

VOLUME 35

AUGUST 1957

NUMBER 8

Canadian Journal of Chemistry

Editor: LÉO MARION

Associate Editors:

HERBERT C. BROWN, *Purdue University*
A. R. GORDON, *University of Toronto*
C. B. PURVES, *McGill University*
Sir ERIC RIDEAL, *Imperial College, University of London*
J. W. T. SPINKS, *University of Saskatchewan*
E. W. R. STEACIE, *National Research Council of Canada*
H. G. THODE, *McMaster University*
A. E. VAN ARKEL, *University of Leiden*

Published by THE NATIONAL RESEARCH COUNCIL

OTTAWA

CANADA

CANADIAN JOURNAL OF CHEMISTRY

(Formerly Section B, Canadian Journal of Research)

Under the authority of the Chairman of the Committee of the Privy Council on Scientific and Industrial Research, the National Research Council issues THE CANADIAN JOURNAL OF CHEMISTRY and five other journals devoted to the publication, in English or French, of the results of original scientific research. Matters of general policy concerning these journals are the responsibility of a joint Editorial Board consisting of: members representing the National Research Council of Canada; the Editors of the Journals; and members representing the Royal Society of Canada and four other scientific societies.

The Chemical Institute of Canada has chosen the Canadian Journal of Chemistry as its medium of publication for scientific papers.

EDITORIAL BOARD

Representatives of the National Research Council

R. B. Miller, *University of Alberta*
H. G. Thode, *McMaster University*

D. L. Thomson, *McGill University*
W. H. Watson (Chairman), *University of Toronto*

Editors of the Journals

D. L. Bailey, *University of Toronto*
T. W. M. Cameron, *Macdonald College*
H. E. Duckworth, *McMaster University*

K. A. C. Elliott, *Montreal Neurological Institute*
Léo Marion, *National Research Council*
R. G. E. Murray, *University of Western Ontario*

Representatives of Societies

D. L. Bailey, *University of Toronto*
Royal Society of Canada
T. W. M. Cameron, *Macdonald College*
Royal Society of Canada
H. E. Duckworth, *McMaster University*
Royal Society of Canada
Canadian Association of Physicians

K. A. C. Elliott, *Montreal Neurological Institute*
Canadian Physiological Society
R. G. E. Murray, *University of Western Ontario*
Canadian Society of Microbiologists
H. G. Thode, *McMaster University*
Chemical Institute of Canada

T. Thorvaldson, *University of Saskatchewan*, Royal Society of Canada

Ex officio

Léo Marion (Editor-in-Chief), *National Research Council*
F. T. Rosser, Vice-President (Administration and Awards), *National Research Council*

Manuscripts for publication should be submitted to Dr. Léo Marion, Editor-in-Chief, Canadian Journal of Chemistry, National Research Council, Ottawa 2, Canada.

(For instructions on preparation of copy, see **Notes to Contributors** (inside back cover).)

Proof, correspondence concerning proof, and orders for reprints should be sent to the Manager, Editorial Office (Research Journals), Division of Administration and Awards, National Research Council, Ottawa 2, Canada.

Subscriptions, renewals, requests for single or back numbers, and all remittances should be sent to Division of Administration and Awards, National Research Council, Ottawa 2, Canada. Remittances should be made payable to the Receiver General of Canada, credit National Research Council.

The journals published, frequency of publication, and prices are:

Canadian Journal of Biochemistry and Physiology	Monthly	\$3.00 a year
Canadian Journal of Botany	Bimonthly	\$4.00 a year
Canadian Journal of Chemistry	Monthly	\$5.00 a year
Canadian Journal of Microbiology	Bimonthly	\$3.00 a year
Canadian Journal of Physics	Monthly	\$4.00 a year
Canadian Journal of Zoology	Bimonthly	\$3.00 a year

The price of single numbers of all journals is 75 cents.

Reprinted in entirety by photo-offset from the original issue.

Canadian Journal of Chemistry

Issued by THE NATIONAL RESEARCH COUNCIL OF CANADA

VOLUME 35

AUGUST 1957

NUMBER 8

THE HYSTERESIS LOOP IN ADSORPTION ISOTHERMS ON POROUS VYCOR GLASS AND ASSOCIATED DIMENSIONAL CHANGES OF THE ADSORBENT. II¹

H. W. QUINN² AND R. MCINTOSH

ABSTRACT

The causes of hysteresis in the adsorption isotherms on porous Vycor glass are discussed, employing as ancillary evidence the dimensional changes of the adsorbent. Diagrams of domain complexions for pores of the ink-bottle type are given and used to develop certain of Everett's theorems. Evidence showing the interdependence of domains or voids is given. The compressibility of the porous adsorbent is evaluated and shown to differ with different adsorbates, which suggests distributions of adsorbed matter specific to the adsorbate. A thermodynamic development is given, which indicates that the most stable states of the system are represented along the adsorption isotherm. Finally, certain anomalous findings in the region of low adsorption and within the hysteresis loop are reported and discussed.

INTRODUCTION

The subject matter discussed in this paper has resulted from a study of the adsorption isotherm and of the expansion of the solid when vapors are adsorbed on porous Vycor glass rods. Some of the results have already been reported in a paper read at the 2nd International Congress of Surface Activity (13) but, owing to the necessity of restricting the length of that submission, details were omitted. The most important observations and conclusions from the investigation have been summarized in the paper referred to, and the discussion of some of them will be elaborated upon. In addition, this paper presents certain observations not previously reported.

THE HYSTERESIS LOOP

Studies have been made of the adsorption on porous glass of butane at -6.2°C. , ethyl chloride at 6.0°C. , and ammonia at -39.2°C. The investigations with butane have been much more extensive than those with the other adsorbates.

As previously noted (13) the adsorption isotherms for these adsorbates all have the same general shape, which corresponds with that found by Amberg and McIntosh (1) for the adsorption of water on porous glass. The similarity of shape also exists for the plots of $\Delta l/l$ vs. volume adsorbed in the cases of butane, ethyl chloride, and water. Both the isotherm and expansion plot for butane and ethyl chloride have hysteresis loops due presumably to the presence of pores in the adsorbent in which adsorbate is taken up irreversibly by capillary condensation. Although the expansion plot was not obtained for the adsorption of ammonia, it is presumed that it would also exhibit hysteresis since the isotherm shows a large hysteresis loop. The upper region of the desorption

¹Manuscript received February 15, 1957.

²Contribution from the Department of Chemistry, University of Toronto, Toronto, Ontario.

³Holder of a National Research Council Studentship. Present address: Research Department, Dow Chemical of Canada, Ltd., Sarnia, Ontario.

isotherm has been found to be reversible in both the adsorption and expansion data. This is illustrated for butane in Table I. Along this region there is a marked contraction of the adsorbent for the removal of a relatively small amount of the adsorbed butane (approximately 12% of the total amount adsorbed). It has been suggested (1) that this marked contraction is due to large negative pressures generated within the pores as a result of the changing radii of concave menisci at the entrances to the pores. Since dimensional changes and adsorption data are reversible, this single mechanism was deemed sufficient to account for these observations.

TABLE I
ADSORPTION AND EXPANSION DATA FOR BUTANE ALONG REVERSIBLE
REGIONS OF THE DESORPTION ISOTHERM

Point No.	% Linear expansion	Volume adsorbed (cm. ³ /g.) S.T.P.	Equilibrium pressure (P/P_0)
24D	0.0812	51.5	0.928
25D	0.0706	49.8	0.885
26A	0.0815	51.5	0.927
27D	0.0718	50.0	0.885
28D	0.0616	48.9	0.837
29D	0.0460	47.2	0.761
30A	0.0614	48.8	0.837

D—a desorption point, *A*—an adsorption point.

SCANNING ACROSS THE HYSTERESIS LOOP

Adsorption and desorption scanning curves have been obtained which rejoin the main branches of the hysteresis loop only at the loop closures. These data support the postulate that the pores in the adsorbent resemble ink bottles in shape (8), each having maximum and minimum dimensions so that, according to the ink-bottle theory of capillary condensation, a pore will fill irreversibly at a pressure governed by its maximum or body radius, where these are related through the Kelvin equation. The same pore will empty irreversibly at a pressure governed by its minimum or neck radius. Because the desorption scanning curves have been found to have reversible regions which are shorter than that on the main desorption isotherm, it has been concluded that the capillaries are not independent of one another and do not empty independently (13).

Adopting the theory of Everett and Smith (4) and Enderby (2), which explains hysteresis in terms of the behavior of independent domains which undergo transitions irreversibly between two possible states (state I and state II) at values of an external variable, λ , governed by parameters of the domains such as domain dimensions, it is possible to obtain complexion diagrams which distinguish those domains in state I and those in state II. Such complexion diagrams have been synthesized for domains represented by ink-bottle-shaped pores for which the domain parameters are r_n and r_b , the radius of the pore neck and pore body respectively. These diagrams are depicted in Fig. 1. The external variable in this case is the pressure (λ). The value of λ at which a pore fills irreversibly is designated by Λ while that at which it empties irreversibly is Λ^* . Since the Kelvin equation applies for these domain transitions, the Λ values are functions of r_b while the Λ^* values are functions of r_n . If the only restriction placed on the possible values of these parameters is that $r_n < r_b$, then the Λ and Λ^* curves will appear on the complexion diagram as shown in Fig. 1(a). The restriction stated implies that all values of $r_n < r_b$ are possible for any given domain. If this were not so the domain complexions would be represented in an area less than that under the sloping straight line, and in this case it would be possible for the number of domains in state II corresponding to a Λ curve to be re-established at some value of λ above that at the inception of the

hysteresis loop. For a system such as that for which the complexation diagram is depicted in Fig. 1(a) it may be proved from complexation diagrams (Fig. 1(c) and 1(d) where the shaded area represents filled pores) that, at a given value of λ , a point on a scanning curve cannot correspond to a point on the main curve except at the closures of

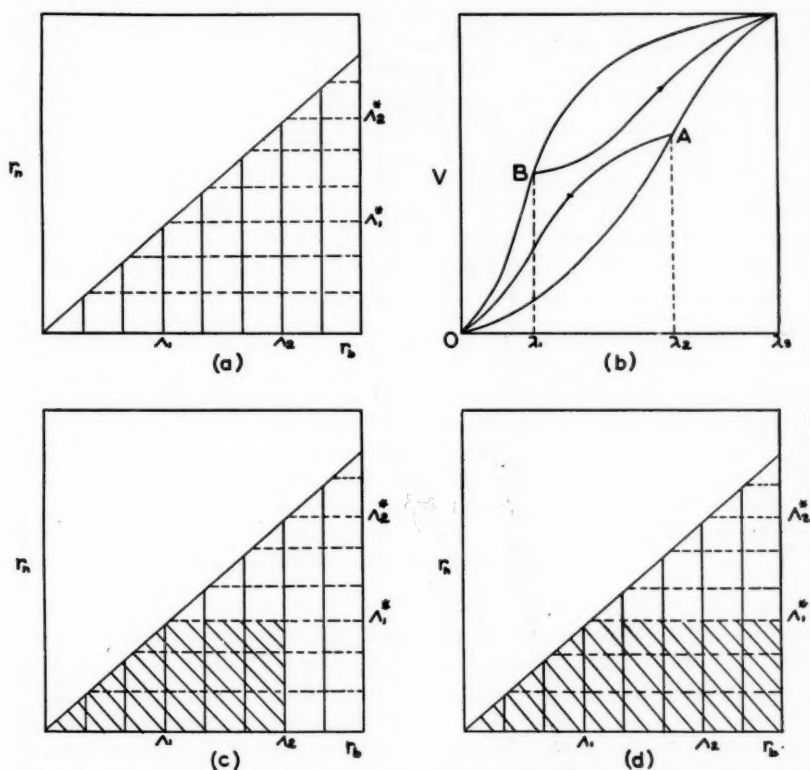


FIG. 1. (a) Complexion diagrams showing Λ and Λ^* curves for ink-bottle pores. (b) Hysteresis loop with scanning curves for the system illustrated in 1(a). (c) Complexion diagrams for ink-bottle pores representing a point on a desorption scanning curve. (d) Complexion diagram for ink-bottle pores representing a point on the main desorption curve.

the hysteresis loop and thus that scanning curves may not join the main curves until these closures have been reached (Fig. 1(b)). Since the experimental fact is that scanning curves go to the lower end of the loop, on the basis of the domain theory it must be concluded that all values of $r_n < r_b$ are possible for any particular r_b . When the pores do not act independently, the independent domain theory cannot be applied and the complexation diagrams depicting domains in state II cannot be obtained.

On the basis of the independent domain theory (3, 4), several theorems have been postulated to predict the behavior of scanning curves. One of these is that, at a given value of the external variable, the slope of any scanning curve must be less than that of the corresponding main curve. With the system butane - porous glass this is not the case for the reversible region of the desorption scanning curves (Fig. 2). It is the interdependence of the pores in the adsorbent which causes this difference from the predicted behavior.

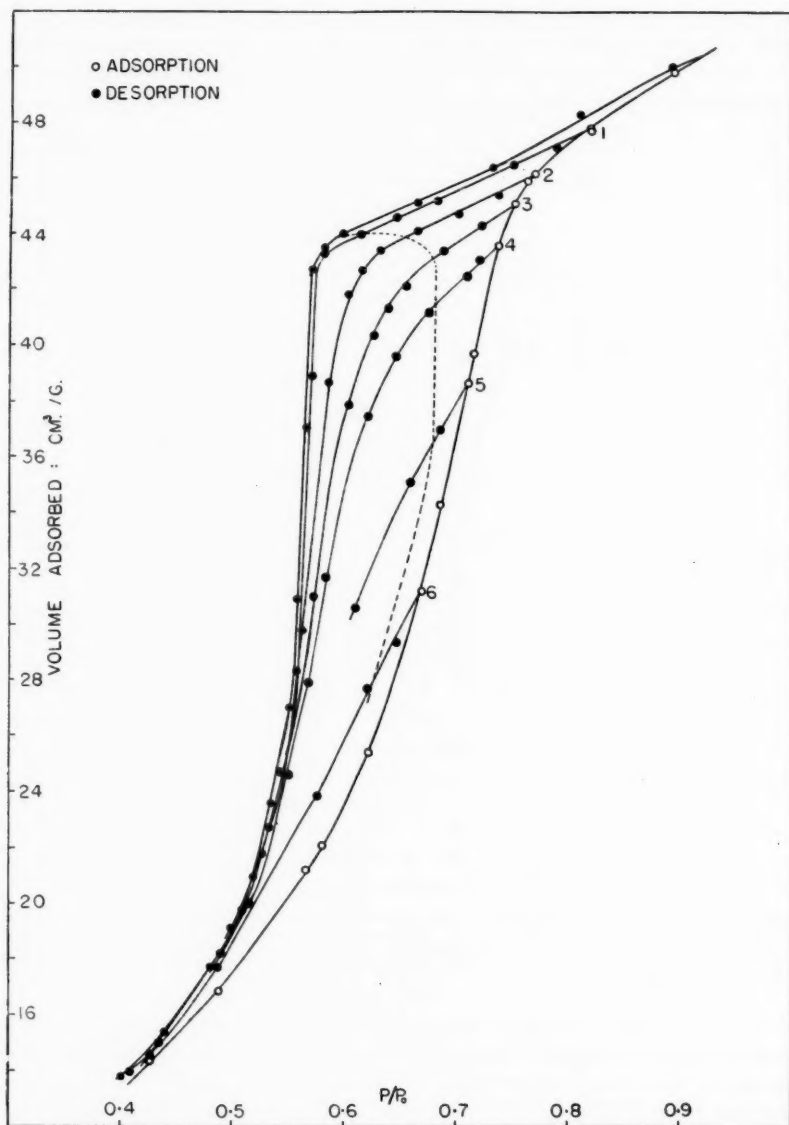


FIG. 2. Desorption scanning for the adsorption of butane on porous glass at -6.2°C . illustrating the region of reversible desorption.

The desorption isotherm has frequently been used in conjunction with the Kelvin equation to obtain an estimate of the size-number distribution of the pores in the adsorbent. When, however, the pores do not empty at the pressures corresponding to their neck radii but are prevented from doing so by pores with smaller necks, the desorption branch can no longer be used to give a reliable distribution. Pores of a shape which

might lead to such behavior have been illustrated in the earlier paper (13). It might be possible to obtain a distribution from the adsorption isotherm if, by partial desorption scanning at frequent intervals along the isotherm, it were possible to separate reversible and irreversible adsorption.

COMPRESSIBILITY OF THE ADSORBENT

It has been observed that, along the reversible region at the top of the hysteresis loop for the systems water - porous glass (1), butane - porous glass, and ethyl chloride - porous glass, there is a linear relationship between $\ln P/P_0$ and $\Delta l/l$ where P is the equilibrium vapor pressure and P_0 the saturation vapor pressure of the adsorbate. If the only mechanism of desorption in this region is the evaporation of adsorbate from the menisci of filled capillaries, it would be expected that, provided the adsorbent obeyed Hooke's law, there would be a linear change of $\Delta l/l$ vs. $\ln P/P_0$. This is because the negative pressure generated in the capillaries by the curvature of the menisci varies directly as the natural logarithm of the relative pressure as given by the equation

$$[1] \quad P' - P = RT/\bar{V} \ln P/P_0,$$

where P' represents the negative pressure under the menisci in atmospheres, \bar{V} the molar volume of the adsorbate, R the gas constant in cc-atmosphere degrees⁻¹ moles⁻¹, and T the absolute temperature. Since all the menisci have the same radius of curvature at a given P/P_0 , the negative pressure within each filled capillary will be the same and there should be a nearly uniform stress distribution throughout the adsorbent provided all capillaries are filled with adsorbate. It is possible to determine $\Delta P'$ between two points on the reversible region and, since there are measurements available of differences of $\Delta l/l$ between these points, a calculation of the compressibility of the adsorbent may be made. The expression applied for such a calculation is

$$[2] \quad \Delta(\Delta l/l) = -\frac{1}{3}\beta'\Delta P',$$

where β' is the compressibility of the adsorbent in atmospheres⁻¹. The compressibility calculated from this relation would not, however, correspond to the compressibility determined by straining the adsorbent with a known stress applied externally since, in this case, the pressure is applied internally.

Mackenzie (11) has derived an expression relating the bulk modulus, k' , of a porous material when stress is applied to the inner surface of the pores to the bulk modulus, k , when the stress is applied externally. The relationship is

$$[3] \quad 1/k' = 1/k - 1/k_0,$$

where k_0 is the bulk modulus of the solid material comprising the body. He adopted the model of spherical holes to represent the pores and each hole is surrounded by an annulus of solid material of thickness such that the density of the hole and the solid material combined is equivalent to the density of the porous medium. The model is illustrated in Fig. 3. On going from state (b), with no applied stress, to state (a), where there is a pressure ($-P$) applied to the internal surface of the hole while the external pressure is still zero, the dilatation is $(\Delta V/V)_1 = -P/k'$. If, however, the pressure P is applied externally while the internal pressure is still zero, (b) \rightarrow (c), the dilatation is $(\Delta V/V)_2 = -P/k$. If state (a) is changed to state (c) by applying an additional hydrostatic pressure P to both the internal and external surfaces, the additional dilatation will be just that produced by the application of an additional pressure P to the solid material and will be expressed by $(\Delta V/V)_3 = -P/k_0$. From Fig. 3, since the process (a) \rightarrow (b) \rightarrow (c) is

equivalent to the process (a) \rightarrow (c), it follows that $(\Delta V/V)_3 = -(\Delta V/V)_1 + (\Delta V/V)_2$ and thus that

$$[4] \quad 1/k' = 1/k - 1/k_0 \text{ or } \beta' = \beta - \beta_0.$$

Thus, if the compressibility of the solid material, β_0 , is known and β' can be calculated from a knowledge of the pressure on the inner surface and of the dilatation, then the compressibility of the porous solid corresponding to the pressure applied externally, β , can

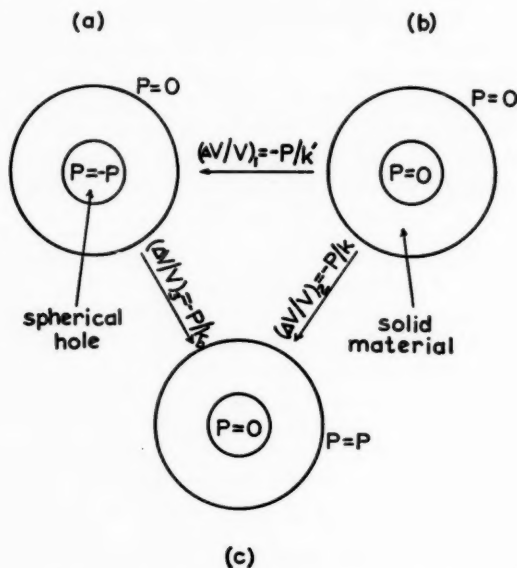


FIG. 3. Mackenzie's model of a pore as a spherical hole surrounded by a shell of solid material.

be calculated and compared with the compressibility obtained by application of a known stress to the external surface.

Employing equation [1] to calculate the pressures within the pores along the reversible region and using the measured values of per cent linear expansion along this region, values of β' have been calculated from equation [2] for the three systems mentioned above. From values of the elastic constants for the solid glass (12), a value of β_0 was determined, assuming isotropy, and found to be 2.04×10^{-7} p.s.i. $^{-1}$. It was thus possible to obtain values of β for the porous glass but there has been no value obtained by the usual methods with which to make a comparison. The calculated values are recorded in Tables II, III, and IV. From Table II the mean value of β for water as adsorbate is 6.03×10^{-7} p.s.i. $^{-1}$, from Table III that for butane is 1.59×10^{-6} p.s.i. $^{-1}$, and from Table IV that for ethyl chloride is 2.69×10^{-6} p.s.i. $^{-1}$.

Flood and Heyding (5) have obtained an expression enabling the calculation (when adsorption is reversible) of the stress in the solid from the adsorption data and a knowledge of the void to solid ratio of the adsorbent. This expression, in conjunction with the Hooke's law relation, allows calculation of an apparent compressibility, βK , where K is a structure constant relating the linear average stress to the volume average stress

TABLE II
COMPRESSIBILITY OF POROUS GLASS DETERMINED FROM ADSORPTION OF WATER

$\Delta P'$ (atm.)	$\Delta (\Delta l/l)$	β' (p.s.i. ⁻¹)	β (p.s.i. ⁻¹)
- 50.01	- 8.3 $\times 10^{-5}$	3.38 $\times 10^{-7}$	5.42 $\times 10^{-7}$
-122.7	-20.9 $\times 10^{-5}$	3.47 $\times 10^{-7}$	5.51 $\times 10^{-7}$
-208.7	-46.7 $\times 10^{-5}$	3.57 $\times 10^{-7}$	6.61 $\times 10^{-7}$
-233.0	-51.8 $\times 10^{-5}$	4.54 $\times 10^{-7}$	6.58 $\times 10^{-7}$

TABLE III
COMPRESSIBILITY OF POROUS GLASS DETERMINED FROM ADSORPTION OF BUTANE

$\Delta P'$ (atm.)	$\Delta (\Delta l/l)$	β' (p.s.i. ⁻¹)	β (p.s.i. ⁻¹)
-22.25	-16.6 $\times 10^{-5}$	1.52 $\times 10^{-6}$	1.72 $\times 10^{-6}$
-46.04	-32.9 $\times 10^{-5}$	1.46 $\times 10^{-6}$	1.66 $\times 10^{-6}$
-68.47	-45.9 $\times 10^{-5}$	1.37 $\times 10^{-6}$	1.57 $\times 10^{-6}$
-92.94	-55.6 $\times 10^{-5}$	1.22 $\times 10^{-6}$	1.42 $\times 10^{-6}$

TABLE IV
COMPRESSIBILITY OF POROUS GLASS DETERMINED FROM ADSORPTION OF ETHYL CHLORIDE

$\Delta P'$ (atm.)	$\Delta (\Delta l/l)$	β' (p.s.i. ⁻¹)	β (p.s.i. ⁻¹)
-32.25	- 44.4 $\times 10^{-5}$	2.81 $\times 10^{-6}$	3.01 $\times 10^{-6}$
-62.72	- 75.8 $\times 10^{-5}$	2.46 $\times 10^{-6}$	2.66 $\times 10^{-6}$
-97.35	-104.2 $\times 10^{-5}$	2.19 $\times 10^{-6}$	2.39 $\times 10^{-6}$

in the solid. Employing this expression for the system at saturation, values of βK have been calculated for water and butane on the porous glass and have been found to be 6.45×10^{-7} p.s.i.⁻¹ and 1.96×10^{-6} p.s.i.⁻¹ respectively. The lack of expansion data for ethyl chloride at saturation prevented calculation of βK for that adsorbate. The values obtained are in good agreement with the values of β which are really apparent compressibilities, obtained for the same two systems assuming that contraction is caused by change of curvature of menisci and that Mackenzie's model applies to the porous glass. The agreement should not be overemphasized, however, since the Flood-Heyding treatment is not correct when the path of integration is not completely reversible as is the case when hysteresis occurs.

It will be observed that the calculated compressibility of the adsorbent is markedly different when water is the adsorbate from that for adsorbed butane and that in turn somewhat different from the compressibility with ethyl chloride. The most logical explanation of this appears to be that there must be a different stress distribution in the solid in the three cases owing possibly to different distributions of adsorbate.

FREE ENERGY CHANGES OF THE ADSORBENT

As has been emphasized (13), several investigators have observed an approximately linear variation of the expansion with computed spreading force of the film for adsorption where the situation is not complicated by the existence of hysteresis. In the case of the porous glass, if the initial part of the adsorption isotherm is considered to be reversible, this relationship is again found. There was noted, however, a substantial difference in

the proportionality constant between extension and spreading force for the several adsorbates. This was considered to be due to different stress distributions which were characteristic of the adsorbate.

If, instead of considering a spreading force of the film, interpretation is based upon a change of chemical potential of the solid as Hill has suggested (7), the dimensional change may be taken as a measure of the variation of chemical potential of the adsorbent. Although changes of stress distribution must undoubtedly occur to some extent as the amount adsorbed is varied, the dimensional variation may be considered to measure the change of chemical potential of the adsorbent even within the hysteresis loop provided that changes of stress distribution are not important. This assumption makes possible an estimate of the relative stability of systems represented by points on or within the hysteresis loop, since the chemical potential of the adsorbate is related to the equilibrium pressure. With systems with the same quantity adsorbed, the comparison is based upon an evaluation of the Helmholtz free energy of the combined adsorbate-adsorbent system in the following way.

According to Hill (7), one may write for a reversible infinitesimal variation of conditions for the total system

$$[5] \quad dE = TdS - PdV + \mu_s dn_s + \mu_{so} dn_{so}$$

where the subscript "s" denotes the adsorbate and "so" the solid adsorbent. For the same quantity of pure solid in the same state of subdivision as that in the combined system, and under the same hydrostatic pressure,

$$[6] \quad dE_{so} = TdS_{so} - PdV_{so} + \mu_{so} dn_{so}$$

On subtraction, the properties of the adsorbed phase are defined by

$$[7] \quad dE_s = TdS_s - PdV_s + \mu_s dn_s - (\mu_{so} - \mu_{so}^*) dn_{so}$$

where

$$E_s = E - E_{so}^*, \text{ etc.}$$

By definition

$$F_s = n_s \mu_s \text{ and } \mu_{so}^* - \mu_{so} = \Phi$$

and the relation

$$[8] \quad -S_s dT + V_s dP + n_{so} d\Phi - n_s d\mu_s = 0$$

follows.

For isothermal conditions,

$$[9] \quad \int n_{so} d\Phi = \int n_s d\mu_s - \int V_s dP$$

It is important to emphasize here that equation [9] is valid for reversible adsorption and may be employed to evaluate $\int n_{so} d\Phi$ from the reversible part of the adsorption isotherm below the hysteresis loop. As mentioned above this leads to a linear relation between $\int n_{so} d\Phi$ and $\Delta l/l$, that is,

$$[10] \quad \int n_{so} d\Phi = k \Delta l/l$$

Clearly, for that part of the isotherm where hysteresis occurs, $\int n_{so} d\Phi$ cannot be evaluated by this means. However, it seems reasonable, on the basis of the experimental result expressed by equation [10], to consider that $\Delta l/l$ may be taken as a measure of $\int n_{so} d\Phi$. If a numerical value is desired it must be based on the value of k obtained from the reversible part of the isotherm. The assumption is thereby made that the value of k may be employed for systems represented by points on or within the hysteresis loop.

As has been pointed out, the value of k , for reversible adsorption, depends upon the adsorbate, and is thus probably dependent upon the distribution of the adsorbed matter. The distribution, for a given adsorbate, may depend upon the quantity of matter adsorbed. The importance of this effect is unknown, but for the purpose of illustrating the method, it will be considered negligible. Therefore, to compare the stability of a system in state (a) (T, n_s, n_{so}, V, P_a) with a system in state (b) (T, n_s, n_{so}, V, P_b), the Helmholtz free energy of the two states is computed. Since $F = A + PV$,

$$A_a - A_b = F_a - F_b - V(P_a - P_b)$$

if the volume of the adsorbed matter is assumed the same for the two states and the volume change of the solid is negligible.

Remembering that

$$F = n_{so}\mu_{so} + n_s\mu_s$$

and that

$$\mu_{so}^* = \mu_{so}^* + \int_{P_a}^{P_b} \bar{V}_{so}^* dP,$$

it follows that

$$[11] \quad A_a - A_b = -n_{so} \int_{P_a}^{P_b} \bar{V}_{so}^* dP - n_{so}(\Phi_a - \Phi_b) + n_s RT \ln P_a/P_b - V(P_a - P_b).$$

Calling $n_{so}\bar{V}_{so}^* = V_s$, the total volume of the solid, the expression may be written

$$[12] \quad A_a - A_b = n_s RT \ln P_a/P_b + (V - V_s)(P_b - P_a) - n_{so}(\Phi_a - \Phi_b).$$

Such calculations have been made for various values of the volume adsorbed on the two branches of the hysteresis loop for the systems water - porous glass and butane - porous glass. The results are shown in Table V, where "a" signifies the adsorption curve

TABLE V
DIFFERENCES OF HELMHOLTZ FREE ENERGY ON THE TWO BRANCHES OF THE HYSTERESIS LOOP

Butane		Water	
Volume adsorbed (cm. ³ /g.) S.T.P.	$A_a - A_b$ (cal. per g. of adsorbent)	Volume adsorbed (cm. ³ /g.) S.T.P.	$A_a - A_b$ (cal. per g. of adsorbent)
18.6	-0.17	0.120	-2.23
22.4	-0.34	0.160	-6.04
26.1	-0.58	0.200	-8.02
29.8	-0.81	0.220	-6.21
33.5	-1.13		
37.3	-1.40		
41.0	-1.66		
44.7	-1.31		
48.4	-0.44		

and "b" the desorption branch. The table shows that the Helmholtz free energy appears to be greater on the desorption curve than on the adsorption curve since $A_a - A_b$ is everywhere negative. This would indicate that the adsorption branch represents the more stable state. It also appears that the free energy difference increases from zero at each loop closure to a maximum at some point on the loop. This is to be expected if there is any free energy difference at all between the two branches since, at the loop

closures, the free energy of the system should be single valued. For a point inside the loop, however, this is not necessarily so since adsorption and desorption scanning curves do not intersect at the same point on the isotherm and expansion plot. The free energy of such a point must thus depend on the path followed in reaching it.

Although the calculated values of the free energy differences may be somewhat in doubt, since it is not known to what extent stress distribution is important, it would appear that the fact that $A_a - A_d$ is always negative provides some support for the suggestion that the main adsorption curve represents the most stable states on the hysteresis loop. When, as is usual in dealing with physical adsorption, the solid is considered inert, the system of lowest equilibrium pressure is thought to be the most stable. In fact the solid is not inert, and if the value of k is chosen as we have outlined, the conclusion is reached that the change of state of the solid is sufficiently great that the system of highest equilibrium pressure may well be the most stable.

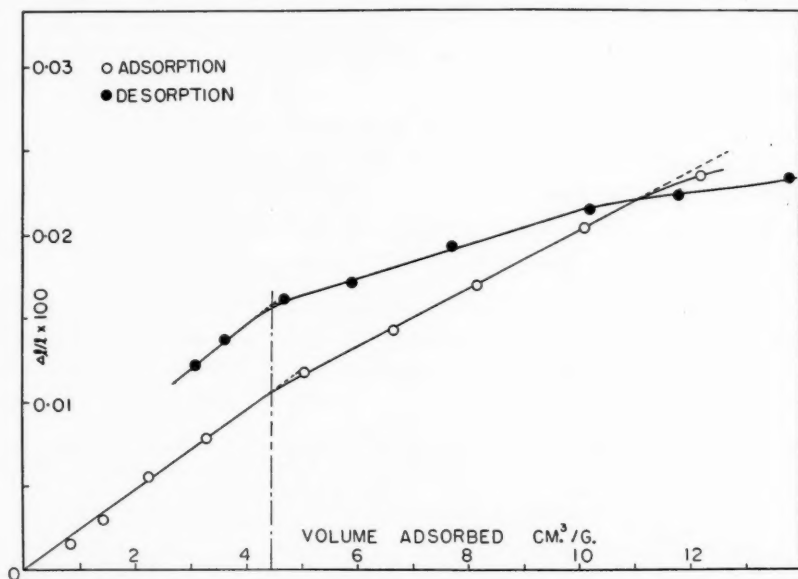


FIG. 4. Expansion plot for butane on porous glass at -6.2°C . showing the crossover on desorption and the change of slope at low pressure.

PECULIARITIES AT LOW ADSORPTION

As reported previously (13), on desorption, the hysteresis loop for butane, ethyl chloride, and ammonia does not close at low pressures but exhibits a long narrow region where the adsorption and desorption isotherms lie almost parallel. Since, on readsorption from this region, carefully studied in the case of butane, the desorption isotherm rejoins the original adsorption curve, the non-closure of the loop is due to something other than error in measurements of adsorbed volumes. It has been found in addition that, on the expansion plot, the desorption curve does not rejoin and follow the adsorption curve at low pressures but actually crosses it and thus lies above it while further desorption occurs. In fact, the original length of the adsorbent is attained only after the remaining butane has been pumped off. The crossover is illustrated in Fig. 4. This figure

also shows an alteration of slope in the change of per cent linear expansion with volume of adsorbed butane at a value of approximately $0.5 \text{ cm}^3/\text{g.}$ on both adsorption and desorption.

The non-closure of the hysteresis loop has also been observed by McDermot and Arnell (9) and McDermot and Lawton (10) for the adsorption of nitrogen on various graphites and has been explained on the basis of swelling of the graphite and penetration of the adsorbate molecules into the crystalline lattice. It does not, however, appear likely that this could occur with butane and glass. It did not occur with water on porous glass (1). If the adsorbent has many small pores into which the large butane molecules can only slowly diffuse, these pores might remain filled until very low pressures are reached, whereas they would not yet have filled at the same pressure on adsorption and non-closure of the loop would be observed. Since, on the desorption curve, the additional adsorbed material makes a contribution to the expansion of the rod, this curve will cross the adsorption curve on the expansion plot and the position of the crossover will correspond roughly to the point at which the pores filling by slow diffusion have all been filled. If such is the case, this phenomenon would be time dependent and a very long time might be required before equilibrium is achieved at a given pressure.

The change of slope in the linear expansion plot for butane on both the adsorption and desorption curves indicates a change in the manner in which the adsorbed butane affects the surface of the glass rod. This could be explained by a change in the position of the surface on which adsorption is occurring. It might be that, at the position of this change of slope, the butane molecules begin to diffuse into small capillaries which are distributed differently throughout the adsorbent than the initial adsorption sites and thus cause a change in the linear expansion as a function of volume adsorbed.

Yates (14) has reported an initial contraction of porous glass when carbon monoxide is adsorbed. This he has attributed to the polar nature of the adsorbate since no such contraction occurs upon adsorption of non-polar gases. In this work, it was not possible to obtain expansion data for ethyl chloride at very low adsorptions so it is not known whether or not there was an initial contraction. With butane, only expansion has been observed even at very low adsorptions. It may be noted that such initial contractions* had already been observed for activated charcoal with both polar and non-polar adsorbates (6). Thus these effects in the region of low adsorption may depend upon the porous structure of the adsorbent and the size of the adsorbate molecule, rather than upon the polar character of the adsorbate or a solution of the gas in the solid.

IRREVERSIBILITY IN EXPANSION OF THE ADSORBENT

It has been found that adsorption from some desorption points within the hysteresis loop, followed by desorption, will return the adsorption data but not the expansion data to the original values. However, a second adsorption followed by further desorption to the point reproduce the $\Delta l/l$ obtained after the first cycle. This is illustrated in Fig. 5. The points exhibiting this phenomenon are those which are reached by much irreversible desorption, presumably after many capillaries have emptied irreversibly. At the moment the only conceivable cause for this effect is some difference in the type or distribution of the film adsorbed on the void walls after rapid irreversible desorption of the capillaries from that of the film remaining after irreversible desorption occurs from a thicker film.

*Dr. E. A. Flood, Pure Chemistry Division, N.R.C., Ottawa, in a private communication, has disclosed his recent observations of marked contractions in zinc chloride activated coconut shell carbon rods on the adsorption of saturated hydrocarbon gases and carbon tetrachloride.

A change of film distribution thus would appear to cause a change in the linear expansion of the adsorbent without any measurable change in the quantity of adsorbed butane and the equilibrium pressure over it.

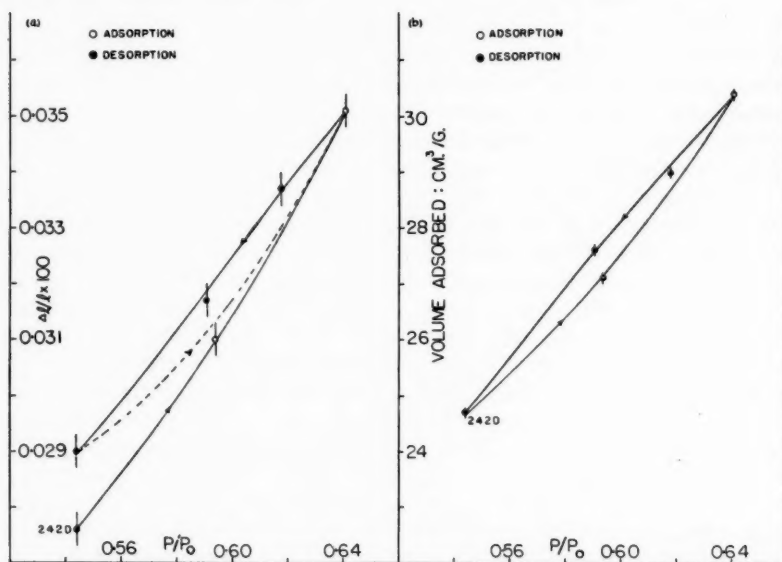


FIG. 5. Adsorption from a desorption point. (a) Irreversibility in length of the adsorbent. (b) Reversibility in amount of adsorbed butane.

SUMMARY

The observation of dimensional changes of the adsorbent in conjunction with adsorption data aids in interpreting the causes of a hysteresis loop in an adsorption isotherm. It also appears that the determination of dimensional changes may aid in settling the relative stability of systems on or within the hysteresis loop. Finally, such measurements reveal that systems considered identical on the basis of adsorption data may indeed be distinct.

ACKNOWLEDGMENT

We would like to acknowledge financial assistance from the National Research Council for this work.

REFERENCES

1. AMBERG, C. H. and MCINTOSH, R. *Can. J. Chem.* **30**, 1012 (1952).
2. ENDERBY, J. A. *Trans. Faraday Soc.* **51**, 835 (1955).
3. EVERETT, D. H. *Trans. Faraday Soc.* **50**, 1077 (1954).
4. EVERETT, D. H. and SMITH, F. W. *Trans. Faraday Soc.* **50**, 187 (1954).
5. FLOOD, E. A. and HEYDING, R. D. *Can. J. Chem.* **32**, 660 (1954).
6. HAINES, R. S. and MCINTOSH, R. *J. Chem. Phys.* **15**, 28 (1947).
7. HILL, T. L. *J. Chem. Phys.* **18**, 246 (1950).
8. KATZ, S. N. *J. Phys. & Colloid. Chem.* **53**, 1166 (1949).
9. McDERMOT, H. L. and ARNELL, J. C. *Can. J. Chem.* **33**, 913 (1955).
10. McDERMOT, H. L. and LAWTON, B. E. *Can. J. Chem.* **34**, 769 (1956).
11. MACKENZIE, J. K. *Proc. Phys. Soc. B*, **63**, 2 (1950).
12. NORDBERG, M. E. Corning Glass, Corning, N.Y. Private communication.
13. QUINN, H. W. and MCINTOSH, R. *Congress of Surface Activity*, April 8-12, 1957. Butterworth's Scientific Publications, London, England.
14. YATES, D. J. C. *J. Phys. Chem.* **60**, 543 (1956).

PREPARATION OF ERUCIC AND NERVONIC ACIDS LABELLED WITH CARBON-14¹

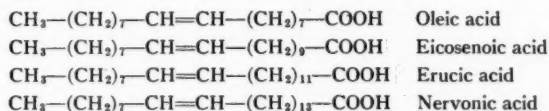
K. K. CARROLL

ABSTRACT

The malonic ester synthesis of nervonic acid (tetracos-15-enoic acid) has been modified so that the product consists of pure *cis* rather than a mixture of *cis* and *trans* isomers. The modified synthesis has been used for the preparation of C¹⁴-labelled erucic and nervonic acids.

INTRODUCTION

The work reported in this paper was undertaken as a result of earlier experiments in this laboratory which indicated that erucic acid in some way influenced cholesterol metabolism in the rat. The addition of this monounsaturated C₂₂ fatty acid to the diet caused an increase in the cholesterol content of the adrenals and liver and an increased excretion of cholesterol in the feces (3). Similar but less marked changes were also obtained by feeding the corresponding C₂₀ (eicosenoic) and C₂₄ (nervonic) acids. Erucic and eicosenoic are major component fatty acids of rapeseed oil (4), which is used in European countries as a salad oil and for incorporation into margarine. Nervonic acid occurs in the cerebroside and sphingomyelin of the central nervous system, and is identical with selacholeic acid isolated from shark liver oil (7).



In studying the mechanism of this effect on cholesterol metabolism, it seemed desirable to have a method for incorporating a C¹⁴ label into these fatty acids. A synthesis of nervonic acid has been described (6, 10) in which erucic acid is reduced to the corresponding alcohol, which is then converted to the bromide and thence to nervonic acid by a malonic ester condensation. This method was used to obtain nervonic acid for our earlier feeding experiments (2), but it is unsatisfactory, particularly from the point of view of incorporating a radiocarbon label, because the final product consists of a mixture of *cis* and *trans* isomers from which it is difficult to obtain a high yield of the desired *cis* isomer.

An investigation of the various reactions of this synthetic route disclosed that the isomerization of the double bond occurred during conversion of the alcohol to the bromide, and it seems likely that hydrogen bromide liberated during the reaction was responsible. By omitting the heating step in this reaction it was possible to obtain nearly pure *cis* nervonic acid in approximately the same yield as the mixture of isomers obtained by earlier workers. The modified method has been used to prepare eicosenoic, erucic, and nervonic acids starting from oleic, eicosenoic, and erucic acids respectively, and the C¹⁴ label was introduced by using radioactive malonic ester for the condensation.

Although this synthesis proved satisfactory for the preparation of labelled fatty acids, the relatively low yield encountered in converting the fatty alcohols to the corresponding

¹Manuscript received April 10, 1967.

Contribution from the Collip Medical Research Laboratory, University of Western Ontario, London, Ontario.

bromides was still a disadvantage in preparing large amounts of unlabelled fatty acids for feeding experiments. An alternative method has been investigated for the preparation of nervonic acid in which erucyl methanesulphonate was used instead of erucyl bromide as the intermediate. This doubled the over-all yield from erucyl alcohol to nervonic acid and resulted in a product which contained no *trans* isomer.

The fact that chain extension by means of a malonic ester condensation can now be achieved without isomerization of the double bond provides further confirmation of the stereochemical configuration of the higher homologues of oleic acid (1, 9).

EXPERIMENTAL

Fatty Alcohols

Erucyl alcohol was prepared by adding 100 g. (0.285 mole) of methyl erucate slowly to a solution of 6.7 g. (0.177 mole) of lithium aluminum hydride in 700 cc. of anhydrous ether in a three-necked flask equipped with stirrer and condenser. The reaction mixture was poured into ice water and acidified with 300 cc. of 3 N sulphuric acid. The ether layer was separated, washed with water, dried over sodium sulphate, and the product distilled. Yield—80 g. (87% of theory), b.p._{0.5}, 188–190° C. Oleyl alcohol and eicosenoyl alcohol were prepared in similar fashion. The methyl eicosenoate and methyl erucate used for these experiments were highly purified preparations provided by Dr. B. M. Craig of the Prairie Regional Laboratory, Saskatoon. Methyl oleate was prepared from oleic acid (Eastman Kodak) and purified by fractional distillation (2).

As an alternative to synthesis, crude oleyl and erucyl alcohols may be obtained from the Archer-Daniels-Midland Company, Midland, Michigan, under the names of ADOL 85 and ADOL 22 respectively. Erucyl alcohol from this source was purified by fractional distillation and used for our large-scale preparations of nervonic acid.

Alkyl Bromides

The method used for converting fatty alcohols to the corresponding bromides is illustrated by the following preparation of erucyl bromide. A solution of 195 g. (0.60 mole) of erucyl alcohol in 600 cc. of toluene was cooled in an ice bath and 60 g. (0.22 mole) of phosphorus tribromide in 300 cc. of toluene was added over a period of 1½ hours with stirring. The temperature of the reaction mixture was maintained between 0° and 5° C. during the addition of the tribromide and the product was worked up immediately without further heating. (In several runs the reaction mixture was allowed to stand for 1–4 hours at room temperature but some isomerization of the double bond occurred even under these conditions.) The toluene was removed *in vacuo* at 40–50° C. and the residue was diluted with 750 cc. of ether and washed first with two 150-cc. portions of a solution containing 10% potassium hydroxide and 10% sodium chloride and then with two 150-cc. portions of 10% sodium chloride solution. Emulsification tends to occur during the washing so the bottom layer was centrifuged after each washing and the upper phase returned to the separatory funnel. It was also found essential to dry the ether solution with magnesium sulphate rather than sodium sulphate; otherwise the mixture foamed badly during the subsequent distillation. Typically, the erucyl bromide distilled at 205–210° C. at 0.6 mm. and towards the end of the distillation the vapor temperature dropped somewhat and a more oily liquid began to distill. This was accompanied by a highly volatile gas which was not condensed in a dry-ice trap and which tended to ignite on contact with air. It is therefore best to discontinue the distillation when the temperature begins to drop, particularly since further distillation does not

appear to increase the subsequent yield of nervonic acid. The erucyl bromide weighed 105 g. (45% of theory).

Malonic Ester Condensation

To a solution of 5.8 g. (0.25 mole) of sodium in 150 cc. of absolute alcohol was added 45.5 g. (0.285 mole) of diethyl malonate. The solution was heated to boiling, then 96 g. (0.25 mole) of erucyl bromide was run in slowly and the mixture was refluxed for 1½ hours. Most of the alcohol was then distilled off and 550 cc. of water containing 5.5 cc. of concentrated hydrochloric acid was added to the residue. The product appeared as an oily top layer which was separated from the aqueous layer and hydrolyzed by refluxing with 160 g. of potassium hydroxide in 1 liter of 60% ethanol for 1½ hours. Part of the alcohol was removed by distillation, then 500 cc. of water was added and the solution was extracted with three 500-cc. portions of ether to remove neutral unreacted material. (This step was included in cases where it was desired to examine the nature of the substituted malonic acids and as a precaution in the preparation of radioactive fatty acids, but ordinarily it can be omitted (6).) The aqueous layer was then acidified with 180 g. of concentrated sulphuric acid in 1500 cc. of water and re-extracted with ether to obtain the crude erucyl malonic acid.

When the original method of Hale, Lycan, and Adams (6) was used for preparing erucyl bromide, the erucyl malonic acid obtained from it consisted of a mixture which was separated by fractional crystallization from chloroform - petroleum ether into two isomers melting at 101–102° C.* and 76.5–79° C. respectively. Calc. for $C_{25}H_{46}O_4$: C, 73.1; H, 11.3; neutral equivalent 205. Found,† high melting isomer: C, 72.5; H, 11.2; neutral equivalent 202; low melting isomer: C, 72.6; H, 11.0; neutral equivalent 204. The high melting isomer gave *trans* nervonic acid when decarboxylated by heating at 175° C. for 30 minutes. The low melting isomer gave *cis* nervonic acid on decarboxylation and was converted to the high melting isomer by treatment with dilute nitric acid and sodium nitrite (6). When the modified method for preparing erucyl bromide was used, the erucyl malonic acid consisted almost entirely of the low melting isomer (m.p. 77.5–78.5° C. after a single recrystallization from petroleum ether (35–50° C.) containing 10% chloroform).

The substituted malonic acids obtained from oleyl bromide and eicosenoyl bromide melted at 65–66° C. and 72–73° C. respectively. Calc. for $C_{21}H_{38}O_4$: C, 71.1; H, 10.8. Found: C, 70.9; H, 10.3. Calc. for $C_{23}H_{42}O_4$: C, 72.2; H, 11.1. Found: C, 72.3; H, 10.8.

Eicosenoic, erucic, and nervonic acids obtained by the modified synthetic method melted at 21–22° C., 31.5–32° C., and 38–39° C. after distillation and recrystallization from methanol. These figures are in general agreement with published data (1, 6, 8, 10). The eicosenoic acid prepared by Fieser and Chamberlain (5) appears to have been mainly the *trans* isomer.

The synthesis of radioactive fatty acids was carried out by essentially the same method as that used for the larger scale preparations. Diethyl malonate-1,3- C^{14} (145 mg. = 1 millicurie) from the Radiochemical Centre, Amersham, was diluted with 18 volumes of non-labelled diethyl malonate and the condensations were carried out on a 1.2 millimole scale. The synthetic fatty acids had specific activities of 6 to 8×10^4 counts/min./mg. (measured in a gas-flow counter—Nuclear, Chicago) after purification by distillation. In

*All melting points are corrected.

†Microanalyses were performed by the Schwartzkopf Microanalytical Laboratory, 56–19 37th Avenue, Woodside 77, N. Y.

these syntheses, approximately half of the radioactivity was lost during decarboxylation of the substituted malonic acids, but this loss could be avoided by using ethyl malonate-2- C^{14} , in which case the fatty acids would be labelled in carbon-2 rather than in the carboxyl carbon.

Erucyl Methanesulphonate

A solution of 48.5 g. (0.150 mole) of erucyl alcohol in 150 cc. of pyridine (dried by distilling from barium oxide and storing over solid potassium hydroxide) was cooled in an ice bath and 18.0 g. (0.157 mole) of methanesulphonyl chloride (Eastman Kodak) was added. The mixture was stirred for 1 hour in the cold and then for 3 hours with the ice bath removed. The reaction mixture was poured into ice water and extracted with ether. The ether extract was washed with dilute hydrochloric acid to remove pyridine, then with water until neutral, and dried with sodium sulphate. Removal of the ether gave a product (54.5 g., 85% of theory) which melted at 33° C. after recrystallization from ethanol. Calc. for $C_{23}H_{46}O_3S$: C, 68.6; H, 11.5. Found: C, 68.5; H, 11.7.

For condensation with ethyl malonate, the crude methanesulphonate was recrystallized from 3 volumes of methanol at 0° C., and the reaction was carried out in a manner similar to that used for erucyl bromide. From 34 g. (0.082 mole) of erucyl methanesulphonate, there was obtained 22 g. (74% of theory) of distilled nervonic acid, b.p. 225–235° C. at 0.1 mm., m.p. 38–39.5° C.

ACKNOWLEDGMENTS

This work was supported by the National Research Council and by a grant from the Life Insurance Medical Research Fund. The author wishes to acknowledge the competent technical assistance of Mr. E. Pedersen.

REFERENCES

1. BOUNDS, D. G., LINSTAD, R. P., and WEEDON, B. C. L. *J. Chem. Soc.* 448 (1954).
2. CARROLL, K. K. *J. Biol. Chem.* **200**, 287 (1952).
3. CARROLL, K. K. and NOBLE, R. L. *Can. J. Biochem. Physiol.* **34**, 981 (1956).
4. CRAIG, B. M. *Can. J. Technol.* **34**, 335 (1956).
5. FIESER, L. F. and CHAMBERLAIN, E. M. *J. Am. Chem. Soc.* **70**, 71 (1948).
6. HALE, J. B., LYCAN, W. H., and ADAMS, R. J. *J. Am. Chem. Soc.* **52**, 4536 (1930).
7. HILDITCH, T. P. *The chemical constitution of natural fats.* John Wiley & Sons, Inc., New York. 1949. p. 30.
8. HOPKINS, C. Y., CHISHOLM, M. J., and HARRIS, J. *Can. J. Research, B*, **27**, 35 (1949).
9. LINSTAD, R. P., WEEDON, B. C. L., and WLADISLAW, B. *J. Chem. Soc.* 1097 (1955).
10. MÜLLER, A. and BINZER, I. *Ber.* **72B**, 615 (1939).

EFFECT OF CHANGES IN HYDRATION ON RECOIL FRAGMENTS IN NEUTRON-IRRADIATED PERMANGANATES¹

J. R. BOLTON AND K. J. McCALLUM

ABSTRACT

Anhydrous and hydrated crystals of sodium and lithium permanganates have been irradiated with neutrons. After irradiation, the crystals were subjected to hydration and dehydration, and the effect of this treatment on the retention of radioactive manganese in the form of the permanganate ion was determined. Hydration of irradiated anhydrous sodium and lithium permanganates decreases the retention observed when the solids are dissolved in basic solutions. Dehydration of the irradiated trihydrate causes little change in the observed retention for sodium permanganate, but a pronounced decrease for lithium permanganate. The significance of the results is discussed.

INTRODUCTION

Libby (2) has studied the reactions of the recoil fragments produced following neutron capture by the manganese atom in potassium permanganate. He found that when irradiated potassium permanganate was dissolved in water, most of the radioactive manganese could be separated with manganese dioxide, but a small percentage, termed the retention, was present in the form of the permanganate ion. When the irradiated solid was dissolved in basic solution, an increase in the retention was observed. He postulated that following the neutron capture reaction, some of the radioactive manganese was present as permanganate ion, but that most existed in the solid in such forms as MnO_3^+ or MnO_2^{+++} . He assumed that these fragments were reduced to manganese dioxide by water. In basic solutions, he postulated that instead they could react with hydroxyl ion to form the permanganate ion, thus accounting for the observed increase in retention. The retention which is observed when the solid is dissolved in water has been termed the inherent retention and may be taken to indicate the percentage of the radioactive manganese present in the solid as the permanganate ion, or at least in a form which yields permanganate ion with water.

Further investigations (3, 5) have verified the nature of the observed changes in retention and have given results which are consistent with the reactions postulated by Libby.

It has been possible to study some of the reactions of the recoil fragments within the irradiated crystals. Heating such crystals before solution increases the retention (5), presumably owing mainly to a recombination of the fragments produced by the recoil process (4), such as a reaction between the manganese containing species and oxygen ions.

Since it is postulated that the recoil fragments undergo reaction with water to form manganese dioxide when the crystals are dissolved, it is possible that they could also undergo reaction with water present as water of hydration during irradiation of the solid. Studies on the retentions in hydrated permanganates (3) have shown that the inherent retentions are usually less, suggesting that some reduction may have occurred. However, since the retentions are still observed to increase in basic solutions, some reactive fragments of the type postulated by Libby apparently still remain.

In the work described here, the effect of hydration changes in irradiated compounds

¹Manuscript received April 15, 1967.

Contribution from Department of Chemistry, University of Saskatchewan, Saskatoon, Sask.

upon the retention has been studied. The resulting rearrangements in the solid could permit the recoil fragments to undergo reactions with other species which are present.

EXPERIMENTAL

Samples of sodium and lithium permanganates were prepared by the reaction between excess silver permanganate and sodium and lithium chlorides. The hydrated permanganates had the compositions $\text{NaMnO}_4 \cdot 2.98\text{H}_2\text{O}$ and $\text{LiMnO}_4 \cdot 3.0\text{H}_2\text{O}$. The anhydrous permanganates prepared from these by drying over magnesium perchlorate had the compositions $\text{NaMnO}_4 \cdot 0.05\text{H}_2\text{O}$ and $\text{LiMnO}_4 \cdot 0.10\text{H}_2\text{O}$.

Samples of these permanganates were bombarded in a paraffin block with neutrons from a radium-beryllium neutron source. Irradiated samples of the hydrated permanganates were dehydrated, partially or completely, in a vacuum desiccator over magnesium perchlorate. Anhydrous permanganates were hydrated in a vacuum desiccator over suitable saturated salt solutions, such as ammonium chloride or calcium nitrate. The samples were then dissolved in water or in sodium hydroxide solutions, and the retentions determined as described previously (3). It was possible to use solutions up to 5 *N* in sodium hydroxide for lithium permanganate. Sodium permanganate appeared to undergo decomposition in solutions more basic than 1 *N* NaOH.

TABLE I
HYDRATION CHANGES IN SODIUM PERMANGANATE

Moles H_2O per mole NaMnO_4		Solvent	% Retention
Solid irradiated	Solid dissolved		
2.98	2.98	Water	11
2.98	0.44	Water	12
2.98	2.98	1 <i>N</i> NaOH	30
2.98	0.21	1 <i>N</i> NaOH	31
0.05	0.05	Water	15
0.05	1.3	Water	16
0.05	0.05	1 <i>N</i> NaOH	79
0.05	0.70	1 <i>N</i> NaOH	58
0.05	0.96	1 <i>N</i> NaOH	40
0.05	1.74	1 <i>N</i> NaOH	24

TABLE II
HYDRATION CHANGES IN LITHIUM PERMANGANATE

Moles H_2O per mole LiMnO_4		Solvent	% Retention
Solid irradiated	Solid dissolved		
3.0	3.0	Water	5
3.0	0.14	Water	7
3.0	3.0	1 <i>N</i> NaOH	16
3.0	0.2	1 <i>N</i> NaOH	12
3.0	3.0	2 <i>N</i> NaOH	30
3.0	0.3	2 <i>N</i> NaOH	17
3.0	3.0	5 <i>N</i> NaOH	55
3.0	0.5	5 <i>N</i> NaOH	31
0.1	0.1	Water	10
0.1	3.0	Water	9
0.1	0.1	1 <i>N</i> NaOH	27
0.1	3.0	1 <i>N</i> NaOH	15
0.1	0.1	2 <i>N</i> NaOH	40
0.1	3.1	2 <i>N</i> NaOH	20
0.1	0.1	5 <i>N</i> NaOH	66
0.1	3.1	5 <i>N</i> NaOH	42

The results for the retention measurements are given in Tables I and II. The values given are the mean of at least two determinations and are precise to within one unit.

The hydration of anhydrous lithium permanganate to form the trihydrate proceeded quite smoothly. The hydration of the sodium permanganate did not proceed so readily. In the time available for the hydration process at humidities which did not cause formation of some liquid phase, the maximum amount of water gained was 1.75 moles of water per mole of permanganate. For sodium permanganate, it was observed that grinding a partly hydrated sample of irradiated permanganate caused a further decrease in retention below the values given in Table I. It was presumed that grinding increased the opportunity for reversible hydration-dehydration processes between different portions of the sample, thus increasing the retention changes with no over-all change in water content. Any such effect was found to be very much smaller with lithium permanganate.

The effect of thermal annealing on irradiated samples which had been subjected to hydration changes was measured. It was found possible to make the measurements only on anhydrous sodium permanganate. The hydrated form of this compound has too low a melting point, while lithium permanganate prepared by dehydration of the trihydrate was found to undergo considerable decomposition under the conditions necessary to cause appreciable changes in the retention.

The samples were heated at 104° C. for 20 minutes, dissolved in water, and the retention determined. Irradiated samples of the trihydrate of sodium permanganate which were then dehydrated and subjected to the heat treatment gave a retention value of 15% compared to 12% in the absence of the heat treatment.

Irradiated samples of anhydrous sodium permanganate subjected to the same heat treatment showed a retention of 37% compared to 15% for unheated samples. Samples of the irradiated anhydrous compound, which were then hydrated to contain 0.6, 0.7, and 1.4 moles of water per mole of permanganate and then dehydrated and heated under the same conditions, gave retentions of 28%, 24%, and 19%, respectively. The hydration-dehydration cycle in these cases resulted in a retention of 15-16% if the heating step was omitted.

DISCUSSION

The reaction between recoil fragments trapped in a hydrated crystal with the water of hydration would, under ordinary conditions, be expected to be slow, because of the slow diffusion processes which would be necessary. If, however, the crystal is subjected to dehydration or hydration steps, reactions could occur.

Dehydration or hydration of irradiated crystals containing recoil fragments might be expected to result in two possible effects. First, if the ions in the crystal undergo a rearrangement during the process, the same processes that occur during thermal annealing might be facilitated. For example, the rearrangement could cause a momentary decrease in the potential barriers hindering diffusion and permit recombination of the fragments produced in the original recoil process to re-form the permanganate ion. This effect would result in an increase in the retention observed when the solid is dissolved in water. Secondly, during the hydration change, the motion of the water molecules through the crystal undergoing a phase change could increase the probability of reaction of the recoil fragments with water. If the products of such a reaction in the solid state were the same as for the reaction in solution, the mechanism proposed by Libby would lead one to expect a reduction of some of the recoil fragments to manganese dioxide. Since when the solid is dissolved in water these fragments are reduced to manganese dioxide in any case, no change in the observed retention should result. However, the decrease

in the number of recoil fragments remaining in the solid should result in a smaller increase in retention when the solid is dissolved in a basic solution. In the extreme case, when all the recoil fragments undergo reduction in the solid to manganese dioxide, no increase in retention in basic solution should be observed.

The results in Tables I and II show that hydration of irradiated anhydrous sodium and lithium permanganates causes little change in retention when water is used as solvent. It appears that during this process there is little reaction of the recoil fragments to form a species yielding permanganate ion with water. Recombination of the initial products of the recoil process does not seem to be facilitated by the hydration process.

However, when either permanganate, after hydration, is dissolved in basic solution, the retention is observed to be lower than that found for the irradiated anhydrous compound dissolved in a solution of the same basicity. This indicates that the hydration process has resulted in a decrease in the number of recoil fragments which react with hydroxyl ions to form permanganate. The manganese-containing species has been changed to one for which the ratio of the rates of reaction with hydroxyl ion and with water has been decreased. A simpler interpretation is that some of the recoil fragments have been reduced to manganese dioxide by water during the hydration reaction. In this case no reaction with hydroxyl ion occurs at all.

The results for the hydration of anhydrous sodium permanganate seem to indicate that for complete hydration to the trihydrate, the retention observed in 1 *N* NaOH would be reduced to the value obtained in water and that complete hydration would result in reduction of all the recoil fragments. The decreases in retention on partial hydration given in Table I are actually even greater than one would calculate on the basis of this assumption. This is ascribed to reversible dehydration-hydration processes between different portions of the sample, so that the fraction of the solid which has gone through the hydration process might be higher than is expected from the observed gain in weight. This explanation is consistent with the observed decrease in retention which resulted from grinding partially hydrated samples of sodium permanganate, a process which should favor such a transfer of water.

Anhydrous lithium permanganate could be readily hydrated to the trihydrate. The retention observed in basic solutions is greater than the value for the anhydrous salt dissolved in water. It appears that hydration in this case does not cause a reduction of all the recoil fragments. If one assumes that the reduction is to a species such as manganese dioxide which does not react at all with hydroxyl ions, it appears that over half of the recoil fragments probably reacts during the hydration.

Tables I and II also give the results following dehydration of the irradiated trihydrates. For sodium permanganate, little effect is evident, both for solutions in water and in 1 *N* NaOH. The slight increase in retention which was observed could indicate some recombination of the original recoil fragments, but the change is within the precision of the experimental results.

The heating experiments on irradiated sodium permanganates which have been subjected to hydration-dehydration processes indicate that changes in the recoil fragments have occurred. The smaller increase in the retention on heating such samples indicates a decrease in the number or reactivity of the recoil fragments, as was concluded from the retention experiments following hydration of sodium permanganate.

In contrast with the results for sodium permanganate, dehydration of irradiated samples of lithium permanganate trihydrate causes decreases in the retention up to 25% in 5 *N* NaOH solution, but no significant change when the solid is dissolved in

water. As in the hydration experiments, it appears that reaction of the radioactive species in the solid has produced a form giving manganese dioxide rather than permanganate ion upon dissolving in basic solution. From the experimental results, it appears that about one-half of the recoil fragments must have undergone such a reaction, since the increase in the retention in basic solution above that in water for the dehydrated samples is about one-half of the corresponding increase for the trihydrate when dissolved directly.

Although the effect of the hydration upon the retention appears to be similar for sodium and lithium permanganate, dehydration of the irradiated trihydrates leads to different results. This difference could be due to a difference in the nature of the recoil species present in the two compounds, or to a difference in the mechanisms of the dehydration processes. It seems unlikely that the recoil species could differ significantly, since the variation of the retention with pH (3) is so similar. Little is known about the details of the changes which occur in these solid permanganate hydrates upon dehydration. For the dehydration of other hydrates, several different mechanisms seem to be possible (1).

A complete understanding of the reactions of the recoil fragments during these hydration changes requires a knowledge of the structural changes which are occurring. On the other hand, studies of the retention changes might conceivably be able to throw some additional light on the changes in the solid state. For example, the observation that extensive reaction of the recoil fragments occurs during the dehydration of the trihydrate of lithium permanganate but not of sodium permanganate suggests that perhaps the simultaneous reorganization of the crystal lattice might be more extensive with the lithium compound. Further discussion must await studies on the structural changes that occur during the changes in hydration.

ACKNOWLEDGMENTS

Grateful acknowledgment is made to the National Research Council for financial support of this work.

REFERENCES

1. GARNER, W. E. *Chemistry of the solid state*. Butterworth Scientific Publications, London, 1955. p. 213.
2. LIBBY, W. F. *J. Am. Chem. Soc.* **69**, 2523 (1947).
3. McCALLUM, K. J. and MADDOCK, A. G. *Trans. Faraday Soc.* **49**, 1150 (1953).
4. MADDOCK, A. G. and DE MAINE, M. M. *Can. J. Chem.* **34**, 275 (1956).
5. RIIFER, W., BRODA, E., and ERBER, J. *Monatsh.* **81**, 657 (1950).

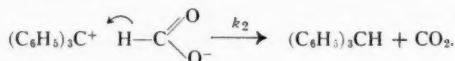
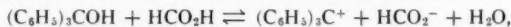
HYDRIDE TRANSFER TO CARBONIUM IONS

I. THE MECHANISM OF THE REDUCTION OF TRIPHENYLMETHYL CARBONIUM ION IN FORMIC ACID¹

ROSS STEWART

ABSTRACT

In an attempt to prove that reduction can take place by hydride transfer, the conversion of triphenyl carbinol in formic acid to triphenylmethane via the carbonium ion was examined. Kinetic and isotopic proof was obtained for the following mechanism:



The rate law based on the above mechanism is

$$-d\{[\text{R}_3\text{C}^+] + [\text{R}_3\text{COH}]\}/dt = k_2[\text{R}_3\text{C}^+][\text{HCO}_2^-],$$

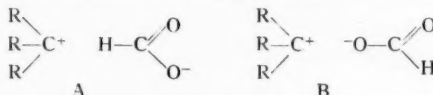
where $\text{R} = \text{C}_6\text{H}_5$, which leads to the integrated rate expression

$$-\log [\text{R}_3\text{C}^+] = \{k_2/(1+1/\alpha)\} [\text{HCO}_2^-] \cdot t, \quad \text{where } \alpha = [\text{R}_3\text{C}^+]/[\text{R}_3\text{COH}].$$

This equation was found to be obeyed under a variety of conditions.

Anhydrous formic-*d* acid was synthesized in good yield by the glycerol catalyzed decomposition of oxalic acid-*d*₂. The concentration of deuterium was shown by nuclear magnetic resonance spectroscopy to be greater than 99%. Use of this material in the reduction gave a kinetic isotope effect and led to isolation of triphenylmethane which had greater than 97% deuterium in the α -position, thus supporting the idea that a hydride ion was transferred from formate ion to the carbonium ion.

The energy and entropy of activation for the rate controlling step have been found to be 18.3 kcal. per mole and -7.5 e.u. The negative ΔS^\ddagger is presumably due to the less likely orientation for the transition state A as compared to B.



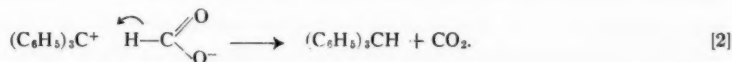
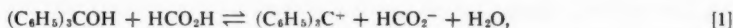
INTRODUCTION

It has been recognized for some time that the mechanism of many reactions which bring about the reduction of organic compounds can best be explained in terms of hydride transfer. Thus it has been suggested that the Cannizzaro (14), Sommelet (1), Meerwein-Ponndorf (22) reactions, the base catalyzed carbonyl-carbinol equilibrium (9), the base catalyzed permanganate oxidation of alcohols (19), and many others take place by such a process and some evidence is available to support such a mechanism. Thus, Doering and Aschner (9) showed that the base catalyzed carbonyl-carbinol conversion proceeds by a two-electron jump. However, a two-electron transition may occur by either the reductant transferring two electrons to the oxidant followed by a transfer of a proton from the solvent to the oxidant, or it may occur by a direct hydride transfer from reductant to oxidant. In an attempt to find more rigorous supporting evidence than has hitherto been obtained for the mechanism of hydride transfer, a search was made of the chemical literature to find a reaction which appeared to be of this type and which would be amenable to a thorough investigation, in particular, a kinetic study. A suitable example was found in a reaction which has been used occasionally for some 60 years,

¹Manuscript received March 6, 1957.

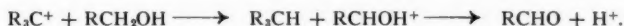
Contribution from the Department of Chemistry, University of British Columbia, Vancouver 8, Canada.

the reduction of triphenyl carbinol to triphenylmethane by formic acid. Formic acid is used as the solvent in the reaction and is sufficiently acidic to cause ionization of the carbinol. It was observed in 1912 by Guyot and Kovache (13) that addition of sodium formate accelerated the reaction and this information appeared to support the following mechanism for the reduction:



However, in 1940 in a semiquantitative study, Bowden, Clarke, and Harris (4) and Bowden and Watkins (5) interpreted this reaction as proceeding via the yellow salt, $(\text{C}_6\text{H}_5)_3\text{C}^+\text{HCO}_2^-$, which decomposed on being heated. They stated that the decomposition temperature for this salt was 49° and that the highly colored triarylmethyl formates are stable at room temperature in the absence of light and moisture, since the carbinol could be completely recovered by hydrolysis of the formate solutions which had stood for several months in the dark. Again, a hydride shift is a plausible route for such a reaction, but it seemed unlikely that the reaction should proceed at a reasonable rate at 49° but not at all at room temperature unless the reaction was reversible. Since the forward reaction in equation [2] is highly favored energetically, the latter possibility did not seem reasonable. Thus the conversion of triphenyl carbinol to triphenylmethane by formic acid seemed a worth-while reaction to investigate, since if the mechanism of Bowden *et al.* involving salt decomposition beginning at a certain temperature was not confirmed, it seemed likely that the reaction was a bimolecular one in solution between $(\text{C}_6\text{H}_5)_3\text{C}^+$ and HCO_2^- , in which case kinetic and other evidence for a hydride shift might be readily obtained.

As this investigation was beginning, there appeared a paper by Bartlett and McCollum in which was reported a thorough investigation of the reduction of carbonium ions in acid solution by alcohols (2). They obtained kinetic evidence which indicated that alcohols in concentrated sulphuric acid can effect the reduction of carbonium ions via a hydride shift,



They measured the deuterium isotope effect for this reaction and showed that reduction of triphenyl carbinol by isopropyl alcohol labelled with deuterium at the α -position gave a ratio, $k_{\text{H}}/k_{\text{D}}$, of either 2.58 or 1.84, depending on the method used. Their system was complicated by the partial conversion of the alcohol to its conjugate acid, but their evidence is convincing enough to establish the hydride shift from neutral alcohol molecule to carbonium ion as the mechanism for the reaction.

EXPERIMENTAL

Reagents

Triphenyl carbinol was crystallized repeatedly from benzene until the mother liquors were colorless. The melting point was $163.5\text{--}164^\circ$ (uncorr.). Stock solutions of the carbinol in reagent grade acetone were made up ranging in concentration from 0.16 *M* to 0.0042 *M*. These solutions were stable over the course of several months.

Formic acid (2 l. of 90%) was twice distilled under reduced pressure and 800 ml. of the middle cut was taken for use as a stock solution. Titration of an aliquot with standard base showed it to be 94.4% formic acid by weight. Anhydrous formic acid

was prepared by shaking 98% commercial formic acid (1 l.) with boron trioxide for 2 days followed by distillation. Three hundred milliliters of the middle cut, m.p. 7.4° , was purified by a simplified but effective version of zone freezing. The bottle of formic acid was immersed in ice water for several hours and when crystallization was well advanced the supernatant liquid was decanted. After two of these operations the m.p. of the residue, about 140 ml., was found to be 8.4° (literature, 8.40° (18)). Titration gave the formic acid content as 99.9%.

Formic-d Acid

Oxalic acid dihydrate (126 g., 1 mole) was heated to about 60° under vacuum using an electric mantle. After dehydration was complete, 75 ml. of 99% D_2O was added and the stoppered flask, complete with mantle, was shaken for 4 days at about 40° . The liquid and water of crystallization were removed as before and 75 ml. of 99.8% D_2O used for a second equilibration. After a third equilibration with 75 ml. of 99.8% D_2O only the excess water was removed from the crystals. This was accomplished by pumping off the water without any heating followed by letting the system sit in equilibrium for a day. That is, the ice collected in the trap was allowed to melt and come to equilibrium with the oxalic acid dihydrate. This is important, since removal of any of the D_2O of crystallization will give a hygroscopic material which will pick up H_2O in subsequent operations.

A sample of glycerol- d_3 was prepared by twice equilibrating 7 ml. of glycerol with 8 ml. of 99.8% D_2O followed in each case by dehydration under vacuum.

The oxalic acid was added in 5 g. portions to the glycerol in a distilling flask heated on a wax bath. The flask was equipped with a long vertical tube with stopper through which the solid could be added. The bath temperature was maintained so that after each addition of acid, distillation took place with the temperature of the vapor rising to $100-102^{\circ}$. After a few minutes distillation ceased and the temperature fell, whereupon more oxalic acid was added. After all the acid had been added, 5 ml. and 3 ml. samples, respectively, of 99.8% D_2O were added and distillation completed as before. Total volume of aqueous deuterio-formic acid obtained was 76 ml., which was analyzed by titration and found to contain 0.0103 equivalents per ml. (78% yield).

The formic acid solution was added with stirring to a solution of lead acetate (155 g.) in 95 ml. of hot water and the resulting solution was chilled in ice water. The precipitate of lead formate was filtered, washed with cold water, and thoroughly dried. Dry hydrogen sulphide gas was led through the solid lead formate while the system was being heated, so that gentle reflux occurred as soon as liquid was liberated by the reaction. After about 4 hours the mixture was subjected to distillation and yielded 24 g. of colorless distillate (51% yield of DCO_2H based on oxalic acid). Redistillation gave 20 g. of product boiling at $30-31^{\circ}$ at 55 mm. and freezing at 8.2° . (The freezing point of anhydrous HCO_2H is 8.4° .) Titration of an aliquot of the material required 4.23 ml. of standard base, whereas titration of an identical volume of anhydrous HCO_2H required 4.25 ml. of the base. Since the molar volumes of H_2O and D_2O are very close, 18.066 and 18.080 respectively, it is assumed that the molar volumes of HCO_2H and DCO_2H will be virtually identical. On this basis the water content of the formic- d acid is about 0.6%. The isotopic purity of the DCO_2H was shown to be greater than 99% by an examination of its nuclear magnetic resonance spectrum.

Isolation of Reaction Products

(a) *Triphenylmethane*.—Triphenyl carbinol (0.4 g.) was added to 20 ml. of 94.4%

formic acid in a glass stoppered Erlenmeyer flask which was then wrapped in black tape and shaken for 2 weeks on a mechanical agitator. At the end of this period the solution was a very pale yellow. Filtration yielded 0.33 g. of white crystals, m.p. 92.5–94.0. They gave no color with concentrated sulphuric acid and when mixed with an authentic sample of triphenylmethane gave no depression of the melting point. A similar experiment with anhydrous formic acid gave the same results.

(b) *Triphenylmethane-d*.—A similar experiment to that described above was conducted with 0.3 g. of triphenyl carbinol and 3 ml. of formic-*d* acid, except that the mixture was kept at a temperature of 35–40° during the course of the shaking by means of a heating mantle. The product obtained (yield 0.26 g.) melted at 92.5–93.5°.

Kinetic Experiments

Rate measurements were made by adding 0.1 ml. of a solution of triphenyl carbinol in acetone of appropriate concentration to 10 ml. of formic acid in a volumetric flask immersed in a constant temperature bath controlled to $\pm 0.02^\circ$. The constant amount of acetone present in all the runs appeared to have little if any effect on the rate apart from a solvent effect. That is, the equilibrium constant governing the ionization of the carbinol and the rate constant governing the reaction rate were undoubtedly altered by the presence of 1% acetone in the system, but the acetone did not appear to take part chemically in the reaction. Using twice as much acetone altered the rate of disappearance of color slightly, presumably by a solvent effect.

The rate of disappearance of triphenyl carbinol was measured by following the drop in the absorption spectrum at 431 m μ , where the carbonium ion absorbs strongly, $\log \epsilon = 4.60$ (8). A Beckman model DU spectrophotometer was used for this purpose. In some experiments a small amount of solution was poured at intervals from the volumetric flask into an absorption cell and the light absorption measured. In other cases the reaction mixture was kept in a ground-glass stoppered absorption cell in the cell compartment of the spectrophotometer. The temperature was controlled by means of thermospacers and temperature fluctuations in the system were very small. Both of these methods gave essentially the same results when applied to the same reaction system.

RESULTS AND DISCUSSION

Ionization of Triphenyl Carbinol in Formic Acid

Triphenyl carbinol ionizes according to the following scheme in strong acids:



Quantitative correlations between extent of ionization of bases of this kind and acid strength of solvent have been made by Gold and Hawes (12) and by Deno, Jaruzelski, and Schriesheim (8) for sulphuric acid as solvent in terms of acidity functions, J_0 and C_0 . Since information on the extent of ionization of triphenyl carbinol in formic acid was required in this work, a study of the effect of a change in concentration of water in formic acid on the ionization of carbinol was undertaken. Fig. 1 shows percentage ionization plotted against percentage formic acid and shows that triphenyl carbinol is essentially completely ionized in solutions of formic acid of strength greater than 99.3%. A thorough study of the relation between the acidity functions, J_0 and C_0 , and extent of ionization of triaryl carbinols in formic acid solutions has been begun and will be reported later.

Evans, Price, and Thomas (10) have recently reported the results of an investigation

of the ionization of, among other things, triphenylmethyl chloride, $(C_6H_5)_3CCl$, in formic acid and they conclude that the ionization produces chiefly ion pairs, since the concentration of the $(C_6H_5)_3C^+$ ion, measured spectroscopically, increased linearly as the concentration of $(C_6H_5)_3CCl$ was raised. Dissociation should produce the usual dependence of ion concentration on the square root of the concentration of un-ionized triphenylmethyl chloride. The formic acid which they used was reported to be 98–100%, but the concentration was not determined by analysis and the acid was undoubtedly wet. Since triphenylmethyl chloride hydrolyzes readily to the carbinol, it is entirely possible that the apparent ionization of triphenylmethyl chloride in wet formic acid is determined by the equilibrium shown in equation [1]. The concentration of triphenylmethyl carbonium ion which is amenable to spectrophotometric measurement is of the

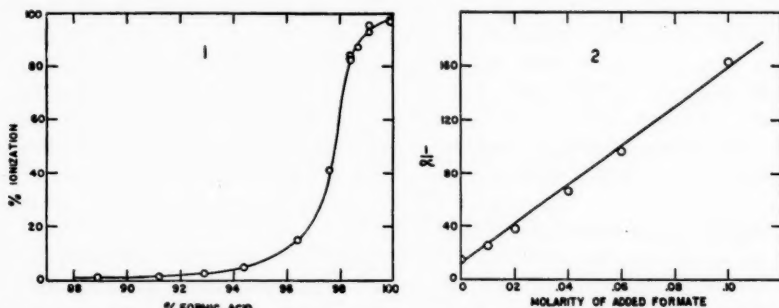


FIG. 1. Effect of a change in formic acid concentration on the ionization of triphenyl carbinol; $T = 25^\circ$.
FIG. 2. Variation of the function $1/\alpha$ with the concentration of added sodium formate; $T = 25^\circ$.

order of $10^{-5} M$. The concentrations of the other components of the equilibrium system, H_2O , HCO_2^- , and HCO_2H , are all much larger than this in wet formic acid. The concentration of formate ion in anhydrous formic acid has been estimated to be $10^{-3} M$ (15) and is probably much larger in wet formic acid. (Some evidence for this statement is discussed later.) Increasing the total concentration of triphenylmethyl species in solution, therefore, should result in a linear increase in the concentration of the carbonium ion whether or not ion pairs are formed.

Adding sodium formate to the solvent decreases the extent of ionization as would be expected if the equilibrium was controlled by equation [1]. When $1/\alpha$, with α defined here as being equal to $[R_3C^+]/[R_3COH]$, or more precisely $[R_3C^+]/[\text{total } R_3COH \text{ added} - R_3C^+]$, where $R = C_6H_5$, is plotted against the concentration of added formate ion, at constant ionic strength, an almost linear relation results (Fig. 2). There is a slight deviation from linearity, caused possibly by a specific salt effect, but it can be seen that the ionization, not merely dissociation of ion pairs is repressed by added formate ion. Adding sodium chloride caused a slight increase in the extent of ionization, presumably by a normal salt effect.

Rate Measurements

The disappearance of the triphenylmethyl carbonium ion was found in all experiments to be first order. A typical rate plot is shown in Fig. 3. The reaction apparently goes to completion at room temperature in the dilute solutions used for the kinetic work. Since Bowden *et al.* had stated that the triphenyl carbinol could be recovered unchanged after several months in the absence of light and moisture at room temperature, experiments were performed using much larger amounts of carbinol than would dissolve in the formic

acid. If these mixtures were allowed to sit without agitation for a month at room temperature, only partial conversion to triphenylmethane was observed, using 99.9% formic acid. If the mixtures were agitated mechanically, however, an almost quantitative yield of triphenylmethane was obtained.

Most of the kinetic work was done with either 94.4% formic acid, where ionization was small, or anhydrous formic acid (99.9%), where ionization was almost complete.

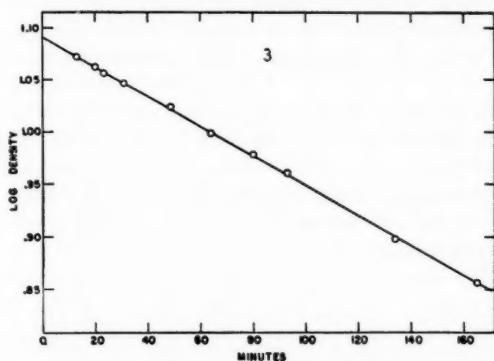


FIG. 3. Rate of disappearance of triphenylmethyl carbonium ion in 94.4% formic acid; $T = 25^\circ$.

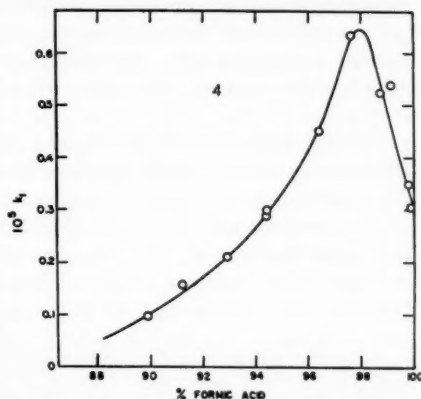


FIG. 4. Variation of first-order rate constant for disappearance of triphenylmethyl carbonium ion with concentration of formic acid; $T = 25^\circ$.

Assuming the mechanism shown in equations [1] and [2] and assuming that the only un-ionized triphenylmethyl species is the carbinol, the following rate expression can be derived:

$$\begin{aligned} -d\{[R_3C^+] + [R_3COH]\}/dt &= k_2[R_3C^+][HCO_2^-], \\ -d\{[R_3C^+](1 + 1/\alpha)\}/dt &= k_2[R_3C^+][HCO_2^-], \\ -\log [R_3C^+] &= \{k_2/2.30(1 + 1/\alpha)\}[HCO_2^-]t. \end{aligned}$$

Since the formate ion concentration is constant, first-order kinetics result and

$$k_1 = k_2\alpha[HCO_2^-]/(1 + \alpha). \quad [3]$$

It follows from the equilibrium constant expression for equation [1] that α varies inversely as the formate ion concentration and, hence, from equation [3] that solutions which differ only in the amount of added sodium formate should give identical values of $k_1(1 + \alpha)$. The results shown in Table I show that this is, indeed, the case in 94.4% formic acid.

TABLE I
EFFECT OF ADDED SODIUM FORMATE ON RATE OF REDUCTION OF
TRIPHENYL CARBINOL AT 25.1° IN 94.4% FORMIC ACID

Added $NaHCO_2^*$ (moles liter $^{-1}$)	$k_1 \times 10^6$ (sec. $^{-1}$)	$k_1(1 + \alpha) \times 10^6$ (sec. $^{-1}$)
—	0.268	0.285
0.01	0.278	0.288
0.02	0.286	0.293
0.04	0.288	0.292
0.06	0.282	0.285
0.10	0.278	0.280

*Ionic strength brought to 0.10 with added sodium chloride.

The effect of a change in the concentration of formic acid on the rate of reaction is shown in Fig. 4. The rate parameter plotted against concentration is the first-order rate constant, k_1 , and it is seen that this value rises as the formic acid concentration rises and then falls again near 100% acid. Since the solvent itself is being changed, any discussion of the effect of changing formic acid concentration on the rate is open to criticism. Nevertheless, one can draw some conclusions about the processes occurring in the reaction. It should be pointed out that k_1 is a function of, first α , which can be measured; second, formate ion concentration, values of which are not known except for the anhydrous acid; and third, the previously referred to specific solvent effect on k_2 . That the peak of the curve in Fig. 4 is not significant can be seen if one examines, instead of k_1 , the function $k_1(1+\alpha)/\alpha$, which is equal to $k_2[\text{HCO}_2^-]$. Values of this function are listed in Table II. The cause of the large decrease in this function as the solution approaches 100% formic acid is mainly a decrease in formate ion concentration, with the solvent effect being of secondary importance. This can be seen by a comparison of the rates for solutions containing added sodium formate. Table III shows that when the added sodium formate concentration is 0.1 M the second-order rate constant, k_2 , does not change markedly between 94.4 and 99.9% acid. These values of k_2 were calculated assuming that all the formate ion arose from the added salt; in 94.4% formic acid there may be a significant contribution of formate ion from the solvent. Since there is a 20-fold increase in the parameter $k_2[\text{HCO}_2^-]$ going from 99.9% to 94.4% acid *without* added sodium formate, and only a $1\frac{1}{2}$ -fold increase *with* added sodium formate, one can conclude that there is, very roughly, a 13-fold increase in the formate ion concentration. Hammett and Deyrup (15) determined the formate ion concentration in anhydrous formic acid to be 0.001 M , and Hammett and Dietz (16) concluded that water is a

TABLE II
EFFECT OF A CHANGE IN SOLVENT COMPOSITION ON THE FUNCTION $k_2[\text{HCO}_2^-]$, $T = 25.1^\circ$

% Formic acid	α	$k_1 \times 10^3$ (sec. ⁻¹)	$k_2[\text{HCO}_2^-] \times 10^3$ (sec. ⁻¹)
88.9	0.0058	0.098	17.1
91.2	0.0132	0.159	12.2
92.9	0.0246	0.210	8.75
94.4	0.0484	0.291	6.30
96.4	0.177	0.450	3.00
97.6	0.690	0.636	1.56
98.4	4.55	0.730	0.89
98.7	6.58	0.525	0.61
99.1	11.5	0.540	0.59
99.8	27.6	0.350	0.36
99.9	39.0	0.303	0.31

*Calculated using equation [3].

TABLE III
EFFECT OF A CHANGE IN SOLVENT COMPOSITION ON THE FUNCTION k_2 , IN SOLUTIONS CONTAINING 0.1 M ADDED SODIUM FORMATE, $T = 25.1^\circ$

% Formic acid	α	$k_1 \times 10^3$ (sec. ⁻¹)	$k_2 \times 10^3$ (l. mole ⁻¹ sec. ⁻¹)
94.4	0.0059	0.278	4.75
98.4	0.0788	2.46	3.36
99.9	0.250	6.02	3.10

*Calculated assuming total formate ion concentration was 0.1 M , using the equation $k_2 = k_1(1+\alpha)/\alpha[\text{HCO}_2^-]$.

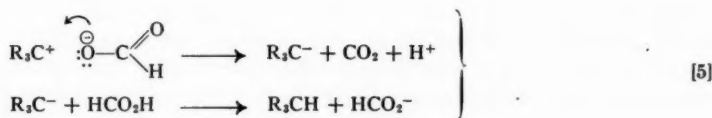
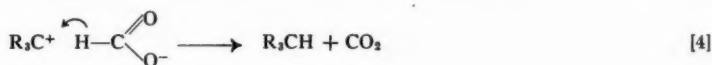
weak base in formic acid. The results reported here confirm the view that water is a weak base in this system, since the molarity of water in 94.4% acid is 3.1, a value very much larger than the concentration of formate ion one can estimate from the above considerations.

Tables II and III show that in 99.9% formic acid addition of sodium formate causes a considerable increase in the value of k_1 , unlike the situation in 94.4% formic acid where the rate is almost independent of added formate. This is because in the 99.9% acid the large increase in the formate ion concentration is not cancelled out by a corresponding decrease in the concentration of the carbonium ion. The catalytic effect of added sodium formate referred to by Guyot and Kovache therefore applies to more concentrated formic acid solutions only.

If one uses Hammett and Deyrup's value of 10^{-3} for the molarity of formate ion in anhydrous formic acid (15), a value can be calculated for k_2 from the data in Table II. Since $k_2 [\text{HCO}_2^-] = 0.31 \times 10^{-5} \text{ sec.}^{-1}$, then $k_2 = 3.1 \times 10^{-3} \text{ l. mole}^{-1} \text{ sec.}^{-1}$. The exact agreement of this value with that appearing in Table III for 99.9% acid containing added formate ion is doubtless fortuitous since the two solutions are at different ionic strengths. The agreement is, nevertheless, gratifying.

Use of Deuterated Formic Acid

One can assume that the reduction of the carbonium ion by formate ion occurs by a two-electron step since triphenylmethane is formed in almost quantitative yield. Two one-electron transitions, unless the second was very fast, would be expected to produce triphenylmethyl peroxide, since the intermediate triphenylmethyl radicals are known to react extremely rapidly with oxygen. There still remains the problem of whether or not the process involves a hydride transfer, equation [4], or a two-electron transfer followed by addition of a proton from the solvent to the carbanion thus formed, equation [5].



A distinction can be made between routes [4] and [5] by use of formic-*d* acid (DCO_2H) as solvent. This material was synthesized in good yield by the glycerol catalyzed decomposition of oxalic acid- d_2 (17). The latter was prepared by equilibrating oxalic acid with heavy water. The ionizable deuteron was then replaced by a proton to give DCO_2H . The isotopic purity was shown to be very high by an examination of the nuclear magnetic resonance (NMR) spectrum. Fig. 5 shows the spectrum of anhydrous formic acid and formic-*d* acid. The almost complete absence of a band for the $\text{H}-\text{C}$ proton indicates an isotopic purity of 99% or more. Fig. 6 shows the spectrum of triphenylmethane and the product obtained using formic-*d* acid as the reductant. The precision of analysis here is less than in the case of formic acid, because the peak for the side-chain hydrogen is small compared to that of the aromatic hydrogen and to the background noise. Identical concentrations and identical sample tubes were used to obtain the two spectra shown in Fig. 6. An estimate of the areas under the curves indicates less than 3% $(\text{C}_6\text{H}_5)_3\text{CH}$

or greater than 97% $(\text{C}_6\text{H}_5)_3\text{CD}$ in the product. The mechanism of the reduction is therefore given by equation [4] and not by equation [5].

Since the carbon-deuterium bond in DCO_2H is broken when the latter is used as reductant, an isotope effect is to be expected. The formic-*d* acid used in this work apparently

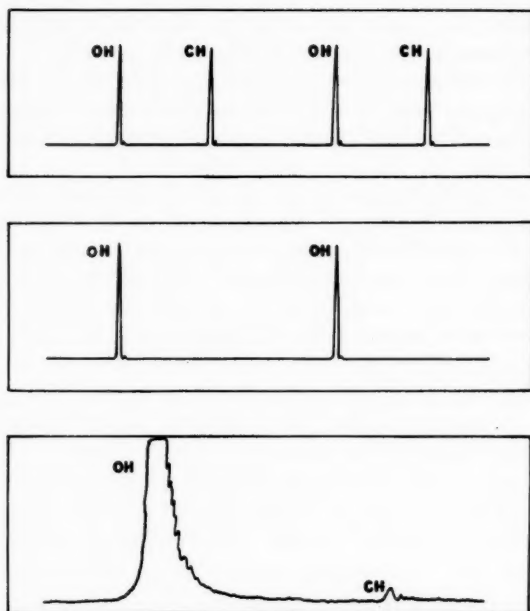


FIG. 5. NMR spectra of HCO_2H (top), DCO_2H (middle), DCO_2H (bottom) with increased amplification showing small residual C—H peak.

contained a very small amount of impurity since an initial, very rapid, disappearance of triphenylmethyl carbonium ion was observed when the triphenyl carbinol was dissolved in the formic-*d* acid solvent. After this initial fast reaction, which consumed over half of the carbinol, the reaction slowed and normal first-order kinetics were obtained

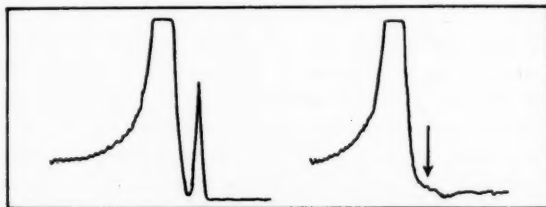


FIG. 6. NMR spectrum of $(\text{C}_6\text{H}_5)_3\text{CH}$ (left) and $(\text{C}_6\text{H}_5)_3\text{CD}$ (right). The arrow shows the position of the side-chain C—H peak in the latter.

for the balance of the reaction. Peroxides are known to react rapidly with triphenylmethyl carbonium ion (2) and may be responsible for the initial reaction. From the amount of carbinol consumed in this way, one can estimate the concentration of the reactive impurity to be of the order of $10^{-5} M$. There was no indication of the fast initial reaction

when 91.5% formic-*d* acid (91.5% DCO_2H , 8.5% H_2O) was used, since the amount of carbinol used is very much larger and any effect of this sort would be masked. At 32.4° the first-order rate constant in anhydrous formic-*d* acid, obtained after the initial rapid reaction had ceased, is 0.16 compared to a value of 0.88 for anhydrous formic acid. The isotope effect, $k_{\text{H}}/k_{\text{D}} = 0.88/0.18 = 4.9$, must be considered to be very rough because of the uncertainty as to the amount of water in the formic-*d* acid, which can affect the value of k_1 very considerably. In more dilute solution uncertainty as to the exact amount of water becomes less important. In formic-*d* acid containing about 8.5% water an isotope effect, $k_{\text{H}}/k_{\text{D}} = 0.163/0.065 = 2.5$, was obtained. This is considerably different from the value obtained under anhydrous conditions and is probably the more reliable. Since the solvent formic acid molecules are all deuterated, some solvent effect may exist. It is clear, at any rate, that the carbon-deuterium bond is broken in the rate controlling step.

Thermodynamic Data

The ionization of triphenyl carbinol in 94.4% formic acid increases, as expected, with increasing temperature. A plot of $\log \alpha$ against $1/T$ shows a satisfactory linear relation and gives a heat of reaction of $\Delta H = +5.2$ kcal. for the ionization reaction. A similar series of determinations for solutions containing added 0.1 *M* sodium formate gave an almost identical value for the heat of reaction.

Fig. 7 shows a plot of $\log k_1/T$ against $1/T$ for 94.4% formic acid, both for solutions with added sodium formate and those without. The rate constants are listed in Table

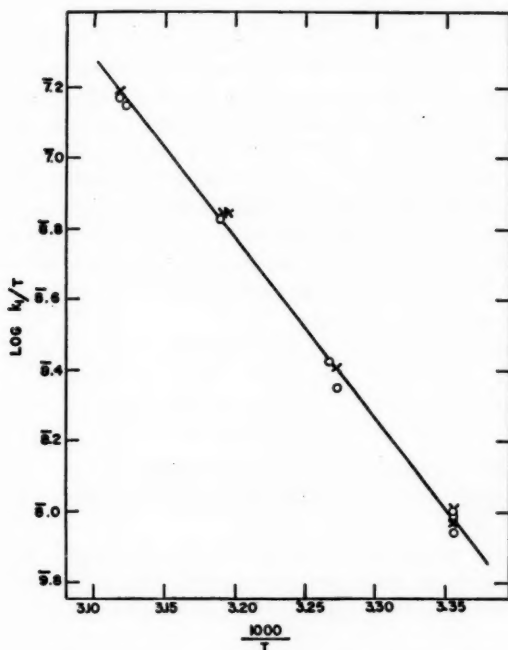


FIG. 7. Effect of temperature change on the rate of disappearance of triphenylmethyl carbonium ion. X—With added 0.1 *M* sodium formate. O—Without added 1 *M* sodium formate.

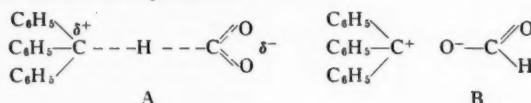
IV. The slope gives an apparent heat of activation of $\Delta H^\ddagger = 23.3$ kcal. This is a composite heat effect which must be corrected for the heat of the preliminary ionization step if significant values of the activation parameters are to be obtained for the rate controlling step, whose rate constant is k_2 . Since $k_1 = k_2\alpha[\text{HCO}_2^-]/(1+\alpha)$, the function can be split and the temperature effect on the term $\alpha[\text{HCO}_2^-]/(1+\alpha)$ determined sepa-

TABLE IV
RATE CONSTANT, k_1 , AND EQUILIBRIUM CONSTANT, α , AS A FUNCTION OF TEMPERATURE

94.4% Formic acid			94.4% Formic acid containing 0.1 M sodium formate		
T	α	$k_1 \times 10^5$ (sec. ⁻¹)	T	α	$k_1 \times 10^5$ (sec. ⁻¹)
25.1	0.0498	0.29	25.1	0.0059	0.31
25.1	0.0471	0.30	25.1	0.0061	0.28
25.1	0.0490	0.26	32.5	0.0077	0.80
32.4	0.0605	0.68	39.9	0.0090	2.23
32.9	—	0.82	40.0	0.0092	2.23
40.4	0.0753	2.10	47.7	0.0132	5.00
47.1	0.0929	4.52			
47.7	0.0905	4.80			

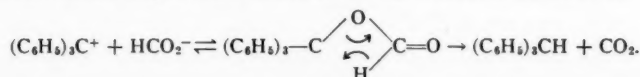
rately for solutions containing added sodium formate. Such a correction gave a heat of activation for the rate controlling step of $\Delta H^\ddagger = 18.3$ kcal. Equation [3] was used to calculate values of k_2 and the entropy of activation was calculated by the method of Cagle and Eyring (6), giving $\Delta S^\ddagger = -7.5$ e.u.

A negative entropy of activation, although small, is at first inspection surprising if the postulated reaction between two oppositely charged ions is correct. A gain in entropy should result from the freeing of the solvated solvent molecules as the transition state is formed. Reactions of this type in aqueous solution have entropies of activation of the order of +10 to +20 e.u. (11). Two factors probably account for the negative ΔS^\ddagger in this reaction. First, formic acid, although a good ionizing solvent, because of its high dielectric constant is believed to be a poorer solvating species than water (18). Thus the ions on forming the neutral transition state have fewer solvent molecules to set free than if the reaction occurred in aqueous solution. Second, in order for reaction to occur, the aldehyde hydrogen atom of the formate ion must approach the central carbon atom of the carbonium ion as in A. The normal electrostatic attraction of the two ions makes the configuration B much more probable.



One could consider the reaction occurring by formation of the ion pair B, followed by rotation of the formate ion to give the transition state A, with a corresponding decrease in entropy.

A final possible route for the reduction should be considered, which would give the same over-all kinetics and the same isotopic results. This is the formation of triphenyl methyl formate which might then undergo an $\text{S}_{\text{N}}1$ reaction, as follows:



The negative entropy of activation would be in agreement with such a mechanism, but it seems an unlikely route for the following reason. Cram (7) has pointed out that reactions which had been regarded as being of the cyclic, S_Ni type proceed more readily in solvents which support ion formation, and his postulate that S_Ni reactions occur through ion pair formation has been supported by other work (3, 20, 21). In view of the fact that the transition state would be highly crowded because of the phenyl groups, and since formate ions and triphenylmethyl carbonium ions are already present in the system, it seems most unlikely that the reaction proceeds by way of ester rearrangement.

ACKNOWLEDGMENT

The author is grateful to the National Research Council for a 1956 Summer Research Associateship under which this work was performed, and also to Dr. C. Reid for the nuclear magnetic resonance spectra referred to herein.

REFERENCES

1. ANGYAL, S. J., PENMAN, D. R., and WARWICK, G. P. *J. Chem. Soc.* 1742 (1953).
2. BARTLETT, P. D. and McCOLLUM, J. D. *J. Am. Chem. Soc.* **78**, 1441 (1956).
3. BOOZER, C. E. and LEWIS, E. S. *J. Am. Chem. Soc.* **75**, 3182 (1953).
4. BOWDEN, S. T., CLARKE, D. L., and HARRIS, W. E. *J. Chem. Soc.* 874 (1940).
5. BOWDEN, S. T. and WATKINS, T. F. *J. Chem. Soc.* 1333 (1940).
6. CAGLE, F. W. and EYRING, H. *J. Am. Chem. Soc.* **73**, 5628 (1951).
7. CRAM, D. J. *J. Am. Chem. Soc.* **75**, 332 (1953).
8. DENO, N. C., JARUZELSKI, J. J., and SCHRIESHEIM, A. *J. Org. Chem.* **19**, 155 (1954).
9. DOERING, W. v. E. and ASCHNER, T. C. *J. Am. Chem. Soc.* **75**, 393 (1953).
10. EVANS, A. G., PRICE, A., and THOMAS, J. H. *Trans. Faraday Soc.* **51**, 481 (1955).
11. FROST, A. A. and PEARSON, R. G. *Kinetics and mechanism*. John Wiley & Sons, Inc., New York, 1953, p. 131.
12. GOLD, V. and HAWES, B. W. V. *J. Chem. Soc.* 2102 (1951).
13. GUYOT, A. and KOVACHE, A. *Compt. rend.* **155**, 838 (1912).
14. HAMMETT, L. P. *Physical organic chemistry*. McGraw-Hill Book Company, Inc., New York, 1940, p. 350.
15. HAMMETT, L. P. and DEYRUP, A. J. *J. Am. Chem. Soc.* **54**, 4239 (1932).
16. HAMMETT, L. P. and DIETZ, N. *J. Am. Chem. Soc.* **52**, 4795 (1930).
17. KIPPING, F. S. and KIPPING, F. B. *Organic chemistry*. W. & R. Chambers, Ltd., London, 1931, p. 147.
18. PINFOLD, T. A. and SEBBA, F. *J. Am. Chem. Soc.* **78**, 5193 (1956).
19. STEWART, R. *J. Am. Chem. Soc.* (In press).
20. STREITWIESER, A. and SCHAEFFER, W. D. *J. Am. Chem. Soc.* **79**, 379 (1957).
21. WIBERG, K. B. and SHRYNE, T. W. *J. Am. Chem. Soc.* **77**, 2774 (1955).
22. WOODWARD, R. B., WENDLER, U. L., and BRUTSCHY, F. J. *J. Am. Chem. Soc.* **67**, 1425 (1945).

FREE RADICALS BY MASS SPECTROMETRY

XIII. THE MERCURY PHOTOSENSITIZED DECOMPOSITION OF ALLENE AND BUTADIENE: THE C_3H_3 RADICAL¹

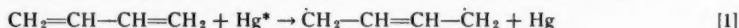
J. COLLIN² AND F. P. LOSSING

ABSTRACT

The $Hg(^3P_1)$ photosensitized decomposition of allene leads to the formation of a C_3H_3 radical. The reaction of this radical with added methyl radicals shows it to have the propargyl ($CH_2-C\equiv CH$) structure rather than the alternative allenyl ($CH_2=C=CH$) structure. The dissociation of 1,2-butadiene proceeds by two modes, one to give $H_2 + C_4H_4$, and the other a split into CH_3 and C_3H_3 radicals. The dissociation of 1,3-butadiene leads to the same final products, a shift of a hydrogen atom being required for the split into free radicals. No evidence was found for a dissociation of 1,3-butadiene into two vinyl radicals. Considerable polymer formation occurred with all three compounds.

INTRODUCTION

The reaction of butadiene, presumably 1,3-butadiene, with $Hg(^3P_1)$ atoms was found by Gee (6) to give mainly an insoluble non-volatile polymer which was deposited on the walls of the reactor. Other products identified were hydrogen and butane. A dimer, assumed to be of cyclic form, was also produced. He concluded that hydrogen played no part in the polymerization but hydrogenated the butadiene to form butane. The primary steps of the mercury photosensitized reaction were postulated to be:



or alternatively



This reaction of butadiene was later examined by Gunning and Steacie (7), who found the pressure-time curve in static runs to have an induction period, followed by a period of linear pressure decrease. The slope of the latter increased with increasing pressure, except below 2 mm. where quenching was probably incomplete. In the static runs the reaction products, aside from polymer formed on the walls, were hydrogen, ethane, an acetylenic compound probably C_4H_4 , and a compound with a boiling point of about 95° C. Analysis of the latter for C and H gave a ratio corresponding to $(C_2H_3)_n$, the same ratio as in butadiene, and it was concluded that the compound was a dimer of butadiene. The yield of dimer was found to be 0.6 mole per mole of butadiene reacted. This amount is stoichiometrically too large, and it is possible that the fraction isolated contained dissolved butadiene. A number of runs were made in a flow system, in which the yields of H_2 and C_4H_4 were considerably higher than in static runs. This suggested that H_2 and C_4H_4 were consumed in the later stages of the reaction. In the static runs the induction period could be prolonged by pumping off the hydrogen produced and eliminated by adding hydrogen initially to the butadiene. The period of linear pressure decrease was consequently considered to be an H-atom initiated polymerization. The following primary steps were suggested:



¹Manuscript received April 12, 1957.

Contribution from the Division of Pure Chemistry, National Research Council, Ottawa, Canada. Issued as N.R.C. No. 4391.

²National Research Council of Canada Postdoctorate Fellow 1956-57.

The rate of reaction was found to be proportional to the light intensity and the quantum yield was approximately unity, in agreement with Gee.

The reaction at pressures above 50 mm. was examined by Volman (15), who found the principal product to be a light yellow oil. Some solid white polymer was produced, and also a non-condensable gas, presumably hydrogen. The reaction was also investigated at pressures of about 2.5 mm. using a flow system and metallic mirrors. Volman found that antimony mirrors were removed, the half-life of the radicals being about the same as for the radicals produced from acetone under the same conditions. Experiments with a guard mirror of lead showed no indication of the presence of hydrogen atoms. He therefore suggested that at low pressures the polymerization is induced by vinyl radicals produced in a primary step rather than by H atoms, and proposed the following modes of decomposition:



followed by



Thus reaction [7] would predominate at low pressures, and reaction [8] at high pressures. The unimolecular decomposition (reaction [4]) was considered not to occur.

Steacie (13) has suggested that the failure to detect H atoms in the above experiments was not conclusive in view of the very rapid rate of the addition reaction:



and that a polymerization initiated by vinyl radicals would not explain the induction period.

From the work discussed above, it would appear that of the excited 1,3-butadiene molecules which dissociate, some do so by loss of H_2 to form C_4H_4 , and others form free radicals of unknown composition. The mercury photosensitized decompositions of the related compounds allene and 1,2-butadiene do not appear to have been studied previously. It was thought that an examination of these reactions using a mass spectrometer adapted for free radical studies might provide more direct evidence as to the nature of the primary dissociation steps. This technique has been useful in determining modes of decomposition in the mercury photosensitized reactions of C_2 - C_4 olefins (9) and of acetone and acetaldehyde (8). The low pressures used in this method are advantageous in that deactivation and polymerization steps are less favored, and the increased lifetime available to excited molecules favors dissociation processes.

EXPERIMENTAL

The arrangement of reaction cell, mercury resonance lamp, and mass spectrometer has been described in previous publications (8, 9). The reactant, at a partial pressure of a few microns, was carried in a stream of helium at 10 mm. pressure over a surface of mercury in a saturator at 55°C ., and through an illuminated zone. From a point 1.5 cm. downstream from the illuminated zone, a small fraction of the gas stream was sampled directly into the ionization chamber of the mass spectrometer. The operation of the reactor and the method of measurement of the concentrations of free methyl radicals and stable species have been described in detail in earlier papers of this series (8, 9). The sensitivity of the instrument to C_3H_3 radicals was not measured.

In the reaction of the butadienes, considerable difficulty was caused by the rapid formation of polymeric material on the walls of the reactor and the consequent decrease in illumination during the time taken to record the spectra. In order to obtain the relative intensity of illumination for a given experiment, the amount of decomposition of ethylene in the reactor under the same conditions was used as a standard of comparison. It was found that in a "non-clean" reactor, when the length of the illuminated zone was reduced to one-half by using the movable shutter, less than half as much ethylene was decomposed. This meant that the deposition of polymer was unequal over the length of the reactor, a proportionally greater amount being deposited at the downstream end. A calibration with ethylene was consequently performed each time the shutter was moved. From these data, an effective "length" of illuminated zone was obtained for each position of the shutter. After a considerable amount of polymer had been deposited, a situation then arose in which equal "lengths" were not quite equal intervals of time. The curves for formation of combination products in Figs. 2 and 3 are therefore slightly distorted.

At the flow rates used, the time of residence in the illuminated zone was 0.34 millisecond per cm. at 55° C.

Materials

A sample of allene was obtained through the courtesy of Dr. L. C. Leitch of these laboratories. The mass spectrum showed the presence of a few per cent of propylene. The effect of this on the course of the reaction was considered to be negligible. Samples of 1,2-butadiene and 1,3-butadiene were Phillips Research Grade gases.

RESULTS AND DISCUSSION

Allene

Three products only were produced by the mercury photosensitized decomposition of allene: hydrogen, a radical of mass 39 (C_3H_3), and a substance of mass 78, evidently the dimer of this radical. In a contact time in which ethylene was decomposed to the extent of 40%, allene was 23% decomposed. A considerable amount of polymer was also formed. The primary step is probably the formation of an excited allene molecule,



The excited molecule then dissociates as follows:

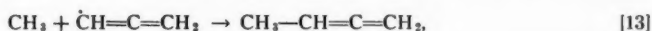


This mode of dissociation appears to be the only one, and no products corresponding to a C—C rupture were found. The spectrum of the dimer was similar to that of 1,5-hexadiyne (di-propargyl). Since the spectra of the other C_6H_6 species, 1,2,4,5-hexatetraene and 1,2-hexadiene-5-yne, were not available for comparison, the identity of the dimer could not be established.

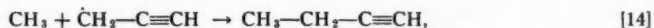
The nature of the C_3H_3 radical is of considerable interest. From the structure of allene it might at first sight be assumed that the C_3H_3 radical would necessarily have the form $H_2C=C=\dot{C}H$ (allenyl). However, an alternative structure differing in electronic configuration is also possible: $H_2C-C\equiv\dot{C}H$ (propargyl). A C_3H_3 radical, thought to be propargyl, has been detected by mass spectrometry in the thermal decomposition of propargyl iodide (2). If the two structures may in fact be regarded as resonance hybrids, the actual structure will be an intermediate one, and it is of interest to know whether the radical reacts as a propargyl or as an allenyl radical or as both. If it reacts

predominantly as one of these forms, it is then not unreasonable to conclude that the actual structure of the radical more closely approximates this form, which is consequently the more stable one.

An identification of the radical from the nature of the dimer was not possible, as mentioned above. It was possible, however, to distinguish between the two forms in the following way. If methyl radicals were to be added to the reaction mixture, the combination of these with C_3H_3 radicals would result in the formation of either 1,2-butadiene,



or 1-butyne,



depending on the structure of the C_3H_3 radical. The identification of the C_4H_6 product as 1,2-butadiene or 1-butyne could then be made on the basis of the ratio of the peaks at mass 53 and 54. A convenient way of bringing about this reaction was to allow a small concentration of mercury dimethyl to flow through the reactor with the allene-helium mixture. The mercury photosensitized decomposition of the mercury dimethyl provided a source of methyl radicals. It was found that in this way a mass 54 peak several centimeters in height could be produced. The mass 53/54 ratio obtained for this product of combination of CH_3 and C_3H_3 , together with ratios for pure samples of 1,2-butadiene and 1-butyne, is given in Table I. It is evident that the combination product is mainly,

TABLE I

Substance	Ratio 53/54
$CH_3 + C_3H_3$	0.474 ± 0.006
1-Butyne	0.478 ± 0.006
1,2-Butadiene	0.420 ± 0.006

if not entirely, 1-butyne, and consequently that the C_3H_3 radical reacts as if it had the propargyl ($\dot{C}H_2-C\equiv CH$) form. It is interesting to speculate as to why the reaction appears to proceed so exclusively by this form, although considerations of resonance suggest that the C_3H_3 radical would have a form intermediate between propargyl and allenyl. A possibility to be considered is that the activated complex resulting from the collision of CH_3 and C_3H_3 can rearrange to form the more stable product. This can be ruled out since the heat of formation of 1-butyne (39.48 kcal./mole) is slightly larger than that of 1,2-butadiene (38.77 kcal./mole) (12), although the difference is not large. The observation that only one product is formed although the heats of formation are so similar suggests that the identity of the product is already implicit in the activated complex, and consequently that the C_3H_3 radical is much more reactive at the CH_2 end. This is consistent with a configuration of C_3H_3 which is nearer to $\dot{C}H_2-C\equiv CH$ than to $CH_2=C=\dot{C}H$, if one assumes that the reactivity is associated with the position of maximum free electron density. This assumption appears to be valid since, if reaction could occur at either end of the radical regardless of the free electron distribution, both butyne and butadiene would be formed whatever the structure of C_3H_3 might be. A further possibility to be considered is that the structure is indeed intermediate between propargyl and allenyl, but the rate of reaction at the "fraction" of the free electron associated with the CH end of the radical is some 20-40 times slower than at the CH_2 end. Since it is hard to see how such a large difference in rate could arise between such similar combination processes, the interpretation given above is to be preferred.

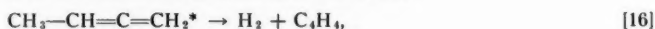
From these considerations it might be expected that the stabilization of the C_3H_3 radical by resonance is considerably less than in the allyl radical, where the resonating structures are identical in energy. The dissociation energies for the propargyl halides, as measured by electron impact (2), are 8–10 kcal./mole greater than those of the corresponding allyl halides (see, for example, Ref. 13). A study of the appearance potentials of $C_3H_3^+$ ions formed from propyne and other compounds, which is to be published shortly, indicates however that the C_3H_3-H bond is only a few kcal./mole greater than the allyl-H bond.

1,2-Butadiene

Using low energy electrons suitable for detecting free radicals, methyl radicals and a radical of mass 39 (C_3H_3) were found to be produced abundantly in the decomposition of 1,2-butadiene. Other parent molecular ions found were those of ethane, hydrogen, and mass 52, presumably C_4H_4 . A small amount of mass 40, allene or propyne, was also produced. No indication of the C_4H_5 radical could be found. A compound of mass 78 was also produced, evidently the dimer of C_3H_3 . Using 50-v. electrons, the spectrum of this dimer was seen to be similar to, but not identical with, that of 1,5-hexadiyne. The formation of considerable amounts of polymer also occurred. The first step in the reaction is probably the formation of an excited 1,2-butadiene molecule:



From the products found, two modes of decomposition can occur:



The ethane and C_6H_6 evidently arose by the dimerization reactions:



Since both CH_3 and C_3H_3 radicals were present, the combination reaction



might be expected. As discussed above in the case of allene, the combination reaction would form 1-butyne or re-form 1,2-butadiene depending on the structure of the C_3H_3 radical. In either case the decrease, on illumination, of the mass 54 peak (using 50-v. electrons) would be less than expected, particularly at the longer contact times where the combination reaction would be favored. This effect is clearly shown by curve 1 in Fig. 1. This curve was obtained by plotting the percentage decrease in the mass 54 peak (measured using 50-v. electrons) against the effective length of the illuminated zone. The percentage decrease was not proportional to the length but fell off as the length was increased. Since the ionization potential of 1-butyne (10.34 v. (4), 10.32 v. (5)) is considerably greater than that of 1,2-butadiene (9.57 v. (5)), a measurement of the mass 54 peak using electron energies between these values permitted a measurement of the amount of 1,2-butadiene without interference from 1-butyne. The relation between the height of the mass 54 peak at low electron energies and the effective length of the illuminated zone is shown by curve 2 in Fig. 1. This relation is much more nearly linear than is curve 1, showing that the curvature of the latter was caused by the formation of 1-butyne. If the curvature of 1 were caused by recombination to form 1,2-butadiene, curve 2 would of course have the same shape as curve 1. It may be concluded, therefore, that the

C_3H_3 radical, as in the case of allene, reacts as if it had the propargyl structure. The measurements at low electron energy consequently give approximately the actual percentage of decomposition of the 1,2-butadiene.

The composition of the products, excepting C_3H_3 , C_4H_6 , and C_4H_4 , at different lengths of the illuminated zone were measured using 50-v. electrons. These concentrations, together with the amount of 1,2-butadiene decomposed, are given in Table II.

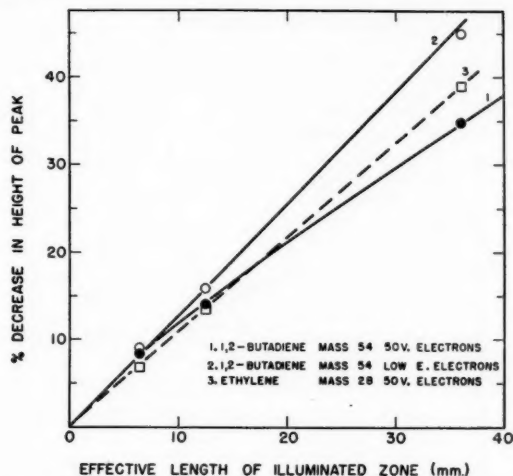
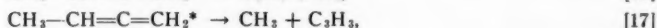
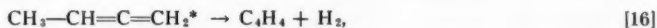


FIG. 1. The curvature of line 1, obtained using 50-v. electrons, shows that a product having a mass of 58 is formed at the longer contact times. The straightening of the line at low electron energies, line 2, shows that this product has a higher ionization potential than 1,2-butadiene. Line 3 shows the calibration of effective length using ethylene.

TABLE II
DECOMPOSITION OF 1,2-BUTADIENE

Butadiene (μ)		Effective length of zone (mm.)	Butadiene decomposed		Ethylene decomposed (%)	Products from butadiene (μ)					Yield of CH_3	Yield of H_2
Lamp off	Lamp on		μ	%		H_2	CH_3	CH_4	C_2H_6	1-Butyne		
2.34	1.29	36	1.05	45.0	39.0	0.11	0.08 ₀	0.01 ₄	0.12 ₂	0.27 ₃	0.59	0.11
2.33	1.96	12.6	0.37	15.9	13.5	0.03 ₄	0.07 ₈	0.00 ₇	0.03 ₂	0.04 ₈	0.53	0.09 ₂
2.27	2.07	6.4	0.20	9.0	6.9 ₂	0.03 ₀	0.04 ₄	0.00 ₃	0.01 ₂	0.03 ₀	0.53	0.15

The change in the composition of the products with the length of the zone can be seen by reference to Fig. 2. Owing to the large amount of polymer formed it was not possible to get a complete mass balance. The amount of C_4H_4 could not be measured, no pure samples of butatriene or vinyl acetylene being available for calibration. An estimate of the proportion of the two modes of decomposition can be made, however, on the basis of the following mechanism:



The proportion of reaction proceeding by reaction [16] can be estimated from the production of H_2 . As shown in Table II the yield of hydrogen per molecule of butadiene decomposed varies between 0.09 and 0.15. The proportion of reaction proceeding by reaction [17] can be estimated from the number of methyl radicals produced per molecule of butadiene decomposed. The total number of methyl radicals is given by the sum $[CH_3] + 2[C_2H_5] + [1\text{-butyne}] + [CH_4]$. From Table II it can be seen that the split into CH_3 and C_3H_3 accounts for 0.53–0.59 of the butadiene molecules decomposed. The remainder of the butadiene ($\sim 35\%$) presumably forms polymer.

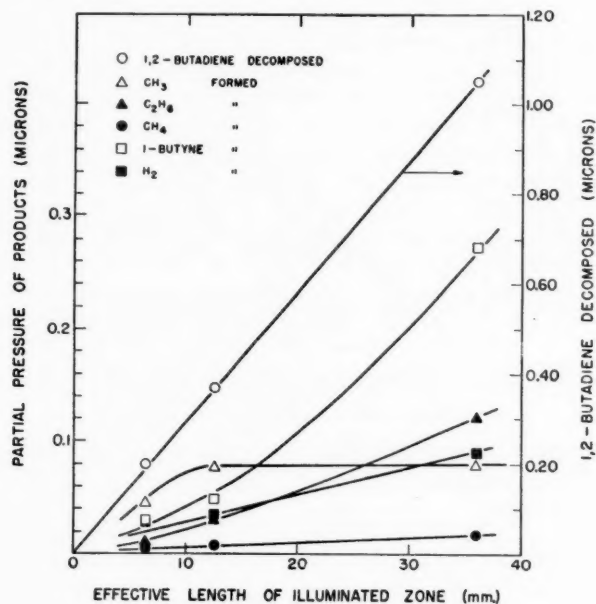


FIG. 2. Decomposition of 1,2-butadiene.

1,3-Butadiene

The dissociation of excited 1,3-butadiene molecules appears to be more complicated than that of allene or 1,2-butadiene. Using low energy electrons, the products of decomposition were found to be H_2 , C_4H_4 , CH_3 and C_3H_3 radicals, ethane, and C_6H_6 . Using 50-v. electrons, the variation in composition of the products with increasing length of the illuminated zone was measured. These results are given in Table III. The effect

TABLE III
DECOMPOSITION OF 1,3-BUTADIENE

Butadiene (μ)		Effective length of zone (mm.)	Butadiene decomposed		C_3H_4 decomposed (%)	Products from butadiene (μ)					Yield of CH_3	Yield of H_2
Lamp off	Lamp on		μ	%		H_2	CH_3	CH_4	C_2H_6	1,2-Butadiene + 1-butyne		
2.46	1.64	36	0.82	33.3	41.0	0.11	0.06 ₂	0.02 ₄	0.00 ₉	0.22	0.35–0.61	0.13
2.44	2.14	13.6	0.30	12.3	15.4	0.01 ₉	0.04 ₄	0.01 ₅	0.03 ₃	0.06 ₇	0.42–0.64	0.06 ₃
2.42	2.27	7.2	0.14 ₉	6.2	8.2	0.01 ₅	0.04 ₄	0.00 ₀	0.01 ₂	0.03 ₆	0.50–0.70	0.10

of varying the length of the zone can be seen in Fig. 3. From these data, there would appear to be two primary modes of decomposition of 1,3-butadiene, one to give H_2 and C_4H_4 , and the other to give CH_3 and C_3H_3 radicals. The latter reaction does not at

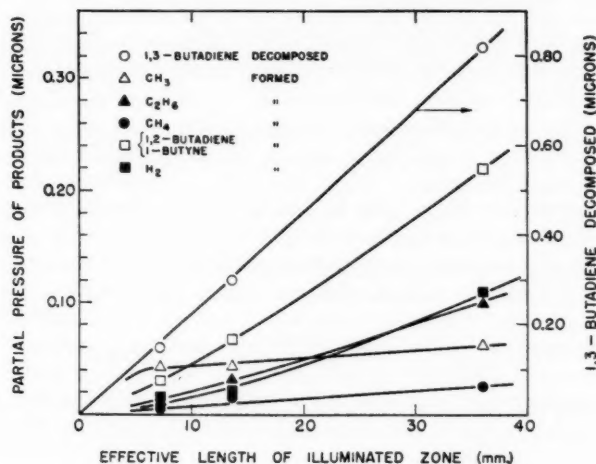
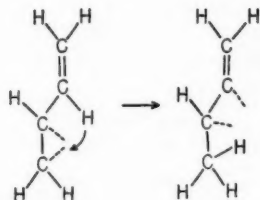


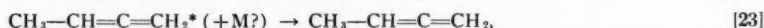
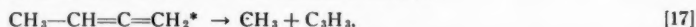
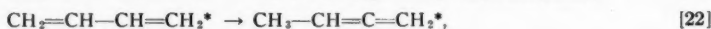
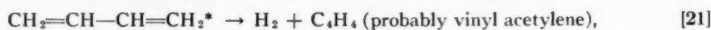
FIG. 3. Decomposition of 1,3-butadiene.

first sight appear very probable, since a hydrogen shift is required. When the configuration of butadiene is taken into account, such a shift appears less unreasonable.



As shown, the excitation of a butadiene molecule probably results in the uncoupling of one pair of electrons in the double bond. The migration of an H atom would give rise to a configuration equivalent to an excited 1,2-butadiene molecule, which could then dissociate into CH_3 and C_3H_3 as was found for 1,2-butadiene. The probability also exists that such an excited molecule could be deactivated to form 1,2-butadiene. The identification of 1,2-butadiene in the presence of 1,3-butadiene and 1-butyne was not unambiguous. Since the ionization potentials of 1-butyne and 1,2-butadiene (see above) are both larger than that of 1,3-butadiene (9.24 (11), 9.18 (5)) low electron energy measurements of the mass 54 peak were not capable of distinguishing between 1,2-butadiene and 1-butyne. Measurements (using 50-v. electrons) of the ratio of the peaks at mass 53 and 54 gave for the product a value intermediate between the ratios for 1,2-butadiene and 1-butyne. Both were probably present. In Table III the two have been lumped together, and the amount calculated using the average of their sensitivities.

The following reactions would account for the products observed:



As in the experiments with allene and 1,2-butadiene, the formation of 1-butyne shows that the C_3H_3 radical reacts as if it had the propargyl configuration. From the data in Table III, reaction [21] accounts for 0.06–0.13 of the butadiene disappearing. The fraction decomposing by reaction [17] depends on what fraction of the 1-butyne/1,2-butadiene product is 1-butyne. Assuming this product to be all 1,2-butadiene, a lower limit is obtained for the extent of reaction [17]. If it is all 1-butyne, an upper limit is obtained. Both limits are given in Table III in the column headed "yield of CH_3 ". The variation in the observed value of the limits with the length of the illuminated zone suggests that an intermediate value of 0.5 is the most probable. The remaining 20–30% of the 1,3-butadiene appears to form polymer.

No evidence could be found for the dissociation into two vinyl radicals proposed in earlier work (15). The radicals detected by Volman were therefore probably methyl radicals and C_3H_3 radicals. His observation that the radicals had a half-life about the same as the radicals from acetone is consistent with this interpretation. It is of interest in this regard to consider possible values for the dissociation energy of the $(\text{CH}_2=\text{CH})-(\text{CH}=\text{CH}_2)$ bond. From electron impact data two values of the heat of formation of vinyl radicals have been obtained: 51.6 kcal./mole (14) and 82.3 kcal./mole (3). From the heat of formation of 1,3-butadiene (26.3 kcal./mole) (12) these lead to two values for the C—C bond as follows:

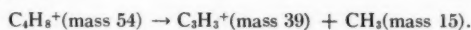
ΔH_f vinyl	$D(\text{C}_2\text{H}_3-\text{C}_2\text{H}_3)$
51.6	76.9
82.3	138.3

Since two C_2H_3 radicals would be formed by rupture of this bond, the discrepancy in the heat of formation appears doubled in the bond dissociation energy. The lower value is considerably less than $D(\text{C}-\text{C})$ in ethane (83.3 kcal./mole (1)) and appears to be much too low. The higher value is considerably higher than $D(\text{C}-\text{C})$ in cyanogen (112 kcal./mole (10)). Such comparisons can be misleading, but a value of about 105 kcal./mole would be easier to understand. Since the energy corresponding to a $\text{Hg}(^3\text{P}_1)$ atom is 112 kcal., it is evident that a dissociation of 1,3-butadiene into two vinyl radicals could not occur if $D(\text{C}_2\text{H}_3-\text{C}_2\text{H}_3)$ were greater than 112 kcal. The non-occurrence of this reaction is not sufficient to prove that $D(\text{C}_2\text{H}_3-\text{C}_2\text{H}_3) > 112$ kcal., but on the other hand it would be surprising that it does not occur if, in fact, the bond were as weak as 77 kcal./mole. The present results may be taken as support for a considerably higher value than 77 kcal./mole for this bond.

It is interesting to note that in the earlier work on the mercury photosensitized re-

action of 1,3-butadiene, the polymerization reaction seems to have predominated over the dissociation reactions. This is understandable on the basis of the great difference in the pressure of butadiene. At pressures above a few millimeters, the excited molecules may not have time to dissociate before suffering collisions leading to polymerization. In addition, the observation of the free radical mode of dissociation would be obscured by the addition of the free radicals to butadiene, resulting in induced polymerization. In static systems at moderate pressures quenching by hydrogen formed in the primary dissociation would, as pointed out by Gunning and Steacie (7), change the course of the reaction from a mercury photosensitized decomposition to an H-atom initiated polymerization. The simplification obtainable by studying such excited molecule reactions at very low pressures and high intensities of radiation is consequently of great assistance in determining the primary modes of dissociation.

Note added in proof.—The migration of a hydrogen atom is also found to occur in the 1,3-butadiene ion. The presence of a relatively large metastable peak at mass 28.2 in the mass spectrum of 1,3-butadiene shows that the following dissociative rearrangement must occur in the $C_4H_8^+$ ion:



This reaction appears to be analogous to that described above as occurring in a 1,3-butadiene molecule after excitation by a 3P_1 Hg atom.

REFERENCES

1. COTTRELL, T. L. The strengths of chemical bonds. Butterworth Scientific Publications, London, 1954.
2. FARMER, J. B. and LOSSING, F. P. Can. J. Chem. **33**, 861 (1955).
3. FIELD, F. H. J. Chem. Phys. **21**, 1506 (1953).
4. FRANKLIN, J. L. and FIELD, F. H. J. Am. Chem. Soc. **76**, 1994 (1954).
5. COLLIN, J. and LOSSING, F. P. To be published.
6. GEE, G. Trans. Faraday Soc. **34**, 712 (1938).
7. GUNNING, H. E. and STEACIE, E. W. R. J. Chem. Phys. **12**, 484 (1944).
8. LOSSING, F. P. Can. J. Chem. **35**, 305 (1957).
9. LOSSING, F. P., MARSDEN, D. G. H., and FARMER, J. B. Can. J. Chem. **34**, 701 (1956).
10. McDOWELL, C. A. and WARREN, J. W. Trans. Faraday Soc. **48**, 1084 (1952).
11. MORRISON, J. A. and NICHOLSON, A. J. C. J. Chem. Phys. **20**, 1021 (1952).
12. ROSSINI, F. D. *et al.* Selected values of physical and thermodynamic properties of hydrocarbons and related compounds. Carnegie Press, Pittsburgh, 1953.
13. STEACIE, E. W. R. Atomic and free radical reactions. 2nd ed. Reinhold Publishing Corporation, New York, 1954.
14. STEVENSON, D. P. J. Am. Chem. Soc. **65**, 209 (1943).
15. VOLMAN, D. H. J. Chem. Phys. **14**, 467 (1946).

THE REACTION OF UNSATURATED CARBOHYDRATES WITH CARBON MONOXIDE AND HYDROGEN

I. BRANCHED-CHAIN CARBOHYDRATE FROM 3,4,6-TRI-*O*-ACETYL-D-GALACTAL¹

A. ROSENTHAL AND D. READ²

ABSTRACT

A new crystalline seven-carbon branched-chain carbohydrate has been synthesized by application of the oxo reaction to 3,4,6-tri-*O*-acetyl-D-galactal. Periodate oxidation of the sugar alcohol was carried out to determine its structure. Crystalline benzoate and *p*-nitrobenzoate derivatives were obtained.

Very few branched-chain carbohydrates have been isolated from naturally occurring products or synthesized in the laboratory. By far the most naturally abundant branched-chain sugar is apiose (9), which is present in parsley and in an Australian pond weed (2). The other branched-chain sugars found in nature—streptose, mycarose, cladinose, and cordycepose—occur as constituents of the antibiotics streptomycin (7), magnamycin (16), erythromycin (24), and cordycepin (3), respectively. In the synthetic field the cyanohydrin reaction has been applied to fructose to furnish branched-chain, seven-carbon sugars (10, 18), and Woods and Neish (26) have used these products as intermediates in preparing other branched-chain sugars. Utkin (22) has reported the synthesis of a new branched-chain sugar by condensation of dihydroxyacetone in alkali and other workers have attempted to prepare branched-chain sugars by the action of Grignard reagents on carbohydrates (6, 14).

Branched and straight-chain aldehydes and alcohols have been produced by the addition of carbon monoxide and hydrogen to olefins, a process known as the oxo reaction (21). The work reported here deals with the application of the oxo reaction to unsaturated sugars and offers proof of the probable structure of the branched-chain carbohydrate that is formed. The present report is subsequent to a preliminary publication on the synthesis (17).

3,4,6-Tri-*O*-acetyl-D-galactal was prepared following the excellent method of Helferich and co-workers (8). The unsaturated carbohydrate was then allowed to react with carbon monoxide and hydrogen in the presence of preformed dicobalt octacarbonyl and ethyl orthoformate at elevated temperature and pressure (1, 15). Chromatographic fractionation of the sirups obtained from two different experiments (see Procedures A and B, Experimental) on acid-washed aluminum oxide yielded non-crystalline components which gave negative unsaturation and Fehling's tests. The infrared spectra of the partially acetylated fractions are shown in the Experimental. Elimination of the band at 1650 cm^{-1} in the spectra of compounds B and C confirmed the saturation of the olefinic bond, whereas the appearance of a new strong band at 3450 cm^{-1} indicated that a hydroxyl group had been added during the reaction.

As the various components obtained in the chromatographic separation of the sirups could not be crystallized, they were deacetylated with sodium methoxide and then

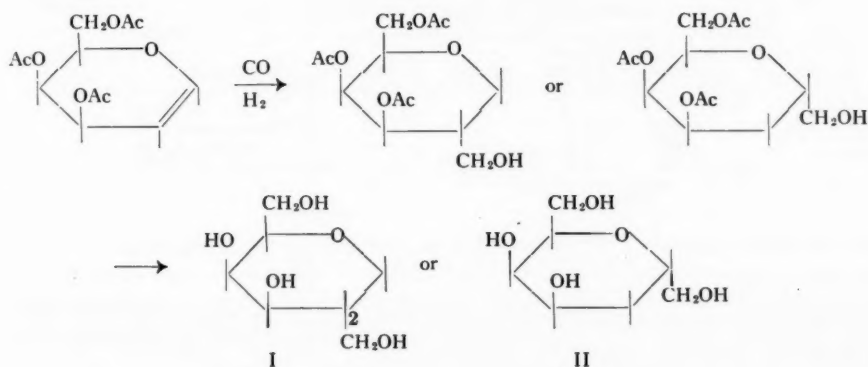
¹Manuscript received in original form October 22, 1956, and, as revised, April 23, 1957.

Contribution from the Department of Chemistry, University of British Columbia, Vancouver, B.C. This paper is based on a thesis submitted by D. Read in partial fulfillment of the requirements for the degree of Master of Science in Chemistry, April, 1956. A preliminary report of this work appears in *Abstracts Papers Am. Chem. Soc.* 128, 10D (1956).

²Present address: Division of Industrial and Cellulose Chemistry, McGill University, Montreal, Que.

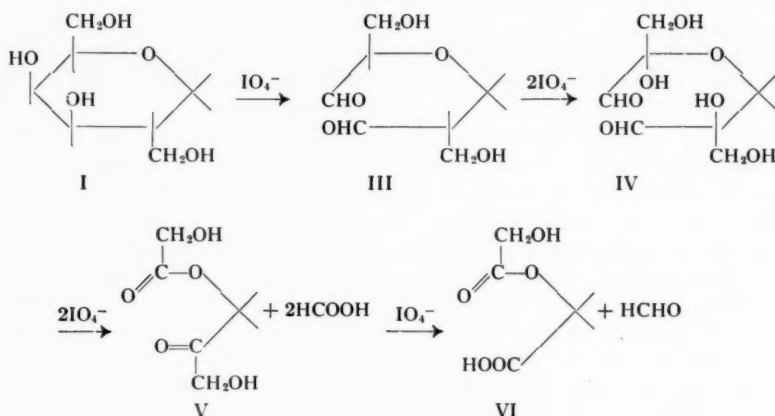
deionized using Amberlite IR-120. Solid products were obtained which were crystallized from methyl alcohol and isopropyl ether. The compounds obtained from each main zone of Procedures A and B (Experimental) were shown to be identical by melting point, mixed melting point, and optical rotation. In addition, each was shown to be chromatographically pure on paper chromatograms and each had the same R_f . The empirical formula of the deacetylated compound was found to be $C_7H_{14}O_6$. Proof that a hydroxymethyl group had been added to the unsaturated carbohydrate was shown by hydroxyl analysis as well as by the analyses of the crystalline benzoate and *p*-nitrobenzoate derivatives.

The formation of the deacetylated compound from 3,4,6-tri-*O*-acetyl-D-galactal may be illustrated by the following sequence of reactions where the sugar alcohol is represented by either I or II. The configuration of carbon-2 is unknown.



Periodate oxidation was used to elucidate the structure of the sugar alcohol. The consumption by compound F of 1.12 moles of oxidant at pH 4.65 within 7 hours showed that there were two vicinal hydroxyl groups in the molecule. From 7 to 40 hours the slow consumption of an additional 0.41 mole of periodate per mole was obviously overoxidation (4). Under slightly different conditions overoxidation of compound F with the same oxidant in sodium hydroxide-sodium dihydrogen phosphate buffer at pH 7 within 900 hours showed a consumption of 6.15 moles of oxidant with the production of 2.45 equivalents of acid and 1.0 mole of formaldehyde per mole. A significant arrest in the progress of the oxidation occurred after 6 moles of periodate were used as shown by the consumption from 900 to 1300 hours of only an additional 0.45 mole of periodate with the production of 0.40 mole of formaldehyde. In a parallel experiment methyl α -D-glucopyranoside consumed 6.0 moles of oxidant per mole of the glycoside within 216 hours. The stability of the glycoside in the buffer solution alone indicated that hydrolysis of the acetal followed by subsequent oxidation did not take place. The additional consumption of 4 moles of oxidant over that required for the cleavage of the C₂-C₃ and C₃-C₄ bonds of the glycoside can be explained on the assumption that, after the formation of the dialdehyde, the hydrogen situated on the original C₅ is activated by the adjacent aldehydic group and is oxidized to a hydroxyl group. Further oxidation of the resulting substance with periodate might then be expected (4). A similar explanation would account for the overoxidation of compound F. The

structure of this compound can be represented by I (configuration of carbon-2 unknown), as the experimental results conform to the reaction scheme depicted below. After the formation of the dialdehyde (III), hydroxylation of C₅ and C₂ occurs (IV), followed by oxidation to yield VI. As the ester (VI) could be expected to be comparatively stable to hydrolysis at pH 7, there would be a levelling off in periodate consumption after 6 moles. If the structure of compound F were represented by II it would be predicted that with the consumption of 6 moles of oxidant no formaldehyde would be produced.



A preliminary nuclear magnetic resonance study (12) of the fully acetylated compound F confirmed structure I. Further N.M.R. studies of closely related acetylated carbohydrates are being carried out and will be subsequently reported.

EXPERIMENTAL

Preparation of 3,4,6-Tri-O-acetyl-D-galactal

3,4,6-Tri-O-acetyl-D-galactal (13) was prepared according to the excellent procedure of Helferich and co-workers (8). The infrared spectrum of the compound showed no hydroxyl band.

Preparation of Dicobalt Octacarbonyl

This compound was prepared from Co-0101-P catalyst (product of Harshaw Chemical Co., Cleveland 6, Ohio) and also from Raney cobalt by procedures previously reported (1). Concentration of dicobalt octacarbonyl in benzene solution was 2.5% as determined by the method of Orchin *et al.* (20).

Reaction of 3,4,6-Tri-O-acetyl-D-galactal with Carbon Monoxide and Hydrogen

Procedure A.—A solution of 3,4,6-tri-O-acetyl-D-galactal (13.5 g., 0.039 mole), ethyl orthoformate (9.2 ml., 0.058 mole), and dicobalt octacarbonyl (0.6 g.) in 35 ml. of anhydrous thiophene-free benzene was placed in the glass liner of a high pressure hydrogenator having a void of 280 ml. To the bomb, which had been freed of air, carbon monoxide (1500 p.s.i.) and hydrogen (1500 p.s.i.) were added. After the hydrogenator was rocked for 5 minutes, the combined gas pressure was 2930 p.s.i. at 22° C. The reactants were heated at 130–140° C. for 4 hours. A pressure drop of 240 p.s.i. at 22° C. was observed. Heating of the dark red solution on a steam bath for 20 minutes was

followed by removal of the cobalt by filtration and subsequent evaporation of the solvent under vacuum; yield, 14 g. of a straw-colored sirup.

Procedure B.—This differed from Procedure A only in that the pressure of carbon monoxide and hydrogen were 200 and 1670 p.s.i. respectively (17).

Continuous Flow Chromatography of Product from Procedures A and B

All solvents used were anhydrous and the benzene was also thiophene-free. A portion of the sirup (6.3 g.) from Procedure A was dissolved in 50 ml. of benzene and added to the top of a glass column containing a 40×7.5 cm. (diam.) adsorbent column of 1700 g. of acid-washed alumina (Merck) which had been prewashed with 1500 ml. of benzene. Development of the chromatogram was effected with benzene and benzene-anhydrous ethanol as indicated in Table I. Solvent ratios were volume:volume before mixing.

TABLE I
CHROMATOGRAPHY OF PRODUCT OF PROCEDURE A

Developer	Volume, l.	Fraction	Fraction yield, g.	Nature of material
Benzene	10.5		0	
99:1 Benzene:ethanol	5	A	0.4	Sirup
95:5 Benzene:ethanol	6	B	3.7	Sirup
90:10 Benzene:ethanol	6	C	1.3	Sirup
			Total 5.4 g. (86%)	

The effluent, collected in 20 ml. fractions by a Technicon T/F Fraction collector, was evaporated under reduced pressure. The main products, B and C, could not be crystallized although a number of solvent combinations were tried. Fraction C was less soluble than B in ether or ethyl acetate. Both B and C gave negative unsaturation tests and were non-reducing to Fehling's solution. Chromatography of the product from Procedure B in the same way yielded two more fractions, D and E. Infrared spectra of B and C (in chloroform) (s, strong; m, medium; w, weak):

B: 3450(s), 2930(s), 1735(s), 1438(w), 1368(s), 1235(s), 1150(w), 1092(m), 1038(m), 907(w).

C: 3430(s), 2920(s), 1725(s), 1435(w), 1370(s), 1235(s), 1158(w), 1090(m), 1035(m).

Deacetylation of Fractions B, C, D, and E

Fraction B (1.5 g.) suspended in 25 ml. of 0.5 N sodium methoxide was maintained at room temperature for 2 hours and then overnight at 0° C. The resultant suspension was dissolved by the addition of 30 ml. of water and then passed through a 22×2 cm. (diam.) column of Amberlite IR-120 (product of Rohm and Haas Co., Resinous Div., Philadelphia, Pa.). Water was removed by evaporation under reduced pressure at 40° C. When it had been left standing for several days *in vacuo* over phosphorous pentoxide, the product (F) deposited crystals which were thrice recrystallized from methanol-isopropyl ether, m.p. 158.5–159.5° C., $[\alpha]_D^{21} +37.6^\circ$ (c, 1.3, in water).

Infrared spectrum data in cm^{-1} of F in Nujol: 3260(s), 2980(w), 1420(w), 1360(m), 1238(m), 1142(m), 1098(s), 1035(s), 930(m), 815(m), 758(w).

Calculated for $\text{C}_7\text{H}_{14}\text{O}_5$: C, 46.91; H, 8.43; OH, 37.9%. Found: C, 47.43; H, 8.16; OH, 37.3% (in duplicate).

Fraction C was deacetylated and recrystallized in the same manner as described for fraction B; m.p. 157–158° C. (corr.), $[\alpha]_D^{21} +36^\circ$ (c, 1.3, water). Mixed m.p. of this compound with F, 157–159°.

Fractions D and E yielded deacetylated products having melting points of 157–159° and 157–158°, respectively. Mixed m.p. of E and F, 156–158°.

Compound F gave a negative Fehling's test.

Paper Strip Chromatography of Products Obtained from the Deacetylation of Fractions A, B, C, and D

Samples of each of the compounds obtained from the deacetylation of A, B, C, and D were chromatographed (5) on Whatman No. 1 paper (50×20 cm.) using *n*-butanol-ethanol-water (40:11:19 v/v) as solvents for 16 hours at a constant temperature of 22° C. Indication was effected on the dried sheets with sodium metaperiodate – alkaline permanganate reagent (11). Each fraction produced only one spot with identical R_f (0.42).

Paper chromatography of each sample using water-saturated *s*-collidine as solvent confirmed the presence of only one substance in each product having an R_f of 0.50.

Characterization of Compound F

1. Benzoylation of Compound F and Flow Chromatographic Purification of Benzoate

A portion of compound F (0.060 g.), obtained from the deacetylation of fraction B, was benzoylated according to the procedure described by Smith and Van Cleve (19); yield, 0.122 g. Infrared analysis of the product showed a trace of hydroxyl to be present.

The above benzoate was dissolved in anhydrous benzene (2 ml.) and added to the top of a glass column containing a 17×2 cm. (diam.) adsorbent column of acid-washed alumina (Merck) prewetted with 50 ml. of anhydrous light petroleum ether. The following mixtures of developer were then added consecutively: 150 ml. of benzene – petroleum ether (25:75 v/v); 150 ml. of benzene – petroleum ether (60:40), which gave crystalline fraction G (0.050 g.); 150 ml. of benzene – petroleum ether (70:30); and 400 ml. of benzene – petroleum ether (80:20), which gave crystalline fraction H (0.061 g.). No chemical analysis was carried out on H, as it was believed that this fraction was partially benzoylated.

Fraction G was thrice recrystallized from methanol–water, m.p. 106–107° C. (corr.), $[\alpha]_D^{22} + 43.5^\circ$ (*c*, 1 in chloroform). Calculated for $C_{36}H_{30}O_9[C_7H_{10}O(OCOC_6H_5)_4]$: C, 70.70; H, 5.04; mol. wt., 594. Found: C, 70.86; H, 4.94; mol. wt., 545 (Rast). Microanalyses by Dr. W. Manser, Nerdstrasse 140, Zurich 37, Switzerland, and by Drs. G. Weiler and F. B. Strauss, 164 Banbury Road, Oxford, England.

*2. *p*-Nitrobenzoylation of Compound F*

A portion of Compound F (0.056 g.) was allowed to react with *p*-nitrobenzoyl chloride according to the method described by Smith and Van Cleve (19). The crude product (yield 0.165 g.) was thrice recrystallized from chloroform – light petroleum ether (b.p. 30–60° C.), m.p. 205–206° C. (corr.), $[\alpha]_D^{20} - 8.7^\circ$ (*c*, 1 in chloroform). Calculated for $C_{38}H_{26}O_{17}N_4$: C, 54.27; H, 3.38; N, 7.24. Found: C, 53.64; H, 3.36; N, 6.91.

3. Acetylation of Compound F

Acetylation of compound F at 0° C. for 2 days with acetic anhydride and anhydrous pyridine gave, after hydrolysis of the excess anhydride with crushed ice, followed by extraction with chloroform, a non-crystalline product. The product was chromatographically purified using acid-washed alumina as adsorbent and anhydrous benzene-ethanol (96:3) as developer, according to the procedure of Woods and Neish (26). Attempts to crystallize the main zone from aqueous ethanol, ether – petroleum ether, or from benzene – petroleum ether were unsuccessful. Acetylation of compound F with

acetic anhydride and twice-fused sodium acetate (25) gave a product having the same properties as that from the acetic anhydride - pyridine procedure.

4. Oxidation by Periodate

(i) *Oxidation of compound F*.—Compound F was oxidized with sodium metaperiodate (0.12 *M*) in buffered solutions (23) according to the procedure outlined by Hirst and co-workers (4). The acid produced during the oxidation was determined by titration with sodium hydroxide (0.02 *N*) using phenolphthalein as indicator. Formaldehyde was determined by precipitation with dimedon. The following results were obtained: A. At pH 4.65 (13–14° C.).

Moles of periodate consumed per mole of compound: 1.12 (7 hours), 1.52 (40 hours).

B. In sodium hydroxide - sodium dihydrogen phosphate buffer at pH 7 (22–25° C.).

Moles of periodate consumed: 1.9 (22 hours), 3.3 (163 hours), 4.2 (330 hours), 5.8 (720 hours), 6.15 (900 hours), 6.45 (1100 hours), 6.55 (1200 hours), 6.60 (1300 hours).

Equivalents of acid formed: 1.15 (163 hours), 2.20 (720 hours), 2.45 (900 hours), 2.85 (1300 hours).

Moles of formaldehyde formed: 0.70 (720 hours), 1.00 (900 hours), 1.40 (1300 hours).

(ii) Oxidation of D-glucose at pH 7

Moles of periodate consumed: 5.00 (22 hours), 5.02 (76 hours), 5.04 (360 hours).

Equivalents of acid formed: 4.92 (22 hours), 4.90 (163 hours).

Moles of formaldehyde formed: 0.95 (163 hours).

(iii) Oxidation of methyl α -D-glucoside at pH 7

Moles of periodate consumed: 2.5 (20 hours), 3.1 (44 hours), 4.8 (118 hours), 6.0 (216 hours), 6.1 (250 hours).

Equivalents of acid formed: 1.9 (118 hours).

A solution of methyl α -D-glucoside in the sodium hydroxide - sodium dihydrogen phosphate buffer showed a constant optical rotation within 120 hours.

ACKNOWLEDGMENTS

The authors are indebted to the National Research Council of Canada for its grants in support of this research. One of us (D. R.) also thanks the Powell River Company Limited for the Scholarship held in 1954–55 and the National Research Council of Canada for the Studentship held in 1955–56.

The authors thank the Canadian Pacific Fisheries Experimental Station, Vancouver, for the microanalyses of the unsubstituted carbohydrate.

REFERENCES

1. ADKINS, H. and KRSEK, G. *J. Am. Chem. Soc.* **70**, 383 (1948); **71**, 3051 (1949).
2. BELL, D. J., ISHERWOOD, F. A., and HARDWICK, N. E. *J. Chem. Soc.* 3702 (1954).
3. BENTLEY, H. R., CUNNINGHAM, K. G., and SPRING, F. S. *J. Chem. Soc.* 2301 (1951).
4. EDINGTON, R. A., HIRST, E. L., and PERCIVAL, E. E. *J. Chem. Soc.* 2281 (1955).
5. FLOOD, A. E., HIRST, E. L., and JONES, J. K. N. *J. Chem. Soc.* 1679 (1948).
6. FOSTER, A. B., OVEREND, W. G., STACEY, M., and VAUGHAN, G. *J. Chem. Soc.* 3308 (1953).
7. GILMAN, H. *Organic chemistry*. Vol. III. John Wiley & Sons, Inc., New York, N.Y. 1953. p. 553.
8. HELFERICH, B., MULCAHY, E. N., and ZIEGLER, H. *Ber.* **87**, 233 (1954).
9. HUDSON, C. S. *Advances in Carbohydrate Chem.* **4**, 57 (1949).
10. KILIANI, H. *Ber.* **18**, 3066 (1885).
11. LEMIEUX, R. U. and BAUER, H. F. *Anal. Chem.* **26**, 920 (1954).
12. LEMIEUX, R. U. and KULLNIG, R. K. *Abstr. Papers Am. Chem. Soc.* 128, 10D (1956).
13. LEVENE, P. A. and TIPSON, R. S. *J. Biol. Chem.* **93**, 644 (1931).
14. OVEREND, W. G. and VAUGHAN, G. *J. Chem. Soc.* 2155 (1954); 3308 (1953).
15. PINO, P. *Gazz. chim. ital.* **81**, 625 (1951); *Chem. Abstr.* **46**, 7079 (1952).

16. REGNA, P. P., HOCKSTEIN, F. A., WAGNER, R. L., and WOODWARD, R. B. *J. Am. Chem. Soc.* **75**, 4625 (1953).
17. ROSENTHAL, A., READ, D., and CAMERON, C. *Science*, **123**, 1177 (1956).
18. SCHMIDT, O. T. and WEBER-MOLSTER, C. C. *Ann.* **515**, 43 (1934).
19. SMITH, F. and VAN CLEVE, J. W. *J. Am. Chem. Soc.* **77**, 3091 (1955).
20. STERNBERG, A., WENDER, I., and ORCHIN, M. *Anal. Chem.* **24**, 174 (1952).
21. STORCH, H. H., GOLUBIC, N., and ANDERSON, R. B. *The Fischer-Tropsch and related syntheses.* John Wiley & Sons, Inc., New York, N.Y. 1951.
22. UTKINS, L. M. *Doklady Akad. Nauk. S.S.S.R.* **67**, 301 (1949); *Chem. Abstr.* **44**, 3910 (1950).
23. VOGEL, A. I. *Quantitative inorganic analysis.* Longmans, Green & Co., Ltd., London. 1951. p. 868.
24. WILEY, P. F. and WEAVER, O. *J. Am. Chem. Soc.* **77**, 3422 (1955); **78**, 808 (1956).
25. WOLFROM, M. L. and SCHUMACHER, J. N. *J. Am. Chem. Soc.* **77**, 3318 (1955).
26. WOODS, R. J. and NEISH, A. C. *Can. J. Chem.* **31**, 471 (1953); **32**, 404 (1954).

THE FRACTIONATION OF POLYSACCHARIDES BY THE METHOD OF ULTRAFILTRATION¹

K. C. B. WILKIE,² J. K. N. JONES,² BARBARA J. EXCELL,³ AND R. E. SEMPLE³

ABSTRACT

Ultrafiltration of an aqueous solution of a synthetic mixture of inulin and clinical dextran has been used to separate the two polysaccharides. A clinical dextran has also been fractionated in the same way to yield five dextran fractions having number-average molecular weights ranging from 11,000 for the lowest to 190,000 for the highest fraction.

The isolation of a chemically homogeneous polysaccharide is desirable prior to the determination of its structure. It is frequently difficult to achieve a satisfactory degree of fractionation owing both to the range of physical properties within a molecular species and to the close physical similarity between the molecules of different species.

Many of the techniques which are employed to achieve fractionation are based upon the fractional dissolution or precipitation of polysaccharides or of their derivatives (5). More recently electrophoretic techniques have been used to achieve such a fractionation (3, 6, 8) but these methods may cause degradation.

Ultrafiltration of colloidal solutions has been used to separate colloids from solutions and, to free liquids from bacteria and from viruses. As far as the authors are aware, it has not hitherto been used to achieve a large scale fractionation of polysaccharides although cellulose derivatives were early fractionated by this method (4). Mould and Syge (10) have reported the small scale fractionation of polysaccharides on strips of collodion membrane by electrokinetic ultrafiltration where the movement of the polysaccharide solution was within the thickness of the membrane. In the work presently reported fractionation of a clinical dextran was achieved by an ultrafiltration technique. The method possesses the advantage over others that there is no risk of degradation of the material under investigation and a high recovery of that material is possible.

Clinical dextran was chosen in the present work as from it we wished to obtain a dextran fraction with a more limited molecular weight distribution, which, it is believed, would be more suitable for use as a plasma expander. In order that clinical dextran should function more efficiently as a temporary plasma expander it is desirable that no major portion of it should be excreted during the first 24 hours after its transfusion into the animal. The clinical dextrans at present commonly in use contain a low molecular weight fraction (*ca.* less than $M_w = 50,000$) which is so rapidly excreted into the urine by man that it is of little use as a plasma expander. There is also evidence that the high molecular weight fraction (above $M_w = ca. 300,000$) of clinical dextrans may be retained by the body for much longer period than is required (11).

EXPERIMENTAL

General

The clinical dextran (Intradex⁴) employed in the present work had been prepared commercially by the partial hydrolytic depolymerization and fractionation of the dextran produced by a culture of *Leuconostoc mesenteroides* (National Regional Research Laboratories strain B-512) grown on a medium containing sucrose.

¹Manuscript received April 15, 1957.

²Contribution from the Department of Chemistry and the Department of Physiology, Queen's University, Kingston, Ontario.

³Department of Chemistry.

⁴Department of Physiology.

⁵Supplied by Glaxo Laboratories, Greenford, Middlesex, England.

The bacteriological filters were supplied by Schleicher and Schuell.⁵ Throughout the work ultrafilters (15 cm.) of the "ultrafine" series were employed. They were clamped in a glass Zsigmondy-Sartorius apparatus⁵ fitted with a pressure top and with a perforated porcelain disk; each ultrafilter was separated from the porcelain disk by a Schleicher and Schuell No. 604 filter paper.

Fractionation of a Synthetic Mixture of Polysaccharides

A preliminary experiment was carried out on a solution of a synthetic mixture of polysaccharides.

An aqueous solution (400 ml.) of the clinical dextran was placed in the ultrafiltration apparatus which had been fitted with a 'superdense' filter, and ultrafiltration was carried out under reduced pressure until the volume of the solution retained in the filtration chamber had been reduced to 100 ml. This residual solution was diluted to its original volume and the ultrafiltration procedure was repeated. It was hoped that that fraction of the dextran able to pass through the 'superdense' filter would then have been removed. Water (300 ml.) was saturated at 30° with inulin and the clinical dextran (12 g.) which had been retained by the 'superdense' filter was dissolved in this solution. The solution of the two polysaccharide species was placed in the filtration apparatus (fitted with a new 'superdense' filter) and the volume of the solution in the filtration chamber was reduced as described above to ca. 250 ml. During the ultrafiltration the solvent evaporated from the ultrafiltrate and crystals were deposited which had $[\alpha]_D^{21} = -32^\circ$ (*c*, 0.2 in water) ($[\alpha]_D^{21} = -37^\circ$ for the non-fractionated inulin, $= +192^\circ$ for then non-fractionated clinical dextran (both *c*, 0.2 in water)). It was evident that practically complete separation of the inulin from the dextran had been achieved.

It was found that the rate of ultrafiltration under reduced pressure became progressively slower as the filtration proceeded owing, in part, to evaporation from the lower side of the filter leading to the retention of a thick sirup on it. Thereafter pressure filtration (ca. 4 lb./sq. in.) was used and the apparatus was shaken gently from time to time.

Fractionation of a Clinical Dextran

Clinical dextran (11 g.), which had not been subjected to any preliminary ultrafiltration, was dissolved in water (500 ml.) and the solution was placed in the filtration chamber of the Zsigmondy-Sartorius apparatus which had been fitted with a 'coarse' filter. After the solution had been subjected to ultrafiltration under pressure no detectable amount of solution or of solute was found to have been retained on the filter. The 'coarse' filter was replaced by a 'medium' filter and as much as possible of the previous ultrafiltrate was forced through it. After a time, owing to the increasing concentration of the solution in the filtration chamber, the rate of ultrafiltration became very slow and the solution was therefore diluted to 500 ml. and the ultrafiltration procedure repeated and continued until the volume of the solution retained in the chamber was reduced to ca. 150 ml. This solution was freeze-dried and then yielded a product which is named 'the medium fraction'; other fractions are named accordingly. The ultrafiltrates which had passed through the 'medium' filter were combined and the solution, and ultrafiltrates subsequently derived from it, were subjected in a similar manner to ultrafiltration using successively a 'dense', a 'very dense', and a 'superdense' filter. The water was removed from the various fractions by freeze-drying.

The specific viscosities (η_{sp}) of solutions of these fractions were determined at different

⁵Apparatus and filters supplied by Carl Schleicher and Schuell Co., Keene, New Hampshire, U.S.A.

concentrations (C) and from them the intrinsic viscosities were calculated by extrapolating straight-line plots of η_{sp}/C vs. C to zero concentration for each fraction. It is apparent from the values of the intrinsic viscosities of the fractions (see table) that the clinical dextran had been separated into fractions having different molecular weight distributions. Ingelman and Halling (9), using the ultracentrifuge, have determined the sedimentation and diffusion constants of various clinical dextran fractions and from them have calculated the weight-average molecular weights (M_w) of the dextrans in the fractions. They have determined that the molecular weights are related to the intrinsic viscosities of aqueous solutions of the dextran samples by the equation:

$$\text{intrinsic viscosity} = 8.2 \times 10^{-7} M_w + 0.18.$$

When the viscosity is in the region of 0.2, or below, the above relationship cannot be applied with any significant accuracy and for that reason the value of M_w of the material in the 'superdense' fraction has not been calculated. Wales, Marshall, and Weissberg (12), having worked with dextrans prepared by the partial acid hydrolysis of native dextrans produced by the B-512 strain of *Leuconostoc mesenteroides*, related the intrinsic viscosities of various dextran fractions to their viscosity-average molecular weights (M_v) by the equation:

$$\text{intrinsic viscosity} = 10^{-3} M_v^{1/2}.$$

Wales *et al.* obtained values indicating that in their work there was comparatively little difference between the value for the weight-average and that for the viscosity-average molecular weight in the region $M_w = 11,000$ – $170,000$. Using both Ingelman's and Wales' equations we have calculated the values of M_w and M_v respectively but the values obtained differ considerably. The values for the ratio M_w/M_n range from 1.6 to 1.8 when using the Ingelman equation whilst using the Wales equation the values for M_v/M_n are 0.9 to 1.4. Using the Ingelman equation our calculated values for M_w correspond reasonably well with those obtained by Granath (7) also working on clinical dextran fractions derived from B-512 cultures. This correspondence together with the improbably low value of M_v/M_n when using the Wales equation suggests that in the present circumstances the Ingelman equation is probably the more applicable.

Owing to the small amount of material in the 'final filtrate' it was not possible to determine its intrinsic viscosity. The number-average molecular weights (M_n) were determined by use of 3,5-dinitrosalicylic acid (1, 2).

Several determinations were made of the rate at which samples of the various dextran fractions migrated on glass paper electrophoretograms (length = 55 cm.) under a potential difference of 110 volts (3). The electrophoretograms had been wetted with a buffer

DATA RELATING TO FRACTIONATED AND NON-FRACTIONATED INTRADEx

Fraction	Weight, g.	$[\alpha]_D^{20} \pm 1\%$	Intrinsic viscosity $\pm 1\%$	$M_v \times 10^{-3}*$	$M_w \times 10^{-3}†$	$M_n \times 10^{-3} \pm 8\%$
Medium	1.76	191	0.462	213	344	190
Dense	6.02	191	0.365	133	225	134
Very dense	2.37	193	0.320	102	171	95
Superdense	0.38	189	0.200	39	—	27
Final filtrate	0.014	190	—	—	—	11
Intradex	—	192	0.328	107	180	114

95.9% of the Intradex subjected to fractionation procedures was recovered.

*Determined using Wales' equation (12).

†Determined using Ingelman's equation (9).

of 0.1 *M* borax in 0.1 *N* aqueous sodium hydroxide. It was found that a sample of the 'dense' fraction moved slightly faster towards the cathode and that it was followed, in order, by samples of the 'final filtrate', the 'medium', the 'very dense', and the 'superdense' fractions. It is of interest to note that the relative rates of electrophoretic migration of the dextran samples cannot be solely dependent upon their molecular weights. Possibly the rates also reflect differences either in the molecular shape or in details of chemical structure or in both.

ACKNOWLEDGMENTS

We are indebted to the Defence Research Board of Canada for grant No. DRB 9530-08 and to the Glaxo Laboratories for the supply of the clinical dextran used in this work.

REFERENCES

1. BOTTLE, R. T. and GILBERT, G. A. *Chemistry & Industry*, 1201 (1954).
2. BOTTLE, R. T. and GILBERT, G. A. *Chemistry & Industry*, 575 (1956).
3. BRIGGS, D. R., GARNER, E. F., and SMITH, F. *Nature*, **178**, 154 (1956).
4. CRAGG, L. H. and HAMMERSCHLAG, H. *Chem. Revs.* **39**, 125 (1946).
5. ERSKINE, A. J. and JONES, J. K. N. *Can. J. Chem.* **34**, 821 (1956).
6. FULLER, K. W. and NORTHCOTE, D. H. *Biochem. J.* **64**, 657 (1956).
7. GRANATH, K. Private communication by Viriding, G.
8. HOCEVAR, B. J. and NORTHCOTE, D. H. *Nature*, **179**, 488 (1957).
9. INGELMAN, B. and HALLING, M. S. *Arkiv Kemi*, **1**, 61 (1949).
10. MOULD, D. L. and SYNGE, R. L. M. *Analyst*, **77**, 964 (1952).
11. SQUIRE, J. R., BULL, J. P., MAYCOCK, W. d'A., and RICKETTS, C. R. *Dextran, its properties and use in medicine*. Blackwell Scientific Publications, Oxford, England. 1955. pp. 23-71.
12. WALES, M., MARSHALL, P. A., and WEISSBERG, S. G. *J. Polymer Sci.* **10**, 229 (1953).

THE STRUCTURE OF ALUMINUM DI- AND TRI-SOAPS¹

A. E. LEGER, R. L. HAINES, C. E. HUBLEY, J. C. HYDE, AND H. SHEFFER

ABSTRACT

Confirmation of the existence of aluminum trilaurate has been obtained by using infrared absorption to follow the course of the reactions of trimethylaluminum and aluminum isopropoxide with lauric acid. The trisoap is shown to exist as micelles of high molecular weight in solution, the size decreasing on dilution or elevation of temperature. On hydrolysis to the disoap, hydrogen bonding does not appear to play a significant role in the formation of polymer structures. Coordination of carboxylate groups with aluminum is shown to be a major feature of the structure of both tri- and di-soaps. Spectral assignments in the 6.0 to 6.4 μ region have been made for various types of inter- and intra-molecular coordination. The effects of dilution, hydrolysis, and hydrochlorination of aluminum trilaurate in solution have been assessed by viscosity, light-scattering, and infrared measurements.

INTRODUCTION

Aluminum soaps, which are widely used as hydrocarbon thickeners in the manufacture of greases, paints, and flame-thruster fuels, are generally made by the aqueous meta-thetic reaction of an aluminum salt and an alkali fatty acid soap. A precipitate is formed consisting mainly of aluminum hydroxy disoap, with small quantities of aluminum dihydroxy monosoap, free fatty acid, and aluminum hydroxide.

In spite of the extensive commercial applications of aluminum disoaps, there is a dearth of fundamental knowledge about aluminum soaps generally. This paper reports some work carried out during the past few years at these laboratories on the physical and chemical properties of aluminum soaps.

It is now generally believed that aluminum mono- and di-soaps are polymeric substances, and McGee (13) and Gray and Alexander (7) have proposed structures in which the polymer chains contain alternating aluminum and oxygen atoms linked by covalent and coordinate bonds.

It is only recently that the synthesis of aluminum trisoap, i.e. an aluminum soap with three acid groups linked to the aluminum atom, has been accomplished. In 1932 McBain and McLatchie (12) recorded that its synthesis in either aqueous or non-aqueous media was impossible. In 1938 Lawrence (11) claimed that trisoaps could be synthesized, but without giving any experimental evidence. More recently new methods for the synthesis of these materials have been proposed. Glazer, McRoberts, and Schulman (6) have reported the attempted synthesis of aluminum trilaurate from trimethylaluminum and lauric acid, and Mehrotra and Pande (14, 15) have synthesized aluminum trisoaps by reacting aluminum isopropoxide and fatty acids dissolved in benzene, with the isopropanol produced being removed by azeotropic distillation. Gilmour *et al.* (5) have reported the isolation of aluminum tristearate by means of pyridine complexing.

In some of the above reports chemical analyses of the reaction product served merely to confirm that the starting materials had been added in the correct stoichiometric proportions. The object of the present work has been to substantiate the existence of aluminum trisoap and to elucidate its structure. Samples of reaction mixtures have been taken at intervals during synthesis and examined by infrared spectroscopy. Upon completion of the synthesis, various studies were carried out on the effects of hydrolysis, hydrochlorination, and dilution, using light-scattering, viscosity, and infrared absorption techniques. These studies have been extended to include aluminum disoaps.

¹Manuscript received April 11, 1957.

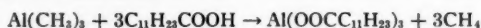
Contribution from the Defence Research Chemical Laboratories, Ottawa, Canada. Also issued as D.R.C.L. Report No. 236.

EXPERIMENTAL

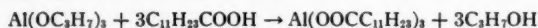
The main experimental refinements in the synthesis of aluminum trilaurate have been dictated by the very reactive nature of the reagents and also the extreme moisture sensitivity of the trisoap. The precautions taken to minimize hydrolysis, e.g. drying of solvents and use of special sampling technique, are dealt with below.

The following reactions were studied:

(1) Trimethylaluminum and lauric acid



(2) Aluminum isopropoxide and lauric acid



All infrared spectra for the reaction mixtures in benzene or carbon tetrachloride were obtained with a Baird double beam instrument, Model AB2, using sodium chloride optics.

Trimethylaluminum and Lauric Acid Reactions

The trimethylaluminum was synthesized by the method of Pitzer and Gutowsky (18). The crude dimethyliodoaluminum from the methyl iodide and aluminum reaction was refluxed in a Todd-type column packed with stainless steel helices, and the trimethylaluminum formed by disproportionation was distilled under vacuum into glass ampoules and sealed. In all subsequent operations, the trimethylaluminum was transferred either by vacuum technique or under a nitrogen atmosphere. The I.R. spectrum of the trimethylaluminum was identical with one published previously (1); chemical analysis showed only trace amounts of iodine to be present; and hydrolysis with water vapor gave the required amounts of methane and aluminum.

Benzene and carbon tetrachloride were distilled in an efficient helix-packed 1-meter column. Most of the water was removed in the first few milliliters of distillate, but about 10% of the solvent was distilled to ensure complete dryness. Although traces of moisture would have caused immediate liberation of methane, there was no evidence of fuming or reaction when trimethylaluminum was dissolved in these solvents.

The lauric acid was Eastman Kodak white label, used without further treatment.

All reactions were run in an atmosphere of nitrogen dried with activated alumina and purified by passing over copper turnings at 400° C. in a tube furnace.

When the soap was prepared by adding trimethylaluminum to lauric acid, the required amount of acid was dissolved in benzene or carbon tetrachloride to make about 800 ml. of a 4% solution. This was transferred to the stillpot of a 1-meter Vigreux column fitted with nitrogen lines and activated-alumina towers; about 200 ml. of solvent was distilled off to dry the apparatus, solvent, and lauric acid; and trimethylaluminum was added dropwise to the lauric acid solution at reflux temperature. Samples were removed at regular intervals by hypodermic syringe for infrared analysis. Addition of trimethylaluminum was continued until the free fatty acid band at $5.85\ \mu$ could no longer be detected.

In the reverse reaction (acid added to trimethylaluminum) the trimethylaluminum was dissolved in predried solvent and the solution was transferred to the stillpot. Acid solution dried as above was added dropwise until the trimethylaluminum had all reacted.

The trilaurate was used in the experiments described below without further treatment as it was found by I.R. analysis that whenever the solvent was removed and the trisoap redissolved hydrolysis occurred from traces of residual moisture in the carefully dried

glassware and solvents. Very little water is required to produce detectable hydrolysis since 1 part of water reacts with about 36 parts (by weight) of aluminum trilaurate.

Aluminum Isopropoxide and Lauric Acid Reactions

The aluminum isopropoxide was made by the reaction of aluminum with isopropyl alcohol (17), vacuum distilled into weighed ampoules, and sealed. The other reagents have all been described above.

The apparatus and techniques used for these reactions were similar to those described above. Using the method of Mehrotra (14) the liberated isopropanol was removed very slowly by azeotropic distillation during reactions.

Infrared Observations

A typical trilaurate spectrum (2–16 μ) is shown in Fig. 1, while changes in the 5 to 7 μ region during reactions in which trimethylaluminum and aluminum isopropoxide were added to lauric acid are shown in Fig. 2. There is gradual disappearance of the 5.85 μ

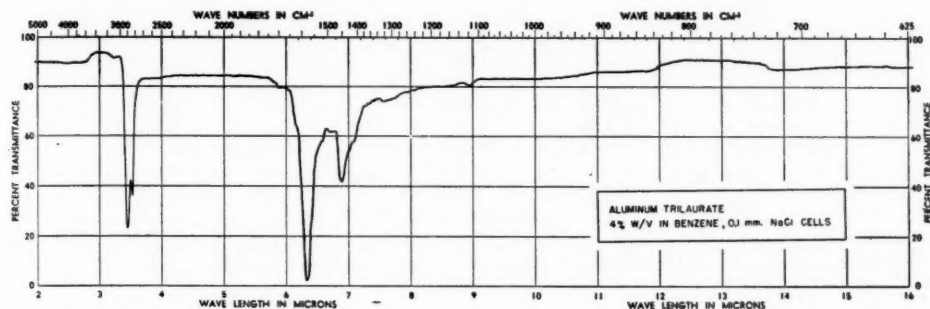


FIG. 1. Infrared spectrum of an aluminum trilaurate sample.

free fatty acid band and appearance and growth of a band at 6.33 μ . The small band appearing at 6.1 μ in the isopropoxide reaction mixture is not considered to disprove the equivalence of the trisoap formed by the two methods, because of the sensitivity of trisoap spectra to environmental conditions and history. As will be shown later the 6.33 μ band can shift to 6.1 μ by mere dilution. In Figs. 3 and 4 the optical densities (OD) of the major bands in the 5 to 7 μ region have been plotted as a function of the molar ratio of acid to aluminum. There is a gradual decrease in intensity of the acid band at 5.85 μ as the 6.33 μ band grows, until a molar ratio of 3:1 is reached. At this stage, which corresponds to section 5, Fig. 2, any increase in the aluminum reagent causes a decrease in the 6.33 μ band intensity and appearance and temporary growth of a 6.0 μ band. The latter band is attributed to a complex formed between the aluminum trilaurate and excess aluminum isopropoxide or trimethylaluminum. There are other variations in the 6.0 to 6.4 μ region which are small compared to those already mentioned.

In Fig. 4 results are given for acid added to trimethylaluminum or aluminum isopropoxide. Here also there is a gradual increase in the 6.33 μ band intensity. The 5.85 μ band makes its appearance after slightly less than 3:1 ratio of acid to aluminum has been attained, probably because of side reactions in which the aluminum compound reacts prematurely with aluminum trilaurate. The lauric acid-trimethylaluminum reaction is more complex because of coordination between trisoap and the large excess of trimethylaluminum. As suggested above, the effect is to suppress formation of the

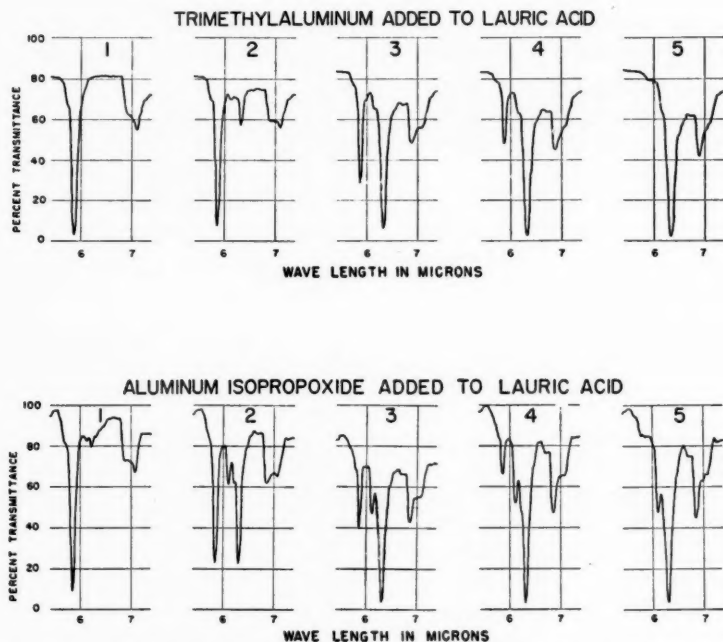


FIG. 2. I.R. spectra of reaction mixtures during addition of trimethylaluminum and aluminum isopropoxide to lauric acid in benzene. Spectra were of 4% solutions in 0.1 mm. NaCl cells.

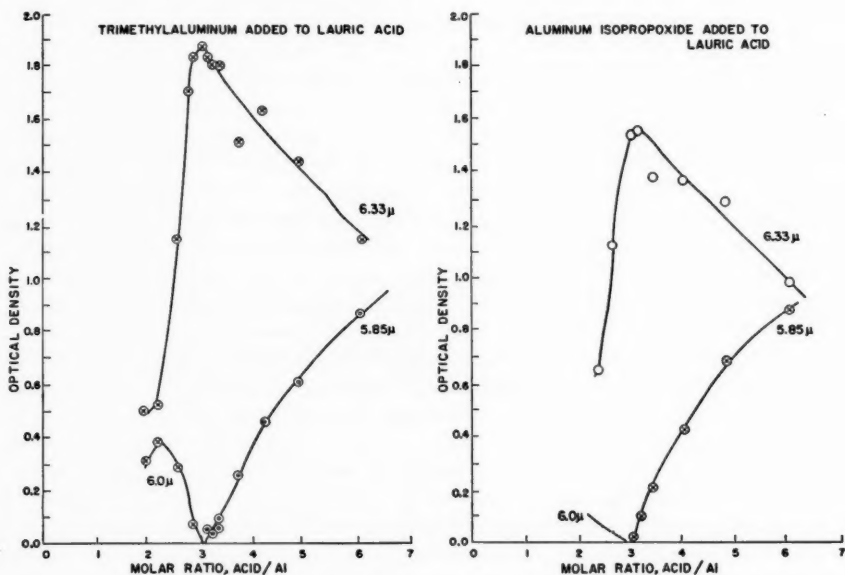


FIG. 3. Optical density during trimethylaluminum and aluminum isopropoxide addition to lauric acid in benzene.

6.33 μ band while favoring growth of a 6.1 μ band. In the case of this reaction in carbon tetrachloride the effect is exaggerated by the presence of HCl produced when trimethylaluminum reacts with the solvent, since bubbling HCl through either di- or tri-soap solution eliminates the 6.33 μ band and causes one to appear at shorter wavelengths (6.1–6.2 μ).

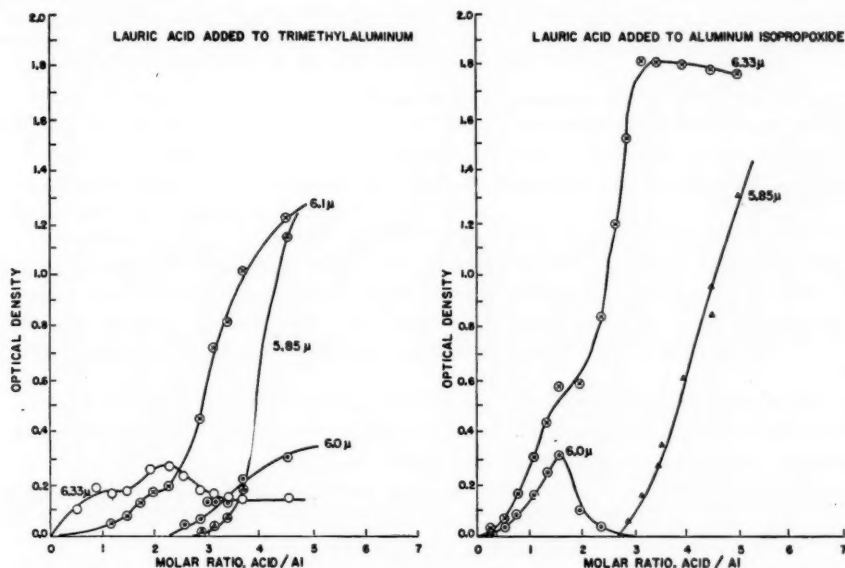


Fig. 4. Optical density during lauric acid addition to trimethylaluminum in benzene and aluminum isopropoxide in carbon tetrachloride.

Viscosity Studies

It was noticed that there was a gradual increase in viscosity of benzene or carbon tetrachloride solutions of aluminum trilaurate during trisoap synthesis. However, an excess of either aluminum isopropoxide or trimethylaluminum caused an immediate drop in viscosity.

The viscosity of the reaction mixture was followed using an ultrasonic viscometer (Model XVH Ultra-Viscoson, Rich-Roth Laboratories, Hartford, Conn.). The gold-plated probe used as the sensing element in this instrument was sealed to a standard ground-glass joint and inserted in the reaction flask. The viscometer was connected to a Brown chart recorder so that a continuous record of viscosity could be obtained.

Fig. 5 shows the variation of viscosity for reaction mixtures as the ratio of acid to aluminum is changed. There is a gradual rise in viscosity as aluminum isopropoxide or trimethylaluminum is added to lauric acid until the 3/1 acid/aluminum ratio is reached, after which there is a sudden fall. While the rise and subsequent fall in viscosity are more noticeable when aluminum reagent is added to lauric acid, this pattern also occurs when lauric acid is added to aluminum isopropoxide. The absence of this behavior in the case of lauric acid added to trimethylaluminum in carbon tetrachloride or benzene is probably due to the viscosity reducing effect of the large excess of trimethylaluminum. In the case of carbon tetrachloride solutions this effect would be augmented by the production of HCl, which prevents viscosity increase mainly by synthesis of non-thickening

chlorodisoap (16). In all other cases discussed, the fall in viscosity must be due to reduction of the trisoap micelle size, probably by coordination occurring between aluminum trilaurate and aluminum alkoxide or alkyl. This is also accompanied by the appearance of an absorption band at 6.0μ , which will be discussed later.

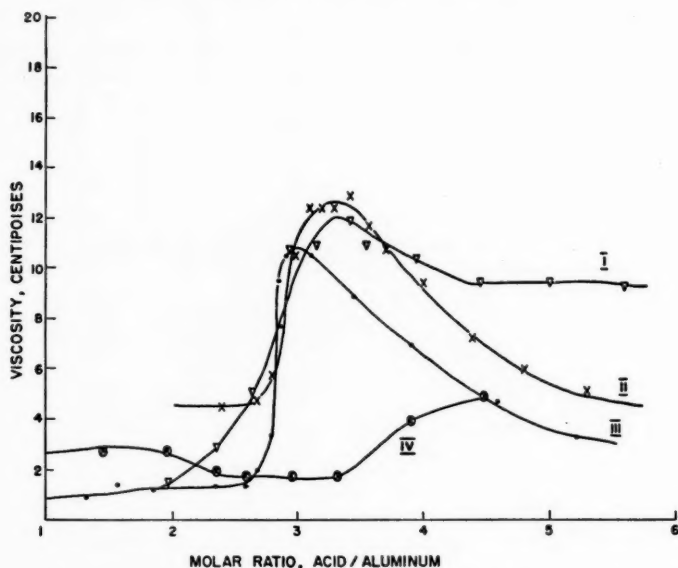


FIG. 5. Viscosity of reaction mixtures during trisoap synthesis: I—lauric acid added to aluminum isopropoxide; II—aluminum isopropoxide added to lauric acid; III—trimethylaluminum added to lauric acid; IV—lauric acid added to trimethylaluminum. All reactions are in carbon tetrachloride at approximately 4% concentration.

Experimental Conditions

During a series of reactions used to determine optimum conditions for trisoap synthesis, the following observations were made:

- (1) There is no apparent difference in behavior between reactions made with stearic acid and those made with lauric acid.
- (2) Aluminum isopropoxide is a superior starting material to aluminum ethoxide since the latter is not very soluble in benzene and cannot be purified by distillation.
- (3) Benzene is the best solvent tested for this reaction. Its freezing point is approximately 5°C ., which permits freeze-drying of the soap. All other solvents tested (carbon tetrachloride, hexane, heptane, and xylene) give very viscous solutions from which the trisoap is isolated only with difficulty and often forms hard gums. Xylene has a boiling point of 138°C . and there seemed to be slight decomposition during the synthesis reaction at reflux temperature. One shortcoming of benzene is the closeness of its boiling point to that of isopropanol-benzene azeotrope, so that a very efficient column is needed to remove the isopropanol from the reaction mixture.
- (4) It is important to employ solutions as concentrated as possible. Hydrolysis due to residual moisture on glassware, etc. will least affect the system when the quantity of soap is large. On the other hand, solutions become rather viscous at high concentrations

and soap is deposited on the wall of the reaction flask. Solutions giving trisoap concentrations of approximately 4 or 5% by weight can be used without undue difficulty.

(5) Although freeze-drying offers the best prospect for trisoap isolation, this technique can be used successfully only for pure trisoap or trisoap containing excess fatty acid. Even then, melting points of the solid trisoap are extremely variable with most values lying in the very broad temperature range 100–120° C. The experimental error in melting-point determinations is undoubtedly exaggerated by hydrolysis, producing traces of fatty acid which act as solvent for the trisoap.

(6) It is advantageous to add the aluminum compound to the lauric acid. This order of addition maintains a large excess of acid in the reaction vessel which should react immediately to give the trisoap. In the reverse addition, i.e. lauric acid added to aluminum reagent, there is high probability that intermediate compounds will be formed initially rather than trisoap.

(7) Variations in reflux time seem to have little effect on the reaction. There is, however, a detectable difference between the reaction product formed when isopropanol is removed continuously and that formed when isopropanol is refluxed for some time before being distilled. In the latter case there is production of ester (5.78 μ band) by an acid-isopropanol reaction and the water formed hydrolyzes the trisoap.

SUMMARY OF EVIDENCE FOR FORMATION OF ALUMINUM TRILAURATE

The addition of trimethylaluminum or aluminum isopropoxide to lauric acid in carbon tetrachloride or benzene under anhydrous conditions yields aluminum trilaurate. Although the aluminum soap produced gives a spectrum whose structural details (due to different types of polymer bonds) vary with concentration (see Fig. 6), it is a distinct

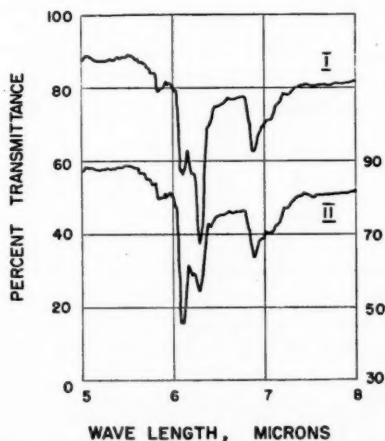


FIG. 6. Changes in I.R. spectra of aluminum trilaurate upon dilution from 4.5% w/v to 0.855% in benzene; curve I—10 minutes; Curve II—158 minutes.

compound and not a mixture of aluminum methyl dilaurate or aluminum isopropyl dilaurate and lauric acid. This is supported by the following evidence:

(1) The free fatty acid absorption band at 5.85 μ decreases on addition of the aluminum reagent and totally disappears when the theoretical amount necessary for trisoap formation has reacted.

(2) The absorption bands at $7.25\ \mu$ and $7.35\ \mu$ due to isopropyl CH deformation in aluminum isopropoxide disappear as the isopropyl alcohol produced in the reaction is distilled. This is also true of other characteristic isopropoxide and trimethylaluminum bands.

(3) The amount of methane produced in the trimethylaluminum - lauric acid reaction is the theoretical amount required for trisoap formation. It is realized, however, that the same amount of methane would be produced if there were water in the system, so this is offered only as corroboratory evidence.

(4) The end products obtained by the trimethylaluminum and aluminum isopropoxide reaction have similar infrared spectra.

(5) Hydrolysis of the trisoap immediately liberates free fatty acid as evidenced by the appearance of the $5.85\ \mu$ band. There is also the immediate appearance of an Al—O—Al band at $10.15\ \mu$ (19), showing that hydrolysis leads to disoap formation. Moreover, the viscosity increases as disoap is produced.

PROPERTIES OF ALUMINUM TRILAURATE

The aluminum trilaurate used in these studies was synthesized by adding trimethylaluminum to lauric acid.

1. Dilution with Dry Benzene

On diluting a benzene solution of aluminum trilaurate by the careful addition of specially dried and purified benzene it was found that the $6.33\ \mu$ band decreased in intensity and a band at $6.1\ \mu$ appeared. Table I gives the ratios of the opacities (I_0/I = the ratio of incident to transmitted energy) of these bands. The change from $6.33\ \mu$

TABLE I
INFRARED DATA ON BENZENE DILUTION OF ALUMINUM TRILAURATE

Conc., g./ml.	A	B	A/B
	I_0/I ($6.33\ \mu$)	I_0/I ($6.1\ \mu$)	
0.00757	2.93	1.23	2.38
0.00652	2.41	1.21	1.99
0.00564	1.98	1.19	1.66
0.00445	1.53	1.17	1.31
0.00367	1.28	1.18	1.08

to $6.1\ \mu$ is not instantaneous, but occurs at a rate and to an extent dependent on the degree of dilution. The data given in Table I are non-equilibrium values and are intended only to show qualitatively the initial behavior of these solutions on dilution. That no hydrolysis occurred during these dilution experiments is established by the complete absence of a $5.85\ \mu$ acid band, which would appear immediately.

Since interpretation of these results is considerably complicated by the successive stepwise additions of solvent, a simpler system comprising a single dilution was studied as a function of time using the properties measured by viscometry and I.R. spectroscopy. The results are recorded in Table II. Obviously the material is polymeric in nature and dilution reduces the size of the micelle.

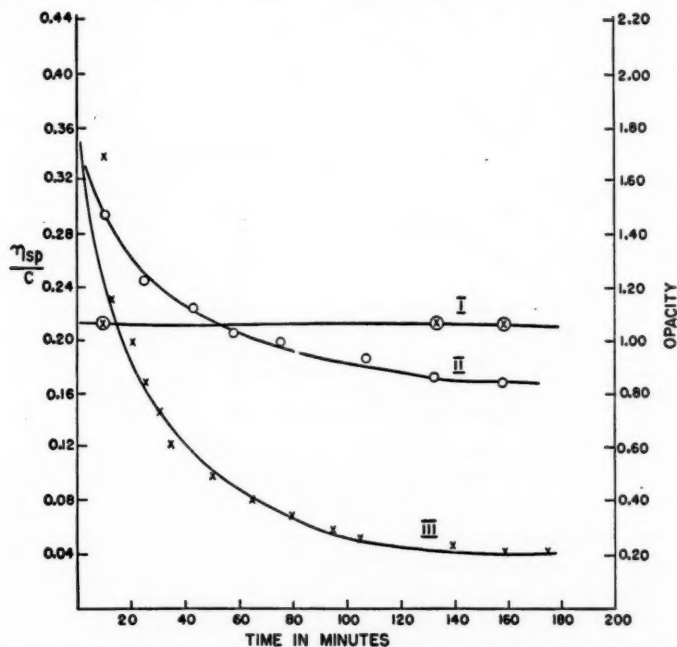
An attempt was also made to follow the degree of polymerization as a function of temperature. It was found that the changes in viscosity and I.R. absorption on dilution were indeed temperature dependent, being very much accelerated by a slight rise in temperature. It is hoped that from experiments still in progress reliable data may be obtained for calculating activation energies for these processes.

TABLE II

CHANGES IN VISCOSITY AND I.R. SPECTRA WITH TIME AFTER BENZENE DILUTION OF ALUMINUM TRILAURATE FROM 3.84% TO 0.77% W/V

Time, min. after dilution	A I_0/I (6.33 μ)	B I_0/I (6.1 μ)	A/B	η_{sp}/c^*
5				0.296
8	2.39	1.23	1.94	
14	2.24	1.25	1.79	0.249
20	2.15	1.25	1.72	0.224
30	2.02	1.27	1.59	0.187
40	1.98	1.31	1.51	0.166
54	1.91	1.35	1.42	0.143
77	1.83	1.36	1.35	0.114
107	1.76	1.40	1.26	
120				0.078
206	1.54	1.51	1.02	0.048

NOTE.—A, B, measured in 0.2 mm. cells, NaCl optics.

* η_{sp}/c , specific viscosity divided by concentration; $c = 0.77$ g./100 ml.FIG. 7. Opacity of various I.R. absorption bands and η_{sp}/c as a function of the time elapsed after dilution: I—opacity of 5.85 μ band; II—ratio of 6.33 μ /6.14 μ band opacities; III— η_{sp}/c .

A 4.5% w/v solution of aluminum trilaurate was diluted with specially dried benzene to 0.855% w/v. Part of this solution was placed in an Ostwald viscometer and its viscosity measured at regular intervals. Changes in the I.R. spectra in the 5 to 7 μ region are given in Fig. 6 while the variations of η_{sp}/c^* and I.R. spectral data for this solution with time are shown in Fig. 7. The 5.85 μ band indicates no increase in the small amount of lauric acid present at the start of the experiment, and therefore no hydrolysis.

*Reduced viscosity = η_{sp}/c , where $\eta_{sp} = \frac{\eta_{\text{solution}} - \eta_{\text{solvent}}}{\eta_{\text{solvent}}}$ and $c = \text{concentration in g./100 ml.}$

The above changes in viscosity and I.R. spectra are thought to be due to a change in the coordination of the carbonyl group and the aluminum atom, and will be discussed in a later section. The drop in viscosity is not instantaneous on dilution and corresponds to a slow breakdown in size of the polymer units.

2. Dilution with Wet Benzene

The benzene used for these dilutions was saturated by distilling with an excess of water and then pipetted into the solution, care being taken that no water droplets were carried over. Infrared and light-scattering data were obtained after each addition. The light-scattering photometer used has been described in a previous publication (8).

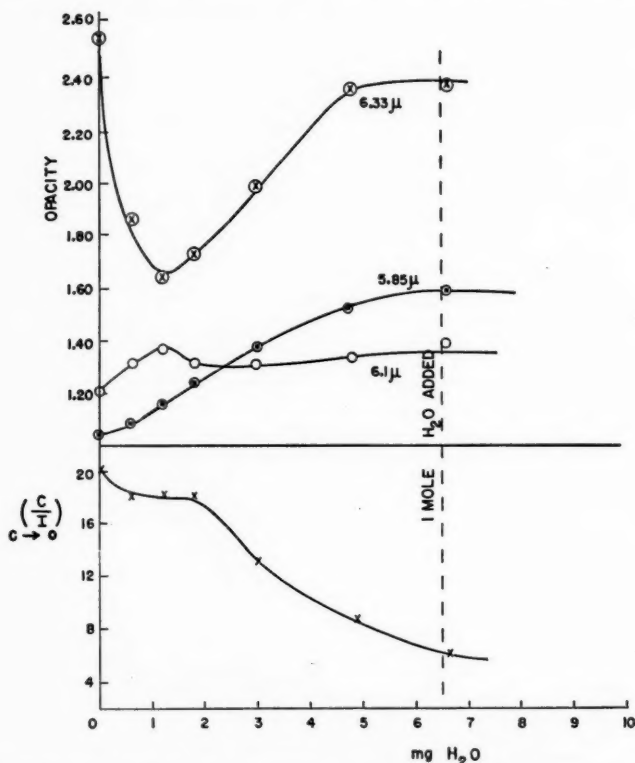


FIG. 8. Opacity of various I.R. bands and $(C/I)_{c \rightarrow 0}$ as a function of the amount of water added to a 0.5% solution of aluminum trilaureate in benzene. I.R. cells were 0.2 mm. NaCl.

These data are plotted in Fig. 8, where each point on the curve represents an addition of water-saturated benzene. The I.R. spectra of the diluted solutions were normalized by reference to the 3.42μ C—H stretching band. The original decrease in the 6.33μ and increase in the 6.1μ band are attributed to the dilution effect discussed above. The light-scattering data are given for qualitative comparison only.* No attempt has been made to calculate precise molecular weight (Mw) values because of the uncertainties

*The light-scattering term used in Fig. 8 is $(C/I)_{c \rightarrow 0}$, the ratio of concentration to reduced intensity at infinite dilution. This is an inverse function of molecular weight.

involved in the measurements of refractive index in a non-equilibrium system, but a marked increase in M_w is evident.

In an effort to separate the viscosity effects of hydrolysis and dilution the following experiment was performed. A 4.5% w/v aluminum trilaurate solution was diluted with wet benzene to give a 0.5% w/v solution, and viscosity was measured as a function of time, giving Curve I in Fig. 9. An initial drop in viscosity occurred in conformity with the dry benzene dilution behavior shown in Fig. 7, followed by a gradual increase as the trisoap hydrolyzed. To eliminate the early dilution effect some 4.5% w/v solution was diluted with dry benzene to 0.69% w/v before further dilution to 0.5% w/v, this time with wet benzene containing the amount of water required for complete hydrolysis

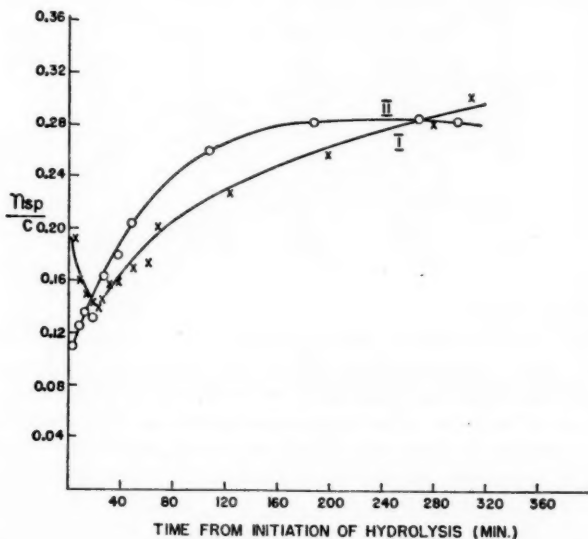


FIG. 9. η_{sp}/c of freshly hydrolyzed aluminum trisopon solutions: I—4.5% solution diluted to 0.5% with wet benzene; II—0.69% solution diluted to 0.5% with wet benzene.

Curve II (Fig. 9) shows the viscosity-time pattern following the final addition. The reduced viscosity, which had been about 0.19 before dry dilution, dropped to 0.10 on equilibration. Final dilution with wet benzene produced an increase in viscosity as the trisoap was hydrolyzed to disoap. After about 5 hours the viscosity reached a maximum which was about the same for both solutions. If the viscosity of these solutions had been followed further there would have been a gradual drop corresponding to breakdown of disoap polymer, as reported previously (20).

The effects of wet dilution were also followed with I.R. absorption (see Table III). As shown by the immediate appearance of the 5.85μ acid band, the hydrolysis reaction was extremely rapid, being complete within the 45 seconds required for preparing the mixtures and measuring their spectra. The very rapid completion of all I.R. spectral changes was in contrast to the slow increase in viscosity.

The slight decrease in the 6.33μ band intensity for the 285-minute observation is probably due to the very slow breakdown of the disoap micelles. Except for this change

in the 6.33μ band and the appearance of a shoulder at 6.2μ all other variations are so slight that they could easily be due to errors in reading charts, etc.

There are no changes in I.R. spectra in the 5.8 to 6.4μ region corresponding to increased viscosity on hydrolysis. This is not surprising since the change in absorption due to the relatively few bonds necessary to explain the rise in viscosity might be well beyond the limits of sensitivity of the I.R. method.

TABLE III
OPACITY (I_0/I) FOR VARIOUS ABSORPTION BANDS

Time, min.	Absorption bands			
	5.85μ	6.1μ	6.33μ	10.15μ
Hydrolysis of 1.35% w/v solution				
1	1.43	1.29	3.84	1.16
5	1.40	1.30	3.81	1.18
12	1.42	1.31	3.81	1.15
30	1.41	1.33	3.64	1.17
75	1.41	1.35	3.72	1.15
135	1.43	1.35	3.64	1.14
Hydrolysis of 0.5% w/v solution				
0.75	1.20	1.03	2.00	1.07
7	1.20	1.04	2.00	1.06
300	1.21	0.03	2.04	1.07

3. Hydrogen Bonding Region

Studies in the 2.5 to 3.0μ region (OH stretching) were made to determine whether hydrogen bonding plays an appreciable role in the viscosity increase on wet-solvent dilution of trisoap. Solutions were prepared in carbon tetrachloride (chosen for its transparency) by removal of benzene under vacuum and addition of dry carbon tetrachloride with a hypodermic syringe to obtain the required soap concentration. The solutions were then further diluted with wet carbon tetrachloride, and samples were placed in the viscometer and in a 1 cm. path length I.R. cell. Fig. 10 gives the changes in η_{sp}/c and opacity of the 2.67μ band, and Fig. 11 the actual spectra in this region.

There is a gradual increase in viscosity with time, paralleling an increase in absorption at 2.67μ . Absorption in this region is normally assigned to non-hydrogen bonded OH, and there is no reason to suspect a different assignment in this instance. However, it is necessary to account for this viscosity-absorption correlation since it seems to run counter to the concept that hydrogen bonding is of any significance in building the soap polymer in this system. Two possible explanations for the phenomenon are offered:

(1) The acid produced by hydrolysis is initially hydrogen bonded to the disoap OH, but on standing transfers gradually into the solvent. Thus the free OH increases slowly,

H

as the acid emerges and the polymer builds up by Al—O—Al coordination. During this process there is a decrease in absorption at 2.9μ , corresponding to a decrease in bonded OH concentration.

(2) Initially, when the disoap is produced by hydrolysis, intramolecular hydrogen bonding of OH and carbonyl oxygen occurs. On standing, the hydrogen bond breaks and the carboxylate groups bond intermolecularly by coordination, thus building up the polymer chain, again accounting for the spectral and rheological behavior observed.

In the hydrolysis studies a band appeared immediately at 2.82μ . This was suspected

of being due to OH absorption from the fatty acid monomer, and this possibility was verified by observing the spectra of lauric acid - carbon tetrachloride solutions diluted in 10-fold steps from a concentration of 3% to 0.003% w/v. By comparing band intensities relative to the $3.42\ \mu$ CH absorption it was found on dilution that the $2.82\ \mu$ band increased and the $5.85\ \mu$ carbonyl band split into a doublet, the $5.7\ \mu$ branch of which became progressively more prominent. These observations are compatible with dissociation of the fatty acid dimer on dilution.

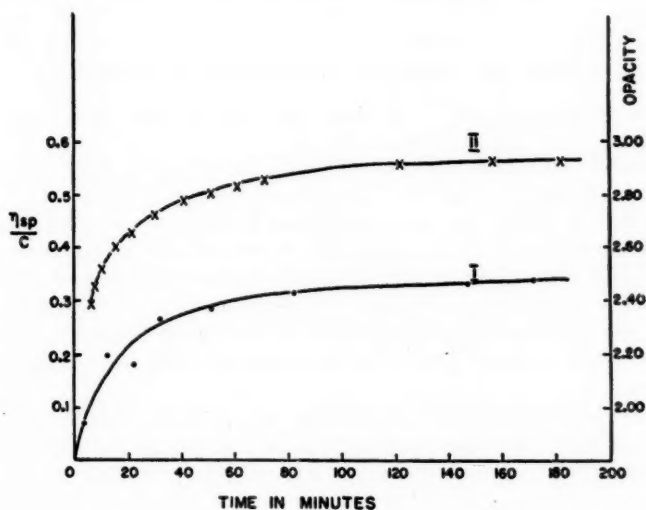


FIG. 10. η_{sp}/c and opacity of the $2.67\ \mu$ band in carbon tetrachloride solution: I— η_{sp}/c ; II—opacity of $2.67\ \mu$ band measured in 1 cm. NaCl cells.

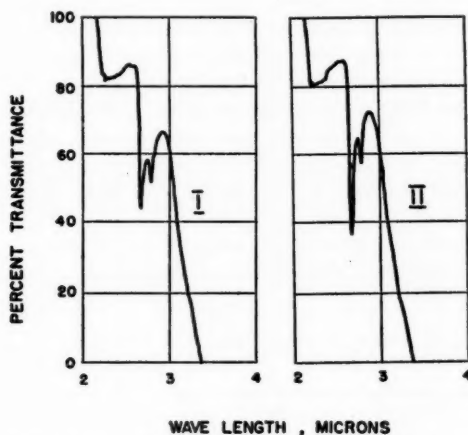


FIG. 11. I.R. spectra of aluminum trilaurate 3 minutes after hydrolysis (I) and 247 min. later (II) Solution of 0.3% w/v in carbon tetrachloride in 1 cm. NaCl cells.

STRUCTURE OF ALUMINUM SOAPS

It is evident from the spectra of aluminum trilaurate solutions in non-polar solvents that carbonyl absorption bands can appear at any of several positions within the 6.0 to 6.4 μ range. For example, the prominent 6.33 μ band in concentrated solutions shifts to 6.1 μ in dilute solutions and under certain conditions there are also strong bands at 6.2 and 6.0 μ . It is proposed in this section to correlate these bands with possible soap structures, using viscosity and other supporting data where appropriate.

Lecomte and co-workers (3) have shown that the carboxylate groups in acetates,

formates, fatty acid soaps, etc., should not be considered as having a $\text{—}\overset{\text{O}}{\underset{\text{O}}{\text{C}}}\text{—}$ structure, but rather the structure $\left[\text{—}\overset{\text{O}}{\underset{\text{O}}{\text{C}}} \right]^-$ where the two oxygen atoms are equivalent.

The antisymmetrical carbonyl vibration of the latter structure gives rise to absorption in the 6.0 to 6.4 μ region.

A carboxylate-type bridge has been postulated at various times to explain physico-chemical properties of coordination compounds. A recent paper by Honig and Singletary (9) reviews this type of bonding and applies it to alkali and alkaline-earth phenylstearates. Küntzel (10) has proposed an analogous structure for fatty acid - chromium complexes. In discussing the mechanism of peptization of aluminum soap - hydrocarbon gels, Bauer *et al.* (19) have assumed a structure in which the carboxylate radicals bridge the aluminum atoms.

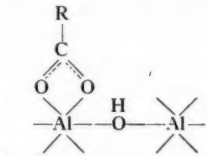
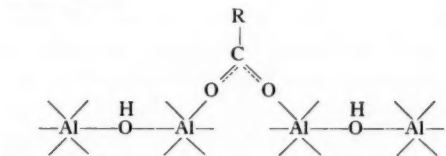
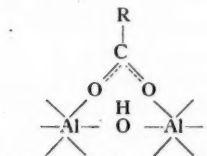
In this paper the hypothesis of carboxylate groups being able to coordinate with aluminum atoms, both intra- and inter-molecularly, is used to explain the spectral and rheological properties of various aluminum soap solutions. In spite of the complexity and variations of spectra in the 6.0 to 6.4 μ region it is possible to offer a reasonable physical picture in support of the assignments given in Tables IV and V.

Structure A represents an intramolecularly bonded fatty acid carboxylate group. In the case of trisoap monomer three such groups occur in each molecule and these are assigned to the higher frequency carbonyl 6.1 μ band since it predominates on trisoap dilution as the most independent (undamped) state is approached. The lower frequency 6.33 μ band is assigned to carboxylate bridge structure B, in which damping of the carbonyl vibration would be maximal. With this type of structure the carboxylate radicals become polymer building links in the same manner as the hydrogen bridges described

TABLE IV
CARBOXYLATE COORDINATION BONDS IN ALUMINUM TRILAURATE

Model		Carbonyl assignment
	Structure A—Intramolecular coordination with one Al atom	6.1 μ
	Structure B—Coordination bridge between two Al atoms	6.33 μ

TABLE V
CARBOXYLATE COORDINATION BONDS IN ALUMINUM DILAURATE

Model	Carbonyl assignment	Molecular weight
 <p>Structure C</p>	6.22 μ	ca. 100,000
 <p>Structure D1</p>	6.33 μ	>1,000,000
 <p>Structure D2</p>	6.33 μ	

by Coulson for aluminum hydride (2). A somewhat analogous shift occurs with acetylacetone, the absorption band moving from 6.04 μ to 6.28 μ on coordination with aluminum in aluminum acetylacetonate (4).

Analogous assignments for aluminum dilaurate are shown in Table V. The molecular weight values given in this table are only very rough approximations for molecular aggregates in which the suggested type of bonding is thought to predominate. The bonding shown in structure C is intramolecular and therefore the difference between the assignment for it (6.2 μ) and that for structure A (6.1 μ) is due to the influence of the OH group on the aluminum-carboxylate bond strength.

The bridge-type links between adjacent atoms described by Bauer (structure D (19)) are assigned to the 6.33 μ band. It is of course coincidental that structures B and D have the same absorption frequencies, but experimentally there is no observable shift in the band position on hydrolysis of the trisoap to disoap. The inference is that although the strength of the aluminum-carboxylate bonds is altered by the OH bridge in structure D, the effect of this group on Al-Al distances is a compensating one and accounts for the identity of the carbonyl absorption frequencies. Structures D1 and D2 are postulated to have similar carbonyl spectra, but D2-type molecules would be linear whereas D1-type would contain crosslinks and give the gel formation observed even at relatively low soap concentrations.

These assignments are consistent with the behavior of aluminum dilaurate on degradation. It is well established that freshly prepared aluminum dilaurate has a 6.33 μ

carbonyl band (19), and that aluminum soap solutions are not stable but exhibit decreasing viscosity and molecular weight on aging (20). It has been found in the present study that during degradation of disoap solutions the $6.33\ \mu$ band decreases while a $6.22\ \mu$ band appears and grows. Fig. 12 shows spectra of disoap solutions before and after degradation by moisture absorbed from a saturated atmosphere. Fig. 13 shows the optical density of the $6.33\ \mu$ and $6.22\ \mu$ bands as a function of molecular weight, determined by light-scattering, at intervals during the aluminum disoap micelle breakdown. Before optical measurements were made the solutions were dried by azeotropic dis-

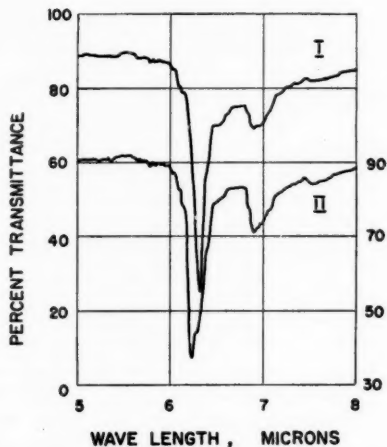


FIG. 12. I.R. spectra of aluminum dilaurate before (I) and after (II) degradation. Solution of 1.0% w/v in benzene in 0.2 mm. NaCl cells.

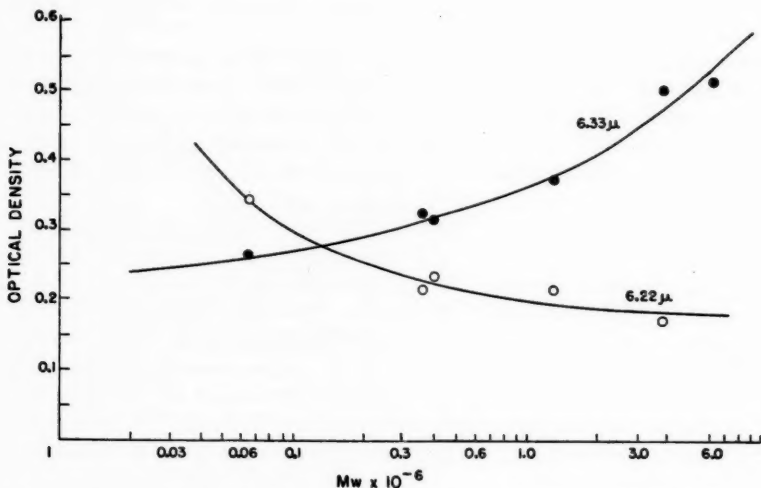


FIG. 13. Optical density of $6.33\ \mu$ and $6.22\ \mu$ bands as a function of molecular weight.

tillation. Structure C (similar to that of Gray and Alexander (7)) is proposed for the lower molecular weight material corresponding to the 6.22μ band.

H

There is little change in the Al—O—Al (10.15μ) band during micelle breakdown, but it has been found that the absorption intensity is somewhat sensitive to water concentration. It varies inversely with the amount of water added to the solution, returning reversibly to its original value when the water is completely removed.

Hydrochlorination of aluminum trilaurate in benzene by bubbling dry HCl through the soap solution produces an immediate decrease in the 6.33μ band intensity. As this band becomes smaller a new band at 6.1μ is formed, the 5.85μ acid band appears, and there is a drop in viscosity similar to that observed on hydrochlorinating dilaurate

H

solution (20). No Al—O—Al absorption occurs at 10.15μ , however, showing that there is no hydrolysis. Since the chlorodisoap thus produced is a non-thickener, its high frequency carbonyl absorption is analogous to that assigned to the non-bridged form of trisoap (structure A). Aluminum chlorodilaurate synthesized by the method of Mysels (16), also a non-thickener, produces the same band.

A slight excess of trimethylaluminum in aluminum trilaurate solutions causes the appearance of an absorption band at 6.0μ , probably because coordination of the alkylate with the trisoap weakens the coordination bond between carbonyl radicals and aluminum atoms. Thus the carbonyl vibrations are damped even less than in structure A and the absorption appears at shorter wavelength. If conditions are such that reaction occurs between trimethylaluminum and trisoap producing methyl disoap, e.g. large excess of trimethyl or reflux temperature, the 6.0μ band disappears.

There are also small bands or weak shoulders which appear in the 6.0 to 6.4μ region, which is not at all surprising considering the variety of molecular species possible with the bond structures shown in Tables IV and V. However, the main spectral features are those dealt with in this paper, and no attempt has been made to explain the secondary inflections in detail.

All spectra of aluminum trilaurate solutions in carbon tetrachloride have strong absorption bands in the 6.7 to 7.2μ region due to symmetrical carboxylate vibrations but this region has not been studied seriously because of the strong background absorption from C—H deformation vibrations.

ACKNOWLEDGMENTS

The authors wish to thank Dr. H. J. Bernstein, National Research Council, Ottawa, for helpful discussions, and Messrs. W. Barnes and A. Grey of the Defence Research Chemical Laboratories for technical assistance.

REFERENCES

1. A.P.I. Project 44. Spectrum No. 1201.
2. COULSON, C. A. Valence. Oxford Univ. Press, London. 1952. p. 321.
3. DUVAL, C., LECOMTE, J., and DOUVILLÉ, F. *Ann. phys.* **17**, 5 (1942).
4. DUVAL, C., FREYMAN, R., and LECOMTE, J. *Bull. soc. chim. France*, 103 (1952).
5. GILMOUR, A., JOBLING, A., and NELSON, S. *J. Chem. Soc.* 1972 (1956).
6. GLAZER, J., MCROBERTS, T. S., and SCHULMAN, J. H. *J. Chem. Soc.* 2382 (1950).
7. GRAY, V. R. and ALEXANDER, A. E. *J. Phys. Colloid Chem.* **53**, 923 (1949); *Proc. Roy. Soc. A*, **200**, 162 (1950).
8. HADOW, H. J., SHEFFER, H., and HYDE, J. C. *Can. J. Research, B*, **27**, 791 (1949).
9. HONIG, J. G. and SINGLETERRY, C. R. *J. Phys. Chem.* **60**, 1114 (1956).

10. KÜNZEL, A., ERDMANN, H., and SPAHRKÄS, H. *Das Leder*, **4**, 73 (1953); **3**, 30 (1952). cf. *Chem Abstr.* **47**, 12087f (1953); **46**, 5479g (1952).
11. LAWRENCE, A. S. C. *J. Inst. Petroleum Technol.* **24**, 207 (1938).
12. MCBAIN, J. W. and McLATCHIE, W. L. *J. Am. Chem. Soc.* **54**, 3266 (1932).
13. MCGEE, C. J. *J. Am. Chem. Soc.* **71**, 278 (1949).
14. MEHROTRA, R. C. *Nature*, **172**, 74 (1953).
15. MEHROTRA, R. C. and PANDE, K. C. *J. Inorg. and Nuclear Chem.* **2**, 60 (1956).
16. MYSELS, K. J. and CHIN, D. M. *J. Am. Chem. Soc.* **75**, 1750 (1953).
17. *Newer methods of preparative organic chemistry*. Interscience Publishers Inc., New York. 1948.
18. PITZER, K. S. and GUTOWSKY, H. S. *J. Am. Chem. Soc.* **68**, 2204 (1946).
19. SCOTT, F. A., GOLDENSON, J., WIBERLY, S. E., and BAUER, W. H. *J. Phys. Chem.* **58**, 61 (1954).
20. SHEFFER, H. *Can. J. Research, B*, **26**, 481 (1948).

EQUILIBRIUM CONSTANTS FOR THE SULPHUR ISOTOPE EXCHANGE BETWEEN SO_2 AND H_2SO_4 ¹

H. B. DUNFORD,² A. G. HARRISON, AND H. G. THODE

ABSTRACT

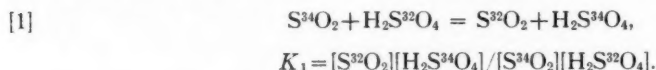
The S^{32} – S^{34} isotope exchange between sulphur dioxide and 100% sulphuric acid has been studied over the temperature range 200° to 400° C. Equilibrium constants of 1.014, 1.011, and 1.008 at 205°, 300°, and 400° C. respectively have been found, favoring the S^{34} in the sulphuric acid. These results agree reasonably well with theoretical calculations made for the sulphur isotope exchange between sulphate ion and sulphur dioxide.

INTRODUCTION

Increasing interest is being shown in the application of isotope abundance measurements to chemical and geological problems. Many such problems can be resolved if it can be assumed that thermodynamic equilibrium has been attained (2).

Tudge and Thode (9) have calculated theoretical equilibrium constants for a large number of sulphur isotope exchange reactions in inorganic systems. However, only in a few cases has it been possible to realize conditions permitting isotopic exchange in the laboratory for confirmation of the theoretical calculations. On the other hand, certain isotopic exchange constants have been determined experimentally, but calculations have not been possible because of the lack of suitable spectroscopic data on the molecules concerned. For example, the equilibrium constant for the sulphur isotope exchange between sulphur dioxide and the bisulphite ion has been measured at room temperature (8), as has the equilibrium constant for the hydrogen sulphide – sulphhydryl ion exchange (9); but spectroscopic data for the bisulphite and sulphhydryl ions are not as yet available. Finally, the characteristic vibrational frequencies for the sulphite ion in solution have been reported (3), and the calculated equilibrium constants involving the sulphite ion will be reported in a forthcoming paper.

Recently the sulphur isotope exchange between sulphur dioxide and concentrated sulphuric acid was studied over the 100°–210° range using S^{35} tracer techniques (6). The half-time for complete exchange was reported to be 7.5 hours at 210° C. Since this exchange was found to take place at a reasonable rate it was decided to measure the equilibrium constant (K_1) at various temperatures for the exchange reaction



Equilibrium constants (K_2) for the reaction



were calculated and compared with the experimental results for reaction [1].

EXPERIMENTAL

Preparation of Reagents

Sulphur dioxide was obtained from the combustion in a quartz tube of a metallic sulphide of known $\text{S}^{34}/\text{S}^{32}$ ratio. The sulphur dioxide was condensed out of the oxygen

¹Manuscript received April 15, 1957.

Contribution from Department of Chemistry, McMaster University, Hamilton, Ontario.

²Present address: Department of Chemistry, Dalhousie University, Halifax, Nova Scotia.

stream used for combustion in traps cooled with liquid air. It was then thoroughly degassed and distilled through a trap cooled with dry ice - acetone to remove any moisture.

Sulphuric acid of 100% strength was made up on the basis of the minimum assay of C. P. conc. sulphuric acid (C.I.L.) and C. P. fuming sulphuric acid (Fisher Scientific). In order to obtain the sulphur isotope ratio of the 100% acid, two 1-drop samples were reduced quantitatively to hydrogen sulphide (7), converted to silver sulphide, and then burned as outlined above. The sulphur dioxide was stored for mass spectrometric analysis.

Procedure for a Typical Sample

A 5-ml. portion of the 100% acid was pipetted into a Pyrex break-seal sample tube of approximately 20 ml. capacity. The sample tube was then immediately sealed to a manifold. The acid was thoroughly degassed and frozen, after which approximately 10 ml. of sulphur dioxide at S.T.P. was admitted from a Toepler pump. The sample tube was then sealed off and heated to an appropriate temperature. After exchange equilibrium was assumed to have been reached, the sample tube was resealed to a manifold and opened by means of a magnetically operated breaker. Sulphur dioxide from the sample tube containing the acid (maintained at room temperature with one exception) was condensed into a second sample tube and stored for mass spectrometric analysis.

Temperature Control

Two sample tubes were heated in refluxing benzyl alcohol ($235^{\circ} \pm 2^{\circ}$), and four others in a small combustion furnace, two at 300° and two at $400^{\circ} (\pm 5^{\circ})$.

Mass Spectrometry

Samples were analyzed on a simultaneous collection mass spectrometer, designed especially to collect the two species $S^{32}O_2$ and $S^{34}O_2$. Details of construction and operation are described elsewhere (12).

Calculations

Simplified partition function ratios $Q_{S^{34}O_2}/Q_{S^{32}O_2}$ and $Q_{S^{34}O_4^-}/Q_{S^{32}O_4^-}$, which have been calculated at 0° and 25° (9), were recalculated at 200° , 300° , and 400° C. using well-known statistical methods (1, 10).

RESULTS AND DISCUSSION

The assignment of the nine fundamental vibration frequencies of the $H_2S^{32}O_4$ molecule appears to be reasonably certain (4, 5); however, until the force equations of the XY_2Z_2 type symmetry, characteristic of sulphuric acid, are worked out, it will not be possible to calculate the shift in the vibrational frequencies caused by S^{34} substitution and therefore it is not possible to calculate the equilibrium constant for equation [1]. Since one would not expect the isotopic shift for sulphuric acid to differ greatly from that found for the sulphate ion and since the calculated partition function is much more dependent on the isotopic shift than the absolute values of the vibrational frequencies, we have calculated in Table I equilibrium constants for the sulphur dioxide - sulphate ion system (equation [2]). These should compare reasonably well with equilibrium constants for equation [1].

There can be no doubt that complete exchange occurred. The original sulphur dioxide was over 1% enriched in S^{34} compared to the sulphuric acid, but the final sulphur dioxide samples were depleted in S^{34} by an average of about 1% with respect to the acid.

TABLE I

CALCULATED EQUILIBRIUM CONSTANTS FOR THE SULPHUR ISOTOPE EXCHANGE BETWEEN SO_2 AND SO_4^{2-}

$Q_{\text{S}^{34}\text{O}_4^{2-}}/Q_{\text{S}^{32}\text{O}_4^{2-}}$	$Q_{\text{S}^{34}\text{O}_2}/Q_{\text{S}^{32}\text{O}_2}$	K_2	Temperature ($^{\circ}\text{C}.$)
1.039	1.021	1.0176	200
1.028	1.016	1.0118	300
1.021	1.012	1.0088	400

It was noted that only about half of the sulphur dioxide was recovered after exchange was completed, presumably because of its solubility in sulphuric acid. Two samples of sulphur dioxide were prepared to test for the possibility of isotope fractionation caused by incomplete recovery of sulphur dioxide. One sample was recovered from over the acid in the usual way and the other was recovered by heating the same sulphuric acid with boiling water to drive off dissolved sulphur dioxide. A difference in the $\text{S}^{34}/\text{S}^{32}$ ratio for the two samples of 0.1% was noted, which is about the limit of accuracy of the determination. Therefore, no correction was applied. Urey and Thode, in testing for simple methods of fractionating isotopes, found that solvent effects gave negligible fractionation (11).

As the acid was present in about 200-fold excess over the sulphur dioxide, it was assumed that the $\text{S}^{34}/\text{S}^{32}$ ratio of the acid was unaffected by the exchange reaction, so that experimental equilibrium constants were obtained for equation [1] using the original $\text{S}^{34}/\text{S}^{32}$ ratio of the acid.

No correction was applied for the exchange of oxygen isotopes between sulphuric acid and sulphur dioxide. Urey has shown that the equilibrium constant for $\text{O}^{16}-\text{O}^{18}$ exchange between sulphur dioxide and sulphate ion is in the range 0.999–1.001 between 400° and 600° K. (10). The oxygen isotope content of the acid would therefore be nearly identical with that of the sulphur dioxide.

It can be seen from the results of Table II that in all cases there is fair agreement between the experimental results for sulphuric acid and the calculated results for sulphate ion; the agreement is better at the higher temperatures. If it were possible to calculate the equilibrium constant for the sulphuric acid – sulphur dioxide system, closer agreement with the experimental results might be expected.

TABLE II

ENRICHMENT FACTORS $(K-1)100$ FOR $\text{S}^{34}/\text{S}^{32}$ EXCHANGE BETWEEN SO_2 AND H_2SO_4 (EXPERIMENTAL) AND SO_2 AND SO_4^{2-} (THEORETICAL)

Temperature ($^{\circ}\text{C}.$)	Exchange time (days)	Enrichment factor	
		Experimental	Theoretical
205	9	1.42	1.76
	16	1.44	
300	5	1.08	1.18
	7	1.08	
400	2	0.76	0.88
	3	0.88	

ACKNOWLEDGMENT

Grateful acknowledgment is made to the National Research Council for financial support of this work and the award of a studentship to A.G.H.

REFERENCES

1. BIGELEISEN, J. and MAYER, M. G. *J. Chem. Phys.* **15**, 25 (1947).
2. CRAIG, H. *Geochim. et Cosmochim. Acta*, **6**, 186 (1954).
3. EVANS, J. C. and BERNSTEIN, H. J. *Can. J. Chem.* **33**, 1270 (1955).
4. FENEANT, S. *Mem. services Chim. état (Paris)*, **34**, 307 (1948).
5. HIBBEN, J. H. *The Raman effect and its chemical applications*. Reinhold Publishing Corporation, New York, 1939.
6. NORRIS, T. H. *J. Am. Chem. Soc.* **72**, 1220 (1950).
7. PEPKOWITZ, L. P. and SHIRLEY, E. L. *Anal. Chem.* **2**, 1709 (1951).
8. THODE, H. G., GRAHAM, R. L., and ZEIGLER, J. A. *Can. J. Research, B*, **23**, 40 (1945).
9. TUDGE, A. P. and THODE, H. G. *Can. J. Research, B*, **28**, 567 (1950).
10. UREY, H. C. *J. Chem. Soc.* 562 (1947).
11. UREY, H. C. and THODE, H. G. Unpublished results.
12. WANLESS, R. K. and THODE, H. G. *J. Sci. Instr.* **30**, 395 (1953).

SENSITIZED PHOTOIONIZATION¹

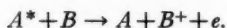
IKUZO TANAKA² AND E. W. R. STEACIE

ABSTRACT

The krypton photosensitized ionization of nitric oxide and acetone has been investigated. At constant nitric oxide pressure, the relation between ion current and krypton pressure is given by $i = a + b(1 - e^{-cp})$, where i is the ion current, a , b , and c are constants, and p is the krypton pressure. It has been further shown that the quenching cross section of nitric oxide for excited krypton is smaller than that of acetone. Sensitized photoionization was also obtained in the cases of xenon and anisole, and argon and nitric oxide. The quenching of excited krypton by helium, hydrogen, and deuterium has been studied. Helium quenches to a negligible extent; the quenching efficiency of hydrogen is rather greater than that of deuterium.

INTRODUCTION

Preliminary sensitized photoionization experiments (5) with nitric oxide and krypton gas using a krypton resonance lamp showed that the following process occurred:



A is an atomic species such as krypton and A^* is a state of A which has been excited by absorbing the resonance line of A . B , whose ionization potential is lower than the energy of the resonance line of A , is a molecular species such as nitric oxide.

In the present work nitric oxide and acetone were examined under various conditions using krypton photosensitization. Sensitized photoionization was also obtained with the xenon and argon resonance lines. The ionization potentials of several substances, as measured by Watanabe (6), and the energies of the resonance lines of argon, krypton, and xenon atoms are listed in Table I. Anisole was used as a substrate for measuring xenon photosensitization and nitric oxide was used for argon photosensitization.

TABLE I

Xenon	1470 Å = 8.40 ev., 1295 Å = 9.53 ev.
Krypton	1235 Å = 10.0 ev., 1165 Å = 10.6 ev.
Argon	1067 Å = 11.6 ev., 1048 Å = 11.8 ev.
Anisole	8.20 ± 0.02 ev.
Nitric oxide	9.25 ± 0.02 ev.
Acetone	9.69 ± 0.01 ev.

If some substance which does not absorb at the wavelength of the resonance line of krypton, for example hydrogen or deuterium, is added to the mixture of nitric oxide and krypton, the krypton atoms which have been excited by absorption of the resonance line of krypton may be quenched by the hydrogen or deuterium. In order to investigate the quenching of excited krypton atoms, the ion currents of mixtures of nitric oxide and krypton were measured in the presence of various partial pressures of hydrogen and deuterium.

¹Manuscript received April 5, 1957.

Contribution from the Division of Pure Chemistry, National Research Council, Ottawa, Canada.

Issued as N.R.C. No. 4403.

²Japanese Government Fellow at the National Research Council of Canada 1954-55, and National Research Council Postdoctorate Fellow 1955-57. Present address: Laboratory of Physical Chemistry, Tokyo Institute of Technology, Tokyo, Japan.

EXPERIMENTAL

The argon resonance lamp (1, 8, 9) is illustrated in Fig. 1. Before the lamp was filled, the tantalum electrodes were heated by an induction heater and pumped for a long time to remove impurities such as carbon monoxide and water until the emission spectra of the latter were undetectable. The lamp was filled with argon at 1 or 2 mm. pressure and after the discharge was run at a current of about 100 milliamperes, the argon together with the small remaining amount of impurity was pumped off. To avoid mercury

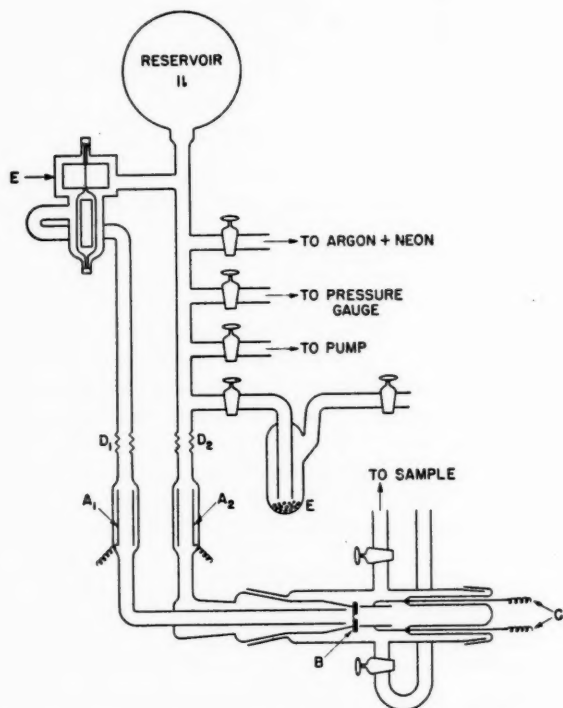


FIG. 1. Apparatus for the argon lamp. A_1 and A_2 , electrodes for the lamp. B, slit. C, electrodes for measuring ion current. D_1 and D_2 , pyrex-quartz graded seals. E, centrifugal pump.

resonance lines a mercury-free vacuum system was used. The window, which was of lithium fluoride 0.5 mm. thick, was painted with colloidal carbon except for a slit 1 mm. by 8 mm. The lamp was filled with argon at about $10\text{--}20\ \mu$ pressure and neon at about 1.5 mm. pressure, and the mixture was circulated using a centrifugal pump. The lamp was operated at 30–40 ma. from a 6000 volt sign transformer. The radiation entered the reaction cell through the slit on the window. In the reaction cell were two parallel plate electrodes 15 mm. apart by means of which the ion current could be measured, using a Keithley electrometer. A potential difference of 22.5 volts or 45 volts was applied between the plates. (The argon lamp was not subsequently used with krypton, since contamination of the krypton with argon was always found.) The krypton resonance

lamp was similar to the argon resonance lamp except that the centrifugal pump was not used.

The xenon resonance lamp is shown in Fig. 2. The electrodes were of pure iron. These electrodes were treated in the same way as those in the argon and krypton lamps to remove impurities. The window was of thin quartz instead of lithium fluoride.

Xenon, krypton, argon, and neon were of spectroscopic purity, obtained from the Linde Air Products Company. Nitric oxide, obtained from an Ohio Chemical Canada

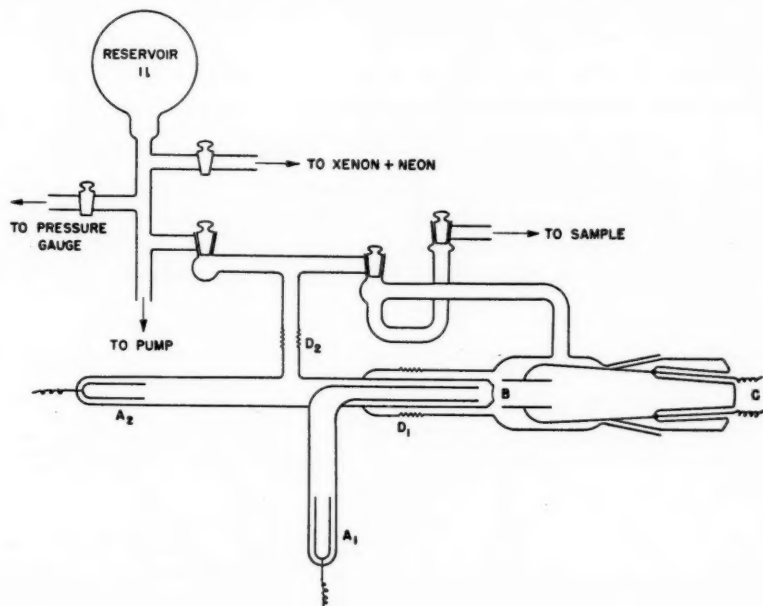


FIG. 2. Apparatus for the xenon lamp. A_1 and A_2 , electrodes for the lamp. B, very thin quartz window. C, electrodes for measuring ion current. D_1 and D_2 , pyrex-quartz graded seals.

Ltd. cylinder, was further purified by repeated bulb-to-bulb distillations *in vacuo*. Acetone, Mallinckrodt Analytical Reagent Grade, and anisole, Eastman Kodak Co., were distilled before use. Hydrogen and deuterium were purified by passage through a palladium thimble. Except for anisole, which was not analyzed, the mass spectra of these gases showed no evidence of impurity.

RESULTS

Krypton and Nitric Oxide System

The preliminary work on the ionization of nitric oxide by krypton photosensitization was done with a potential between the two electrodes of 22.5 volts. In the present investigation, the effect of this voltage on the ion current was examined using 22.5 volts and 45 volts. The ion currents found at various pressures of nitric oxide gas alone are shown in Fig. 3.

Assuming no recombination of $\text{NO}^+ + e$ before the NO^+ ion arrived at the electrode, the curve of ion current vs. pressure of NO should be given by $i \propto I_0 - I = I_0(1 - e^{-\alpha P - I})$,

where i is the ion current, $\alpha = N\sigma$, I is the intensity of radiation transmitted by a column of gas l cm. long at a pressure p (measured in atmospheres after reduction to $0^\circ\text{C}.$), I_0 is the intensity of the incident radiation, $N = 2.69 \times 10^{19}$ molecules/cc., and σ is an ionization cross section given in cm^2 . This leads to a relation between the ion current and the pressure of nitric oxide of the form $i = k_1(1 - e^{-k_2 p})$. The ionization cross section can thus be calculated from the ion currents observed. For example, in the expression:

$$i_2/i_1 = (1 - e^{-\alpha p_2 l}) / (1 - e^{-\alpha p_1 l})$$

if $i_2 = 1.5 \times 10^{-7}$ amp., $p_2 = 0.60$ mm. Hg,
 $i_1 = 0.9 \times 10^{-7}$ amp., $p_1 = 0.30$ mm. Hg,
 and $l = 4$ cm.,

the ionization cross section of nitric oxide is given as

$$\sigma = 1.31 \times 10^{-17} \text{ cm}^2 = 13.1 \text{ mb.}, \quad \text{where } 1 \text{ mb.} = 10^{-18} \text{ cm}^2$$

In contradistinction with our value for the photoionization of nitric oxide, Watanabe *et al.* (7) obtained a cross section of 1.0 mb. at 1300 Å, rising to about 6 mb. at 1100 Å. It is difficult to decide where the source of the discrepancy lies; the relative values may depend to a large extent on differences in the degree of recombination of NO^+ and an electron (10).

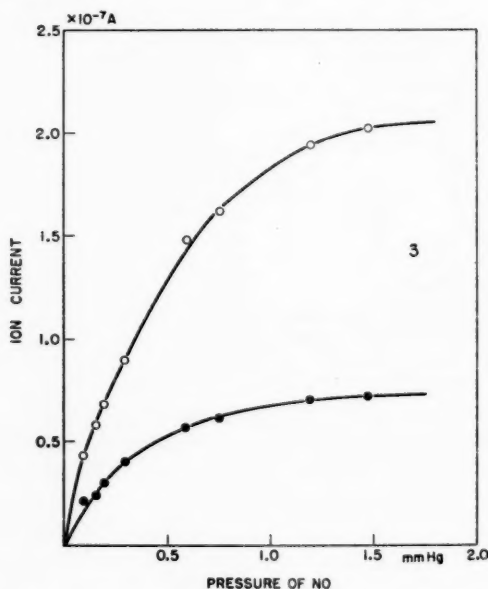


FIG. 3. Ion current of NO gas without krypton. Voltage between the two electrodes = ●, 22.5 v.; ○, 45 v.

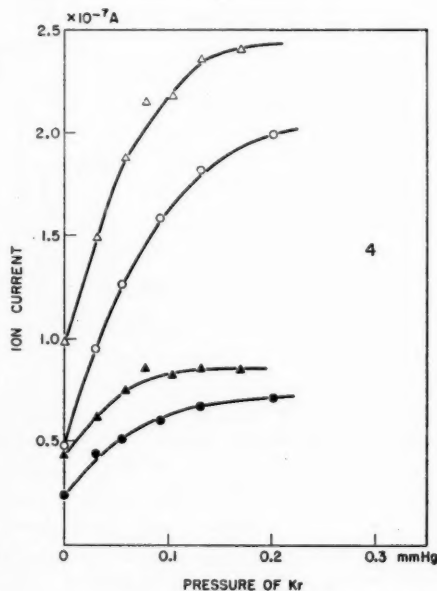


FIG. 4. Ion current of NO gas with krypton.

	Voltage between the electrodes
●	22.5 v.
▲	22.5 v.
○	45 v.
△	45 v.

Pressure of NO gas
0.11 mm. Hg
0.29 mm. Hg
0.11 mm. Hg
0.29 mm. Hg

The curves of ion current vs. krypton pressure at two electrode voltages and nitric oxide pressures are shown in Fig. 4.

Krypton and Acetone System

The ion current at various pressures of acetone is shown in Fig. 5. The curve for acetone appeared similar to that of nitric oxide, although the saturation ion current occurred at a lower pressure of acetone.

The curves of ion current vs. krypton pressure for mixtures of acetone and krypton are shown in Fig. 6.

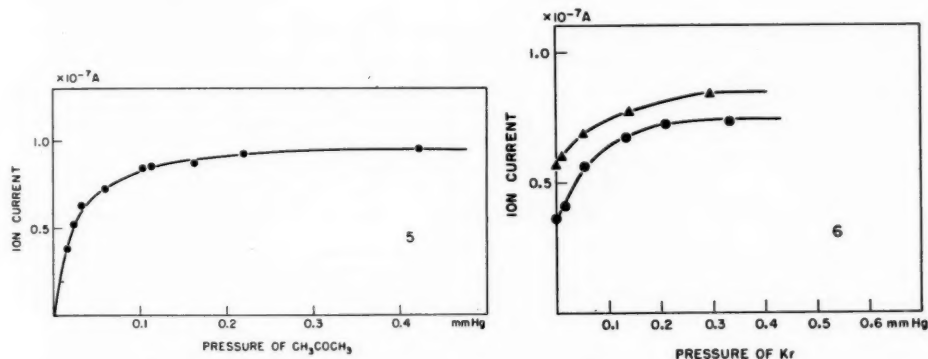


FIG. 5. Ion current of acetone without krypton. Voltage between the electrodes = 22.5 v.

FIG. 6. Ion current of acetone with krypton. Voltage between the electrodes = 22.5 v. ●, pressure of acetone = 0.006 mm. Hg. ▲, pressure of acetone = 0.026 mm. Hg.

Xenon and Anisole System

There are few compounds whose ionization potentials are less than the energy of the resonance line of xenon. However, aniline (I.P. = 7.70 ± 0.02 ev.), 1-methylnaphthalene (I.P. = 7.96 ± 0.02 ev.), and anisole (I.P. = 8.20 ± 0.02 ev.) can be used as samples (6). In this experiment anisole was convenient, as its ionization has been observed by mass spectrometry (2) using photoionization as the source of ions.

Although the thin quartz window absorbs appreciably below 1500 Å, the transmission of the xenon resonance line 1470 Å was adequate and a measurable ion current was obtained even when the pressure of anisole was low. The various pressures of anisole below 0.1 mm. were obtained by expansion of a measured sample from a small volume to a large volume. Since the anisole was absorbed to some extent by Apiezon grease, the ion current was measured twice at each pressure. These results are shown in Fig. 7 and Fig. 8. The shapes of the curves obtained in the case of anisole and the mixture of anisole and xenon are similar to those of nitric oxide and the mixture of nitric oxide and krypton.

Argon and Nitric Oxide System

Propane was used to determine whether the lithium fluoride window was sufficiently transparent to the argon resonance lines. Since the ionization potential of propane is 11.08 ev., only the argon lines could ionize it, and radiation from impurities, such as krypton and xenon, in the argon would have no effect on the propane. An ion current

of 0.40×10^{-7} amp. at a propane pressure of 2 mm. was obtained, showing that appreciable argon resonance radiation passed through the window.

For a comparison with the results of krypton photosensitization nitric oxide was used. The results for nitric oxide and the mixture of nitric oxide and argon, shown in Figs. 9 and 10, are similar to those for nitric oxide and the mixture of nitric oxide and krypton

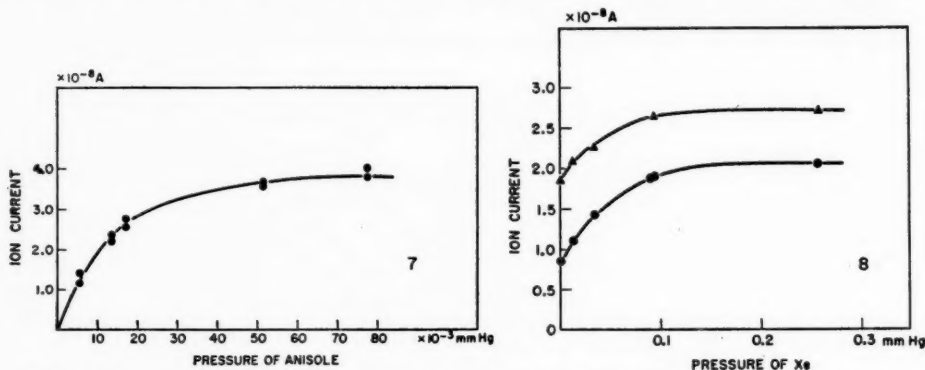


FIG. 7. Ion current of anisole without xenon. Voltage between the electrodes = 22.5 v.

FIG. 8. Ion current of anisole with xenon. Voltage between the electrodes = 22.5 v. ●, pressure of anisole 3×10^{-3} mm. Hg. ▲, pressure of anisole 9×10^{-3} mm. Hg.

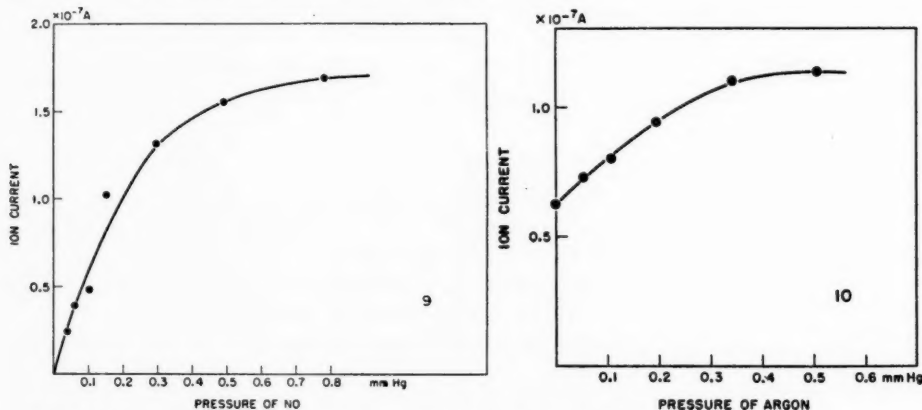


FIG. 9. Ion current of NO gas without argon. Voltage between the electrodes = 22.5 v.

FIG. 10. Ion current of NO gas with argon. Voltage between the electrodes = 22.5 v. Pressure of NO gas = 0.107 mm. Hg.

using a krypton resonance lamp, although the saturation ion current occurred at a lower pressure. This means that the absorption cross section of nitric oxide at 1068 or 1048 Å is greater than at 1236 and 1165 Å (6). The main source of difficulty in this experiment was that the transmission of the lithium fluoride window decreased rapidly owing to the progressive action of the discharge.*

*An electrodeless lamp activated by a microwave generator, a Raytheon CMD-7, was tried. In this case the transmission of the window did not change as rapidly as above. The resonance lines of argon, krypton, and xenon were strong enough to give measurable sensitized photoionization. The pressure of these gases in each case was about 10 microns, diluted with 2-4 mm. of neon.

Quenching

The effect of an added gas which does not absorb radiation might be one or more of the following:

- to quench excited atoms A^* or Kr^* without ionization, consequently decreasing the yield of ions;
- to act as a third body for ion-electron recombination, consequently decreasing the yield of ions;
- to broaden the absorption lines of the krypton or argon atoms, consequently increasing the yield of ions.

The ion current of nitric oxide in the absence of sensitizing gas was influenced slightly by the presence of helium, hydrogen, and deuterium, the decrease in ion current being least with helium. These results are shown in Fig. 11. The decrease owing to the presence

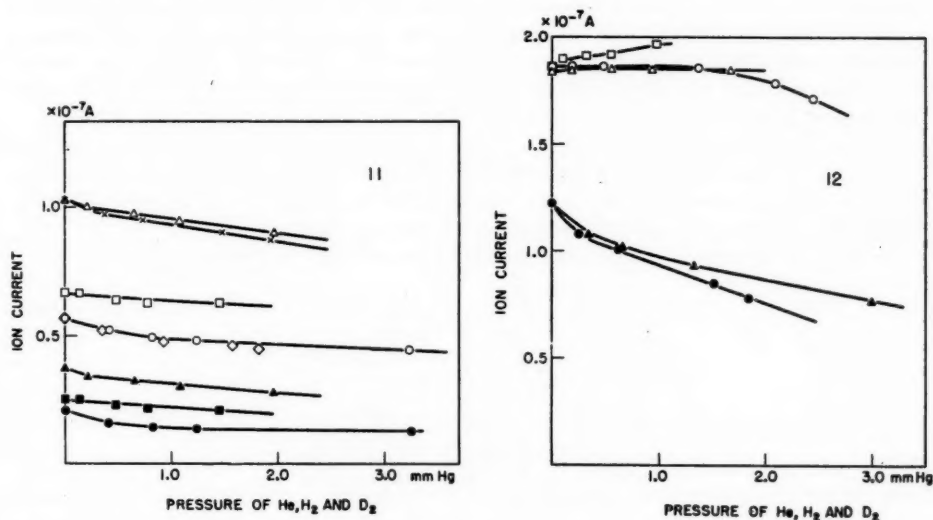


FIG. 11 Ion current of NO gas with He or H₂ or D₂.

	Quenching gas	Voltage between the electrodes	Pressure of NO
△	D ₂	45 v.	0.36 mm. Hg
×	H ₂	45 v.	0.36 mm. Hg
□	He	45 v.	0.20 mm. Hg
◇	H ₂	45 v.	0.15 mm. Hg
○	D ₂	45 v.	0.15 mm. Hg
▲	D ₂	22.5 v.	0.36 mm. Hg
■	He	22.5 v.	0.20 mm. Hg
●	D ₂	22.5 v.	0.15 mm. Hg

FIG. 12. Ion current of mixture of NO gas and krypton with He or H₂ or D₂.

	Quenching gas	Pressure of NO	Pressure of krypton
□	He	0.36 mm. Hg	0.090 mm. Hg
○	H ₂	0.36 mm. Hg	0.090 mm. Hg
△	D ₂	0.36 mm. Hg	0.086 mm. Hg
●	H ₂	0.085 mm. Hg	0.090 mm. Hg
▲	D ₂	0.085 mm. Hg	0.090 mm. Hg

of hydrogen or deuterium was rather greater, hydrogen showing a slightly larger effect than deuterium. These substances may act as third bodies for the recombination of nitric oxide ions and electrons rather than as quenchers of the excited state of nitric oxide, because nitric oxide in the excited state ionizes almost immediately.

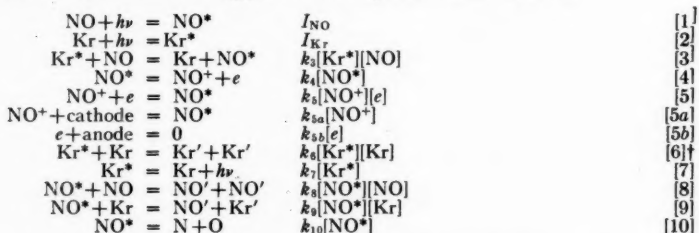
The ion currents of the mixtures of nitric oxide and krypton with helium, hydrogen, or deuterium are shown in Fig. 12. The upper curves were obtained using a relatively high pressure of nitric oxide, so that the ion currents were high. It is seen that the pressure broadening of the krypton absorption line is greater than the quenching effect of the added gas. In the lower set of curves, where the nitric oxide pressure is smaller, the quenching of excited krypton by hydrogen or deuterium is marked.

DISCUSSION

We consider first the results on the direct photoionization of NO, acetone, and anisole using argon, krypton, and xenon lamps, but with no rare gas in the ionization chamber. The plots of ion current versus pressure of sample are all of the same form. In agreement with the work of Zelikoff and Aschenbrand (10), the ion current with NO increased markedly with electrode voltage, but, with increasing pressure of NO, the ion current at the two voltages tended to limiting values, probably decreasing again at still higher pressures of NO.

Next, we consider the results in the sensitized photoionization of NO, acetone, and anisole, using argon, krypton, and xenon lamps and with rare gas in the ionization chamber. The ion current curves were similar, and, as representative of the results as a whole, we consider the reaction mechanism for the system Kr-NO.

The following reaction mechanism is suggested to explain these results:



If the lifetime of NO^* is very short, this set of equations is modified as follows: [1] and [4] are replaced by [11]; [10] is replaced by [12]; [5] is omitted; [8] and [9] are replaced by [13] and [14].



For the purpose of working out the rate equations, the unmodified scheme is used; both modified and unmodified schemes should lead to the same rate equation as the lifetime of NO^* approaches zero. From equations [1] to [10], neglecting [5],‡ we may write:

$$[\text{NO}^*] = \frac{I_{\text{NO}} + k_2[\text{Kr}^*][\text{NO}]}{k_4 + k_{10} + k_8[\text{NO}] + k_9[\text{Kr}]}$$

$$[\text{Kr}^*] = \frac{I_{\text{Kr}}}{k_3[\text{NO}] + k_6[\text{Kr}] + k_7}$$

†The reaction $\text{Kr}^* + \text{Kr} = \text{Kr} + \text{Kr}^*$ can be ignored in this calculation.

‡If [5] is not neglected, then the ion current becomes approximately proportional to the square root of the pressure of the absorbing species at low pressure, in disagreement with the experimental results (Fig. 3).

If it is assumed that k_6 and k_9 are very small, then approximately

$$[\text{NO}^+] \propto [\text{NO}^*] = \frac{I_{\text{NO}} + k_3 I_{\text{Kr}} [\text{NO}] / (k_3 [\text{NO}] + k_7)}{k_8 [\text{NO}] + k_4 + k_{10}}$$

If the pressure of NO is constant, the variation of ion current with the pressure of krypton conforms to the equation $i = a + b(1 - e^{-cp})$, where a , b , and c are constants and p is the pressure of krypton. The experimental results coincide approximately with this relation. Our data do not permit the calculation of the absolute quenching cross section for NO or acetone, but the ratio of the two cross sections can be obtained, qualitatively at least, in the following manner.

Considering the quenching of Kr^* by NO, one obtains when the pressure of krypton is zero

$$[\text{NO}^*]_{\text{Kr}=0} = \frac{I_{\text{NO}}}{k_8 [\text{NO}] + k_4 + k_{10}}$$

and when the pressure of krypton is " a " mm. Hg,

$$[\text{NO}^*]_{\text{Kr}=a} = \frac{I_{\text{NO}} + k_3 I_{\text{Kr}} [\text{NO}] / (k_3 [\text{NO}] + k_7)}{k_8 [\text{NO}] + k_4 + k_{10}},$$

$$\frac{i_a}{i_0} = \frac{[\text{NO}^+]_{\text{Kr}=a}}{[\text{NO}^+]_{\text{Kr}=0}} = \frac{[\text{NO}^*]_{\text{Kr}=a}}{[\text{NO}^*]_{\text{Kr}=0}} = 1 + \frac{I_{\text{Kr}}}{I_{\text{NO}}} \frac{k_3 [\text{NO}]}{k_3 [\text{NO}] + k_7};$$

i_a = ion current in presence of " a " mm. Kr.

i_0 = ion current in absence of Kr.

In the same manner for acetone

$$\frac{i_a'}{i_0'} = \frac{[\text{Ac}^+]_{\text{Kr}=a}}{[\text{Ac}^+]_{\text{Kr}=0}} = \frac{[\text{Ac}^*]_{\text{Kr}=a}}{[\text{Ac}^*]_{\text{Kr}=0}} = 1 + \frac{I_{\text{Kr}}}{I_{\text{Ac}}} \frac{k_3' [\text{Ac}]}{k_3' [\text{Ac}] + k_7};$$

i_a' = ion current in presence of " a " mm. Kr,

i_0' = ion current in absence of Kr.

In these equations, k_3 is proportional to the quenching cross section of NO, k_3' to that of acetone, and k_7/k_3' is the desired ratio.

The ratio k_7/k_3 can be calculated from values of i_a at the two pressures of NO, together with values of i_0 . The ratio k_7/k_3' is also calculated from acetone data. From these ratios k_3/k_3' is obtained.

The accuracy of our data is not sufficient to allow the precise value of k_7/k_3' to be obtained. It appears, however, that k_7/k_3' is unity or less and hence the quenching cross section of NO is rather less than that of acetone. The relations obtained above are approximate, and no claim is made that the mechanism is unique, although it gives results in agreement with experiment. It does indicate, however, that it is possible to give a reasonable explanation of the experimental results.

The curves in Fig. 12 have already been described, and it was seen that, at higher pressures of nitric oxide (upper curves), the ion current was increased by the addition of He, while H_2 and D_2 have initially little or no effect. However, at lower pressures of nitric oxide (lower curves), the ion current is decreased by the addition of H_2 and D_2 . These phenomena are readily explained. At the higher nitric oxide pressure, there is

sufficient nitric oxide present to quench almost completely the krypton excited state, and the addition of He, H₂, or D₂ results only in broadening of the krypton absorption line, with a consequent rise in the number of excited krypton atoms available for reaction with nitric oxide. At the lower pressure of nitric oxide, quenching of the excited krypton by nitric oxide is by no means complete, and the addition of H₂ or D₂ leads to further quenching, and a consequent decrease in ion current.



or



Then

$$[\text{NO}^*] = \frac{I_{\text{NO}} + k_3 I_{\text{Kr}} [\text{NO}] / (k_3 [\text{NO}] + k_{16} [x] + k_7)}{k_8 [\text{NO}] + k_{16} [x] + k_4 + k_{10}}$$

Thus

$$i \propto [\text{NO}^*] \propto [\text{NO}^*] = \frac{I_{\text{NO}} + e I_{\text{Kr}} / (a + b[x])}{c + d[x]},$$

where a , b , c , d , and e are constants at constant $[\text{NO}]$ and $[\text{Kr}]$. If $d = 0$,

$$i = \frac{I_{\text{NO}} + e I_{\text{Kr}} / (a + b[x])}{c} = \frac{I_{\text{NO}}}{c} + \frac{e}{c} \cdot \frac{I_{\text{Kr}}}{a + b[x]}.$$

This equation is that of an hyperbola, where

$$i = \frac{I_{\text{NO}}}{c} + \frac{e}{c} \cdot \frac{I_{\text{Kr}}}{a} = i_0$$

when $[x] = 0$, and

$$i = \frac{I_{\text{NO}}}{c}$$

when $[x] \rightarrow \infty$

The curvature of the plots of i vs. pressure of hydrogen or deuterium is directly related to the term $k_{16}[\text{Kr}][x]$, where x is quenching gas; thus, the greater k_{16} , the greater is the curvature of the plot. It is seen, therefore, that hydrogen is a more efficient quencher of Kr^* than is deuterium, as is also the case in the quenching of Cd^* (4) and K^* (3).

The recombination of ions and electrons forms excited molecules which may decompose into radicals or atoms. The reactions of these excited molecules, and the relation between photoionization and photolysis, will be investigated in further work.

ACKNOWLEDGMENTS

The authors wish to thank Dr. F. P. Lossing for helpful advice during the course of this work and also Dr. K. O. Kutschke and Dr. G. W. Taylor for discussions. They would also like to thank Mr. G. Ensell for the benefit of his experience and skill in the design and construction of the lamps.

REFERENCES

1. DACEY, J. R. and HODGINS, J. W. Can. J. Research, B, **28**, 90 (1950).
2. LOSSING, F. P. and TANAKA, I. J. Chem. Phys. **25**, 1031 (1956).
3. SMITH, W. M., STEWART, J. A., and TAYLOR, G. W. Can. J. Chem. **32**, 961 (1954).

4. STEACIE, E. W. R. and LEROY, D. J. *J. Chem. Phys.* **11**, 164 (1943).
5. TANAKA, I. and STEACIE, E. W. R. *J. Chem. Phys.* **26**, 715 (1957).
6. WATANABE, K. *J. Chem. Phys.* **22**, 1564 (1954).
7. WATANABE, K., MARMO, F. F., and INN, E. C. Y. *Phys. Rev.* **91**, 1155 (1953).
8. WIJNEN, M. H. and TAYLOR, H. A. *J. Chem. Phys.* **21**, 233 (1953).
9. ZELIKOFF, M. and ASCHENBRAND, L. M. *J. Chem. Phys.* **22**, 1680 (1954).
10. ZELIKOFF, M. and ASCHENBRAND, L. M. *J. Chem. Phys.* **25**, 674 (1956).

THE REACTION OF NITROUS ACID WITH 4-SUBSTITUTED-THIOSEMICARBAZIDES¹

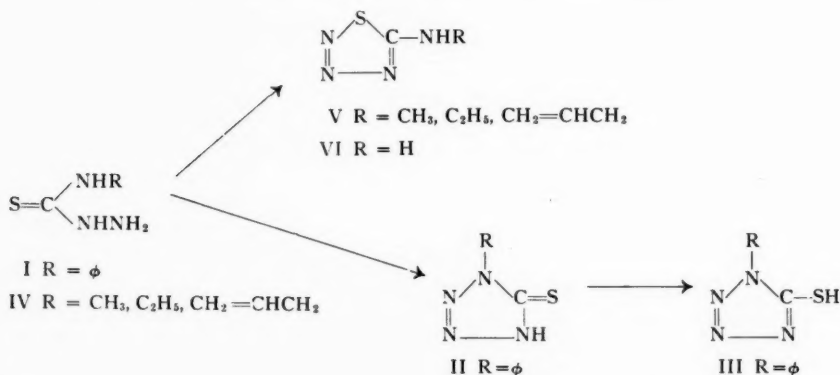
EUGENE LIEBER,² C. N. PILLAI,³ AND RALPH D. HITES⁴

ABSTRACT

The reaction of nitrous acid with 4-alkyl- or 4-aryl-thiosemicarbazides, as well as the reaction of alkyl- or aryl-isothiocyanates with hydrazoic acid, leads to the identical 5-(substituted)amino-1,2,3,4-thiatriazole. This has been established by infrared absorption and chemical degradation studies. The reaction of the 5-(substituted)amino-1,2,3,4-thiatriazoles with aqueous bases leads to two competitive reactions: (1) degradation to an isothiocyanate and azide ion, and (2) isomerization to a 1-substituted-tetrazole-5-thiol, the extent of path (1) or (2) depending on the nature of the substituent. Path (1) predominates when the substituent is alkyl, whereas when the substituent is aryl both paths (1) and (2) occur, the relative proportion depending on the electrical nature of the aromatic group, path (2) increasing as the electronegativity increases. The 1-aryl-tetrazole-5-thiols were found to be thermally unstable at their melting points, degrading more or less violently to one mole proportion of pure nitrogen with the formation of sulphur and organic products of lower melting point as yet unidentified. Theories to account for these observations are presented and discussed.

INTRODUCTION

In 1895, Freund and Hempel (9) reported that when 4-phenylthiosemicarbazide (I) was treated with nitrous acid, a substance was produced to which the structure II was assigned. II was reported to be a stable compound, not decomposed by cold sulphuric



acid or boiling hydrochloric acid. On melting, however, it decomposes more or less violently depending on the rate of heating. Freund and Hempel (9) reported that it could be recovered unchanged from cold alkaline solution, but on being heated, II was isomerized to a compound of different properties to which they assigned structure III. Structure III was supported by adequate chemical evidence (9). On the other hand, when R was an alkyl group (IV), Freund and Schwarz (11) assigned the structure V, on the basis of degradative evidence and of its marked instability in comparison

¹Manuscript received April 11, 1957.

²Contribution from the Departments of Chemistry of De Paul University and the Armour Research Foundation of the Illinois Institute of Technology, Chicago, Illinois.

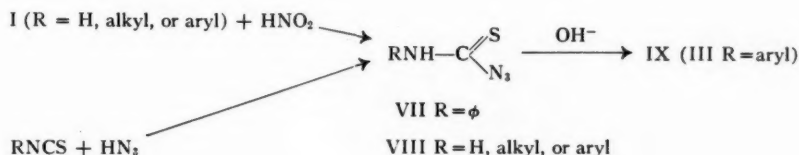
³De Paul University, to whom all requests for reprints and additional information should be addressed.

⁴Eli Lilly Research Fellow, 1956-1957, Research Corporation Fellow, 1957, De Paul University.

⁵Armour Research Foundation.

with structure II. Structures of type V were very similar in properties to that of VI obtained by the reaction of thiosemicarbazide with nitrous acid (10).

In 1913, Oliveri-Mandala and Noto (23) discovered that the reaction of hydrazoic acid with phenylisothiocyanate produced a compound, VII, that had properties very similar to those described for II. In continuation of these studies, Oliveri-Mandala (20, 21, 22) found that these compounds had properties more in conformance with a thiocarbamyl azide structure, VIII, and suggested that the initial diazotization products of thiosemicarbazides and their 4-alkyl- and 4-aryl-substitution products were identical with the condensation of an isothiocyanate with hydrazoic acid and that the differences observed by Freund (9, 10, 11) were not differences in structure but rather differences



due to variations in stability depending on the nature of the R substituent. On the other hand, when VIII (R = aryl) was treated with bases, Oliveri-Mandala (20, 21) obtained the 1-aryl-tetrazole-5-thiols, IX, identical with the products described by Freund and Hempel (9).

The present investigation is part of a general study of azole chemistry with the specific object of resolving the conflicts concerning the structure of the initial diazotization products of 4-alkyl- and 4-aryl-thiosemicarbazides.

EXPERIMENTAL^{5,6}

1,3-Diaryl-2-thioureas, RNHC(S)NHR.—These were prepared by refluxing an alcoholic solution of the arylamine with carbon disulphide until the evolution of hydrogen sulphide ceased. On cooling, the product crystallizes and is purified by recrystallization from alcohol. The following gives the R, % yield, m.p., and literature m.p.: benzyl, 90, 147–148°, 147–148° (27); *o*-tolyl, 53, 158–159°, 161° (7); *p*-tolyl, 63, 177–178°, 177° (3); *p*-anisyl, 95, 185–186°, 186.5° (7); *o*-anisyl, 82, 132–133°, 134° (8); *p*-hydroxyphenyl, 95, 223.5–224°, 223–224° (7).

Organic isothiocyanates, RNCS.—Of these R = CH₃, C₂H₅, *n*-C₄H₉, *n*-C₇H₁₅, phenyl, and allyl are commercially available. R = *p*-tolyl, *o*-tolyl, *o*-anisyl, and *p*-anisyl were prepared by refluxing the corresponding thiourea with acetic anhydride by the method of Werner (28). This method, however, gave only a very poor yield for R = benzyl, which was best prepared by the method of Moore and Crossley (19) in 75% yield. R = 4-Cl-C₆H₄ was prepared in 32% yield, based on *p*-chloroaniline, from 1-(4-chlorophenyl)-3-phenyl-2-thiourea (from *p*-chloroaniline and phenylisothiocyanate) by steam distilling in the presence of sulphuric acid by the method of Chattaway, Hardy, and Watts (5), m.p. 40–45°, b.p. 110–115° at 4 mm. Refluxing 1,3-di-(*p*-hydroxyphenyl)-2-thiourea with acetic anhydride leads to *p*-acetoxo-phenylisothiocyanate (16), non-volatile with steam, purified by vacuum fractional distillation, the fraction being collected

⁵All melting points are uncorrected.

⁶Microanalyses by Dr. C. Weiler and Dr. F. B. Strauss, Oxford, England.

at 167–175° at 8 mm., 58 g. (84%) from 93 g. of the thiourea; solidifies on cooling, recrystallized from ethanol, m.p. 33.5–34.5°. Anal. Calc. for $C_9H_7NO_2S$: N, 7.25; S, 16.6. Found: N, 7.28; S, 16.5.

4-Substituted-thiosemicarbazides (Table I).—All of the isothiocyanates readily underwent hydrazination to form the corresponding 4-substituted-thiosemicarbazide, purification being effected by repeated recrystallization from ethanol. The products so prepared are summarized in Table I. Para-acetoxyphenylisothiocyanate was found to undergo hydrazinolysis as well as hydrazination.

TABLE I
4-SUBSTITUTED-THIOSEMICARBAZIDES

RNHC(S)NHNH ₂ R =	% Yield	M.p., ° C.		Formula	Calc.	Found
		Found	Reported			
CH ₃	93	136.5–137	137–138 ^a	C ₂ H ₇ N ₃ S	39.98	40.00
C ₂ H ₅	87	83.5–84	84 ^b	C ₃ H ₉ N ₃ S	35.25	35.20
C ₃ H ₇ ^c	86	96.5–97	88–89 ^a	C ₄ H ₉ N ₃ S	32.02	32.40
<i>n</i> -C ₄ H ₉	89	74–74.5	70 ^d	C ₅ H ₁₁ N ₃ S	28.54	28.40
<i>n</i> -C ₅ H ₁₁	92	53–54	54–55 ^e	C ₆ H ₁₃ N ₃ S	22.20	22.60
C ₆ H ₅ CH ₃	70	129.5–130.5	130 ^f	C ₈ H ₁₁ N ₃ S	23.30	23.40
4-CH ₃ C ₆ H ₄	95	137	137 ^g	C ₈ H ₁₀ N ₃ S	23.30	23.00
2-CH ₃ C ₆ H ₄	98	148	148 ^g	C ₈ H ₁₀ N ₃ S	23.30	23.20
4-CH ₃ OC ₆ H ₄	95	150–151	144 ^h	C ₉ H ₁₀ N ₃ OS	21.31	21.20
2-CH ₃ OC ₆ H ₄	95	154	156 ^g	C ₉ H ₁₀ N ₃ OS	21.31	21.20
4-ClC ₆ H ₄	95	180	180 ^h	C ₇ H ₇ ClN ₃ S	20.84	20.60 ⁱ

^aPulvermacher, *Ber.* **27**, 622 (1894).

^bFreund and Schwarz, *Ber.* **29**, 2483 (1896).

^cAllyl.

^dHogarth and Young, *J. Chem. Soc.* 1582 (1950).

^eBaird, Burns, and Wilson, *J. Chem. Soc.* 2527 (1927).

^fGuha and Ray, *J. Am. Chem. Soc.* **47**, 387 (1925).

^gFromm, Soffner, and Frey, *Ann.* **434**, 285 (1923).

^hBusch and Ulmer, *Ber.* **35**, 1714 (1902).

ⁱCalc.: S, 15.91; Cl, 17.59. Found: S, 15.50; Cl, 17.75.

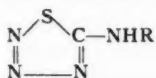
4-(p-Hydroxyphenyl)-thiosemicarbazide.—To a solution of 54 g. (0.28 mole) of *p*-acetoxyphenylisothiocyanate in 200 ml. of ethanol was added 15 ml. of 95% hydrazine hydrate diluted with 10 ml. of water. The mixture was shaken for a few minutes and cooled. The precipitate was recovered by filtration. Yield, 40 g. (80%); recrystallized from ethanol, m.p. 170–171° (decomp.). Anal. Calc. for $C_7H_9N_3SO$: C, 45.86; H, 4.95; N, 22.94; S, 17.50. Found: C, 45.68; H, 4.94; N, 23.60; S, 17.40.

1-Benzylidene-4-(p-hydroxyphenyl)-thiosemicarbazide.—From 1 g. of 4-(*p*-hydroxyphenyl)-thiosemicarbazide and 1 g. of benzaldehyde in ethanol in the presence of nitric acid. Recrystallized three times from ethanol and dried at 100° at 4 mm.; m.p. 184–185°. Anal. Calc. for $C_{14}H_{13}N_3SO$: C, 61.95; H, 4.83; N, 15.50; S, 11.82. Found: C, 61.53; H, 4.56; N, 15.30; S, 11.60.

4,4-Dimethylthiosemicarbazide.—From 70 g. (0.39 mole) of *N,N*-dimethylthiocarbamylthioglycolic acid, m.p. 144–146° (13), 7 g. of sodium hydroxide in 170 ml. of water, and 35 ml. of 85% hydrazine hydrate. Recrystallized from water, m.p. 151–152° (reported (13) value is 156–157°).

1-Benzylidene-4,4-dimethylthiosemicarbazide.—Recrystallized from ethanol, m.p. 161–162°. Anal. Calc. for $C_{16}H_{15}N_3S$: N, 20.28; S, 15.48. Found: N, 20.50; S, 15.50.

The reaction of 4-substituted-thiosemicarbazides with nitrous acid, 5-(substituted)amino-1,2,3,4-thiadiazoles (Table II).—The preparation of 5-anilino-1,2,3,4-thiadiazole was

TABLE II
 5-(SUBSTITUTED)AMINO-1,2,3,4-THIATRIAZOLES


R ¹ =	% Yield	M.p., ° C.		Formula	Analysis							
					% C		% H		% N		% S	
		Found	Reported		Calc.	Found	Calc.	Found	Calc.	Found	Calc.	Found
CH ₃	60	93-96	96 ^c	C ₇ H ₆ N ₄ S					48.25	48.40	27.61	27.50
C ₆ H ₅	62	66-67	66-67 ^c	C ₈ H ₆ N ₄ S					43.05	42.70	24.64	24.84
n-C ₄ H ₉ ^a	80	40-41	—	C ₉ H ₁₀ N ₄ S	37.93	37.96	6.37	6.31	35.42	35.60	20.27	20.50
n-C ₇ H ₁₅ ^d	97	75-75.5	—	C ₁₂ H ₁₆ N ₄ S	47.95	48.33	8.05	7.92	27.98	27.60	16.01	15.80
C ₆ H ₅	89	142-143	142-145 ^d	C ₇ H ₆ N ₄ S	47.15	47.10	3.40	3.51	31.45	31.60	18.00	17.60
4-CH ₃ C ₆ H ₄	94	142-144	140-144 ^e	C ₈ H ₈ N ₄ S	50.00	50.22	4.17	4.39	29.17	28.90	16.67	16.90
2-CH ₃ C ₆ H ₄	90	114-115	120 ^f	C ₈ H ₈ N ₄ S	50.00	50.11	4.17	4.40	29.17	29.00	16.67	16.50
4-CH ₃ OC ₆ H ₄ ^a	85	136-137	—	C ₉ H ₈ N ₄ OS	46.12	46.24	3.87	3.91	26.92	27.10	15.40	15.00
C ₆ H ₅ CH ₂ ^a	90	80.5-81	—	C ₈ H ₈ N ₄ S	50.00	50.07	4.17	4.25	29.17	29.00	16.67	16.70
4-ClC ₆ H ₄ ^{a,g}	75	147-148	—	C ₇ H ₄ ClN ₄ S	39.50	40.54	2.39	2.16	26.35	26.00	15.08	15.18
(CH ₃) ₂ ^{2a,b}	31	49-51	—	C ₈ H ₈ N ₄ S	27.66	27.90	4.65	4.53	43.05	42.80	24.64	24.40
CH ₂ =CHCH ₂	72	53-53.5 ^h	54 ^c	C ₈ H ₈ N ₄ S	33.78	33.81	4.26	4.47	39.42	39.41	22.56	22.65
2-CH ₃ OC ₆ H ₄ ^a	85	89-90	—	C ₉ H ₈ N ₄ OS	46.12	46.29	3.87	3.96	26.92	26.60	15.40	15.45

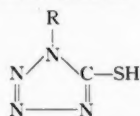
^a New compounds.^b R = CH₃, H = CH₃.^c Freund and Schander, *Ber.* **29**, 2491 (1899).^d Freund and Hempel, *Ber.* **28**, 74 (1895).^e Oliveri-Mandala, *Gazz. chim. ital.* **44**, I, 670 (1914).^f Oliveri-Mandala, *Gazz. chim. ital.* **51**, II, 195 (1921).^g Calc. % Cl, 16.68; Found % Cl, 16.38.^h Recrystallization must be made from non-aqueous solvents in order to avoid decomposition; a mixture of ether-petroleum ether was found best.ⁱ All products showed the absence of the azido-group frequency in the infrared.

typical. To a stirred and cooled mixture of 16.7 g. (0.10 mole) of 4-phenylthiosemicarbazide and 76 ml. of 15% hydrochloric acid was added 6.9 g. (0.10 mole) of sodium nitrite in 50 ml. of water. The white powdery material, which rapidly turns pale pink, was filtered. Yield, 16 g. (89%), m.p. 136-137° (decomp.). Recrystallization from methanol yields colorless needles, m.p. 142-143° (decomp.).

Reaction of nitrous acid with 4-phenylthiosemicarbazide in different acid environments.—Diazotizations were carried out in 50% aqueous acetic acid, in anhydrous acetic acid, and in hydrochloric acid of pH 3 and 5, respectively. In all cases a product melting at 142-143° was obtained. Mixed melting points showed all the products to be identical with 5-anilino-1,2,3,4-thiatriazole obtained above.

Reaction of phenylisothiocyanate and hydrazoic acid.—A mixture of 13.5 g. (0.1 mole) of phenylisothiocyanate and 6.5 g. (0.1 mole) of sodium azide was cooled to 0° and 25 ml. of 4 N hydrochloric acid added over a period of 30 minutes. After the addition of the acid, the reaction mixture was warmed on the water bath for 30 minutes and then cooled in an ice bath. The product was recrystallized from ethanol, m.p. 142°; no depression of m.p. with 5-anilino-1,2,3,4-thiatriazole. An infrared analysis showed the absence of the azido-group frequency.

Reaction of methylisothiocyanate and hydrazoic acid.—Hydrazoic acid from 2 g. (0.03 mole) of sodium azide was distilled into a solution of 2 g. (0.02 mole) of methylisothiocyanate in 25 ml. of ethanol. When the mixture was cooled, after concentration under

TABLE III
 1-SUBSTITUTED-TETRAZOLE-5-THIOLS


					Analysis							
R =	% Yield	M.p., ° C.		Formula	% C		% H		% N		% S	
		Found	Reported		Calc.	Found	Calc.	Found	Calc.	Found	Calc.	Found
C ₆ H ₅	34	148-148.5	147-159 ^a	C ₇ H ₆ N ₄ S	47.15	47.33	3.40	3.61	31.45	31.40	18.00	17.70
4-CH ₃ C ₆ H ₄	30	150	150-151 ^b	C ₈ H ₈ N ₄ S	50.00	50.41	4.17	4.17	29.17	28.90	16.67	16.20
2-CH ₃ C ₆ H ₄	22	121-123	129 ^c	C ₈ H ₈ N ₄ S	50.00	50.18	4.17	4.38	29.17	28.80	16.67	16.60
4-CH ₃ OC ₆ H ₄ ^d	30	150	—	C ₉ H ₈ N ₄ OS	46.12	46.19	3.87	4.02	26.92	27.00	15.40	15.30
2-CH ₃ OC ₆ H ₄ ^d	24	139-140	—	C ₉ H ₈ N ₄ OS	46.12	46.38	3.87	4.08	26.92	26.60	15.40	15.15
C ₆ H ₅ CH ₂ ^{d,e}	25	138-139	—	C ₈ H ₈ N ₄ S	50.00	50.21	4.17	4.33	29.17	29.20	16.67	16.64
4-ClC ₆ H ₄ ^{d,e}	37	156-157	—	C ₇ H ₄ ClN ₄ S	39.50	38.85	2.39	2.18	26.35	26.20	15.08	15.60
4-HOC ₆ H ₄	None											
CH ₃	None											
n-C ₇ H ₁₅	None											

^aFreund and Hempel, *Ber.* **28**, 74 (1895).^bOliveri-Mandala, *Gazz. chim. ital.* **44**, I, 670 (1914).^cOliveri-Mandala, *Gazz. chim. ital.* **51**, II, 195 (1921).^dNew compounds.^eCalc. % Cl, 16.68. Found % Cl, 16.40.

reduced pressure, colorless crystals were obtained which were recrystallized from ethanol, m.p. 96°; no depression of the melting point with 5-methylamino-1,2,3,4-thiatetrazole. An infrared analysis showed the absence of the azido-group frequency.

1-Substituted-tetrazole-5-thiols (1-substituted-5-thiatetrazolones) (Table III).—The procedure used for the preparation of 1-phenyltetrazole-5-thiol was typical. A mixture of 2.2 g. (0.012 mole) of 5-anilino-1,2,3,4-thiatetrazole and 25 ml. of 10% aqueous sodium hydroxide (4 moles) was refluxed for several minutes. The solution, which was at first a green color, turned yellow and turbid. On acidification, hydrogen sulphide was liberated and a faint yellow crystalline material precipitated. Recrystallization was effected from ethanol.

Alkaline steam degradation of 5-anilino-1,2,3,4-thiatetrazole.—A mixture of 9 g. (0.05 mole) of 5-anilino-1,2,3,4-thiatetrazole, 9 g. (0.23 mole) of sodium hydroxide, and 250 ml. of water was steam distilled. The steam distillation was continued for a period of 1 to 2 hours in order to make certain that no further steam-volatile degradation products were being produced. Aniline, identified by conversion to benzanilide, m.p. 161°, was found in the distillate. Acidification of the residue in the distillation flask gave the familiar odor of hydrogen sulphide and a crystalline precipitate, which after recrystallization from ethanol melted at 148°. It was identified as 1-phenyltetrazole-5-thiol by mixed melting point with an authentic specimen. Hydrazoic acid was also identified in the steam distillation residue by distilling the acidified mixture into a solution of ferric chloride. The characteristic blood-red coloration (6) due to the ferric-azide ion complex resulted. When the experiment was repeated in the presence of a stoichiometric quantity of sodium hydroxide, the distillate contained initially phenylisothiocyanate followed by 1,3-diphenyl-2-thiourea, identified by its m.p. of 154° (12) and analysis.

Anal. Calc. for $C_{11}H_{12}N_4S$: C, 68.37; H, 5.30; N, 12.28; S, 14.05. Found: C, 68.15; H, 5.37; N, 12.00; S, 13.90. The residue, on acidification, again yielded 1-phenyltetrazole-5-thiol, hydrogen sulphide, and hydrazoic acid. The 1-phenyltetrazole-5-thiol, recovered from the residue of the alkaline steam degradation, was resubmitted to steam distillation in the presence of 4 moles of sodium hydroxide over a period of 1 hour. No volatile product of any type was found in the distillate and the 1-phenyltetrazole-5-thiol was recovered unchanged and in quantitative yield. Neither hydrogen sulphide nor hydrazoic acid could be detected.

Thermal behavior of 1-phenyltetrazole-5-thiol.—On melting at 147–148°, 1-phenyltetrazole-5-thiol undergoes a marked decomposition with evolution of a gas and the development of a yellow coloration. On cooling, a grease-like substance of lower melting point was obtained. Quantitative experiments were carried out by mixing weighed quantities of 1-phenyltetrazole-5-thiol with white sand, in order to moderate the violence of the decomposition, and collecting the evolved gas over concentrated potassium hydroxide solution. Replicate runs showed that very nearly 1 mole of gas was liberated per mole of 1-phenyltetrazole-5-thiol. Mass spectrometric analysis⁷ of the evolved gas showed it to be pure nitrogen. Sulphur was isolated and identified. A white crystalline material has been isolated whose identity is as yet unknown. Studies on the identity of this product are in progress.

The reaction of 5-(substituted)amino-1,2,3,4-thiatriazole with hydrogen sulphide.—Aqueous solutions of 5-methylamino-, 5-*n*-heptylamino-, and 5-anilino-1,2,3,4-thiatriazole, respectively, were saturated with hydrogen sulphide and allowed to stand overnight, at room temperature, under a slight excess pressure of hydrogen sulphide. All of the thiatrazoles were recovered quantitatively and unchanged.

Potentiometric titrations of 1-(substituted)phenyltetrazole-5-thiols.—The apparent acidic dissociation constants were determined by potentiometric titration in 50% aqueous ethanol using a photovolt pH meter. The titration curves for the compounds studied were of the moderately strong acid type. The data obtained for 1-*p*-chlorophenyl-, 1-phenyl-, and 1-*p*-methoxyphenyl- were, respectively, in pK_a units 3.3, 3.4, and 3.4.

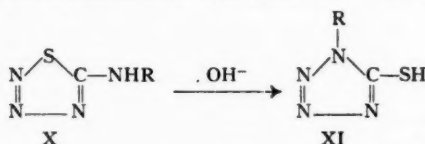
DISCUSSION

The most important observation arising from this study is the fact that all of the initial diazotization products summarized in Table II, as well as identical substances produced by the reaction of phenyl- and methyl-isothiocyanates with hydrazoic acid, show no azido-group frequency in the infrared. This at once eliminates the assertion of Oliveri-Mandala (20, 21, 22, 23) that the products of the above reaction are thio-carbamyl azides, VII and VIII, in spite of the almost overwhelming chemical evidence in favor of this hypothesis. The most important of this chemical evidence is the formation of the azide and sulphide ions by alkaline degradation. Thus, the alkaline degradation of VIII ($R = H$) (10) corresponds almost exactly to that of guanyl azide nitrate (25) in which the azido-group frequency in the infrared is quite marked (17). On the other hand, the inertness of VII and VIII to hydrogen sulphide is in agreement with the infrared spectroscopy data. The facile reducibility of the azido-group by hydrogen sulphide has been frequently demonstrated (14, 18, 25, 26). Freund (9) placed a great deal of stress on his observation that the initial diazotization product of I showed marked stability

⁷Consolidated Engineering Corporation, Pasadena, California.

in alkaline medium⁸ and on this basis assigned the structure II to his product. Unfortunately, Freund's (9) observations and deductions were incorrect and incomplete.

The present study has shown that from the infrared absorption spectroscopy and the chemical properties the initial diazotization products of 4-alkyl- and 4-aryl-thiosemicarbazides, as well as the alkyl- and aryl-isothiocyanate-hydrazoic acid reaction products, are best represented as possessing the 1,2,3,4-thiatriazole ring structure, X, regardless of whether R is represented as hydrogen,⁹ alkyl, or aryl. The most significant



observation arising out of the conversion of X (R = ϕ) to XI (R = ϕ) is the fact that on warming in alkali, the odor of phenylisothiocyanate is almost immediately discernible and that on acidifying the alkaline mixture, in order to isolate the tetrazole XI, hydrogen sulphide is abundantly present. Further, XI was obtained in much less than stoichiometric yield (Table III). Since these observations indicated that some extensive degradation of X was taking place, the experiments were repeated in such a manner that the volatile degradation products could be collected and identified. All of the results can be interpreted on the basis that the initial reaction involves the degradation of X to phenylisothiocyanate and hydrazoic acid:



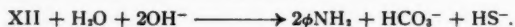
followed by the basic hydrolysis of the phenylisothiocyanate:



In the presence of one mole proportion of sodium hydroxide, the hydrolysis of the phenylisothiocyanate is somewhat retarded owing to the consumption of the base by the formation of the azide ion. That alkaline hydrolysis does occur is evidenced by the formation of 1,3-diphenyl-2-thiourea, XII:



found in both the residue and the steam distillate.¹⁰ In the presence of a large excess of sodium hydroxide, aniline is the only volatile product. This could arise solely from the phenylisothiocyanate or by alkaline hydrolysis of XII:



In either case, on acidification of the steam distillation residue, the additional volatile products are due to the neutralization of the azide, bicarbonate, and bisulphide ions, the non-volatile residue XI (R = ϕ), of course, arising from the same cause. XI (R = ϕ), isolated from these alkaline steam degradation studies, is identical with the so-called

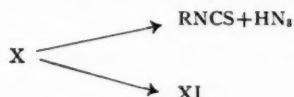
⁸It is interesting to point out that Freund and Hempel (9) in preparing a large quantity of III (R = ϕ) by digestion with aqueous sodium carbonate, at 50–60°, found 1,3-diphenyl-2-thiourea (reporting a m.p. of 150°) in the residue and indicated that the odor of phenylisothiocyanate was discernible and that at the same time aniline appeared. However, they completely disregarded the significance of these observations.

⁹The chemistry of 5-amino-1,2,3,4-thiatriazole will be reported in a separate communication.

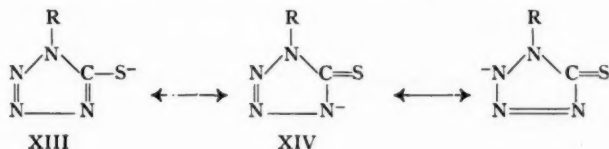
¹⁰Independent experiments have shown that the reaction of alkyl- or aryl-isothiocyanates with one to two molar proportions of aqueous sodium hydroxide leads to substantial yields of symmetrical disubstituted thioureas. This work will be reported in a separate communication.

base-tautomerized II ($R = \phi$) of Freund (9) and to the base-tautomerized phenylisothiocyanate-hydrazoic acid reaction product, IX, of Oliveri-Mandala (20, 21).

The presence of XI ($R = \phi$) in the alkaline steam degradation of X ($R = \phi$) can be accounted for on the basis that two competitive reactions are taking place:



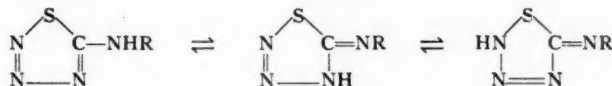
and that the driving force leading to XI depends on the stabilization afforded by the anion of XI in the alkaline medium, XIII and XIV ($R = \text{aryl}$):



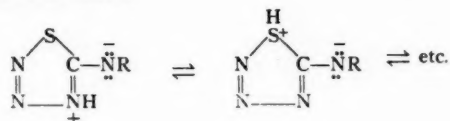
This was demonstrated by the fact that when the 1-phenyltetrazole-5-thiol (XI, $R = \phi$), recovered from the initial alkaline steam degradation, was resubmitted to steam distillation in the presence of a large excess of sodium hydroxide, it was recovered quantitatively unchanged and no volatile product of any type was detectable in the steam distillate. These facts lead immediately to the conclusion that the initial diazotization products of 4-arylthiosemicarbazides cannot possess the tetrazole ring structure as demanded by the structural assignment II ($R = \text{aryl}$) of Freund (9) since its anion, XIV, is identical with the anion of III ($R = \text{aryl}$) and should exhibit the same stability in alkaline medium.

The conclusion that both the initial diazotization products of 4-substituted-thiosemicarbazides and the isothiocyanate-hydrazoic acid reaction products are 5-(substituted)-amino-1,2,3,4-thiatriazoles (structure X) clarifies many of the observations recorded in the literature and in this communication. Some of these points will now be considered.

While structure X can now be assigned to the initial diazotization products of 4-substituted-thiosemicarbazides, the high melting points and crystalline character can best be explained by assuming that X may not exist only as a tautomeric mixture of two or more forms:

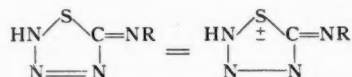


but more probably in zwitterion form:



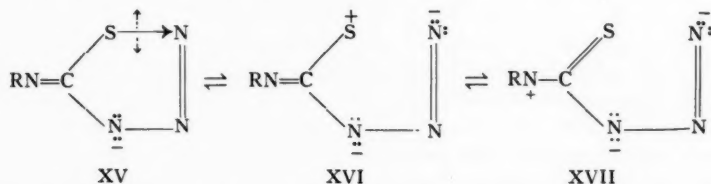
In view of the large number of such charged structures which can be written for

5-(substituted)amino-1,2,3,4-thiatriazoles, it is not inappropriate to consider a mesoionic structure (1):

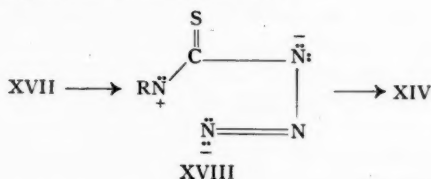


as a possibility.¹¹

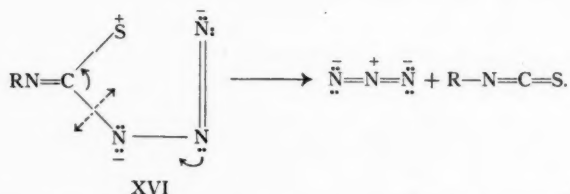
The basic degradation of the 5-(substituted)amino-1,2,3,4-thiatriazoles can readily be accounted for on the basis that the anion produced, XV, undergoes heterolytic cleavage to XVI. The positive (+) charge resulting from this ring opening can then be distributed between the sulphur and nitrogen atoms, as in XVI and XVII, the contribution of each of these high energy forms being dependent on the electrical character of the substituent R:



This is due to the fact that it would be more natural for the positive (+) charge to reside on the sulphur atom rather than on the nitrogen atom because of the greater electronegativity of the nitrogen over sulphur. However, if the electron density of the 5-amino nitrogen atom is decreased by the electron-withdrawing ability of the substituent R, the structure XVII should make a marked contribution to the ground state of the anion, XV. Structure XVII has exactly the charge distribution needed for the formation of the tetrazole ring, which is readily accomplished by the rotation of the azido-group about the carbon atom to produce structure XVIII:



which on ring closure produces the anion of the 1-(substituted)-5-thiatetrazolone, structure XIV being equivalent to structure XIII. On the other hand, the anion structure XVI can readily stabilize itself by the ejection of the more stable azido ion in the following manner:



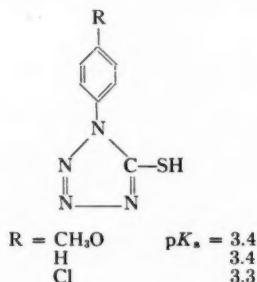
¹¹Spectral, absorption studies in the U.V. region are in progress. Surprisingly, 5-amino-1,2,3,4-thiatriazole shows a very strong absorption maximum at 267 mμ, while the introduction of a CH₃ in the 5-amino position causes a marked bathochromic shift. Similar evidence (15) has been used to show the mesoionic character of 2-methyl-5-alkylaminotetrazoles, which has been also verified by X-ray crystal structure analysis (4).

These considerations lead to the prediction that the tetrazole formation will be favored if R is electronegative, whereas isothiocyanate and azido ion formation will be favored if R is electropositive. This theory is approximately confirmed by the yields of 1-(substituted)-tetrazole-5-thiols summarized in Table III. Note that when R is alkyl or the phenoxide ion, the formation of tetrazole is excluded and that as the electronegativity of R increases there is an approximate trend of increasing tetrazole formation. This is brought out more clearly by a comparison of the following parasubstituted R substituents:

XVIII R	% Yield of 1-R-tetrazole-5-thiol
(4) $^-OC_6H_4$	None
4- $CH_3OC_6H_4$	24
4- $CH_3C_6H_4$	30
4- HC_6H_4	34
4- ClC_6H_4	37

In spite of the complexity of the reactions taking place in alkaline medium, the correlation is reasonably good.

Freund and Hempel (9) on the basis of qualitative observations reported that 1-phenyltetrazole-5-thiol, III ($R = \phi$), possessed strong acidic properties and attributed this to the mercapto-group. The present investigation has confirmed this quantitatively by potentiometric titration of a series of 1-(substituted)phenyltetrazole-5-thiols with the following results:

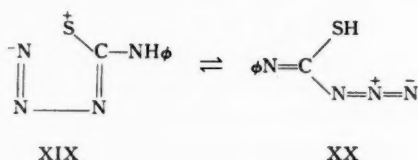


The lack of response in acidity to the inductive effect of the R substituent is surprising in view of the fact that Schwarzenback and Egli (24) found a marked effect of groups on the dissociation of metasubstituted phenylthiols.

The unexpected thermal instability of 1-phenyltetrazole-5-thiol should be noted in view of the marked stability that has previously been reported (2) for the tetrazole ring system. So violent is the degradation at the melting point of the substance that it must be moderated by initially mixing the substance with sand before it can be studied quantitatively. One mole proportion of pure nitrogen is evolved and sulphur is precipitated. The violence of the thermal decomposition suggests the hypothesis that isomerization to the thiatrazole takes place at the melting point:



followed by a heterolytic bond breaking to produce structure XIX:



which is equivalent to phenylthiocarbamyl azide, XX. The presence of the thiol- and azido-groups then leads, at the temperature involved, to an explosive internal oxidation-reduction involving these two groups, producing nitrogen and sulphur. It is possible that this rapid internal oxidation-reduction may take place before isomerization to the thiatriazole ring has taken place. This is comparable to the relatively easy external reduction of the azido-group by hydrogen sulphide (14, 18, 26), the products being the same. A general investigation of the thermal behavior of 1-substituted-tetrazole-5-thiols is in progress.

ACKNOWLEDGMENTS

The authors gratefully acknowledge the receipt of research grants from the Eli Lilly Company, Indianapolis, Ind., and the Research Corporation, New York, N.Y., which made this study possible.

REFERENCES

1. BAKER, W., OLLIS, W. D., and POOLE, V. D. *J. Chem. Soc.* 307 (1949).
2. BENSON, F. R. *Chem. Revs.* **41**, 1 (1947).
3. BOST, R. W. and SMITH, W. F. *J. Am. Chem. Soc.* **53**, 652 (1931).
4. BRYDEN, J. H. *Acta Cryst.* **9**, 874 (1956).
5. CHATTAWAY, F. D., HARDY, R. K., and WATTS, H. G. *J. Chem. Soc.* 1552 (1924).
6. DENNIS, L. M. and BROWNE, A. W. *J. Am. Chem. Soc.* **26**, 577 (1904).
7. DYSON, G. M. and GEORGE, H. J. *J. Chem. Soc.* 1702 (1924).
8. DYSON, G. M., GEORGE, H. J., and HUNTER, R. F. *J. Chem. Soc.* 436 (1927).
9. FREUND, M. and HEMPEL, H. *Ber.* **28**, 74 (1895).
10. FREUND, M. and SCHANDER, A. *Ber.* **29**, 2500 (1896).
11. FREUND, M. and SCHWARZ, H. P. *Ber.* **29**, 2491 (1896).
12. FRY, H. S. *J. Am. Chem. Soc.* **35**, 1539 (1913).
13. JENSEN, K. A. *J. prakt. Chem.* **159**, 189 (1941).
14. HANTZSCH, A. and VAGT, A. *Ann.* **314**, 362 (1900).
15. HENRY, R. A., FINNEGAN, W. G., and LIEBER, E. *J. Am. Chem. Soc.* **76**, 2894 (1954).
16. KALCKHOFF, F. A. *Ber.* **16**, 1825 (1883).
17. LIEBER, E., LEVERING, D. R., and PATTERSON, L. *Anal. Chem.* **23**, 1594 (1951).
18. LIEBER, E., SHERMAN, E., HENRY, R. A., and COHEN, J. *J. Am. Chem. Soc.* **73**, 2327 (1951).
19. MOORE, M. L. and CROSSLEY, F. S. *Organic syntheses*. Vol. 21. John Wiley & Sons, Inc., New York, 1941. p. 81.
20. OLIVERI-MANDALA, E. *Gazz. chim. ital.* **44**, I, 670 (1914).
21. OLIVERI-MANDALA, E. *Gazz. chim. ital.* **51**, II, 195 (1921).
22. OLIVERI-MANDALA, E. *Gazz. chim. ital.* **52**, II, 98 (1922).
23. OLIVERI-MANDALA, E. and NOTO, F. *Gazz. chim. ital.* **43**, I, 304 (1913).
24. SCHWARZENBACK, G. and EGLI, H. *Helv. Chim. Acta*, **17**, 1194 (1934).
25. THIELE, J. *Ann.* **270**, 1 (1892).
26. TURRENTINE, J. W. *J. Am. Chem. Soc.* **34**, 385 (1912).
27. UNDERWOOD, H. G. and DAINS, F. B. *J. Am. Chem. Soc.* **57**, 1768 (1935).
28. WERNER, A. *J. Chem. Soc.* 396 (1891).

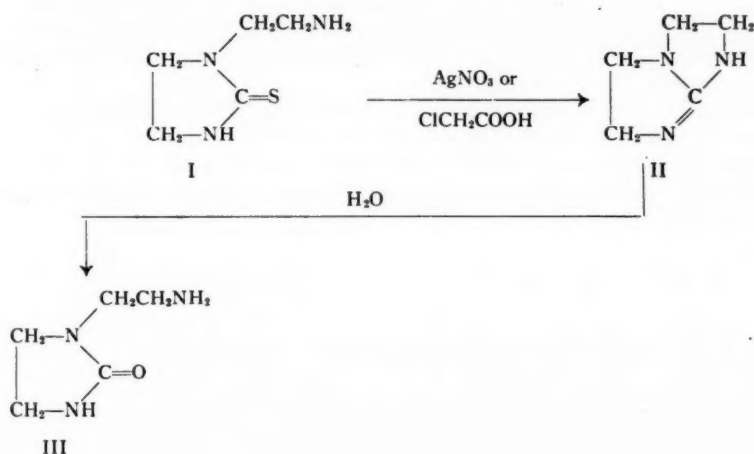
CHEMISTRY OF 2,3,5,6-TETRAHYDRO-1-IMIDAZ(1,2-a)IMIDAZOLE¹

A. F. MCKAY, M.-E. KRELING, G. Y. PARIS, R. O. BRAUN, AND D. J. WHITTINGHAM

ABSTRACT

A new synthesis of 2,3,5,6-tetrahydro-1-imidaz(1,2-a)imidazole is described. This bicyclic compound is hydrolyzed to 1-(β -aminoethyl)-2-imidazolidone. The preparation of 1-(β -hydroxyethyl)- and 1-vinyl-2,3,5,6-tetrahydro-1-imidaz(1,2-a)imidazole also is described.

Recently (5) a synthesis of 2,3,5,6-tetrahydro-1-imidaz(1,2-a)imidazole (II) from 2-(β -hydroxyethylamino)-2-imidazoline by chlorination and dehydrohalogenation was described. Compound II has now been synthesized by the simultaneous desulphurization and cyclization of 1-(β -aminoethyl)-2-imidazolidinethione (I) by silver nitrate, mercuric oxide, or preferably chloroacetic acid. When product II was isolated as its picrate the last reagent gave an 86% yield. This yield was decreased by attempting to isolate the bicyclic compound (II) as the free base. It was found later that the free base in water at room temperature hydrolyzed slowly. The hydrolysis product, 1-(β -aminoethyl)-2-imidazolidone, does not form a picrate under the conditions used for precipitation of 2,3,5,6-tetrahydro-1-imidaz(1,2-a)imidazole as its picrate.



The preparation of 2,3,5,6-tetrahydro-1-imidaz(1,2-a)imidazole by the reaction of ethylenediamine with cyanogen bromide was claimed by Pierron (7). A comparison of the properties of the product from ethylenediamine and cyanogen bromide with the properties of 2,3,5,6-tetrahydro-1-imidaz(1,2-a)imidazole and 2-(β -aminoethylamino)-2-imidazoline as shown in Table I indicates that Pierron had obtained the latter compound. 2-Substituted-amino-2-imidazolines (or their tautomers) have been shown (3) to hydrolyze readily into the corresponding amine and ethyleneurea. On the other hand,

¹Manuscript received April 10, 1957.

Contribution from the L. G. Ryan Research Laboratories of Monsanto Canada Limited, Ville LaSalle, Quebec.

TABLE I
COMPARISON OF 2,3,5,6-TETRAHYDRO-1-IMIDAZ(1,2-a)IMIDAZOLE WITH
2-(β -AMINOETHYLAMINO)-2-IMIDAZOLINE

Compound	M.p. or b.p., °C. (mm.)	Picrates, m.p., °C.	Hydrolysis products
Product from cyanogen bromide and ethylenediamine ^a		203 ^d	Ethylenediamine + ethyleneurea
2-(β -Aminoethylamino)-2-imidazoline (Ref. 4)	200–208 (2) ^b 188–191 (0.7)	205–206.5 ^d	Ethylenediamine + ethyleneurea
2,3,5,6-Tetrahydro-1-imidaz(1,2-a)-imidazole	158.5–159.5 ^c	220–221	1-(β -Aminoethyl)-2-imidazolidone

^aDinitrate m.p. 138° C. (7); dihydrobromide m.p. 224° C. (7).

^bBoiling point.

^cMelting point.

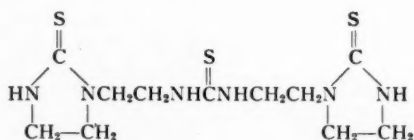
^dDipicrates.

^eMonopicrate.

2,3,5,6-tetrahydro-1-imidaz(1,2-a)imidazole (II) is hydrolyzed to 1-(β -aminoethyl)-2-imidazolidone (III). Further hydrolysis of the latter compound would not be expected to yield ethylenediamine. Furthermore, 2,3,5,6-tetrahydro-1-imidaz(1,2-a)imidazole is monobasic while Pierron's compound is dibasic like 2-(β -aminoethylamino)-2-imidazoline.

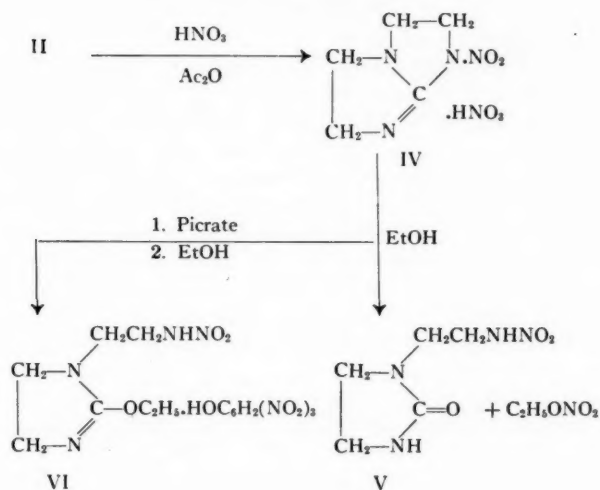
The intermediate, 1-(β -aminoethyl)-2-imidazolidinethione (I), used in the preparation of the bicyclic compound II was prepared from carbon disulphide and diethylenetriamine by the method of Hurwitz and Auten (1).

We were unable to obtain the high yields of 1-(β -aminoethyl)-2-imidazolidinethione reported; instead a mixture of 1-(β -aminoethyl)-2-imidazolidinethione, unreacted diethylenetriamine, and a compound melting at 228–229° C. was obtained. The compound melting at 228–229° C. gave analytical values in excellent agreement with those calculated for the following structure:

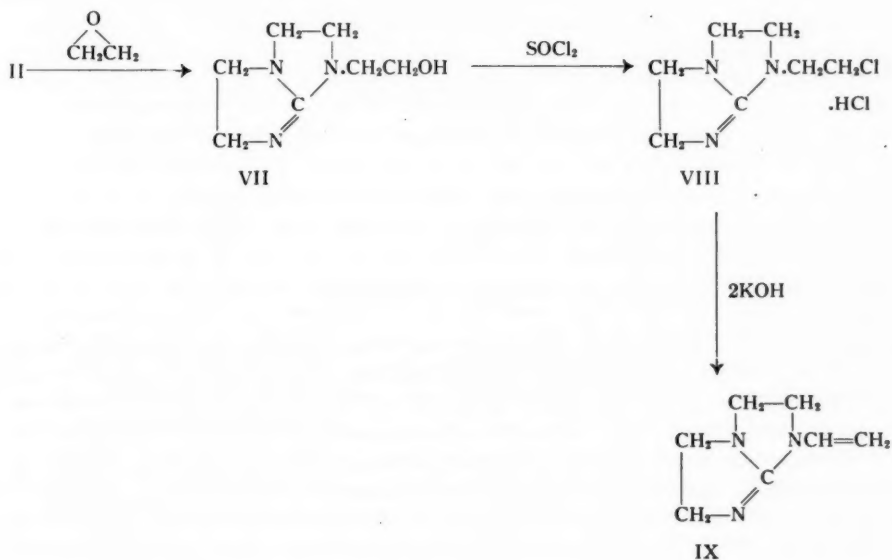


Although Hurwitz and Auten (2) claim the preparation of compounds of similar structure they do not describe their properties.

1-Nitro-2,3,5,6-tetrahydro-1-imidaz(1,2-a)imidazole nitrate (IV) (5) on being refluxed with absolute ethanol gave a 76% yield of 1-(β -nitraminoethyl)-2-imidazolidone (V). The water necessary for the conversion of the bicyclic derivative (IV) into 1-(β -nitraminoethyl)-2-imidazolidone must come from the formation of ethyl nitrate. Attempts to isolate 1-(β -aminoethyl)-3-nitro-2-imidazolidone from the products of this reaction were unsuccessful. When the picrate salt of 1-nitro-2,3,5,6-tetrahydro-1-imidaz(1,2-a)imidazole was refluxed with absolute ethanol, then the picrate (m.p. 112.5–113.5° C.) of a new compound was formed. This compound gave analytical values in agreement with structure VI.



Ethylene oxide combines with 2,3,5,6-tetrahydro-1-imidaz(1,2-a)imidazole (II) to give 1-(β -hydroxyethyl)-2,3,5,6-tetrahydro-1-imidaz(1,2-a)imidazole (VII). The latter compound on chlorination with thionyl chloride and dehydrohalogenation with methanolic potassium hydroxide gave 1-vinyl-2,3,5,6-tetrahydro-1-imidaz(1,2-a)imidazole (IX).



EXPERIMENTAL²*1-(β-Aminoethyl)-2-imidazol'dinethione*

1-(β-Aminoethyl)-2-imidazolidinethione was prepared previously (5) in 34% yield from carbon disulphide and diethylenetriamine by the method of Hurwitz and Auten (1). It has now been prepared in 35.5% yield from thiourea and diethylenetriamine as described by Hurwitz and Auten (2). Since both these reactions gave low yields of 1-(β-aminoethyl)-2-imidazolidinethione, the reaction between carbon disulphide and diethylenetriamine was subjected to closer examination. A solution of diethylenetriamine (103 g., 1.0 mole) in benzene (250 cc.) was placed in a 3-l. three-necked flask fitted with a stirrer, dropping funnel, and thermometer. This solution was cooled with an ice bath, and carbon disulphide (76 g., 1.0 mole) in benzene (200 cc.) was added over a period of 45 minutes. After the carbon disulphide was added, the ice-water bath was replaced by a heating mantle and the reaction mixture was heated under reflux for 10 hours. It was impossible to stir the reaction mixture at the beginning of the reflux period because the solid had caked. After 1 hour at the reflux temperature the solid was converted into a dark green insoluble oil. Hydrogen sulphide was evolved throughout the entire reflux period.

After the benzene was removed *in vacuo*, the residue was extracted with absolute ethanol (3×100 cc.). The ethanol insoluble material melted at 218.5–219° C., yield 16.7 g. The ethanol filtrate was concentrated to 250 cc. and benzene (150 cc.) was added. When it had been in the refrigerator overnight, this solution deposited more crystals melting at 218–219° C., yield 3.3 g. A continuation of this method of separating the reaction products gave a total yield of 29.6 g. (18%) of product melting at 218–229° C. One crystallization from nitromethane gave material melting at 228–229° C. The material gave analytical values in good agreement with those calculated for N,N'-di-(β-1-(2-thioimidazolidinylethyl) thiourea. Anal. Calc. for C₁₁H₂₀N₄S₃: C, 39.73; H, 6.06; N, 25.28; S, 28.93%. Found: C, 39.80; H, 5.94; N, 25.36; S, 28.45%.

The filtrate from the high melting compound gave 86.5 g. of crude 1-(β-aminoethyl)-2-imidazolidinethione (m.p. 86–101° C.). Crystallization of this material from ethanol-benzene gave 44.9 g. (31%) of crystals melting at 109–111° C. The mother liquors from the crude 1-(β-aminoethyl)-2-imidazolidinethione on fractional distillation gave 8.8 g. (8%) of a pale yellow oil (b.p. 59° C. at 0.48 mm.). This oil gave the tripicrate of diethylenetriamine on treatment with a saturated aqueous solution of picric acid. This tripicrate melted at 210–211° C. alone and on admixture with a known sample of diethylenetriamine tripicrate (m.p. 210–211° C.).

*Preparation of 2,3,5,6-Tetrahydro-1-imidaz(1,2-a)imidazole**Method A*

A solution of 1-(β-aminoethyl)-2-imidazolidinethione (1.0 g., 0.007 mole) and silver nitrate (2.34 g., 0.014 mole) in 35 cc. of 85% aqueous ethanol was refluxed for 1 hour and 15 minutes. The precipitate of silver sulphide was removed by filtration. The filtrate was adjusted to a pH of 1.0 with 20% nitric acid solution and the remaining silver nitrate was precipitated as silver chloride. After the silver chloride was removed, the filtrate was evaporated to dryness. A portion (0.227 g.) of the residual oil (1.278 g.) was treated with a saturated aqueous picric acid solution. A crystalline picrate (m.p. 208–210° C.) was obtained, yield 0.197 g. One crystallization from ethanol raised the melting point

²All melting points are uncorrected. The microanalyses were performed by Micro-Tech Laboratories, Skokie, Illinois.

to 219–221° C. This picrate did not depress the melting point of a known (5) sample of 2,3,5,6-tetrahydro-1-imidaz(1,2-a)imidazole picrate (m.p. 220–221° C.). The yield of 2,3,5,6-tetrahydro-1-imidaz(1,2-a)imidazole based on picrate formation is 47%. A similar experiment using mercuric oxide without heating in place of silver nitrate gave a 33% yield of 2,3,5,6-tetrahydro-1-imidaz(1,2-a)imidazole.

Method B

A solution of 1-(β -aminoethyl-2-imidazolidinethione (5.00 g., 0.034 mole) and chloroacetic acid (3.21 g., 0.034 mole) in water (100 cc.) was refluxed for 4 hours. The solution, on evaporation *in vacuo*, gave an oily residue, yield 7.2 g. An analysis of this oil for 2,3,5,6-tetrahydro-1-imidaz(1,2-a)imidazole by picrate formation showed that this bicyclic was formed in 77% yield. The melting point of the picrate was raised from 219° C. to 221° C. by crystallizing from water. A mixture melting point determination with 2,3,5,6-tetrahydro-1-imidaz(1,2-a)imidazole picrate (5) (m.p. 220–221° C.) gave no depression.

The oil (7.0 g.) was dissolved in water (160 cc.) and this solution was passed through a column (diam. 1.8 cm., length 47 cm.) of IRA-400 resin (in the hydroxyl form). The resin was washed with water (740 cc.) and the eluate and washings were evaporated to dryness *in vacuo*. This oil (4.03 g.) was dissolved in acetone and the acetone solution was cooled. The deposited crystals (m.p. 158–159° C.) were removed by filtration, yield 0.7 g. (19%). A mixture melting point determination between these crystals and a known sample of 2,3,5,6-tetrahydro-1-imidaz(1,2-a)imidazole (5) (m.p. 158.5–159.5° C.) gave no depression.

The oil obtained from the acetone mother liquors contained 46.8% 2,3,5,6-tetrahydro-1-imidaz(1,2-a)imidazole as determined by picrate analysis but it could not be isolated as the free base. Similar experiments gave 2,3,5,6-tetrahydro-1-imidaz(1,2-a)imidazole picrate in yields varying between 71 and 86%.

A sample of 1-nitro-2,3,5,6-tetrahydro-1-imidaz(1,2-a)imidazole nitrate (5) (0.19 g.) was dissolved in water and treated with an aqueous solution of picric acid (15 cc.). The picrate (m.p. 145–147° C. with decomposition) was purified by one crystallization from water after which it melted at 146.5–147.5° C. with decomposition, yield 0.177 g. (53%). Anal. Calc. for $C_{11}H_{11}N_7O_9$: C, 34.28; H, 2.88; N, 25.45%. Found: C, 34.34; H, 3.12; N, 25.72%.

Reaction of 1-Nitro-2,3,5,6-tetrahydro-1-imidaz(1,2-a)imidazole Nitrate in Ethanol

1-Nitro-2,3,5,6-tetrahydro-1-imidaz(1,2-a)imidazole nitrate (0.57 g., 0.0026 mole) in absolute ethanol (50 cc.) was refluxed for 2½ hours. The resulting solution was concentrated to 5 cc. *in vacuo* and then stored in the refrigerator for 2 hours. The crystalline precipitate (m.p. 175° C.) was removed by filtration, yield 0.346 g. (76%). One crystallization from ethanol raised the melting point to 180° C. A mixture melting point with an authentic sample of 1-(β -nitraminoethyl)-2-imidazolidone (5) (m.p. 180–182° C.) was not depressed. The filtrate from 1-(β -nitraminoethyl)-2-imidazolidone did not yield any further identifiable products.

Reaction of 1-Nitro-2,3,5,6-tetrahydro-1-imidaz(1,2-a)imidazole Picrate with Ethanol

1-Nitro-2,3,5,6-tetrahydro-1-imidaz(1,2-a)imidazole picrate (0.132 g.) on crystallizing three times from absolute ethanol (30 cc./g.) gave 70 mg. (47%) of a new picrate which melted sharply at 112.5–113.5° C. Anal. Calc. for $C_{13}H_{17}N_7O_{10}$: C, 36.20; H, 3.97; N, 22.74%. Found: C, 36.40; H, 4.27; N, 22.56%.

Hydrolysis of 2,3,5,6-Tetrahydro-1-imidaz(1,2-a)imidazole

2,3,5,6-Tetrahydro-1-imidaz(1,2-a)imidazole (314.8 mg., 0.003 mole) in water (5 cc.) was refluxed for 50 minutes. After the water was removed *in vacuo* the residual colorless oil (361 mg.) was dissolved in absolute ethanol (10 cc.). Gaseous hydrogen chloride was passed into this ethanolic solution until a pH of 3 was obtained. A crystalline solid was precipitated on addition of ether (5 cc.), yield 375 mg. (81%). This product melted at 175.5–177° C. alone and on admixture with a known sample of 1-(β -aminoethyl)-2-imidazolidone hydrochloride (m.p. 176–177° C.) (6). 1-(β -Aminoethyl)-2-imidazolidone does not give a picrate on addition of saturated aqueous or ethanolic solutions of picric acid. When 2,3,5,6-tetrahydro-1-imidaz(1,2-a)imidazole was dissolved in water at room temperature, 93% was recovered as its picrate, while after 16½ hours only 86% was recovered in this manner.

1-(β -Hydroxyethyl)-2,3,5,6-tetrahydro-1-imidaz(1,2-a)imidazole

A solution of 2,3,5,6-tetrahydro-1-imidaz(1,2-a)imidazole (19 g., 0.17 mole) in absolute methanol (85 cc.) was treated with a solution of ethylene oxide (8.3 g., 0.188 mole) in absolute methanol (40 cc.) at 0° C. This solution was heated to reflux temperature and it was refluxed for 1½ hours. After the solvent was removed *in vacuo* under nitrogen a light yellow oil was obtained, yield 23.5 g. (86%). The oil on distillation (b.p. 125.5–126° C. at 0.13 mm.) gave a crystalline (m.p. < 60° C.) product, yield 17.4 g. Two crystallizations from ethyl acetate (ca. 6 cc./g.) raised the melting point to a constant value of 68.5–69.5° C. Anal. Calc. for $C_7H_{13}N_3O$: C, 54.16; H, 8.44; N, 27.06%. Found: C, 54.13; H, 8.46; N, 26.83%.

A sample of the crude waxy crystals (410 mg., 0.0026 mole) in ethyl acetate (20 cc.) was treated with a saturated ethyl acetate solution of picric acid. The crystalline picrate (m.p. 110.5–111.5° C.) was obtained in 72.4% (734 mg.) yield. Anal. Calc. for $C_{13}H_{16}N_6O_8$: C, 40.62; H, 4.20; N, 21.87%. Found: C, 40.92; H, 4.26; N, 22.06%.

Several runs on the preparation of 1-(β -hydroxyethyl)-2,3,5,6-tetrahydro-1-imidaz(1,2-a)imidazole gave yields of pure product varying between 56 and 72%.

1-(β -Chloroethyl)-2,3,5,6-tetrahydro-1-imidaz(1,2-a)imidazole Hydrochloride

To 1-(β -hydroxyethyl)-2,3,5,6-tetrahydro-1-imidaz(1,2-a)imidazole (80 g., 0.513 mole) in absolute methanol (55 cc.) was added a 10% excess of 5 N HCl in methanol. The solution was taken to dryness *in vacuo* to yield a light yellow viscous oil, yield 99 g. (100%). A solution of 1-(β -hydroxyethyl)-2,3,5,6-tetrahydro-1-imidaz(1,2-a)imidazole hydrochloride (17.7 g., 0.09 mole) and freshly distilled thionyl chloride (15 g., 0.126 mole) in pure chloroform (60 cc.) was refluxed for 2 hours and 20 minutes. After the solvent and excess thionyl chloride were removed *in vacuo* under nitrogen, a semicrystalline oil was obtained, yield 19.5 g. (100%). A picrate of this oil was formed from aqueous solution in the usual manner. Two crystallizations from water raised the melting point from 117–120° C. to 120–121° C. Anal. Calc. for $C_{13}H_{15}ClN_3O_7$: C, 38.76; H, 3.75; N, 20.87; Cl, 8.80%. Found: C, 38.94; H, 3.79; N, 20.48; Cl, 8.76%.

In some runs it was found that the oily product of 1-(β -chloroethyl)-2,3,5,6-tetrahydro-1-imidaz(1,2-a)imidazole hydrochloride contained 5–12% of 2,3,5,6-tetrahydro-1-imidaz(1,2-a)imidazole hydrochloride. The latter compound was separated by treating the original oil with boiling acetone (11–12 cc./g.). The acetone solution on cooling deposited crystals (m.p. 153–156° C.) of 2,3,5,6-tetrahydro-1-imidaz(1,2-a)imidazole hydrochloride. The melting point was raised to 156.5–157.5° C. by crystallizing from methanol. This product was identified as its picrate (m.p. 219.5–222° C.) by a mixed

melting point determination with an authentic sample (5) of 2,3,5,6-tetrahydro-1-imidaz(1,2-a)imidazole picrate (m.p. 220–221° C.). The original acetone mother liquors on evaporation gave 1-(β -chloroethyl)-2,3,5,6-tetrahydro-1-imidaz(1,2-a)imidazole hydrochloride as an oil.

1-Vinyl-2,3,5,6-tetrahydro-1-imidaz(1,2-a)imidazole

1-(β -Chloroethyl)-2,3,5,6-tetrahydro-1-imidaz(1,2-a)imidazole hydrochloride (8 g., 0.038 mole) in absolute methanol (25 cc.) was placed in a three-necked flask fitted with a condenser, stirrer, and dropping funnel. After the solution was refluxing, methanolic potassium hydroxide solution (49.6 cc. of 1.53 *N* KOH in methanol) was added over a period of 20 minutes. After the methanolic potassium hydroxide solution was added, the dropping funnel was replaced with a capillary nitrogen lead-in. The refluxing was continued for 2 hours under nitrogen. This solution, when it was left standing under nitrogen in the refrigerator, deposited crystals of potassium chloride. The potassium chloride was removed by filtration and the filtrate was taken to dryness *in vacuo* under nitrogen. The residue was extracted with ether (5×50 cc.). Evaporation of the combined ethereal extracts gave 4.5 g. (86.5%) of a mobile light yellow oil. This product on distillation gave a colorless oil (b.p. 85.5–86° C. at 0.275 mm.). Anal. Calc. for $C_7H_{11}N_3$: C, 61.29; H, 8.08; N, 30.63%. Found: C, 60.93; H, 8.09; N, 30.83%.

A sample (233.5 mg.) of this oil in ethyl acetate (2 cc.) on treatment with a saturated ethyl acetate solution of picric acid gave 508 mg. (81%) of a crystalline picrate (m.p. 170–171.5° C.). Two crystallizations from ethyl acetate raised the melting point to 171.5–172.5° C. Anal. Calc. for $C_{13}H_{14}N_6O_7$: C, 42.63; H, 3.88; N, 22.94%. Found: C, 42.94; H, 3.91; N, 23.06%. Several preparations of 1-vinyl-2,3,5,6-tetrahydro-1-imidaz(1,2-a)imidazole gave similar results.

REFERENCES

1. HURWITZ, M. D. and AUTEN, R. W. U.S. Patent No. 2,613,211 (October 7, 1952).
2. HURWITZ, M. D. and AUTEN, R. W. U.S. Patent No. 2,613,212 (October 7, 1952).
3. MCKAY, A. F., BUCHANAN, M. N., and GRANT, G. A. J. Am. Chem. Soc. **74**, 766 (1949).
4. MCKAY, A. F., COLEMAN, J. R., and GRANT, G. A. J. Am. Chem. Soc. **72**, 3205 (1950).
5. MCKAY, A. F., HATTON, W. G., and BRAUN, R. O. J. Am. Chem. Soc. **78**, 6144 (1956).
6. MCKAY, A. F., PARIS, G. Y., and KRELING, M.-E. J. Am. Chem. Soc. (In press, 1957).
7. PIERRON, P. Ann. chim. et phys. [9], **11**, 361 (1919).

THE PRODUCTION OF TITANIUM TRICHLORIDE BY ARC-INDUCED HYDROGEN REDUCTION OF TITANIUM TETRACHLORIDE¹

T. R. INGRAHAM, K. W. DOWNES, AND P. MARIER

ABSTRACT

Finely powdered titanium trichloride of high purity was prepared by an arc-induced reaction of titanium tetrachloride with hydrogen. The hydrogen chloride by-product was passed over heated titanium, and the regenerated hydrogen and titanium tetrachloride were recirculated to the arc. The method in effect utilizes the reducing power of the titanium metal to produce titanium trichloride from titanium tetrachloride.

INTRODUCTION

Titanium trichloride (TiCl_3) is a highly reactive substance which is rapidly hydrolyzed by water and is pyrophoric in air. It has a much higher solubility than titanium tetrachloride (TiCl_4) in molten salts and is readily ionized. In molten salt media it has been used as a titanium source material for the recovery of metallic titanium by electrolysis (3) and disproportionation (7).

Titanium trichloride has been prepared by reducing TiCl_4 with hydrogen at high temperatures (1), in silent electrical discharge (2), and by reduction with metals such as aluminum (15), antimony, lead, sodium amalgam (13), titanium (4), and zinc.

When prepared by hydrogen reduction, the system must include a generation and purification train for hydrogen and a means for economically disposing of the by-product, HCl . When prepared by metal reduction, the product contains TiCl_2 and the chloride of the reducing metal. Since the quantitative separation of titanium subchlorides from each other (6) and from many other metal chlorides is difficult, and since the generation and purification of hydrogen is not without danger, a simplified method of preparing pure TiCl_3 was sought.

In this paper, it will be shown that titanium can be used to regenerate hydrogen and TiCl_4 from the HCl by-product of an arc-induced hydrogen- TiCl_4 reaction, and that a cyclic system can be built, into which TiCl_4 and titanium are fed and out of which pure TiCl_3 is removed.

APPARATUS

The apparatus in which TiCl_3 , 13, was produced is shown diagrammatically in Fig. 1. The apparatus was constructed principally of 25 mm. pyrex glass tubing with brass ball valves, 7 and 9, joined to the pyrex by a copper to pyrex seal. One ball valve, 7, served to control the access of TiCl_4 , 5, to the system; the other, 9, sealed the system from vacuum, argon, and hydrogen sources. Teflon gaskets were used in the ball valves. Where it was necessary to open the apparatus for the discharge of product, a pyrex glass pipe fitting with a Teflon gasket, 16, was used.

The electrode section of the apparatus, 12, consisted of pyrex tubing reduced from 25 mm. to 6.5 mm. inside diameter over a length of 10 mm. Tungsten electrodes were sealed in the pyrex in such a way that the space through which the arc passed was 22 mm. in length. The top electrode was placed deeper within the constricted zone than the bottom electrode, to aid in directing the reaction product downward through the arc.

¹Manuscript received January 22, 1957.

Contribution from the Extractive Metallurgy Section, Mineral Dressing and Process Metallurgy Division, Mines Branch, Department of Mines and Technical Surveys, Ottawa; published with the permission of the Deputy Minister.

In this way, the rapidly expanding gases from the arc forced the TiCl_3 product, 13, preferentially in the direction of the collection container, 14.

High voltages to produce the required arc within the gas were provided by either a Tesla coil leak tester or the igniting circuit from a Pfeilsticker spectrographic source unit, 11. The titanium, 3, used for the regeneration of hydrogen was heated by an external tube furnace, 10, automatically controlled to $\pm 2^\circ \text{C}$. The control range did not

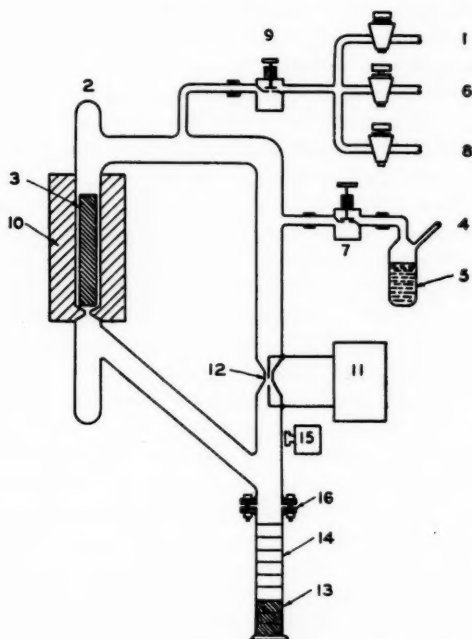


FIG. 1. Apparatus used for production of TiCl_3 .

represent the uniformity of temperature throughout the furnace, owing to the vertical position of the furnace, the upward flow of gas, and the inevitable temperature gradient in an open-ended furnace. Nevertheless, for short titanium coupons, the titanium temperature was effectively the mid-point temperature of the furnace.

PROCEDURE

Before a run was started, the apparatus was evacuated to a pressure of 10^{-4} mm. of mercury and checked for leaks. When the apparatus was found to be free from leaks and any moisture introduced during assembly, helium was admitted through 1, and an opening was made at 2 through which the titanium was placed at 3. The titanium consisted of strips, rods, or pellets which were reasonably free of surface oxide coatings. The system was then sealed with a torch at 2 and an opening made at 4. Through the opening at 4, against a gentle countercurrent of helium, a specified volume of TiCl_3 was admitted to the apparatus at 5. The opening at 4 was then sealed with a torch, the helium supply cut off, and the TiCl_3 frozen with liquid air. Because of its lower freezing point, helium was used in preference to argon. When freezing was complete, the apparatus

was thoroughly evacuated through 6, and valve 7 closed. The TiCl_4 at 5 was then melted and brought to room temperature. While this was taking place, hydrogen was admitted through 8 to a specified pressure measured by a McLeod gauge, then valve 9 was closed and the furnace 10 surrounding the titanium was brought up to temperature. When equilibrium had been reached, exciter 11 was started, valve 7 was opened, and the vapor of TiCl_4 was admitted to the system.

The immediate result of exciting the arc was the production of finely powdered TiCl_3 , which collected on the inside of orifice 12 and was blown down the tube by the circulating gas stream. The powdered TiCl_3 , 13, settled in the graduated container, 14. Because the powder was electrostatically charged, some of it was attracted to the glass walls of the vertical tubing, from which it was continuously dislodged by a mechanical vibrator, 15.

At the end of a run, when the reservoir 14 was filled with TiCl_3 , valve 7 was closed and the gaseous atmosphere of the apparatus was removed by pumping through 6. Helium was then admitted through 1, and clamp 16 loosened. Against a gentle counter-current of helium, container 14 was removed and replaced by a duplicate container, previously flushed with helium. After the clamps were tightened at 16, the system was again evacuated to 10^{-4} mm. of Hg and cylinder hydrogen admitted through 8 to a specified pressure. Valve 9 was closed and valve 7 opened. When the arc was struck, reaction was resumed and additional product was formed. The run was continued without further interruption or attention until another TiCl_3 container had been filled, or the titanium or the TiCl_4 supply exhausted. Occasionally it was found necessary to replenish the hydrogen in the system when a large amount of TiCl_3 had been formed, owing presumably to the adsorption of hydrogen on the finely divided TiCl_3 .

As an alternative to injecting hydrogen into the system at the beginning of an experiment, it was found that if the TiCl_4 supply were renewed each time the TiCl_3 product was removed, it was possible to use a solution of TiCl_4 saturated with HCl for charging the system. The volume of TiCl_4 -HCl solution introduced into the system was calculated so that when the HCl was released from it under vacuum and converted to hydrogen at the titanium, the pressure of hydrogen in the system was equivalent to that obtained from optimum hydrogen injections. A convenient method for determining the amount of HCl dissolved in TiCl_4 was developed and used in this work (8).

OPTIMUM OPERATING CONDITIONS

During experiments on the conversion of mixtures of TiCl_4 and hydrogen to TiCl_3 and HCl, it was found that the reaction was affected by the type of excitation used for the discharge. It was found that certain types of discharges gave appreciably larger yields of product. For example, while a 60-cycle alternating current arc had virtually no effect on the mixture, the discharge produced by a Tesla coil leak tester or by the igniting circuit from a Pfeilsticker spectrographic source unit was quite effective. The most efficient discharge found for promoting the reaction was characterized as follows (5): A high voltage oscillatory spark discharge, heavily damped, with a frequency of approximately 200 kc./seconds and a total duration of about 5×10^{-8} seconds. Discharges were produced in groups of four with each half cycle and were initiated at about 1000 volts and maintained at about 10 volts and 100 amperes.

The optimum dimensions for the area surrounding the discharge were determined experimentally in a series of runs. It was found that this area should be sufficiently small to permit effective activation of all of the gas stream passing through the constrict-

tion but not so small that the glass wall enclosing the constriction attained temperatures appreciably above 50° C. on the outside. An inside diameter for the constricted area of 5–9 mm. over a length of 8–12 mm. when used with a discharge length of 15–30 mm. seemed to satisfy the required conditions. Average values within the above ranges were found to be optimum values.

The TiCl_4 pressures in the apparatus were maintained, in most runs, at the equilibrium vapor pressure at room temperature, i.e. 10–13 mm. of mercury at 20–25° C. Qualitative results at lower pressures showed that with decreasing TiCl_4 pressure a lower rate of TiCl_3 production was obtained. Owing to the nature of the apparatus, and to the fact that if higher TiCl_4 pressures were to be studied the temperature of all parts of the apparatus would have to be raised uniformly, few attempts were made to study the effects of higher TiCl_4 pressures. From the qualitative results of the higher pressure experiments, it was concluded that excessive contamination of the titanium with TiCl_2 took place. For these reasons, subsequent studies were made at equilibrium TiCl_4 pressure at room temperature.

The range of hydrogen pressures compatible with TiCl_4 at its vapor pressure of 10–13 mm. of mercury was found to be between 1 and 7 mm. of mercury in the system investigated. Below 1 mm., the rate of TiCl_4 conversion was extremely slow; above 7 mm. it was observed that the amount of HCl remaining unconverted to hydrogen in the system was sufficient to alter the excitation characteristics of the arc, with the result that the rate of TiCl_3 formation in the arc was appreciably reduced. Pressures between 4 and 5 mm. were found to give the highest rates of production and hence were used throughout the experiments.

To convert the HCl by-product from the arc reaction to hydrogen for re-use at the arc, several materials were used. It was found that lead, aluminum, and titanium were satisfactory. When lead and aluminum were used, the by-products were lead and aluminum chlorides. These accumulated in the furnace and were difficult to recover. In addition, neither is an economically desirable by-product.

When titanium, which had previously been cleaned so that its surface was reasonably free of titanium oxides, was used to convert the HCl from the arc reaction to hydrogen, it was found that the apparatus could be operated continuously for extended periods with a minimum of attention. It was found desirable to heat the titanium only to a temperature at which hydrogen diffusion into the titanium was relatively slow and at which the reaction of HCl at the titanium had a favorable rate. At the end of each run, determinations were made of the weight of titanium consumed, the approximate volume of TiCl_4 consumed, the weight of TiCl_3 recovered from the reservoir, and the weight and distribution of TiCl_2 and TiCl_3 in the mixed product surrounding the titanium in the furnace.

RESULTS

The data to be presented in this section were obtained in a single apparatus which incorporated optimum orifice size, electrode separation, arc excitation conditions, and hydrogen pressure. The experiments were designed to show the effects of titanium temperature on the rate of production and final yield of TiCl_3 and to provide observations which might be used to deduce the mechanism of the processes by which TiCl_3 was produced in the system.

The data obtained from a series of runs in which the rate of TiCl_3 production as a function of titanium temperature was studied at an initial hydrogen pressure of 4 mm. of mercury and a TiCl_4 pressure of 13 mm. of mercury are shown in Fig. 2.

Fig. 2 shows that the threshold temperature for initiating the conversion by titanium of HCl to hydrogen is 375° C. Fig. 2 also shows that the rate of TiCl_3 production in the arc increased with increasing titanium temperature up to 460° C., decreased slightly to 525° C., and then increased again with further temperature increase to 550° C. (the limiting temperature obtainable in a pyrex apparatus under partial vacuum). From Fig. 2, the optimum temperature appears to be near 460° C.

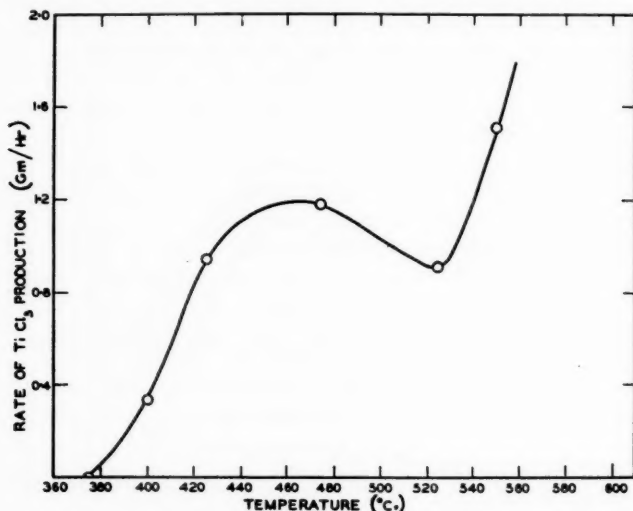


FIG. 2. Rate of TiCl_3 production as a function of the temperature of the metallic titanium in the system.

Since it appeared impossible to eliminate the reaction of TiCl_4 with titanium in the furnace while operating at good production rates, a small operating loss of titanium and TiCl_4 to form TiCl_2 and TiCl_3 in the furnace chamber was accepted.

Fig. 3 shows that the yield of TiCl_3 decreased continuously with increasing temperature of the titanium. At the maximum rate of TiCl_3 formation (460° C.), the recovery of TiCl_3 was 91%.

The reduction of TiCl_3 yield from 97% to 71% with increasing temperature corresponded with an increase in the amount of TiCl_2 and TiCl_3 formed in the vicinity of the titanium. It was observed that the composition of this titanium chloride mixture varied with the temperature to which the titanium was heated. In Fig. 4, the mole percentage of TiCl_3 in the mixture is shown as function of the temperature of the titanium.

Fig. 4 shows that, in the low temperature experiments, equimolar quantities of TiCl_3 and TiCl_2 were recovered from the region surrounding the titanium. As the temperature was increased to near 460° C., where the optimum rate of TiCl_3 production was obtained (Fig. 2), the product contained about 90 mole per cent TiCl_3 (Fig. 4).

The TiCl_3 recovered from the arc reaction was formed initially as a brownish-red powder. When the material fell into the receiver, its color changed to a stable purple. Depending on the depth of packing in the receiver and the intensity of vibration imparted by the vibrator attached to the apparatus, the powder settled to apparent densities varying from 0.07 to 0.25 g./cm.³ When analyzed for chlorine and titanium, the product

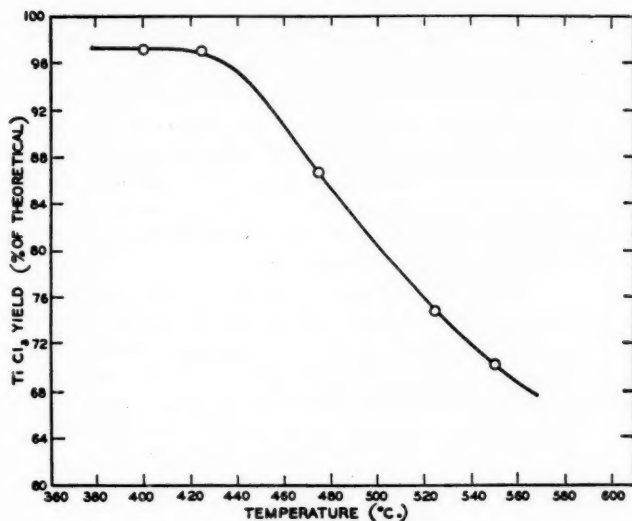


FIG. 3. $TiCl_3$ yield (percentage of the theoretical) as a function of the temperature of the metallic titanium in the system.

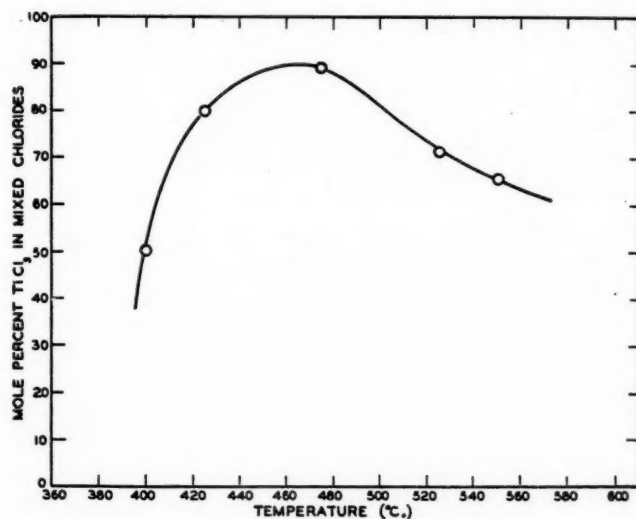


FIG. 4. Mole percentage $TiCl_3$ in the subchloride mixture on the surface of the metallic titanium as a function of the titanium temperature.

gave ratios varying between 2.99:1.00 and 3.01:1.00. With the exception of analytical errors, the low ratio has been explained by the presence of small amounts of $TiCl_2$, and the high ratio by adsorbed $TiCl_4$. Where analysis was accomplished without air oxidation, the product was shown to be 99.8% $TiCl_3$.

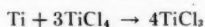
TYPICAL SAMPLE RUN

Internal orifice diameter	6.5	mm.
Electrode separation	22	mm.
Volume of system (approx.)	1750	cm. ³
Titanium temperature	425° C.	
Initial hydrogen pressure	4.33	mm. Hg
Duration of run	23.0	hours
TiCl ₄ consumed (approx.)	13	cm. ³
Titanium consumed	1.7554	g.
Theoretical TiCl ₃ yield, based on titanium consumed	22.60	g.
Primary TiCl ₃ recovered	21.96	g.
Primary TiCl ₃ recovery	96.9%	
Average rate primary TiCl ₃ production	0.95	g./hour
Ratio Cl/Ti in secondary product	2.81:1.00	
Secondary TiCl ₃ recovered	0.48	g.
Secondary TiCl ₂ recovered	0.12	g.

DISCUSSION

It is well known that titanium absorbs hydrogen readily, and that the equilibrium attained is a function of the titanium temperature and hydrogen pressure (12). At the temperatures and pressures used in these experiments, the rate of hydrogen absorption has been shown to be slow, relative to the rate of removal of titanium. Hence, since no effective absorption could take place, the mechanism of the reaction which will be suggested will make no reference to hydrogen absorption by the titanium.

To calculate the yield of TiCl₃ in the foregoing experiments, the over-all reaction



is applicable to the system. This reaction suggests that, in effect, the titanium may be considered both as a reducing agent for TiCl₄ and as a component of the product TiCl₃.

The stepwise reactions through which the above functions are achieved will be elucidated by discussing separately the reactions taking place in the arc and at the titanium.

Reactions in the Arc

When pure TiCl₄ vapor was passed through the arc in experiments without hydrogen, no visible decomposition of the TiCl₄ resulted. The same observation has been made by Gutman (6) during studies using electrodeless discharges. However, when small amounts of hydrogen were admitted to the system, a blue glow developed in the reaction zone; TiCl₃ formed and was precipitated on the walls of the reaction vessel. This blue glow is commonly observed in electrically stimulated hydrogen reactions and is attributed to excitation of molecular hydrogen. Failure to observe the reddish glow associated with hydrogen atoms was attributed both to a relatively low concentration of hydrogen atoms in the reaction zone and to the masking effects of the reddish colored TiCl₃ precipitated on the walls of the vessel in the reaction zone. If the reactions



are considered to represent the formation of TiCl_3 in the arc, the observed sensitivity of TiCl_3 production in the arc to small variations in its power supply may be explained by the sharp dependence of hydrogen atom generation on the mode of excitation used. In addition, the strong temperature dependence of the secondary H-H_2 recombination reaction taking place on the walls of the reaction vessel would explain the observations that when the diameter of the orifice through which the arc passed was decreased, and the temperature of the orifice increased appreciably beyond 50°C ., TiCl_3 production diminished. Hence, temperature effects on the H-H_2 recombination reaction may explain the low reaction rate obtained with small diameter orifices, while only partial reaction of the gas stream would explain the low reaction rate when a large diameter orifice was used. Thus, an optimum diameter for the orifice was indicated.

When hydrogen was added initially to the system to promote the TiCl_4 decomposition reaction in the arc, it was found that 4–5 mm. of mercury pressure of hydrogen gave the best results in terms of TiCl_3 yield. When lesser amounts were used, the lower rate of TiCl_3 production was explained by there being insufficient hydrogen to promote reactions [1] and [2] effectively. When larger amounts were used, the lower rate of TiCl_3 production was explained by a combination of two effects. In the first instance, the generation of hydrogen atoms in a system is a function of both the partial pressure of hydrogen and the total gas pressure in the system. When either is increased, as would be the case when hydrogen pressure in excess of 4–5 mm. was used, the production of hydrogen atoms would be reduced; hence a decreased yield of TiCl_3 would be expected and was in fact observed. The second effect, to which the decreasing yield of TiCl_3 with high hydrogen pressures may be attributed, is predictable from equation [2]. If it is assumed that the regeneration capacity of the system for converting HCl to hydrogen is fixed, then the presence of an initial excess of hydrogen beyond that required for steady state conditions would lead to the accumulation of a circulating load of HCl in the system. This in turn would decrease the efficiency of reaction [2] and thus lead to a reduction in the rate of TiCl_3 production with excess hydrogen. Fixing of the regeneration capacity of the system will be discussed by reference to temperature effects on reactions at the titanium.

Reactions at the Titanium

In any system containing heated titanium and gaseous TiCl_4 , reactions to form TiCl_2 and TiCl_3 can be expected to occur (4, 10, 9). Both of these products have been detected on the surface of the titanium during a run. The presence of hydrogen and HCl in the system did not appear to prevent the formation of subchlorides, but it was observed that the presence of HCl did prevent their accumulation up to the point where their lack of volatility would protect the titanium from further reaction.

The production of TiCl_2 and TiCl_3 at the titanium can be represented by the reactions:



Since both reaction products have a relatively low volatility, any accumulation of these products in the vicinity of the titanium must result in decreased yield of TiCl_3 recovered from the arc and based on the disappearance of titanium. This reduction in yield is shown in Fig. 3. At a titanium temperature of 400°C ., 97.2% of the titanium reacted was converted to recoverable TiCl_3 in the arc and 2.8% accumulated as mixed chlorides at the titanium. At 550°C ., a substantial reduction in the TiCl_3 yield to 71.1% was

observed to accompany the accumulation of 28.9% of the reacted titanium as mixed chlorides. Since the accumulated mixed chlorides at the titanium are undesirable and are difficult to recover pure, efficiency considerations require the temperature of the titanium to be as low as possible consistent with favorable conversion of HCl to hydrogen.

The reaction by which HCl is converted to hydrogen at the titanium may be deduced from Fig. 2 and Fig. 4. Fig. 2 shows that the optimum rate of TiCl_3 formation in the arc, which reflects the most efficient regeneration of hydrogen from HCl at the titanium, occurs at a titanium temperature near 460°C . Fig. 4, showing the relative distribution of TiCl_3 and TiCl_2 in the mixed chlorides at the titanium, indicates that at 460°C . the product at the titanium is principally TiCl_3 . Thus, it may be reasoned that the conditions which produce a preponderance of TiCl_3 over TiCl_2 at the titanium are the most favorable for hydrogen regeneration from HCl or, conversely, that maximum hydrogen regeneration is accompanied by maximum TiCl_3 availability at the titanium. Either might be construed to indicate that TiCl_3 and H_2 formation accompany each other:



Although this reaction is thermodynamically favorable, it indicates that the regeneration of hydrogen would be accompanied by the accumulation of TiCl_3 at the titanium in quantities equivalent to the amount of hydrogen regenerated. Since from the percentage of TiCl_3 recovered, as shown in Fig. 3, it may be deduced that 10 to 30 times as many moles of hydrogen as moles of TiCl_3 are regenerated at the titanium, it follows that under favorable reaction conditions all hydrogen regeneration cannot take place by reaction [5].

To avoid the accumulation of TiCl_3 , as inferred from reaction [5], while still permitting the regeneration of hydrogen, the following thermodynamically less favorable reaction is suggested (11):



Both products from this reaction are volatile and may be fully utilized in the system. Thus, reactions [3], [4], and [6], with possibly a small contribution from [5], are consistent with the observation of almost complete utilization of the titanium for the regeneration of hydrogen and the return of TiCl_4 to the system.

The validity of reaction [6] for the regeneration of hydrogen indirectly from the titanium was checked by placing TiCl_3 in the furnace chamber instead of titanium. It was found that the hydrogen chloride was effectively removed from the system, hydrogen satisfactorily regenerated, and the titanium trichloride consumed.

Having thus placed the burden of hydrogen regeneration on the consumption of TiCl_3 formed on the surface of the titanium, it is now possible to explain the decrease in the rate of TiCl_3 production in the arc shown in Fig. 2 at titanium temperatures above 460°C . Above 460°C ., TiCl_3 is unstable and disproportionates at low TiCl_4 pressures to TiCl_2 (14):



This is borne out by Fig. 4, which shows that the proportion of TiCl_3 to TiCl_2 in the mixed chlorides on the titanium decreases with increasing temperature. From the argument previously developed to show hydrogen regeneration to be a function of the TiCl_3 available at the titanium, it is evident that when TiCl_3 becomes unstable owing to disproportionation, hydrogen regeneration would decrease and hence the yield of TiCl_3 in the arc would decrease.

In Fig. 2, the sharp increase in TiCl_3 production in the arc with titanium temperature increase above 525°C . cannot be adequately explained. It is suggested, however, that at these temperatures the heterogeneous reactions [4] and [6] might occur rapidly and homogeneously in the gas phase.

REFERENCES

1. BAEZINGER, N. and RUNDLE, R. E. *Acta Cryst.* **1**, 274 (1948).
2. BÖCK, F. and MOSER, L. *Monatsh. Chem.* **33**, 1407 (1912).
3. CORDNER, G. D. P. and WÖRNER, H. W. *Australian J. Appl. Sci.* **2**, 358 (1951).
4. FAST, J. D. *Z. anorg. u. allgem. Chem.* **241**, 42 (1939).
5. GRAY, M. W. Personal communication.
6. GUTMAN, V., NOWOTNY, H., and OFNER, G. *Z. anorg. u. allgem. Chem.* **278**, 78 (1955).
7. INGRAHAM, T. R. Research Report MD173, Mines Branch, Dept. of Mines and Technical Surveys, Ottawa, Canada (1954).
8. INGRAHAM, T. R. *Can. J. Chem.* **33**, 1731 (1955).
9. JORDAN, J. F. U.S. Patent No. 2,670,270 (1954).
10. KLEMM, W. and GRIMM, L. *Z. anorg. u. allgem. Chem.* **249**, 198 (1942).
11. KRIEVE, W. F. and MASON, D. M. *J. Chem. Phys.* **25**, 524 (1956).
12. McQUILLAN, A. D. *Proc. Roy. Soc. A*, **204**, 309 (1950).
13. PFORDTEN, O. *Liebigs Ann. Chem.* **237**, 217 (1887).
14. RUFF, O. and NEUMANN, F. *Z. anorg. u. allgem. Chem.* **128**, 81 (1923).
15. SUNDSTROM, R. F. *J. Am. Chem. Soc.* **55**, 596 (1933).

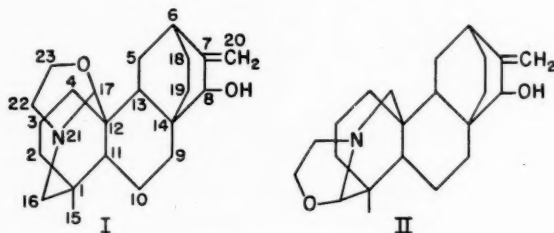
ATISINE: FURTHER DEGRADATION¹

D. DVORNIK² AND O. E. EDWARDS

ABSTRACT

The oxazolidine rings of atisine and isoatisine have been removed by a novel Hofmann-type reaction, giving a C₂₀-azomethine alcohol. Atisine was resynthesized from this, locating the azomethine double bond and the oxazolidine relative to each other. The azomethine alcohol was further degraded to the azomethine C₁₉H₂₅N, XIII, the unsubstituted ring system of atisine. This will be useful for relation of other *Delphinium* and *Aconitum* alkaloids to atisine.

The diterpenoid structures I and II have been suggested (14, 19) for the *Aconitum* alkaloids atisine and isoatisine respectively, but no rigorous proof of this skeleton has been presented. In order to facilitate the testing of these structures, and to obtain the



unsubstituted ring system as a point of comparison with similar *Aconitum* and *Delphinium* alkaloids we undertook systematic removal of the functional groups of atisine.

The N-oxyethyl group has been removed previously by pyrolysis of atisine hydrochloride (6), by pyrolysis of atisine in the presence of selenium (1) or nickel on calcium carbonate (9), and by the action of lead tetraacetate on tetrahydroatisine (6). By the first three procedures C₂₀-azomethine ketones were obtained in modest yields. We have now been able to eliminate this group in good yield under mild conditions and to obtain a C₂₀-azomethine containing the original allyl alcohol system.

In a previous communication (7) we showed that both atisine and isoatisine hydrochlorides in boiling acetic anhydride gave the same atisine acetate hydrochloride. This was shown by Pelletier and Jacobs (15) to be a diacetate hydrochloride. These authors were only able to obtain atisine monoacetate when they liberated the base from this salt. We have found, however, that by avoiding hydrolytic conditions, atisine diacetate (III) may be prepared from it readily. On being warmed in non-polar solvents it decomposed smoothly to a base C₂₂H₃₁O₂N and a volatile compound which could be rapidly hydrolyzed to acetaldehyde. The new base was a monoacetate, containing the original exocyclic methylene group (I.R. max. at 920 cm.⁻¹) and an azomethine group (I.R. max. at 1653 cm.⁻¹). The >C=N-bond was readily reduced (lithium aluminum hydride or sodium borohydride), giving a secondary amine. On the basis of formula I for atisine, the new

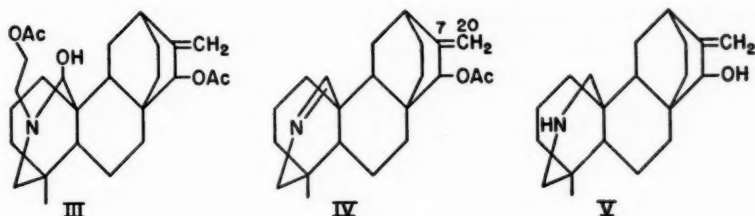
¹Manuscript received May 8, 1957.

Contribution from the Division of Pure Chemistry, National Research Council, Ottawa, Canada. A preliminary account of some of this work was published earlier (4).

Issued as N.R.C. No. 4406.

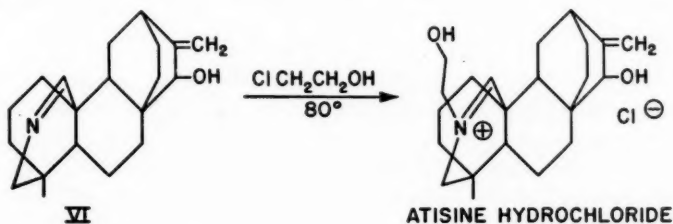
²National Research Council Postdoctorate Fellow, 1955-57.

monoacetate appeared to be IV and the secondary amine-alcohol derived from it to be V.



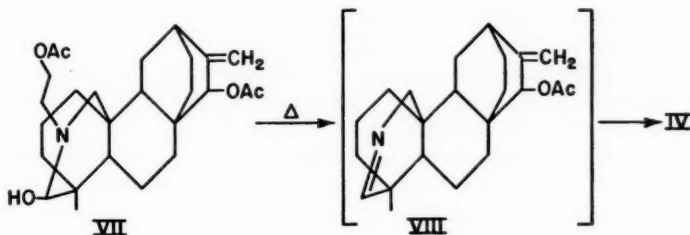
Proof of this was provided by synthesis of dihydroatisine hydrochloride by the action of ethylene chlorohydrin on V in the presence of potassium carbonate.³

A more significant experiment, which located the >C=N- , was the direct synthesis of atisine hydrochloride from VI by warming it with ethylene chlorohydrin in dimethylformamide. Since atisine is a very much stronger base ($\text{p}K_a > 12$) than VI ($\text{p}K_a$ 6 in 80% alcohol) no potassium carbonate was necessary to ensure complete quaternization.



Under the same reaction conditions isoatisine hydrochloride did not rearrange to atisine hydrochloride. Hence the synthesis provides strong evidence that the azomethine double bonds in IV and VI are on the same side of the nitrogen as the oxazolidine ring in atisine.

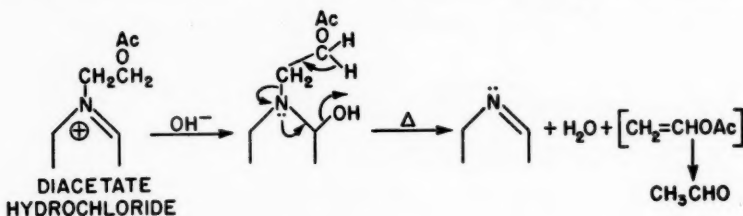
By acetylating isoatisine hydrochloride under mild conditions it has now been possible to prepare isoatisine diacetate hydrochloride. Isoatisine diacetate VII prepared from this is distinct ($[\alpha]_D -100^\circ$ in carbon tetrachloride) from atisine diacetate ($[\alpha]_D -35^\circ$ in carbon tetrachloride) but in boiling carbon tetrachloride it decomposed smoothly to IV. It seems likely that VIII is formed first, but that the azomethine double bond migrates with



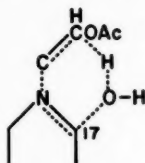
³Since our preliminary communication (4) Pelletier and Jacobs (16) have described base VI as a by-product of the permanganate oxidation of atisine and also resynthesized dihydroatisine from V.

great facility to the "atisine side" of the nitrogen. The probable driving force for this migration is discussed below.

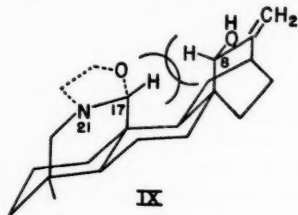
We consider the decomposition of atisine and isoatisine diacetates to be a novel type of Hofmann degradation, with the most likely mechanism being that shown below:



The remarkable facility with which this elimination takes place seems to be a result of the low energy of the cyclic transition state represented below:



The C—O bond breaking is undoubtedly aided by the marked tendency of carbon 17 to assume a trigonal state. Both Wiesner and Edwards (20) and Pelletier and Jacobs (15) have discussed the factors favoring the trigonal state of carbon 17. In structure I, if one assumes the 11,12-*trans* 12,13-*anti* ring fusion common to most diterpenes, the van der Waals radius of the hydrogen on C-17 overlaps seriously with that of the closest hydrogen on the bicyclooctane system⁴ as illustrated in the conformational drawing:⁵



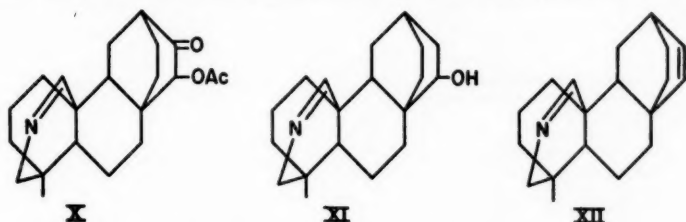
In the trigonal state of C-17 (i.e. $\Delta^{17(21)}$) however, the lone hydrogen on C-17 is coplanar with C-17—N—C-16 and the non-bonded interaction between the hydrogens on C-17 and C-8 (or C-19) is markedly diminished. This then seems to be the factor which provides the driving force for the ready transformation of isoatisine hydrochloride to diacetyl atisine hydrochloride (7) and the azomethine VIII to IV.

In order to obtain the unsubstituted atisine ring system, the functional groups on the bicyclooctane system of IV were removed in the following manner. Oxidation of the C-7—C-20 double bond with the elegant osmium tetroxide—periodate combination

⁴Evidence for the presence of this system will be presented in the next paper of the series.

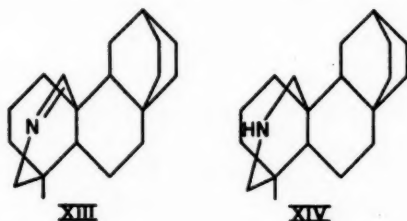
⁵The allyl alcohol may be on the other branch of the bicyclooctane system, but this does not affect the argument. The closest hydrogen would then be on C-19.

(13) in 80% acetic acid gave the ketol acetate X. On Wolff-Kishner reduction X gave a mixture of the alcohol XI and the oxygen-free unsaturated azomethine XII. The formation



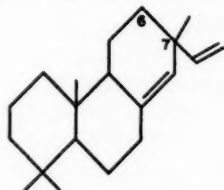
of saturated and unsaturated compounds on Wolff-Kishner reduction of α -ketols has been observed in several instances (2, 17). The infrared absorption spectrum of XII contained a sharp band at 706 cm^{-1} characteristic of a *cis*-disubstituted double bond, which disappeared on hydrogenation.

The alcohol XI was oxidized to the corresponding ketone, which was then reduced by the Wolff-Kishner method to XIII. Any alkaloid having the ring system of atisine and substituents that are readily removed can be converted to XIII or compounds readily derived from it.⁶



In order to locate the >C=N- in XII and XIII the corresponding oxazolidine salts were synthesized under the same conditions used for the synthesis of atisine from VI. The pK_a of the corresponding bases was greater than 12, again providing evidence that the azomethine bond in the whole series lies between the nitrogen and carbon 17 since isoatisine-type oxazolidines are much weaker bases. An apparently general correlation appears to be that the infrared absorption due to the >C=N^{\oplus} on the "atisine side" ($\Delta^{17(21)}$) is close to 1680 cm^{-1} while the corresponding bond on the isoatisine side ($\Delta^{18(21)}$) absorbs near 1690 cm^{-1} as illustrated in Table I.

Wenkert has suggested a very plausible biogenetic pathway to atisine and the *Garrya* alkaloids (18) from the pimaradiene precursor shown:

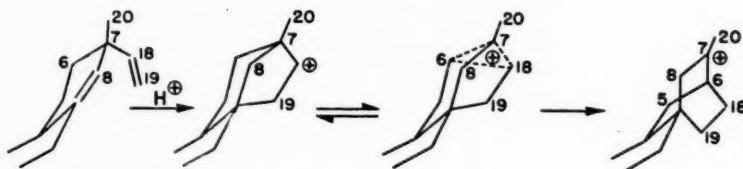


⁶The Delphinium alkaloid ajaconine has recently been converted to XIII (5).

TABLE I.

Compound	I.R. max. (nujol) for $\text{C}=\text{N}^+$, cm. ⁻¹
Atisine hydrochloride	1680
Atisine diacetate hydrochloride	1679
Methiodide of VI	1684
Methiodide of IV	1684
β -Hydroxyethochloride of XIII	1678
Isoatisine hydrochloride	1692
Isoatisine diacetate hydrochloride	1690
Isomethiodide from VI	1696

The two possible configurations of the substituents at C-7 could give rise to atisine-type skeletons with the allyl alcohol system *cis* or *trans* to the heterocyclic bridge.⁷ The cyclization to give the *cis* bridging as in IX is illustrated below:



On this basis the numbering system in I follows directly from that assigned to pimarane by Klyne (11).

EXPERIMENTAL

The melting points were determined with a Kofler micro melting point apparatus. Rotations were determined in absolute ethanol unless stated otherwise, the cited temperature being that of the room. The activities of aluminum oxide were determined according to Brockmann (3). The pK_a values cited are the pH values at half-titration. The ultraviolet spectra were determined on solutions using a Beckmann D.U. Spectrophotometer. Infrared spectra were determined on a Perkin-Elmer model 21 double-beam spectrophotometer.

Atisine Diacetate Hydrochloride

This was prepared as described earlier (7), and recrystallized from ethanol-light petroleum ether, m.p. 243–245° with decomposition, $[\alpha]_D^{21} -17.5^\circ$ (c, 2.4); $[M]_D -81^\circ$. Found: acetyl, 18.39. Calc. for $C_{26}H_{37}NO_4 \cdot HCl$ (464.03): acetyl, 18.55.

Atisine Diacetate Degradation

To a vigorously agitated ice-cold emulsion of 10 ml. of chloroform and 5463 mg. (11.71 mM.) of atisine diacetate hydrochloride in 8 ml. of water there was added 14 ml. of ice-cold 40% aqueous potassium hydroxide and the agitation continued for 2 minutes. The layers were separated and the aqueous layer extracted twice with 15 ml. portions of chloroform. The combined dried chloroform solution⁸ was then heated to the boiling point over a period of 45 minutes with evaporation of the solvent. The dark residue was

⁷A study of the stereochemistry of atisine is in progress.

⁸The corresponding solution in an experiment following the same procedure, but with carbon tetrachloride instead of chloroform, had $[\alpha]_D^{22} -35^\circ$ (c, 1.8).

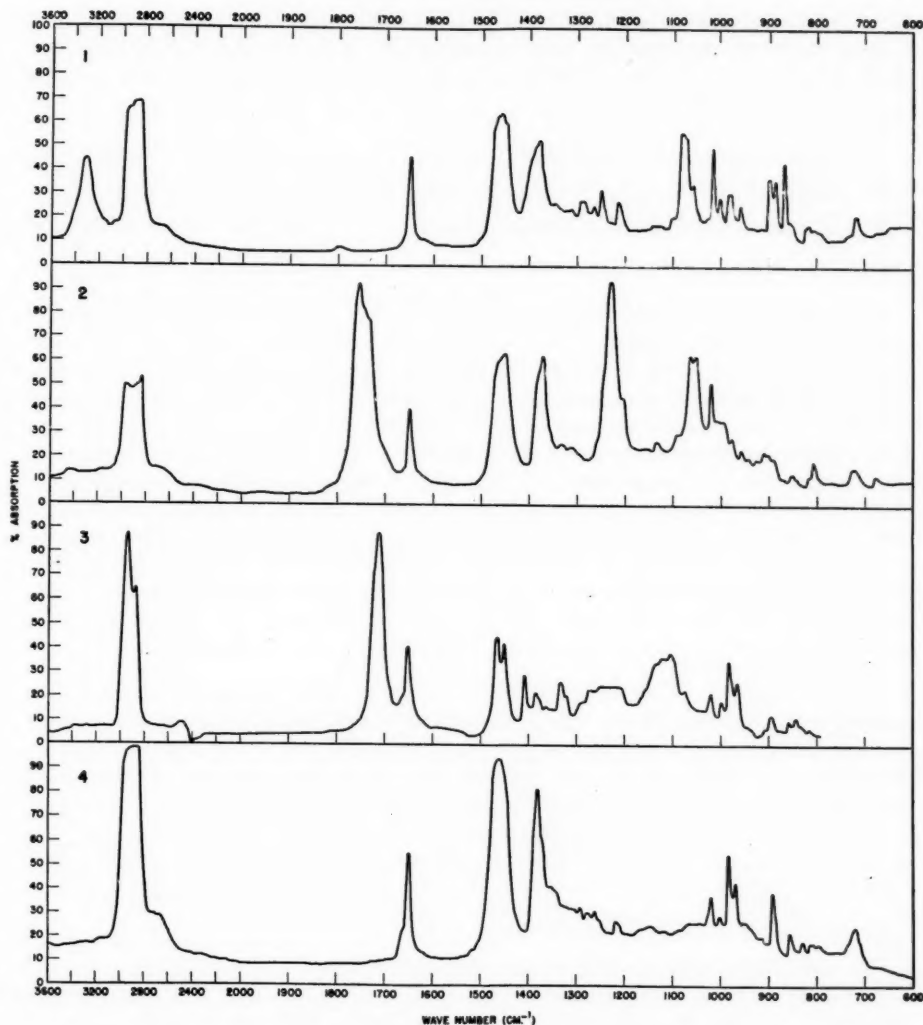


FIG. 1. Infrared spectra: (1) C_{20} -azomethine alcohol VI (nujol mull), (2) C_{20} -azomethineketol acetate X (nujol mull), (3) C_{19} -azomethine ketone ($CHCl_3$), (4) C_{19} -azomethine XIII (nujol mull).

diluted with fresh chloroform, shaken with 3 *N* aqueous sodium carbonate solution, dried, and evaporated to dryness *in vacuo*. The residue was dissolved in ether, filtered from some insoluble amorphous material (116 mg.), and evaporated to dryness *in vacuo*. The crystalline residue (3764 mg.) was taken up in hot *n*-hexane, filtered from some insoluble material, and evaporated to dryness *in vacuo*, giving 3431 mg. (85.7% of theory) of crystalline, faintly yellow residue. This residue was dissolved in *n*-hexane and decolorized by passing through a column of neutral aluminum oxide (1:5.5, activity III). Hexane and benzene-hexane (75:25) eluted 3190 mg. of the base IV, which on repeated crystallization from

light petroleum ether (b.p. 30–50°) had m.p. 151–152°; $[\alpha]_D^{24} - 60^\circ$ (c , 2.00); $[M]_D - 205^\circ$. Found: C, 77.49; H, 9.31; N, 4.02; acetyl, 12.02. Calc. for $C_{22}H_{31}O_2N$ (341.48): C, 77.37; H, 9.15; N, 4.10; acetyl, 12.60. I.R. max. (nujol mull): 1732, 1240 cm^{-1} (OAc); 1653 cm^{-1} (>C=N); 920 cm^{-1} (>C=CH_2).

The *methiodide* had m.p. 264–265° (acetone–ethyl acetate); $[\alpha]_D^{25} - 50^\circ$ (c , 1.84); $[M]_D - 242^\circ$. Found: C, 57.32; H, 7.20. Calc. for $C_{23}H_{34}O_2NI$ (483.43): C, 57.15; H, 7.09. I.R. max. (nujol mull): 1740, 1237 cm^{-1} (OAc); 1684 cm^{-1} (>C=N^{\oplus}); 1660, 913 cm^{-1} (>C=CH_2).

An experiment was made using 11.1 g. (24.95 mM.) of atisine diacetate hydrochloride following the same procedure but using carbon tetrachloride as solvent. The carbon tetrachloride was distilled slowly over a period of 1½ hours, 60% of the original 100 ml. being collected under a suspension of 4 g. of *p*-nitrophenylhydrazine in 20 ml. of water plus 5 ml. of acetic acid and 5 ml. of methanol. The resulting suspension was heated to give a clear two-phase system and separated while hot. The carbon tetrachloride layer contained a *p*-nitrophenylhydrazone, m.p. 125°. The aqueous layer gave another large crop of crystals. The derivative was dissolved in chloroform, washed with 3 *N* hydrochloric acid, dried, and evaporated to dryness *in vacuo* giving 2.38 g. (56% of theory) of a *p*-nitrophenylhydrazone, which after recrystallization had m.p. 124–128° and showed no m.p. depression with an authentic sample of acetaldehyde *p*-nitrophenylhydrazone.

*C*₂₀-Azomethine Alcohol (VI)

Base IV, 664 mg. (1.94 mM.), was refluxed for 3 hours with a solution of 1.5 g. of potassium hydroxide in 20 ml. of 75% aqueous methanol, the methanol partially removed *in vacuo*, water added, and the solution extracted with methylene chloride. Removal of the solvent gave 550 mg. of crude product, which was dissolved in a benzene–pentane mixture and passed through a column of aluminum oxide (1:10, act. II). After repeated crystallization from benzene–pentane the product melted at 184–186°; $[\alpha]_D^{22} - 15^\circ$ (c , 2.17); $[M]_D - 44^\circ$; pK_a 6.0 in 80% ethanol. Found: C, 80.16; H, 9.59. Calc. for $C_{20}H_{29}NO$ (299.44): C, 80.22; H, 9.76. I.R. max. (Fig. 1): 3310 cm^{-1} (OH); 1650 cm^{-1} (>C=N-); 898 cm^{-1} (>C=CH_2).

The *methiodide* had m.p. 253° (methanol–acetone); $[\alpha]_D^{25} - 14^\circ$ (c , 1.65); $[M]_D - 62^\circ$; pK_a greater than 12 (95% ethanol). Found: C, 57.09; H, 7.20. Calc. for $C_{21}H_{33}ONi$ (441.40): C, 57.15; H, 7.31. I.R. max. (nujol mull): 3360 cm^{-1} (OH); 1684 cm^{-1} (>C=N^{\oplus}); 1654, 897 cm^{-1} (>C=CH_2). This methiodide could be crystallized from potassium hydroxide solution.

The “*isomethiodide*” (the isoatisine analogue of the above methiodide) was prepared as follows: A solution of 232 mg. of methiodide in 7 ml. of methanol containing 400 mg. of potassium hydroxide was refluxed for 3 hours. The methanol was removed under reduced pressure, the residue taken up in water, and the base extracted into benzene. The 189 mg. of pale yellow gum from the benzene was dissolved in methanol and exactly neutralized with hydriodic acid in methanol. The solvent was removed under reduced pressure and the residue crystallized from acetone. After two recrystallizations from acetone containing a trace of methanol the “*isomethiodide*” melted at 245–246.5° (par-

tially liquefied when put on the hot stage at 220°, then resolidified). It was dried 5 hours at 100°, 5×10^{-4} mm. pressure; $[\alpha]_D^{25} - 13^\circ$ (c, 1.74); $[M]_D - 57^\circ$; pK_a 10.6 (95% ethanol). Found: C, 56.56, 56.63; H, 7.24, 7.16. Calc. for $C_{21}H_{32}ONI$ (441.40): C, 57.15; H, 7.31.

I.R. max. (nujol mull): 3380 cm^{-1} (OH); 1696 cm^{-1} (>C=N^{\oplus}); 1634, 896 cm^{-1} (>C=CH_2).

The *ethiodide* had m.p. 261.5–263.5 (methanol–ethyl acetate); $[\alpha]_D^{25} - 4^\circ$ (c, 1.00); $[M]_D - 18^\circ$. Found: C, 58.06; H, 7.37. Calc. for $C_{22}H_{34}ONI$ (455.42): C, 58.02; H, 7.52.

I.R. max. (nujol mull): 3390 cm^{-1} (OH); 1678 cm^{-1} (>C=N^{\oplus}); 1665, 895 cm^{-1} (>C=CH_2).

Secondary Amino Alcohol (V)

(a) *With lithium aluminum hydride*.—A solution of 396 mg. (1.12 mM.) of the azomethine alcohol VI and 1.2 g. of lithium aluminum hydride in 40 ml. of ether was refluxed for 3 hours. After it had been left overnight at room temperature the mixture was chilled and the excess of the reagent destroyed by the addition of 8 ml. of ethyl acetate. Forty milliliters of a cold, saturated aqueous Rochelle-salt solution and 10 ml. of water were added and the mixture extracted with ether. Evaporation of the solvent gave 327 mg. (93.5%) of the crude dihydro derivative V, which after several recrystallizations from acetone–pentane and sublimation *in vacuo* melted at 154–154.5°; $[\alpha]_D^{24} - 15^\circ$ (c, 1.85); $[M]_D - 44^\circ$. Found: C, 79.60; H, 10.28; N, 4.80%. Calc. for $C_{20}H_{31}NO$ (301.46): C, 79.67; H, 10.37; N, 4.65%. I.R. max. (carbon disulphide): 3600 cm^{-1} (OH); 1653, 900 cm^{-1} (>C=CH_2).

(b) *With sodium borohydride*.—To a solution of 74 mg. (0.25 mM.) of the azomethine alcohol VI in 7 ml. of 80% aqueous methanol 51 mg. of sodium borohydride was added. After it had been left for 3 hours at room temperature, the solution was evaporated to dryness *in vacuo*, water added, and the base extracted with ether. The crude product was purified by passing its benzene solution through aluminum oxide (1:30, act. II). It melted at 153.5–155°, giving no m.p. depression with a sample obtained from the lithium aluminum hydride reduction.

Dihydroatisine from V (16, 21)

A mixture of 95 mg. (0.32 mM.) of the secondary amino alcohol V, 330 mg. of anhydrous sodium carbonate, 1 ml. of 2-chloroethanol, and 9 ml. of anhydrous methanol was refluxed. After 22 hours 320 mg. of anhydrous sodium carbonate and 1 ml. of 2-chloroethanol were added and the refluxing continued for an additional 24 hours. The methanol was removed *in vacuo*, water added, and the mixture extracted with chloroform. Evaporation of the water-washed solution yielded 102 mg. (94.5%) of an oily product which crystallized on being sprayed with ether. When recrystallized from aqueous methanol the product melted at 158–160°. It showed no melting point depression with a pure sample of dihydroatisine (6); $[\alpha]_D^{23} - 44.5^\circ$ (c, 1.82); $[M]_D - 154^\circ$. Its infrared spectrum (chloroform) was identical with that of authentic dihydroatisine.

Synthetic Atisine Hydrochloride

A solution of 112 mg. (0.37 mM.) of the C_{20} -azomethine alcohol VI and 1 ml. of 2-chloroethanol in 10 ml. of dimethylformamide was warmed for 24 hours over refluxing

benzene. On cooling, 65 mg. of crystals separated. By adding petroleum ether to the mother liquor an additional 53 mg. of crystalline material separated. After recrystallization from methanol-ethyl acetate the salt melted at 318–319° with decomposition, and showed no melting point depression with a sample of pure atisine hydrochloride. Its infrared spectrum (nujol mull) was identical with that of authentic atisine hydrochloride; $[\alpha]_D^{22.5} + 28^\circ$ (*c.* 1.0 in water); $[M]_D + 93^\circ$. Found: C, 69.36; H, 9.02; Calc. for $C_{22}H_{33}NO_2 \cdot HCl$ (379.96): C, 69.55; H, 9.02.

When a sample of this hydrochloride was reduced by being left overnight with an excess of sodium borohydride in 80% aqueous methanol, the product melted at 158–160°, and did not depress the melting point of dihydroatisine. The infrared spectrum (in chloroform) was identical with that of pure dihydroatisine.

When a solution of isoatisine hydrochloride in dimethylformamide was heated for 24 hours at 80° C. it was recovered unchanged.

Isoatisine Diacetate Hydrochloride

Isoatisine hydrochloride (405 mg., 1.065 mM.) was dissolved in 10 ml. of 1:1 acetic acid-acetic anhydride. After 4 hours' heating over refluxing benzene the rotation had changed from $[\alpha]_D -1^\circ$ to $[\alpha]_D -52^\circ$. The solution was concentrated under reduced pressure until it crystallized, giving 405 mg., m.p. 232°, and 88 mg. of less pure salt. The first crop, after four recrystallizations from methanol-acetone, had m.p. 239° (immersed at 210°); $[\alpha]_D^{22} -45^\circ$ (*c.* 1.87); $[M]_D -209^\circ$. Found: C, 67.00; H, 8.08; acetyl, 18.45. Calc. for $C_{26}H_{37}O_4N \cdot HCl$ (464.03): C, 67.30; H, 8.25; acetyl, 18.55. I.R. max. (nujol mull): 1740, 1240 cm^{-1} (OAc); 1690 cm^{-1} (>C=N^+); 1655, 900 cm^{-1} (>C=CH_2).

Isoatisine Diacetate Degradation

Isoatisine diacetate hydrochloride (302 mg., 0.65 mM.) in solution in 4 ml. of ice-cold water was emulsified with 10 ml. of carbon tetrachloride. Four milliliters of ice-cold 20% aqueous potassium hydroxide solution was added while the agitation was continued. The layers were separated after 1 minute and the aqueous layer extracted with fresh carbon tetrachloride. The combined organic solution was dried and filtered. The solution had $[\alpha]_D^{25} -100^\circ$ (*c.* 1.6). This solution was slowly distilled to half the original volume over a period of 45 minutes. The brownish-red solution was then taken to a froth under reduced pressure. The residue was taken up in fresh carbon tetrachloride, the solution shaken with 3 *N* aqueous sodium carbonate solution, dried, and evaporated, giving 232 mg. of residue. This was dissolved in ether, filtered, and petroleum ether (b.p. 30–50°) added after concentration to a small volume. After filtration and evaporation the petroleum ether yielded 180 mg. of froth. This was adsorbed from petroleum ether (b.p. 30–50°) on neutral aluminum oxide (1:11, activity III). Petroleum ether (120 ml.) eluted 75 mg., which crystallized spontaneously. Benzene-petroleum ether (20:80) eluted a further 39 mg. of colorless crystalline product. After one recrystallization from petroleum ether these melted at 151–153°; $[\alpha]_D^{22} -63 \pm 1^\circ$ (*c.* 1.46). The mixed melting point with the base IV from atisine was 151–154° and its infrared spectrum (nujol mull) was identical with that of IV.

Thirty-five milligrams of this acetate was hydrolyzed using potassium hydroxide in aqueous methanol. The 33 mg. of basic product was chromatographed on neutral aluminum oxide (1:10, activity III). Benzene-petroleum ether (1:1, 45 ml.) eluted 20 mg. which

crystallized spontaneously, m.p. 180–182°; $[\alpha]_D^{22} - 14^\circ$ (c, 1.10). This showed no melting point depression with the corresponding alcohol obtained from atisine.

C₁₉-Azomethineketol Acetate (X)

A solution of 1.03 g. (3.01 mM.) of the C₂₀-azomethine acetate (IV) in 11 ml. of 80% aqueous acetic acid containing 85 mg. (0.33 mM.) of osmium tetroxide was left for 15 minutes at room temperature, in which time the solution had turned dark brown. A solution of 1.82 g. (6.2 mM.) of sodium paraperiodate (Na₃H₂IO₆) in 30 ml. 80% aqueous acetic acid was added, and the mixture left at room temperature for 4 hours. The colorless suspension of crystals was filtered, and the filtrate taken to dryness under reduced pressure. The crystalline residue was taken up in methylene chloride, shaken with cold 3 N aqueous sodium carbonate solution, and the emulsion filtered. The layers were separated and the aqueous layer extracted twice with methylene chloride. The dried methylene chloride solution yielded on evaporation *in vacuo* 1.05 g. of product which crystallized when ether was added. The first crop (638 mg.) melted at 150–168°. A benzene solution of this was filtered through a column of neutral aluminum oxide (1:5, activity II). The eluate, after three recrystallizations from ether, melted at 175–178°; $[\alpha]_D^{24} - 140 \pm 2^\circ$ (c, 1.80 in pure chloroform); $[M]_D - 481^\circ$. Found: C, 73.25; H, 8.44. Calc. for C₂₁H₂₉O₃N (343.45): C, 73.43; H, 8.51. I.R. max. (nujol mull) (Fig. 1): 1755 cm.⁻¹ (carbonyls); 1650 cm.⁻¹ (>C=N-); 1230 cm.⁻¹ (OAc). (The partly crystalline material from the main mother liquor had an infrared spectrum practically identical with the pure ketol acetate.)

Wolff-Kishner Reduction⁹ of the C₁₉-Azomethineketol

A solution of 77 mg. (0.23 mM.) of the ketol acetate X in 2 ml. of triethylene glycol and 1 ml. of 95% hydrazine was heated to 145°, 700 mg. of potassium hydroxide added, and the temperature gradually raised to 200° over a period of 2 hours. After it was heated for an additional 4 hours at 200 ± 10° the solution was cooled, diluted with water, and extracted with chloroform. The crude product was chromatographed on neutral aluminum oxide (1:20, activity II). The first benzene fraction crystallized spontaneously, m.p. 93–143°. The low-melting component, the unsaturated base XII, was removed by repeated extractions with boiling *n*-pentane. The residue, the alcohol XI, had m.p. 153–162.5°, and was further purified by sublimation at 145° at 0.1 μ , m.p. 165–166°; $[\alpha]_D^{24} - 48^\circ$ (c, 0.85); $[M]_D - 139^\circ$. Found: C, 79.42; H, 10.14. Calc. for C₁₉H₂₉NO (287.43): C, 79.39; H, 10.17. I.R. max. (nujol mull): 3440, 3110 cm.⁻¹ (OH); 1651 cm.⁻¹ (>C=N-).

The later benzene fractions and the *n*-pentane washings were combined, evaporated, dissolved in *n*-pentane, passed through neutral aluminum oxide (1:10, activity I), and the filtrate carefully chromatographed on neutral aluminum oxide (1:50, activity I). The unsaturated base XII was eluted with benzene-ether (95:5). After sublimation it had m.p. 105–105.5°; $[\alpha]_D^{25} - 73^\circ$ (c, 1.22); $[M]_D - 197^\circ$; p*K_a* 6.0 in 80% ethanol. Found: C, 84.54; H, 10.14. Calc. for C₁₉H₂₇N (269.41): C, 84.70; H, 10.10. I.R. max. (nujol mull): 1650 cm.⁻¹ (>C=N-); 706 cm.⁻¹ (*cis*-disubstituted double bond).

The *picrate* of the unsaturated base XII, crystallized from chloroform-methanol, had m.p. 251–253°. Found: C, 60.13; H, 6.19. Calc. for C₂₅H₃₀N₄O₇ (498.52): C, 60.23; H, 6.07.

Later, the procedure was improved as follows: the crude crystalline mixture of the

⁹Procedure modified according to Huang-Minlon (8).

alcohol XI and the unsaturated base XII was repeatedly recrystallized from boiling *n*-hexane and the crystalline alcohol washed with hot *n*-pentane. The mother liquors and *n*-pentane washings were combined, the solvents removed, and the residue chromatographed on neutral aluminum oxide (1:10, activity I). The combined *n*-pentane and *n*-hexane eluates were evaporated and the crystalline residue converted to the picrate, which was purified by crystallization from chloroform-methanol, m.p. 251–253°. The base liberated from this picrate gave on crystallization from aqueous acetone the pure unsaturated base XII, m.p. 105–105.5°. The rest, i.e. the alcohol XI, was eluted from the column with methanol-ether (1:99) and converted to the picrate, which was purified by crystallization from chloroform-ethyl acetate, m.p. 273–275°. Found: C, 58.30; H, 6.29. Calc. for $C_{25}H_{32}N_4O_8$ (516.54): C, 58.13; H, 6.24.

Hydrogenation of XII

A solution of 13.7 mg. (0.051 mM.) of the unsaturated base XII in 4 ml. of glacial acetic acid was hydrogenated in the presence of 13.3 mg. of platinum oxide. The first mole of hydrogen was taken up after 10 minutes, the second after 16 hours. The hydrogen uptake was 2.35 ml. Calculated for 2 moles, 2.50 ml. After the hydrogenation the catalyst was removed and the filtrate evaporated, the residue distributed between ether and aqueous 3 *N* sodium carbonate solution, the solvent evaporated, and the residue passed through neutral aluminum oxide (1:5, activity I). The amine XIV was eluted with methanol-ether (4:96), evaporated, and the residue sublimed at 85–90° at 0.4 μ giving a colorless viscous oil. Found: C, 83.52; H, 11.59. Calc. for $C_{19}H_{31}N$ (273.45): C, 83.45; H, 11.43.

C_{19} -Azomethine Ketone from XI

(a) *Kiliani procedure* (10, 12).—To a solution of 17 mg. (0.06 mM.) of the alcohol XI in 1 ml. of glacial acetic acid 0.4 ml. of the Kiliani solution was added over a period of 2 minutes. After it was left at room temperature for an additional 12 minutes, the solution was chilled and the excess of the oxidizing agent destroyed by the addition of 1 ml. of methanol. The ice-cold solution was made alkaline (pH 9) with aqueous ammonia (1:1) and extracted with ether. The residue (16 mg., 94%), after the solvent was evaporated, crystallized spontaneously, m.p. 169–171°. The analytical sample was sublimed at 145° at 0.5 μ ; m.p. unchanged; $[\alpha]_D^{24} -14^\circ$ (*c*, 0.42); $[M]_D -41^\circ$. Found: C, 80.13; H, 9.65. Calc. for $C_{19}H_{27}NO$ (285.41): C, 79.95; H, 9.54. The ultraviolet spectrum in 95% ethanol showed λ_{max} 250 $m\mu$ ($>C=N-$), $\log \epsilon$ 2.23, and a shoulder with $\log \epsilon$ 2.00 at 290 $m\mu$ ($>C=O$). I.R. max. (chloroform) (Fig. 1): 1713 cm^{-1} ($>C=O$); 1651 cm^{-1} ($>C=N-$).

(b) *Mild oxidation*.—To a solution of 94 mg. (0.33 mM.) of the alcohol XI in 1 ml. of glacial acetic acid a solution of 29 mg. of chromium trioxide in 3 ml. of 90% aqueous acetic acid was added; after it was left for 4 hours at room temperature an additional 23 mg. of chromium trioxide was added and the solution kept overnight at 0°. Excess of the oxidizing agent was destroyed by adding sodium bisulphite, the mixture chilled, made alkaline with aqueous ammonia (1:1), and extracted with ether. The residue (81 mg., 87%), after the solvent was evaporated, crystallized spontaneously, m.p. 167–171°. After recrystallization from aqueous acetone the product was identical with that obtained by the Kiliani procedure.

Wolff-Kishner Reduction of the C₁₉-Azomethine Ketone

A solution of 428 mg. (1.5 mM.) of the C₁₉-ketone in 5 ml. of triethylene glycol and 5 ml. of 95% hydrazine was immersed in a preheated bath at 110°, and the temperature gradually raised to 165°. Potassium hydroxide (2.6 g.) was added and the mixture heated at 200±5° for 3 hours. After cooling, water was added and the mixture extracted with chloroform. The residue, after the solvent was evaporated, was dissolved in hot *n*-pentane, filtered through neutral aluminum oxide (1:10, activity II), and the column washed with *n*-pentane. Evaporation of the solvent gave 378 mg. (93%) of the base XIII, which on recrystallization from aqueous acetone had m.p. 111–113°. The sample for analysis was sublimed at 95–105° at 0.5 μ ; m.p. 111.5–114.5°; $[\alpha]_D^{24}$ -31° (c, 1.11); $[M]_D$ -84°; p*K*_a 6.0 in 80% ethanol. Found: C, 84.10, 84.03; H, 10.59, 10.60. Calc. for C₁₉H₂₉N (271.43): C, 84.07; H, 10.77. I.R. max. (nujol mull) (Fig. 1): 1649 cm.⁻¹ (>C=N-).

The *picrate*, recrystallized from methanol-chloroform, had m.p. 268–269°. Found: C, 59.97; H, 6.30. Calc. for C₂₅H₃₂N₄O₇ (500.54): C, 59.99; H, 6.44.

 β -Hydroxy-ethochloride of XIII

A solution of 51 mg. (0.19 mM.) of the base XIII and 0.5 ml. of 2-chloroethanol in 5 ml. of dimethylformamide was warmed for 24 hours over refluxing benzene. After cooling, the solvent was partially evaporated *in vacuo*. On addition of ether 62.5 mg. (94.5%) of crystals separated, which were recrystallized twice from methanol-benzene and finally from methanol-ethyl acetate. The air-dry crystals melted at 264–267° with decomposition; $[\alpha]_D^{23}$ +13 (c, 0.55 in water); $[M]_D$ +46°; p*K*_a > 12 in 95% ethanol. Found: C, 70.20; H, 9.42. Calc. for C₂₁H₃₃NO $\cdot\frac{1}{2}$ H₂O (360.96): C, 69.87; H, 9.77 (contains no methoxyl). I.R. max. (nujol mull): 3210 cm.⁻¹ (OH); 1678 cm.⁻¹ ($\text{>C=N}^{\oplus}\text{-}$).

 β -Hydroxy-ethochloride of XII

This was prepared from 58 mg. (0.22 mM.) of the unsaturated base XII as described for the base XIII. Yield, 74 mg. (98%). After several recrystallizations from methanol-benzene and finally from methanol-ethyl acetate, the air-dried salt had m.p. 258–259° with decomposition; $[\alpha]_D^{23}$ +13.5° (c, 0.89 in water); $[M]_D$ +50°; p*K*_a > 12 in 95% ethanol. Found: C, 68.96; H, 8.98. Calc. for C₂₁H₃₁NO \cdot H₂O (367.96): C, 68.55; H, 9.31 (contains no methoxyl). I.R. max. (nujol mull): 3210 cm.⁻¹ (OH); 1677 cm.⁻¹ ($\text{>C=N}^{\oplus}\text{<}$); 698 cm.⁻¹ (*cis*-disubstituted double bond).

ACKNOWLEDGMENTS

The authors wish to thank Mr. M. Lesage for technical assistance, Mr. H. Seguin for the analyses, and Mr. R. Lauzon for taking the infrared spectra.

REFERENCES

1. BARTLETT, M. F., EDWARDS, J. A., TAYLOR, W. I., and WIESNER, K. *Chemistry & Industry*, 323 (1953).
2. BARTON, D. H. R. and ROBINSON, C. H. *J. Chem. Soc.* 3045 (1954).
3. BROCKMANN, H. and SCHODDER, H. *Ber.* 74, 73 (1941).
4. DVORNIK, D. and EDWARDS, O. E. *Chemistry & Industry*, 248 (1956).
5. DVORNIK, D. and EDWARDS, O. E. *Chemistry & Industry* (In press, 1957).
6. EDWARDS, O. E. and SINGH, T. *Can. J. Chem.* 32, 465 (1954).
7. EDWARDS, O. E. and SINGH, T. *Can. J. Chem.* 33, 448 (1955).
8. HUANG-MINLON, J. *Am. Chem. Soc.* 68, 2487 (1946).
9. HUEBNER, C. F. and JACOBS, W. A. *J. Biol. Chem.* 170, 515 (1947).
10. KILIANI, H. and MERK, B. *Ber.* 34, 3562 (1901).

11. KLYNE, W. J. *Chem. Soc.* 3072 (1953).
12. MIJOVIC, M. V., SUNDT, E., KYBURZ, E., JEGER, O., and PRELOG, V. *Helv. Chim. Acta*, **38**, 231 (1955).
13. PAPPO, R., ALLEN, D. S., LEMIEUX, R. U., and JOHNSON, W. S. *J. Org. Chem.* **21**, 478 (1956).
14. PELLETIER, S. W. and JACOBS, W. A. *J. Am. Chem. Soc.* **76**, 4496 (1954).
15. PELLETIER, S. W. and JACOBS, W. A. *Chemistry & Industry*, 1385 (1955).
16. PELLETIER, S. W. and JACOBS, W. A. *J. Am. Chem. Soc.* **78**, 4144 (1956).
17. TURNER, R. B., ANLIKER, R., HELBLING, R., MEIER, J., and HEUSSER, H. *Helv. Chim. Acta*, **38**, 411 (1955).
18. WENKERT, E. *Chemistry & Industry*, 282 (1955).
19. WIESNER, K., ARMSTRONG, R., BARTLETT, M. F., and EDWARDS, J. A. *Chemistry & Industry*, 132 (1954).
20. WIESNER, K. and EDWARDS, J. A. *Experientia*, **15**, 255 (1955).
21. WIESNER, K., TAYLOR, W. I., FIGDOR, S. K., BARTLETT, M. F., ARMSTRONG, R., and EDWARDS, J. A. *Chem. Ber.* **86**, 800 (1953).

Bis-ORGANOMAGNESIUM REACTIONS

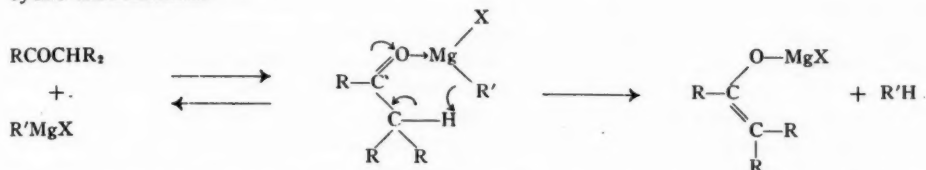
I. EFFECT OF SOLVATION ON ENOLIZATION¹

C. A. GUTHRIE, E. Y. SPENCER, AND GEORGE F WRIGHT

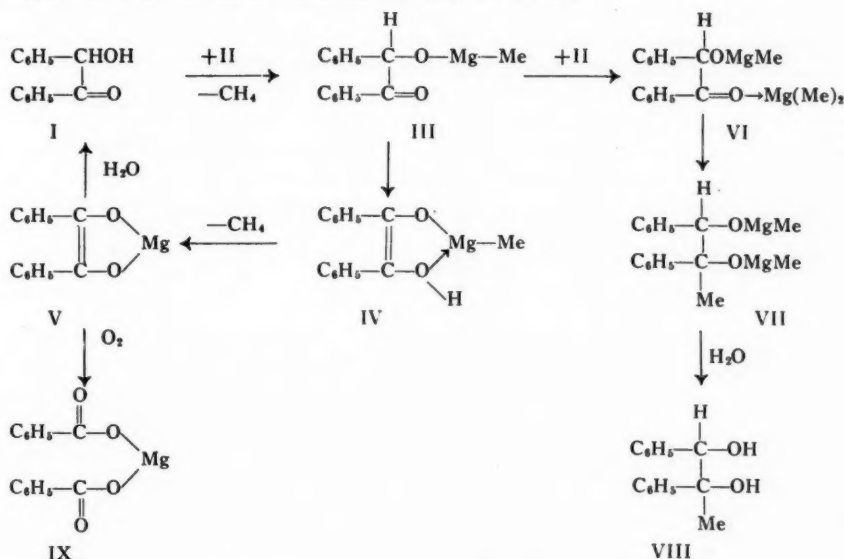
ABSTRACT

The reaction of bis-organomagnesium compounds with benzoin has been used to determine the effect of co-ordinative solvents on these halogen-free organometallic compounds after the test reaction has been re-examined to establish its reliability. Although the reaction of ether-free dimethylmagnesium is sufficiently different from reactions in which ethers of varying basicity are present to show that co-ordination is significant, this co-ordination seems to be relatively unimportant by contrast to organometallic systems containing halogen.

Generally it is recognized that enolate formation during Grignard reactions does not actually involve enolization but, instead, is a consequence of appropriation by the organic group of a Grignard reagent co-ordinated with carbonyl of an element on the carbon alpha to that carbonyl group. With some exceptions (8) this element usually is hydrogen (2). The reaction is alternative to Grignard addition when the latter is geometrically unfavorable, and it may be expressed (11) in terms of a quasi-six-membered transitory cyclic intermediate.



However in one instance (14) true enolization seems to occur so as partially to preclude addition. The description of this reaction of dimethylmagnesium (II) with benzoin may be improved over the earlier formulation (14) as follows:



¹Manuscript received April 18, 1957.

Contribution from the Department of Chemistry, University of Toronto, Toronto, Ontario.

The initial reaction of R_2Mg with hydroxyl in benzoic acid is to be expected, both because carbonyl is less co-ordinative than hydroxylic oxygen and also because this difference is accentuated by the low reactivity of R_2Mg (14). Subsequently the alkoxide III may intramolecularly co-ordinate, leading to IV which loses methane to give the enediolate V. Alternatively, III with a second mole of R_2Mg may co-ordinate to VI which subsequently rearranges to the dimethomagnesium diolate, VII. Obviously IV and V may also be represented as polymeric forms.

Upon hydrolysis the diolate VII leads to 1,2-diphenyl-1,2-propanediol, VIII, while V regenerates benzoic acid. But if the reddish reaction system (in this dioxane medium) is bleached by introduction of oxygen, then V or its equivalent is oxidized to magnesium benzoate, IX, the salt, VII, being unaltered by this treatment. The Grignard reaction variants may be evaluated by estimation of the diol and the benzoic acid after oxidation.

In consideration of this formulation it is of interest to compare the yields when benzoic acid in dioxane is added to excess dimethylmagnesium in dioxane (direct addition) with the yields when addition is "inverse", i.e., when excess of dimethylmagnesium is added to benzoic acid. The data in Table I show that benzoic acid yields are greater when addition is "inverse" while yields of the glycol, VIII, are greater when addition is direct ($II \leftarrow I$). Thus a paucity of organomagnesium reagent favors the intramolecular formation of the enediolate, V, whereas the yield of VIII is greatest when direct addition brings a small amount of benzoic acid into a large amount of dimethylmagnesium.

The association of the reddish color of the system with the presence of V seems to be warranted. The color is the same when diphenylmagnesium is added to benzoic acid in dioxane medium. Oxidation of such a system proceeds normally, yielding 6% of benzoic acid and 20% of triphenyl-1,2-ethanediol. Likewise a similar red color is bleached by oxygen addition into the system prepared by slow introduction of excess diethylmagnesium (in dioxane) to benzoic acid. Both benzoic acid (4.3%) and 1,2-diphenyl-1,2-butanediol (37%) are the products.

TABLE I
REACTION OF DIMETHYLMAGNESIUM (II) WITH BENZOIC ACID (I)

Concn. basic Mg, mole/l.	Concn. of I, mole/l.	Mole ratio II:I	Time of addn., min.	Time of oxdn., hr.	Mode of addition	Products, mole %	
						Benzoic acid	Glycol
0.29	0.20	4.84	15	2.5	$II \rightarrow I$	12	46
0.29	0.20	4.84	20	2.6	$II \leftarrow I$	7	70
0.29	0.20	4.84	20	3.7	$II \rightarrow I$	15	54
0.29	0.20	4.84	15	3.7	$II \leftarrow I$	12	63
0.20	0.16	5.00	11	4.0	$II \rightarrow I$	21	67
0.20	0.16	5.00	10	4.0	$II \leftarrow I$	14	76

The foregoing description attests the reliability of the reaction between *bis*-organomagnesium and benzoic acid. It seemed worth while to use this reaction of competitive addition or enolization to evaluate the effect of the reaction medium on these alternatives. Consequently a solution of dimethylmagnesium (prepared as usual by dioxane precipitation of the Grignard components containing chlorine) has been heated at 150–155° for 3 hours under nitrogen at a pressure of 3 mm. of mercury in order to remove all diethyl ether and dioxane. The near-white residue is immediately inflammable, spontaneously in air. Neither of the ethers can be detected in the hydrolyzate of this powder. Since it has not otherwise been altered by heat treatment (9, 13, 6), it provides a source of *bis*-organomagnesium reconstituted in media containing no dioxane.

The powder is almost insoluble in benzene. Although the suspension gives a strong Gilman test with Michler's ketone the supernatant layer from the centrifuged suspension gives only a faint test. On the other hand the powder is very soluble in 2,5-dioxahexane with evolution of heat; titration for basic magnesium shows that a 1.08 *M* solution is not saturated. However the powder is less soluble in other ethers. For the study of dimethylmagnesium in media other than dioxane-ether we have used only the suspension in benzene and the solution in dioxahexane.

When a solution of benzoin in benzene is treated with an excess of non-solvated dimethylmagnesium the characteristic red color is deeper than has been observed with these reagents in any other system. Passage of oxygen through this reaction mixture is dangerous (in one instance a violent explosion occurred) but a successful experiment has yielded 8% of benzoic acid and 92% of 1,2-diphenyl-1,2-butanediol, VII, a quantitative recovery.

The yield of VII is lower (79%) when benzoin in 2,5-dioxahexane is treated with the dry dimethylmagnesium but the yield of benzoic acid (8%) is about the same. Notable in this instance is the observable heat of solvation of the organometallic compound and the absence of the red color which is characteristic of the reaction in other media. This is in accord with the strongly co-ordinative power of 2,5-dioxahexane which has been observed previously (4, 3). It would seem that the enediolate, V, is not solvated except in media of high "basicity" like dioxahexane.

It would appear from these experiments that the co-ordinative effect of ethers on dimethylmagnesium is existent, but it is slight by comparison with the strong co-ordinate bonds in ordinary Grignard reagents containing halogen. This information is not new, although it seems to have been neglected. Actually, in 1931 Schlenk (13) reported that diethyl ether was only weakly bound to crystalline diethylmagnesium below 25° and not at all above this temperature. This small extent of co-ordination is reflected in the similarity of reaction with benzoin in strongly co-ordinating solvents like dioxahexane versus weak ones like dioxane. Only in benzene suspension wherein dipole interaction is insignificant is the reaction unique because of a quantitative yield of the two products.

Of some interest is the red color of the reaction product from benzoin and dimethyl-, diethyl-, or diphenyl-magnesium. This color has been attributed to magnesium diphenyl-ethenediolate, V, or its polymeric modification. The extremes of behavior in benzene and dioxahexane seem to indicate that this salt, V, is visibly colored only when it is not co-ordinated with an ether.

EXPERIMENTAL*

Dimethylmagnesium

The methyl chloride Grignard reagent was prepared by bubbling 5 moles of dry methyl chloride through 5 atoms of magnesium in about 50 moles of ether under nitrogen. Part of the reagent (0.37 mole) obtained in this way (0.78 *N*) was filtered, then stirred while 2.2 moles of dioxane was added dropwise. When the suspension settled, the etherous phase was filtered off through a glasswool plug and the precipitate was washed with 1.1 mole of dioxane. This washing was repeated until the effluent gave a negative Gilman test. According to acid titration of an aliquot the combined filtrates contained dimethylmagnesium to the extent of 5.5% of the basic magnesium in the original reagent.

When the methyl chloride Grignard reagent was prepared from 3.6 moles of methyl

*Melting points have been corrected against standards according to *Can. J. Technol.* **34**, 89 (1956).

chloride into 6 atoms of magnesium in 50 moles of ether the reagent (0.45 mole, 0.74 *M*) was precipitated by 3.4 moles of dioxane but it required 7.9 moles of dioxane before the filtrate gave a negative Gilman test. The combined filtrates contained 54% of the basic magnesium in the original reagent.

This discrepancy in yield corresponds to the 4–6% (14, 1) versus 57% (5) reported previously. The difference probably is due to impurities in the surface layer on the magnesium. Reagents of high dimethylmagnesium content form a precipitate during preparation which is largely if not entirely magnesium chloride etherate. The chloride content of the supernatant layer is lower than that in reagents which do not precipitate this magnesium chloride. Precipitation of chloride is not related to coupling, as the following experiment shows.

The gradual introduction during 6 hours of 22.8 g. (0.45 mole) of dry methyl chloride into 35 g. (1.45 g-atoms) of distilled magnesium (courtesy of Dominion Magnesium Co., Haley, Ontario) in 400 ml. of anhydrous peroxide-free ether under nitrogen caused initial precipitation of a white solid within 10 minutes of initiation, but lack of expansion of a rubber sack attached to the system showed that ethane was not formed in appreciable amount. The amount of precipitate increased during reaction and was finally filtered off under nitrogen, then was ether-washed. Filtrate and washings, evaluated by acid titrations of an aliquot, contained Grignard reagent in 87% yield. Separation by use of dioxane as described above showed a halogen-free basic magnesium content corresponding to 61% of dimethylmagnesium.

The solvent could be removed from these solutions of dimethylmagnesium by distillation from a nitrogen-filled Claisen flask, first at 100° under 12 mm. and then for 3 hours at 150–153°. Portions of the pyrophoric residue were transferred under nitrogen to volumetric flasks to which were added 2,5-dioxahexane, dioxane, diethyl ether, and diisooamyl ether. After they had been shaken overnight at 20° aliquots withdrawn into standard acid and titrated with alkali gave molarities of the saturated solutions. The powder is very soluble in 2,5-dioxahexane with evolution of heat; titration for basic magnesium shows that a 1.08 *M* solution is not saturated. However solubility in other ethers is limited. Saturated solutions in diethyl ether, dioxane, and isoamyl ether are 0.62, 0.23, and 0.08 *M* respectively while molarity in 4:1 ether-dioxane is 0.44.

Dimethylmagnesium with Benzoin

A. In Dioxane-Ether

These reactions were carried out as described previously (14) but with attention to addition of a solution of one reagent to the stirred solution of the other during about 10 minutes.

B. In Benzene

To 0.21 g. (0.001 mole) of benzoin in 15 ml. of dry benzene was added at once 0.82 g. (0.015 mole) of dimethylmagnesium (previously heated at 150–160° and 12 mm. for 8 hours). An intense red color appeared during 3 minutes. After 18 hours (positive Gilman test) dry oxygen was passed slowly through the system during 10 hours. The system was then poured into sulphuric acid – ice mixture and extracted with ether. The extract was washed thoroughly with aqueous sodium bicarbonate and then evaporated. The residue was treated with Girard P reagent (7) to detect whether benzoin was present (0%). The mixture of diphenylpropanediols was then isolated (14) and weighed, 0.21 g. (92%). The combined aqueous bicarbonate washings were acidified, extracted with ether, and the residue was sublimed to ascertain the benzoic acid yield (0.021 g., 8.5%).

C. In 2,5-Dioxahexane

When 0.35 g. (0.0065 mole) of dimethylmagnesium (heated to 155°) was added to 0.21 g. (0.001 mole) of benzoic acid in 15 ml. of dry 2,5-dioxahexane no red color was observed but the temperature increased by a few degrees. The resulting yellow solution was treated at 20° with dry oxygen for 12 hours. Subsequent processing as described above gave 0.020 g. (8%) of benzoic acid, 0.18 g. (79%) of non-ketonic material (VII), and no benzoic acid.

Diphenylmagnesium

To 0.275 equivalents of bromobenzene Grignard reagent (200 ml. vol. in diethyl ether) was added 100 ml. of dry peroxide-free dioxane during 40 minutes while it was stirred under nitrogen. After 12 hours for digestion and settling, the solution was filtered by nitrogen pressure through a glasswool plug above the stopcock at the bottom of the flask. The remaining precipitate was washed (by 3-minute agitation, 30-minute settling, and then filtration) with five 50-ml. portions of dioxane during 30 hours or until the filtrate gave a negative Gilman test. The entire filtrate was halogen-free and contained 50% of the basic magnesium in the original reagent.

In a modification of this procedure 25 ml. of 0.5 M magnesium bromide dietherate solution (10) was added to 0.083 equivalents (80 ml.) of bromobenzene Grignard reagent. The opalescent system separated into two phases when 15 ml. more of the dietherate solution was added. The lesser upper phase was 1.16 N, the lower phase 1.31 N with respect to bromide. Then 100 ml. of dioxane was stirred into the system in a centrifuge jar equipped with serum bottle cap. After centrifugation the solution was withdrawn by hypodermic syringe. After the precipitate was shaken with 100 ml. of dioxane (introduced through the serum cap) and centrifuged, the solution was withdrawn. This washing process was repeated six times, or until the washing liquor gave a negative Gilman test. The total solution contained 26.5% of the basic magnesium in the original reagent.

Solvent-free diphenylmagnesium was prepared by treatment under nitrogen from 25° to 160° under 12 mm. mercury pressure, first for 30 minutes at 160°. The residue, only slightly soluble in diethyl ether, was reheated at 160° for 30 minutes more, after which it was about 60% soluble in diethyl ether. Subsequent heating to 190° for 5 minutes left a residue almost completely soluble in ether. Titration showed that no destruction of the organometallic compound had occurred.

Diphenylmagnesium and Benzoic Acid

A. In Ether-Dioxane

To a solution of 1 g. (0.005 mole) of benzoic acid in 25 ml. of dioxane was added with stirring 0.064 mole of diphenylmagnesium in 500 ml. of the ether-dioxane solution in which it had been prepared. The clear reaction system was first deep-red, then orange in color as the addition was completed. Twelve hours later dry carbon-dioxide-free oxygen was passed through at 8° for 10 hours, leaving a yellow gel. After treatment with dilute sulphuric acid the ether extract was 4 times extracted with aqueous sodium bicarbonate, then evaporated and treated with Girard reagent to demonstrate that no benzoic acid was present. The non-ketonic portion, triphenyl-1,2-ethanediol, m.p. 167°, weighed 0.27 g. (20%) while the acidified and ether-extracted bicarbonate washings yielded 0.75 g. (6.5%) of sublimed benzoic acid.

B. In Diethyl Ether

A solution of 0.47 g. (0.002 mole) of benzoic acid in 75 ml. of dry ether was added to a

solution of 0.045 basic magnesium equivalents of solvent-free diphenylmagnesium in 50 ml. of diethyl ether. Subsequent processing as described in A yielded 0.27 g. (42%) of triphenylethanol, m.p. 168°, and 0.02 g. (4%) of benzoic acid.

Diethylmagnesium and Benzoin

An ethyl ether - dioxane solution prepared as described for the dimethyl homologue from ethyl bromide Grignard reagent contained 28% of the basic magnesium equivalence, as contrasted to the 42% found in the original study (12). Such a solution (0.029 equiv.) was added to 1.0 g. (0.0047 mole) of benzoin in 50 ml. of dioxane forming a deep-red solution which gradually turned orange in color. With oxygenation and subsequent processing as described above there was obtained 0.05 g. (4%) of benzoic acid, 0.42 g. (37%) of diphenylbutanediol, m.p. 116-117°, and no benzoin.

REFERENCES

1. BARTLETT, P. D. and BERRY, C. M. J. Am. Chem. Soc. **56**, 2684 (1934).
2. BREDT-SAVELSBURG, M. J. prakt. Chem. [2], **107**, 65 (1924).
3. BROOK, A. G., COHEN, H. L., and WRIGHT, G. F. J. Org. Chem. **18**, 447 (1953).
4. COHEN, H. L. and WRIGHT, G. F. J. Org. Chem. **18**, 432 (1953).
5. COPE, A. C. J. Am. Chem. Soc. **57**, 2238 (1935).
6. GILMAN, H. and SCHULZE, F. J. Am. Chem. Soc. **49**, 2328 (1927).
7. GIRARD, A. and SANDULESCO, G. Helv. Chim. Acta, **19**, 1095 (1936).
8. LUTZ, R. E. and KIBLER, C. J. J. Am. Chem. Soc. **62**, 360 (1940).
9. MEISENHEIMER, J. and SCHLICHENMAIER, W. Ber. **61B**, 720 (1928).
10. MENSCHUTKIN, B. N. Z. anorg. Chem. **49**, 34, 207 (1906).
11. Organic analysis. Vol. 1. Interscience Publishers Inc., New York. 1953. p. 191.
12. SCHLENK, W. Ber. **64B**, 734 (1931).
13. SCHLENK, W. Ber. **64B**, 736 (1931).
14. WRIGHT, G. F. J. Am. Chem. Soc. **61**, 1152 (1939).

DÉTERMINATION DU DEGRÉ DE SOLVATATION DU MONO-*n*-BUTOXYTRICHLOROTITANE DANS LE BUTANOL¹

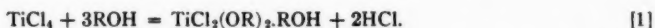
JACQUES ARCHAMBAULT² ET ROLAND RIVEST

RÉSUMÉ

Les mesures de densité, de viscosité et de conductivité des solutions de mono-*n*-butoxytrichlorotitane dans le butanol normal nous ont permis de déterminer le degré de solvation de ce composé du titane. Les mesures de viscosité indiquent une forte interaction entre le solvant et le soluté; les mesures de densité et de conductivité nous permettent de conclure à la présence de trois composés solvatés $\text{TiCl}_3\text{OBu.6BuOH}$, $\text{TiCl}_3\text{OBu.2BuOH}$ et $(\text{TiCl}_3\text{OBu.BuOH})_2$.

INTRODUCTION

Le tétrachlorure de titane peut réagir avec les alcools pour donner des composés de substitution. Jennings, Wardlaw et Way (8) ont proposé l'équation générale suivante pour ce genre de réaction:



Cette équation est assez représentative de la réaction générale des alcools sur le tétrachlorure; cependant, la facilité d'obtention de ces composés diminue à mesure que la chaîne carbonée de l'alcool allonge. Ainsi, si le *n*-butanol réagit avec le tétrachlorure de titane à température ordinaire, il y a formation du composé monosubstitué TiCl_3OBu , mais pour obtenir le composé disubstitué, il faut refluer à la température d'ébullition du butanol pendant 52 heures. De plus, des composés trialkoxy et tetraalkoxy peuvent être obtenus si l'alcoolate de sodium (3) est utilisé à la place de l'alcool pour faire la réaction. La réaction [1] montre que les composés disubstitués du tétrachlorure sont normalement monosolvatés; cependant, la stabilité de la liaison du ROH au reste de la molécule varie beaucoup d'un composé à l'autre, et seulement un certain nombre de composés solvatés ont pu être isolés. La littérature chimique ne mentionne aucun autre travail sur la solvation de ce genre de composés en solution. Nous avons pensé qu'une étude physicochimique d'un système solvant-soluté donné pourrait fournir des informations plus complètes sur le sujet.

Nous avons choisi d'étudier le système *n*-butoxytrichlorotitane - butanol normal à cause de la possibilité de faire les mesures physico-chimiques sur ce système à une température raisonnablement basse, i.e. à 60° C. Nous avons déterminé la variation de la viscosité, de la densité et de la conductivité en fonction de la concentration moléculaire du soluté dans le solvant, et l'interprétation des résultats obtenus nous a permis de conclure que le soluté pouvait être mono, di ou hexa solvato.

TRAVAIL EXPÉRIMENTAL

Purification des produits chimiques

On a utilisé pour ce travail le tétrachlorure de titane "Purified" de la Compagnie Fisher. Ce composé a été repurifié d'après la méthode de Gilchrist (4) et ses collaborateurs. Cette méthode a été éprouvée et donne un produit de haute pureté. Le butanol a été desséché sur du sulfate de calcium anhydre, reflué pendant 2 heures en présence de phtalate de butyle, puis soumis à une distillation fractionnée (12). La fraction médiane

¹Manuscrit reçu le 1 avril, 1967.

²Contribution du Département de Chimie de l'Université de Montréal, Montréal, Québec.

³Boursier de l'Office des Recherches Scientifiques de la Province de Québec.

distillant entre 116° et 117° C. a une conductivité de $2.3 \text{ à } 2.4 \times 10^{-7}$ mhos/cm. et une viscosité de 2.5 centipoises à 25° C.

Préparation du mono-n-butoxytrichlorotitane

Le composé est préparé par addition directe du tétrachlorure de titane en excès dans le butanol, à 0° C., contre un courant de gaz carbonique anhydre. Le système obtenu est ensuite débarrassé de l'acide chlorhydrique formé en le soumettant à un vide de 1 ou 2 cm. de mercure. Le composé est soumis à plusieurs lavages successifs avec le cyclohexane anhydre, ce qui enlève l'excès de tétrachlorure, et desséché à température ordinaire, sous un vide de 10 mm. de mercure. Ce composé ainsi préparé est blanc, et à l'analyse, donne les résultats suivants: Ti = 20.5%, Cl = 45.44%; les calculs théoriques donnent Ti = 21.1%, Cl = 46.8%. Si on fait le rapport Ti/Cl, on trouve 1/2.995 (théorique: = 1/3.0). La différence entre les valeurs théoriques et les valeurs expérimentales de l'analyse est probablement due à la présence d'un peu de butanol inclus dans le composé.

Mesures de conductivité

Les mesures de conductivité ont été effectuées à l'aide d'un pont de conductivité opérant en courant alternatif à haute fréquence tel que proposé par Jones et ses collaborateurs, et muni d'un "Wagner Ground" tel que conçu par Taylor et Acree, et amélioré par Jones et Joseph (9). Cet appareil nous permet d'obtenir une sensibilité de l'ordre d'une partie par million dans les meilleures conditions, et une précision de 0.01% pour des résistances de 1000 à 11000 ohms et de 0.05% pour des résistances de 11000 à 111000 ohms.

La cellule à conductivité utilisée était analogue à celle conçue par Kraus (6), c'est-à-dire que son compartiment à électrodes est situé en dehors de la cellule. Le volume contenu dans cette cellule n'est pas un facteur critique, pourvu que le compartiment à électrodes soit rempli. Ceci permet de faire des dilutions dans la cellule même. Nous avons pu ainsi réaliser plusieurs mesures de conductivité sur des solutions de concentrations différentes à partir de la même solution. Les mesures ont été effectuées dans un bain à température constante à l'huile de paraffine, maintenu à une température de $60 \pm 0.01^\circ \text{C}$.

Mesures de densité

Les densités ont été déterminées à l'aide de picnomètres d'environ 10 ml. gradués au millième de ml. Lors d'une mesure, nous pouvons facilement apprécier une demie division de la graduation, c'est-à-dire 0.0005 ml., ce qui représente l'erreur maxima sur une lecture de volume. Admettant une erreur maxima de 0.1 mg. sur chaque pesée et de 0.0005 ml. sur chaque lecture de volume, on obtient pour la densité une erreur absolue maxima allant de 0.0001 gramme par ml. pour les faibles densités à 0.00015 pour les densités voisines de 1.3. Les picnomètres ont été calibrés à l'eau distillée à la température de $60 \pm 0.01^\circ \text{C}$.

Mesures de viscosité

Les viscosités ont été mesurées à l'aide de deux viscosimètres Ostwald numérotés V₁ et V₂, à une température de $60 \pm 0.01^\circ \text{C}$. Le viscosimètre V₁ a été calibré avec le butanol et V₂ avec une solution de viscosité connue à l'aide de V₁. Pour déterminer les temps d'écoulement des solutions, nous avons utilisé un chronomètre gradué au dixième de seconde. L'erreur relative sur la moyenne des temps d'écoulement a toujours été inférieure à 0.3%, ce qui signifie que le chiffre de la viscosité en centipoises est au moins précis à 0.6%, si l'on suppose que les autres sources d'erreur sont négligeables par rapport à celle discutée.

Précautions à prendre dans la manipulation d'un composé étudié

Le monobutoxytrichlorotitane (composé "c") peut réagir avec l'eau pour donner de l'hydroxyde de titane, du butanol et de l'acide chlorhydrique. Cependant, la vitesse de la réaction d'hydrolyse varie beaucoup suivant la concentration du soluté dans le butanol. Pour les solutions de concentration moléculaire plus petite que 70% du composé "c" dans le butanol la réaction avec l'humidité de l'air est plutôt lente de sorte que les solutions peuvent être exposées à l'air libre pendant une minute sans être altérées. Ceci a été vérifié par des mesures de conductivité. Ces dernières seraient certainement les plus affectées par la réaction d'hydrolyse mentionnée, car l'acide chlorhydrique formé est plus dissocié que toute autre espèce chimique présente dans les solutions concernées. Dans les solutions plus concentrées que 70%, le composé "c" est plus sensible à l'humidité de l'air et il faut éviter son contact avec l'air libre. Pour ce faire, nous avons toujours transvasé le produit sous une atmosphère de gaz carbonique anhydre. Ainsi, pour introduire le composé "c" dans la cellule à conductivité, on place sur le ballon contenant le composé, un bouchon à joint rodé muni d'un tube allant jusqu'à environ deux centimètres de la surface du liquide et d'un autre tube par lequel on peut faire passer l'aiguille d'une seringue. On fait entrer le gaz carbonique par un des tubes et par l'autre on soutire le composé au moyen d'une seringue. Le composé est immédiatement versé dans la cellule à conductivité munie d'un dispositif analogue à celui ci-avant décrit. De cette façon, le composé "c" ne vient pas en contact avec l'air libre et n'est pas altéré par la manipulation. Une technique analogue a été utilisée pour les mesures de densité et de viscosité. Même si ce n'était pas rigoureusement nécessaire nous avons utilisé cette technique à toutes les concentrations. Cette technique s'est révélée satisfaisante puisqu'il nous a été facile de reproduire nos résultats à partir de différentes solutions-mères.

RÉSULTATS ET DISCUSSION

Densité

Les résultats obtenus par les mesures de densité sont consignés dans le tableau I et représentés graphiquement dans la figure 1.

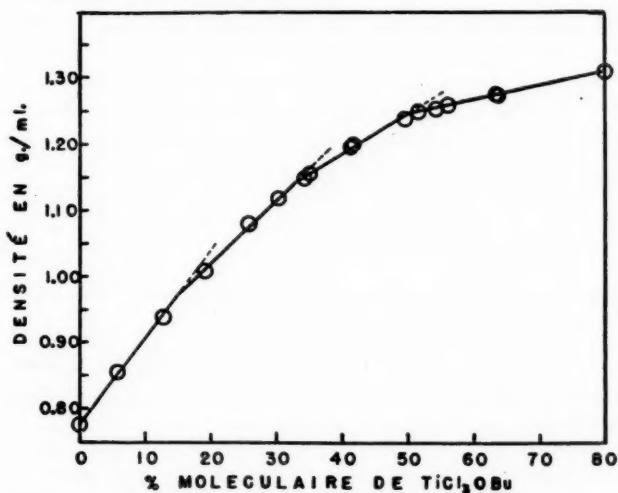
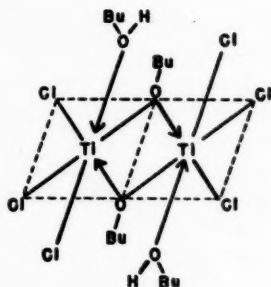


FIG. 1.

TABLEAU I

Solution No.	Concentration en moles % de TiCl_3OBu	Densité, g./ml.
1 d	0.00	0.7779
2 d	5.74	0.8550
3 d	12.69	0.9392
4 d	19.06	1.0095
5 d	25.69	1.0800
6 d	30.20	1.1190
7 d	34.33	1.1501
8 d	35.07	1.1567
9 d	41.43	1.1973
10 d	41.61	1.2008
11 d	49.61	1.2389
12 d	51.56	1.2499
13 d	54.24	1.2543
14 d	55.99	1.2605
15 d	63.42	1.2774
16 d	63.77	1.2747
17 d	80.00	1.3100

L'isotherme de densité du système consiste en quatre sections linéaires qui se rencontrent vers 14%, 33% et 50% du soluté dans le butanol. Un isotherme de ce genre pour la densité est le signe d'une interaction chimique prononcée entre le solvant et le soluté et les points de rencontre des sections linéaires coïncident habituellement avec la composition d'une espèce chimique définie (11). La courbe représentée dans la figure 1 semble donc indiquer la présence de trois composés solvatés: un composé hexasolvaté $\text{TiCl}_3\text{OBu} \cdot 6\text{BuOH}$ à 14%, un composé disolvaté $\text{TiCl}_3\text{OBu} \cdot 2\text{BuOH}$ à 33.3% et un composé monosolvaté $\text{TiCl}_3\text{OBu} \cdot \text{BuOH}$ à 50%, qui comme l'indique Wardlaw (2) et ses collaborateurs dans leur mémoire récent, existe probablement sous forme dimérique et peut être représenté par la formule suivante:



Cette formule explique assez bien les résultats obtenus par les mesures de conductivité.

Viscosité

Les mesures de viscosité ont donné les résultats inclus dans le tableau II. La figure 2 donne la courbe de la viscosité en fonction de la concentration moléculaire du monobutoxytrichlorotitane.

L'association intermoléculaire dans un système donné a toujours une répercussion sur la viscosité du système. Selon Bingham (1) et Dunstan (7), si la présence d'un maximum de viscosité est le signe indubitable d'une interaction chimique entre les deux constituants,

TABLEAU II

Solution No.	Concentration en moles % de TiCl_3OBu	Viscosité en centipoises
1 v	0.00	1.04
2 v	5.74	1.81
3 v	13.54	4.21
4 v	20.32	9.18
5 v	25.69	17.10
6 v	30.20	26.60
7 v	34.62	39.66
8 v	35.32	43.81
9 v	38.67	48.29
10 v	42.57	48.87
11 v	47.08	42.25
12 v	51.25	33.44
13 v	56.99	20.86
14 v	63.79	10.50
15 v	71.00	5.24
16 v	81.46	2.69
17 v	100.00	1.00

la position du maximum ne peut généralement nous renseigner de façon précise sur la composition du complexe. La position du maximum coïncidera avec la composition du complexe seulement quand celui-ci est stable, et quand les viscosités relatives des constituants sont à peu près identiques à la température du mélange. L'isotherme de viscosité représenté dans la figure 2 passe par un maximum très net à une composition de $41 \pm 1\%$ de soluté dans le butanol. Il est assez curieux de constater que la concentration au maximum de viscosité ne corresponde à aucun composé défini. Cependant, comme les composés solvatés ne sont pas très stables, on ne peut s'attendre à une détermination de la composition des complexes formés par l'étude de l'isotherme de viscosité. Cet isotherme nous indique qu'il y a formation d'au moins un complexe entre le solvant et le soluté et le fait que le maximum soit à mi-chemin entre les deux concentrations correspondant à des complexes définis est peut-être significatif.

Conductivité

Les mesures de la conductivité spécifique des différentes solutions étudiées sont compilées dans le tableau III. Nous avons inclus dans le même tableau les résultats obtenus pour la conductivité spécifique corrigée pour la variation de viscosité avec la concentration. Ces résultats sont représentés graphiquement dans la figure 3.

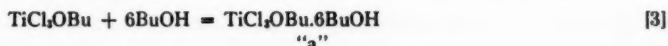
La conductivité d'un système donné dépend de la concentration ionique, de la mobilité des ions et de la viscosité du milieu. Nous avons éliminé l'effet de viscosité en corrigeant la conductivité spécifique par rapport à cet effet. Il est connu que la conductivité spécifique est inversement proportionnelle à la p -ième puissance de la viscosité où p est dépendant de la nature de l'ion. Dans tous les cas où p est connu, sa valeur est assez voisine de l'unité (10). On a alors la relation:

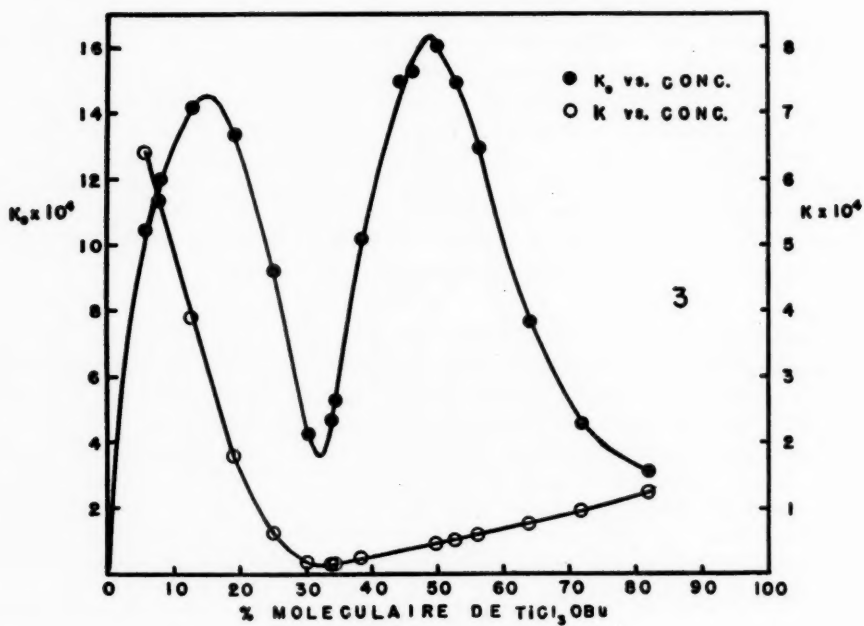
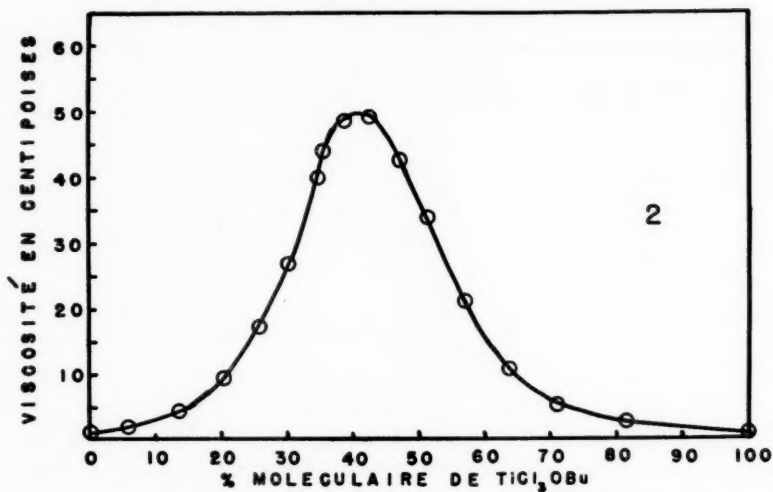
$$K_0 = K(n/n_0)^p \quad [2]$$

où K est la conductivité spécifique à la viscosité n du système et K_0 la conductivité spécifique à la viscosité n_0 du solvant pur.

Les différentes réactions qui ont lieu dans le système, à mesure que la concentration du complexe du titane augmente, peuvent être représentées par les équations suivantes:

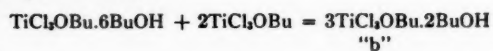
Solvatation du complexe du titane:





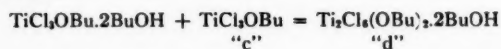
FIGS. 2 AND 3.

Formation du complexe dissolvé:



[4]

Formation du dimère:



[5]

TABLEAU III

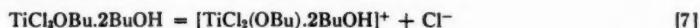
Solution No.	Concentration en moles % de TiCl_3OBu	Conductivité spécifique non corrigée $\times 10^4$	Conductivité spécifique corrigée $\times 10^4$
1 c	5.56	6.395	10.45
2 c	7.76	5.663	11.98
3 c	12.69	3.874	14.15
4 c	19.06	1.775	13.31
5 c	25.02	0.595	9.16
6 c	30.26	0.153	4.22
7 c	33.80	0.127	4.65
8 c	34.33	0.140	5.24
9 c	38.28	0.222	10.15
10 c	44.00	0.330*	14.90
11 c	46.00	0.360*	15.20
12 c	49.61	0.450	16.00
13 c	52.61	0.508	14.85
14 c	55.99	0.578	12.89
15 c	63.77	0.756	7.63
16 c	71.67	0.951	4.57
17 c	81.79	1.239	3.10

* Valeurs obtenues par interpolation sur la courbe de la conductivité spécifique.

Dissociation du composé "a":



Dissociation du composé "b":



Dissociation du dimère:



Dissociation du composé "c":



À l'aide de ces équations, nous pouvons expliquer les points importants de la courbe A de la figure 3.

La conductivité spécifique corrigée augmente d'abord jusqu'à la concentration de 14% à cause de l'augmentation de la concentration du composé "a" hexasolvaté dissocié d'après l'équation [6].* Il est normal de supposer que "a" sera plus dissocié que le composé "b" parce que les six doublets d'électrons fournis par les six molécules de butanol rendent le titane plus électrorépuilif dans le composé "a" que dans le composé "b" et ainsi favorisent davantage le départ d'un ion chlorure du composé "a". Ceci explique le maximum de conductivité à 14% et la diminution subséquente de conductivité avec la diminution de la concentration du composé "a" dans le système. Le minimum observé à 33% est ainsi attribuable à la disparition du composé "a" du système et correspond à la composition du composé "b". Dès que la concentration devient supérieure à 33%, le dimère "b" se forme d'après l'équation [5] et se dissocie comme l'indique l'équation [8]. On observe une augmentation de conductivité due à la dissociation plus grande du dimère que du monomère. La littérature fournit en effet un grand nombre d'exemples analogues où l'agglomération de molécules augmente la dissociation.

Il y aura donc augmentation de la conductivité avec augmentation de la concentration du dimère "b" jusqu'à l'obtention d'un maximum de conductivité à la concentration

*Ce degré de solvation n'est pas impossible puisque Cueilleron et Charest (5) ont trouvé que dans l'ammoniac liquide, le tétrachlorure de titane donne le composé $\text{TiCl}_4.6\text{NH}_3$.

équivalente au dimère pur. A l'addition de plus de TiCl_3OBU dissocié d'après l'équation [9], il y a diminution de la conductivité parce que la dissociation du composé "c" est moins grande que celle des deux composés "b" et "d". En effet, dans le cas des deux derniers, les deux doublets d'électrons additionnels fournis par les molécules de butanol rendent le titane plus électrorépuulsif, favorisant ainsi le départ d'un ion chlorure. Le composé "c" sera donc moins dissocié que les deux autres, parce qu'il ne contient dans sa structure aucune molécule de solvation, ce qui explique la diminution régulière de la conductivité à mesure que la concentration de "c" augmente.

La courbe de la figure 3 semble donc indiquer la présence dans notre système de trois états de solvation du composé "c", c'est-à-dire le composé "a" hexasolvaté, le composé "b" disolvaté et le composé "d" dimérique, où il y a une molécule de butanol de solvation par atome de titane.

REMERCIEMENTS

Les auteurs de ce mémoire remercient le Conseil National des Recherches pour la subvention (R. R.) accordée en vue de ce travail, et l'Office Provincial des Recherches Scientifiques de Québec pour la bourse accordée à l'un d'eux (J. A.).

BIBLIOGRAPHIE

1. BINGHAM, E. C. Fluidity and plasticity. McGraw-Hill Book Co. Inc., New York. 1922. p. 160.
2. BRADLEY, D. C., GAZE, R. et WARDLAW, W. J. Chem. Soc. 469 (1957).
3. BRADLEY, D. C., HANCOCK, D. C. et WARDLAW, W. J. Chem. Soc. 2773 (1952).
4. CLABAUGH, W. S., LESLIE, R. T. et GILCHRIST, R. J. Research Natl. Bur. Standards, **55**, 261 (1955).
5. CUEILLERON, J. et CHAREST, M. Bull. soc. chim. France, **5**, 802 (1956).
6. DAGGETT, H. M., Jr., BAIR, E. J. et KRAUS, C. E. J. Am. Chem. Soc. **73**, 799 (1951).
7. DUNSTAN, A. E. et THOLE, F. B. The viscosity of liquids. Longmans, Green & Co., Ltd., London. 1914. pp. 44-51.
8. JENNINGS, J. S., WARDLAW, W. et WAY, W. M. R. J. Chem. Soc. 637 (1936).
9. JONES, G. et JOSEPH, R. C. J. Am. Chem. Soc. **50**, 1049 (1928).
10. KRAUS, C. E. The properties of electrically conducting systems including electrolytes and metal. Chemical Catalog. Co., New York. 1922.
11. OSIPOV, O. A. et SUCHKOV, V. J. Gen. Chem. (U.S.S.R.) (Traduction anglaise), 1177 (1952).
12. VOGEL, A. I. Practical organic chemistry. Longmans, Green & Co., Ltd., London. 1951. p. 161.

STRESSES AND STRAINS IN ADSORBATE-ADSORBENT SYSTEMS

IV. CONTRACTIONS OF ACTIVATED CARBON ON ADSORPTION OF GASES AND VAPORS AT LOW INITIAL PRESSURES¹

M. L. LAKHANPAL² AND E. A. FLOOD

ABSTRACT

When active adsorbents, such as active carbon and porous glass, adsorb relatively large quantities of vapors, normally the adsorption is accompanied by considerable swelling of the adsorbent. It has been observed by McIntosh, Yates, and others that when the quantities adsorbed are small in some cases the adsorption is accompanied by an appreciable shrinkage of the adsorbent. We have studied this phenomenon experimentally and theoretically and some of the results obtained are presented in this paper. It is suggested that the shrinkage is due to "bridging" of sites by adsorbate molecules, the "bridging" being associated with highly anisotropic forces acting on adsorbate molecules and with considerable tensile stresses along some of the bonds of the adsorbed molecules.

INTRODUCTION

When porous adsorbents are immersed in incompressible fluids or in fluids which are not adsorbed appreciably, the volumes of the porous bodies decrease as the hydrostatic pressures of the enveloping fluids are increased. However, when a porous body adsorbs appreciable quantities of a fluid and the quantity adsorbed increases as the pressure increases, generally the porous body swells as the hydrostatic pressure of the enveloping fluid is increased. Generally, in such cases, the dimensional changes of the porous adsorbent are roughly proportional to the changes of the Gibbs free energy of the solid material. In cases where considerable adsorption hysteresis occurs, considerable net swelling may be observed along adsorption paths while considerable net shrinkages may be observed along desorption paths (1, 11, 12, 14, 17).

This rather paradoxical adsorption-extension behavior can be deduced from thermodynamic and statistical considerations while still retaining the simplifying assumption that the adsorbent and the adsorbate may each be treated thermodynamically as single component assemblies (8, 9, 11). Such considerations lead quite naturally to fairly simple relations (Equations [1], [2], and [3]) between the small changes in linear dimensions and the quantities adsorbed. The linear change in dimensions of the adsorbent may be expressed by the equation

$$[1] \quad \delta L/L = -A(1-B \delta \bar{p}_e^L) \delta \bar{p}_e^L,$$

where $\delta L/L$ is the elongation per unit length along a direction L , A and B are constants characteristic of the solid, and $\delta \bar{p}_e^L$ is the change in the linear mean stress intensity of the solid along the direction L . For isotropic materials A is roughly one-third the bulk compressibility and B measures the variation of compressibility with compression, i.e., B is a small correction to Hooke's law.

When the change in the state of stress of the solid is purely a change in uniform hydrostatic pressure of the solid, $\delta \bar{p}_e^L$ is the same as the change in volumetric mean state of stress, δp_e^V , so that $\delta \bar{p}_e^L = \delta p_e^V$, and δp_e^V can be obtained directly from the adsorption isotherm.

¹ Manuscript received March 25, 1957.

Contribution from the Division of Pure Chemistry, National Research Council, Ottawa, Canada.

Issued as N.R.C. No. 4408.

² National Research Council of Canada Postdoctorate Fellow 1955-1957. On leave of absence from the Department of Chemistry, Punjab University, India.

Thus we can write (9, 10, 11)

$$\delta v_{at} \cdot dp_{at} + \delta v_{ct} \cdot dp_{ct} = (\delta v_{at} + \delta v_{ct}) dP,$$

where δv_{at} and δv_{ct} are elements of volume of the adsorbate and adsorbent respectively, p_{at} and p_{ct} are their corresponding stress intensities, and P is the hydrostatic pressure of the fluid enveloping the system. For the assembly, after summation and integration over the range 0 to P , we have

$$v_a \cdot \bar{p}_a^V + v_c \cdot \delta \bar{p}_c^V = (v_a + v_c) P$$

and

$$\delta \bar{p}_c^V = (1 + v_a/v_c) P - (v_a/v_c) \bar{p}_a^V.$$

Since $\bar{p}_a^V = \int_0^P (\bar{\rho}_a^V / \rho) dP$, where $\bar{\rho}_a^V$ is the volumetric mean density of the adsorbate and ρ is the density of equilibrium gas whose pressure is P , the value of \bar{p}_a^V can be obtained graphically from the adsorption isotherm. Putting $\bar{p}_a^V = \alpha P$ (defining α), and $v_a/v_c = \phi$, we can write

$$[2] \quad \delta \bar{p}_c^V = [1 + \phi - \phi \cdot \alpha] P.$$

When the cross-sectional areas of the solid are not uniform and the changes in surface potentials are correlated with the structure, $\delta \bar{p}_c^L$ will in general differ materially from $\delta \bar{p}_c^V$. In such cases it can be shown that $\delta \bar{p}_c^L$ may be related to $\delta \bar{p}_c^V$ through the relation

$$\delta \bar{p}_c^L = K_p \cdot K_s (\delta \bar{p}_c^V - P) + P,$$

and hence

$$[3] \quad \delta \bar{p}_c^L = [1 + K_p \cdot K_s \cdot \phi (1 - \alpha)] P,$$

where K_s is a numerical factor ≥ 1 which is characteristic of the solid alone and constitutes a measure of the variation in "wall thickness" of the capillary spaces of the porous body. K_p measures the statistical correlation between the surface potentials of the capillary regions and their wall thicknesses. When the density of the adsorbate is constant everywhere for given changes in hydrostatic pressure, K_p is necessarily unity for such changes. While K_s is independent of the pressure and nature of the adsorbable fluid, K_p will, in general, vary with the pressure and nature of the fluid. It has been found that K_p approaches unity when the quantity adsorbed is large, i.e., for large α and P . When $\alpha \gg 1$ and K_p is unity, $\delta L/L = -K_s \cdot \phi \cdot \alpha \cdot P$. Thus the elongation becomes proportional to the change in Gibbs free energy of the solid (since $v_a \cdot \bar{p}_a^V + v_c \cdot \delta \bar{p}_c^V = (v_a + v_c) P$ is equivalent to $\Delta F_a + \Delta F_c = \Delta F_{ac}$ and when ΔF_{ac} is small $\Delta F_a = -\Delta F_c = v_a \cdot \bar{p}_a^V = v_a \cdot \alpha \cdot P$).

It has been observed that small initial contractions sometimes occur at low pressures with certain gases and that these contractions occur along paths of increasing equilibrium pressure, i.e., along paths of increasing P . (Negative adsorbate pressures cannot be formed along thermodynamically reversible increasing pressure paths.) These contractions seem quite independent of adsorption hysteresis and are more or less reversible with increasing or decreasing equilibrium pressures. Accordingly, if such cases are describable by Equations [1], [2], and [3], $\delta \bar{p}_c^L$ must be negative and of considerable numerical magnitude. Such a situation indicates a highly anisotropic stress distribution which is specific for the different adsorbates. It is to be emphasized that $\Delta \bar{F}_c^V$ must be negative in order that appreciable adsorption can occur. Hence $\delta \bar{p}_c^V$ must also be negative. The fact that $\delta L/L$ is negative indicates that $\delta \bar{p}_c^L$ is positive; accordingly $\delta \bar{p}_c^V$ and $\Delta \bar{F}_c^V$ must contain positive components or elements.

A considerable volume of literature (1, 2, 3, 4, 10, 11, 12, 14, 15, 17, 18, 19) exists concerning the over-all adsorption-extension behavior of adsorbents at high surface coverages, where relatively large expansions occur and where the adsorption-extension behavior can be described very well by means of Equations [1], [2], and [3], K_p being taken either as unity or as an empirical function differing but little from unity (9, 11). However, the small specific contractions which occur in some cases at low "surface coverages" have not been systematically examined.

In what follows we present the results of experimental measurements of the adsorption-extension behavior of activated carbon rods exposed to low pressures of a number of gases and vapors, special emphasis being placed on the cases where contractions occur or where negative K_p values are indicated.³

EXPERIMENTAL DETAILS AND RESULTS

Materials

(a) *Carbon rod*.—The carbon rod, No. 4, used in these investigations is similar to the carbon rod, No. 1, used by Flood and Heyding (10) since they have both been selected out of the same group of activated carbon rods. Before use this carbon rod was heated to 500° C. in low pressures of helium for 5 hours. The dimensions of the rod are as given below:

Length	103.02 mm.
Diameter	1.69 mm.
Total volume	0.2315 cc.
Void volume ⁴	0.1390 cc.
∴ Carbon volume	0.0925 cc.

The measurement of void volume has been carried out in accordance with the procedure outlined by Flood (9).

(b) *Ethane, n-propane, n-butane, and 2,2-dimethylpropane*.—These gases were supplied by The Matheson Co. Inc. and the purity of the gases was 99%, 99.5%, and 99.9% respectively. Before use the gases were condensed in a liquid air trap or in CO₂ snow traps to assure absence of more volatile constituents, and the gases were then introduced later into the apparatus by slowly raising the temperature of the trap so that any of the more condensable gases or vapors present may not enter the apparatus.

(c) *n-Pentane*.—It was a "high research grade" obtained from the special products division of the Phillips Petroleum Co. and was used as received.

(d) *Carbon tetrachloride and methanol*.—These were obtained from The Mallinckrodt Chemical Works and Brickman and Company respectively and were used after redistillation.

Procedure

The adsorption values for the various gases were obtained volumetrically and adsorption-extension measurements carried out simultaneously. In most cases the volumetric

³It may be pointed out that in the Appendix of the paper by Flood and Heyding (10) the expressions K_p and K_v are used. The K_p of the earlier paper is quite different from the K_p used later. Thus the K_p used by Flood and Heyding refers to the special case where p_a^0 is constant. Thus K_p (Flood and Heyding) is K_s in the later papers. K_v on the other hand is based on a constant γ and accordingly $K_v = K_p K_s$ of the later papers.

⁴The values of 1.1 for α used by Flood (9), calculated from the data of Steele and Halsey (16), are based on micropore volume only. The total volume being approximately double the micropore volume, the correction gives the value of $\alpha = 1.05$. Accordingly on the basis of $\alpha = 1.05$, the void volume and the carbon volume of rod No. 4 are 0.1324 cc. and 0.0991 cc. respectively.

adsorption measurements were obtained by expansion from known volumes into the carbon-rod-containing vessel and, by application of ideal gas laws, the quantities adsorbed were obtained in PV units.

At higher equilibrium pressures constant adsorption-extension values were usually obtained within 1 to 2 hours, while at low relative pressures in the neighborhood of the maximum contractions, equilibrium required many hours or several days. This is especially the case on desorption.

The measurement of length changes was carried out in exactly the same way as was done by Flood (9). All observations were carried out at a constant temperature of 24.8° C. The length changes were reproducible to within $\pm 5.0 \times 10^{-4}$ mm. The length changes of the carbon rod and the amounts of the various gases adsorbed are reported in Tables I to III and plotted in Figs. 1 to 6.

Radial changes on adsorption of carbon tetrachloride have been made on a similar carbon rod (No. 5) to verify the isotropic behavior of these rods during both expansion and contraction. Comparative data of the linear and radial changes in dimensions of the carbon rods are given in Table IV. While the radial and axial dimensional changes reported refer to different carbon rods, it is evident that the dimensional changes are essentially isotropic. The apparatus used for these radial changes is the one described by Flood and Heyding (10).

DISCUSSION

The data presented in Tables I to IV and in Figs. 1 to 6 indicate quite clearly that in the case of these particular carbon rods initial contractions along increasing adsorbate equilibrium pressure paths are by no means limited to a particular adsorbate. In general these initial contractions are reasonably reproducible, are more or less independent of the pressure path, and are not directly associated with adsorption hysteresis. While some extension hysteresis is exhibited, it is considered that this is in the main due to the very slow rates of attainment of equilibrium at these low pressures.

Evidently these contractions are highly specific and bear no obvious relation to the change in Gibbs free energy of the solid or to the change in solid surface free energy. Any considerable "chemical reaction", "chemisorption", or "solution effect" will give rise to dimensional changes of the rods that are highly specific and that bear little or no relation to the changes in the thermodynamic potential of the carbon and bear no relation to the elastic properties, structure, etc. of the pure carbon. In such cases Equations [1], [2], and [3] cannot describe the extensions in any literal sense.

It is, of course, evident that if K_p in Equation [3] is a function of P which may have comparatively large positive or negative values without restriction, the Equations [1], [2], and [3] are capable of describing empirically almost any adsorption-extension behavior including cases where the underlying assumptions are not even approximately valid. In the latter cases, the constants and variables will not have the physical significance assigned to them and accordingly the equations will be quite useless as a means of interpreting the data.

It seems very unlikely that such a variety of adsorbates can give rise to reasonably reversible "chemisorption" or "solution" complexes without permanent change of the carbon and without the formation of other chemical species or decomposition products. Accordingly, we shall regard the contractions as arising primarily from physical adsorption phenomena. The physical factors which might be expected to give contractions fall into two broad categories: (a) The phenomena are largely the result of thermodynamically

TABLE I
ADSORPTION-EXTENSION DATA
Carbon rod No. 4
Straight chain hydrocarbons (24.8° C.)

Substance	Adsorption			Desorption		
	Relative pressure† $p_s/p_0 \times 10^3$	Quantity sorbed, PV units* $\times 10^{-2}$	Length change $\delta L/L \times 10^3$	Relative pressure† $p_s/p_0 \times 10^3$	Quantity sorbed, PV units* $\times 10^{-2}$	Length change $\delta L/L \times 10^3$
Ethane ($p_0 = 3144$ cm.)	0.24	0.88	- 3.5	—	—	—
	0.80	1.75	- 5.7	7.45	—	+22.4
	1.01	2.09	- 4.9	3.30	—	+ 1.4
	1.29	2.50	- 4.6	2.41	—	- 1.8
	2.05	3.37	- 4.0	1.25	—	- 5.0
	3.75	4.77	+ 0.5	1.00	—	- 5.7
	6.12	6.28	+ 9.0	0.41	—	- 5.5
	10.11	8.00	+23.5	0.18	—	- 4.8
	19.28	10.40	+42.7	—	—	—
	23.83	11.30	+68.4	—	—	—
	26.76	11.61	+81.6	—	—	—
	—	—	—	—	—	—
	—	—	—	—	—	—
Normal propane ($p_0 = 703.3$ cm.)	0.16	1.46	- 7.3	—	—	—
	0.24	1.95	-11.6	13.24	—	+74.0
	0.62	3.30	-12.4	2.26	—	- 0.3
	0.96	4.10	-10.5	0.94	—	- 7.3
	2.77	6.47	- 5.6	0.51	—	- 8.1
	3.93	7.36	+ 3.6	0.31	—	- 8.5
	4.23	7.58	+ 5.1	0.22	—	- 6.2
	6.41	8.68	+21.9	0.15	—	- 5.3
	9.28	9.60	+37.6	—	—	—
	10.17	9.79	+43.9	—	—	—
	18.74	11.28	+72.3	—	—	—
Normal butane ($p_0 = 200$ cm.)	0.11	0.53	- 4.2	—	—	—
	0.22	1.43	-10.1	51.20	12.65	+269.6
	0.57	2.51	-16.4	8.20	9.97	+103.7
	1.32	4.19	-16.7	2.87	8.28	+41.4
	2.72	6.85	+ 2.5	1.71	7.25	+20.1
	5.51	8.76	+48.5	1.18	6.60	+ 5.0
	16.78	10.63	+134.1	0.87	6.10	- 2.1
	50.30	12.36	+249.6	0.68	5.71	- 6.5
	93.37	13.21	+314.0	0.56	5.39	- 9.4
	—	—	—	0.45	5.13	-11.7
	—	—	—	0.40	4.72	-14.7
	—	—	—	0.32	4.40	-15.3
	—	—	—	0.28	4.25	-16.8
Normal pentane ($p_0 = 50$ cm.)	0.07	1.31	-12.2	—	—	—
	0.15	3.60	-22.7	8.88	8.63	+161.0
	0.20	3.64	-23.3	4.36	8.00	+113.8
	0.67	3.90	-22.2	2.68	7.60	+91.8
	0.80	4.27	-19.5	1.26	6.80	+42.5
	2.40	5.35	- 3.1	0.90	6.26	+27.8
	9.12	6.67	+62.6	0.78	5.80	+17.5
	48.34	8.30	+239.7	0.46	5.36	+ 6.2
	—	—	—	0.40	5.20	- 0.5
	—	—	—	0.23	4.99	-16.5
	—	—	—	0.212	4.72	-20.5
	—	—	—	0.150	4.57	-17.9

*PV units sorbed are expressed in pressure (cm. Hg) multiplied by volume (cc.), and can readily be converted to moles or volumes at standard pressure.

† p_s = equilibrium pressure, p_0 = saturation pressure.

TABLE II
ADSORPTION-EXTENSION DATA
Carbon rod No. 4
Symmetrical molecules (24.8° C.)

Substance	Adsorption			Desorption		
	Relative pressure† $p_e/p_0 \times 10^3$	Quantity sorbed, PV units* $\times 10^{-2}$	Length change $\delta L/L \times 10^3$	Relative pressure† $p_e/p_0 \times 10^3$	Quantity sorbed, PV units* $\times 10^{-2}$	Length change $\delta L/L \times 10^3$
2,2-Dimethylpropane ($p_0 = 128.5$ cm.)	0.10	1.60	- 21.3	544.900	11.72	+476.5
	0.17	3.13	- 26.6	245.56	9.54	+407.8
	0.26	4.46	- 22.0	115.40	8.47	+346.4
	0.55	4.93	+ 30.4	60.03	7.80	+287.2
	15.40	6.81	+152.0	30.42	7.17	+224.7
	50.08	7.87	+250.9	9.946	6.36	+149.6
	126.30	8.76	+367.4	2.716	5.17	+ 66.10
	282.70	9.58	+398.9	1.720	4.41	+ 42.5
	544.90	11.72	+476.5	0.607	4.14	+ 16.1
				0.300	4.01	+ 2.8
				0.245	3.90	- 4.5
				0.206	3.81	- 11.2
				0.079	—	- 12.7
				0.047	—	- 10.4
Carbon tetrachloride ($p_0 = 11.45$ cm.)	0.65	1.20	- 17.9	389.69	15.20	+538.9
	0.72	3.01	- 38.6	217.12	14.17	+464.4
	0.76	3.90	- 39.8	70.48	12.79	+355.7
	1.13	4.31	- 40.3	27.25	11.72	+261.4
	1.21	5.38	- 36.5	11.79	10.35	+153.1
	1.55	6.46	- 26.4	0.987	9.53	+ 96.8
	1.90	7.65	- 3.0	2.620	8.23	+ 61.7
	5.24	9.03	+ 73.2	1.485	7.49	+ 37.7
	17.47	9.96	+167.4	1.048	6.97	+ 24.3
	55.98	10.94	+298.2	0.227	—	+ 0.2
	143.23	11.88	+395.9	0.131	—	- 11.6
	249.69	12.99	+463.6	0.065	—	- 15.9
	322.44	13.83	+467.5	0.044	—	- 19.2
	572.92	15.48	+538.9	0.017	—	- 12.0

*†See Table I, footnote.

TABLE III
ADSORPTION-EXTENSION DATA
Carbon rod No. 4
Polar molecule (24.8° C.)

Substance	Adsorption			Desorption		
	Relative pressure† $p_e/p_0 \times 10^3$	Quantity sorbed, PV units* $\times 10^{-2}$	Length change $\delta L/L \times 10^3$	Relative pressure† $p_e/p_0 \times 10^3$	Quantity sorbed, PV units* $\times 10^{-2}$	Length change $\delta L/L \times 10^3$
Methanol ($p_0 = 11.5$ cm.)	3.9	1.27	+12.6	650.9	38.85	+500.9
	13.0	2.67	+ 5.4	425.2	35.65	+306.4
	22.1	4.60	- 1.9	225.6	32.62	+139.4
	25.6	5.58	- 3.4	115.5	29.09	+ 43.2
	29.7	8.16	-12.8	84.7	25.74	+ 1.7
	34.3	9.85	-18.8	55.0	17.34	- 18.7
	40.3	12.35	-22.2	34.8	12.04	- 12.3
	46.7	13.58	-25.5	18.3	9.24	- 2.5
	53.6	14.74	-25.6	12.3	7.37	+ 4.8
	59.1	16.21	-25.9	12.0	5.54	+ 7.0
	70.0	19.11	-18.2	9.3	4.12	+ 7.1
	99.0	23.22	+ 9.0	9.1	2.73	+ 8.2
	227.1	29.42	+165.0	6.4	1.74	+10.1
	475.0	35.33	+310.8	3.0	1.27	+15.6
	650.9	38.85	+500.9	1.2	1.11	+ 8.9
				0.0	0.00	+ 6.0

*†See Table I, footnote.

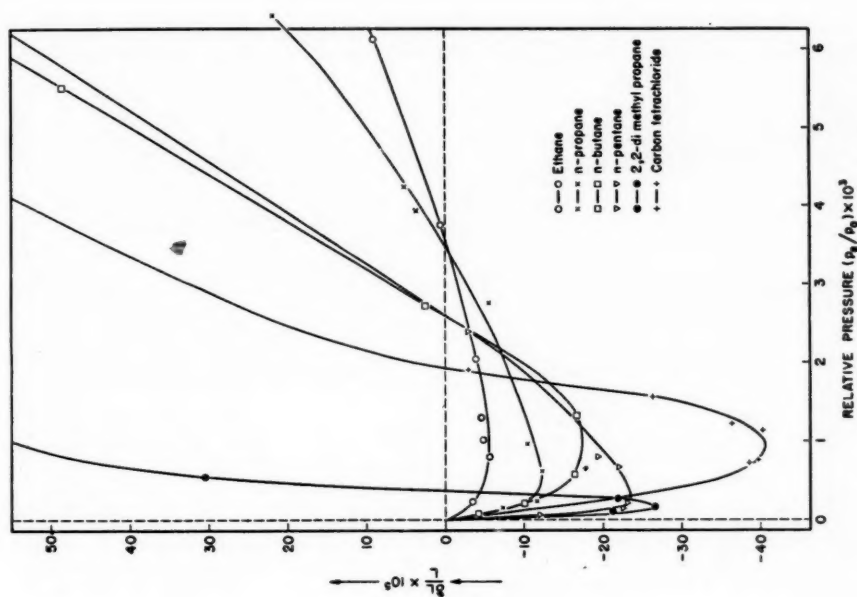


FIG 2. $\delta L/L$ on adsorption of C_2H_6 , $n-C_3H_8$, $n-C_4H_{10}$, $n-C_5H_{12}$, $(CH_3)_2C$, and CCl_4 at increasing relative pressures.

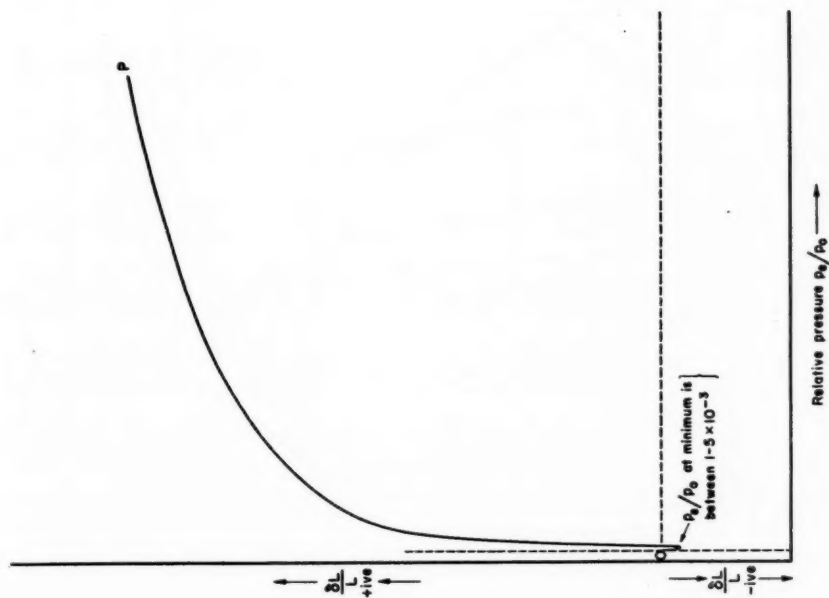


FIG. 1. The general trend of the plot of $\delta L/L$ against p/p_0 of the various adsorbates.

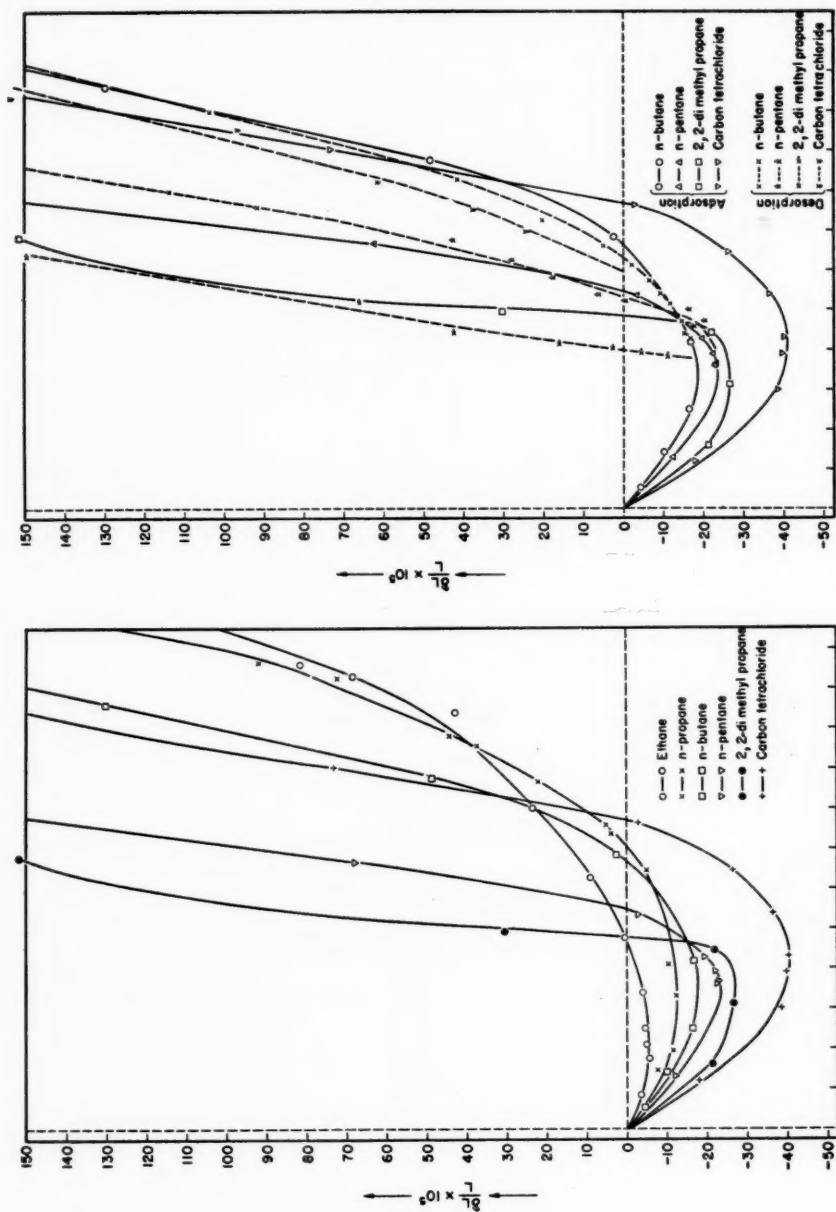


FIG. 3. $\delta L/L$ plotted against the PV units of the various gases adsorbed.

FIG. 4. $\delta L/L$ plotted against the PV units of n -C₄H₁₀, n -C₅H₁₂, (CH₃)₂C, and CCl₄ (during adsorption and desorption).

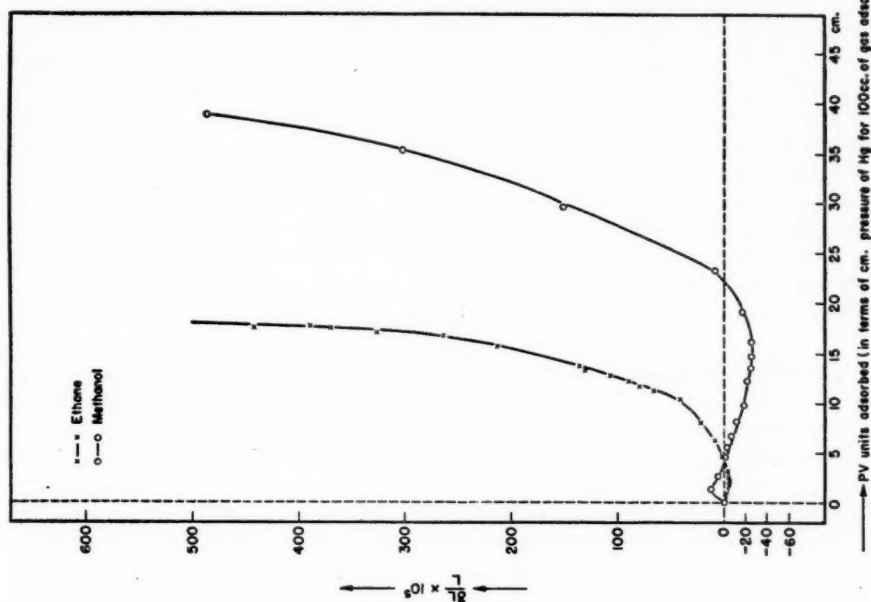


Fig. 6. $\delta L/L$ plotted against PV units of ethane and methanol adsorbed.

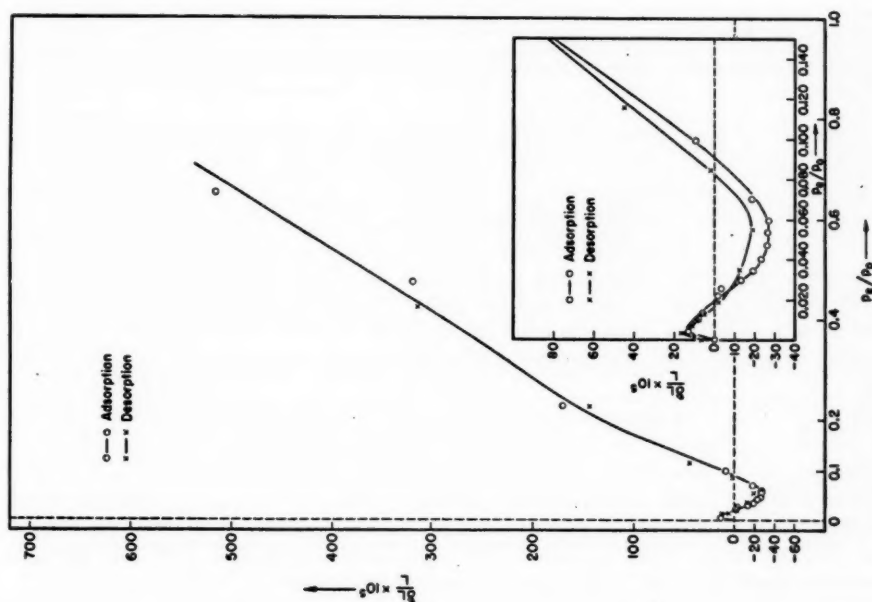


Fig. 5. $\delta L/L$ plotted against p_s/p_0 of methanol (during adsorption and desorption).

irreversible processes and consequently Equations [1], [2], and [3] cannot hold accurately over the whole of the pressure range 0 to P (Fig. 1). (The irreversible formation of condensed states having net negative pressures, the states being reached along increasing pressure paths, as in "capillary condensation" theories, would render the equations inaccurate.) (b) The phenomena are the result of inherently thermodynamically reversible processes and are described by Equations [1], [2], and [3]. K_p thus measures the statistical correlations indicated by the theoretical development, the negative K_p values being due to the action of highly anisotropic surface forces throughout the elements of the more or less isotropic assembly. The lack of isotropy may be ascribed to (i) polar character of adsorbate molecules, (ii) hydrogen bonding, (iii) co-operative van der Waals' forces between neighboring adsorbate molecules, (iv) bridging by single adsorbate molecules of neighboring sites, the sites bridged being either on the same solid surface or on opposite sides or faces of small pores.

TABLE IV
COMPARATIVE DATA OF LINEAR* AND RADIAL* CHANGES IN DIMENSIONS
OF CARBON RODS ON ADSORPTION OF CARBON TETRACHLORIDE AT
DIFFERENT RELATIVE VAPOR PRESSURES
($p_0 = 11.45$ cm.)

Serial number	$p_r/p_0 \times 10^3$	Linear changes $\delta L/L \times 10^3$	Radial changes† $\delta r/r \times 10^3$
1	1.13	- 4.0	- 3.2
2	12.22	+12.6	+14.1
3	21.39	+18.7	+22.6
4	38.83	+24.1	+26.9
5	74.45	+31.4	+31.7
6	296.50	+46.2	+48.6

*Radial changes were done on carbon rod No. 5 and axial changes on carbon rod No. 4. (Both rods are of essentially similar characteristics.)

†The radial contractions reported above are the mean values of a large number of measurements at each individual point and at small dimensional changes the percentage error may be as much as 50% while at higher changes it is about 5%.

The absence of appreciable adsorption hysteresis, together with the reproducibility of the contractions, their independence of approach along the pressure coordinate, etc., suggests that the phenomena belong in class (b). (It is to be emphasized that these contractions must not be confused with the generally much larger contractions associated with desorption when hysteresis is marked.) While the contractions might be interpreted as evidence of capillary condensation it can easily be shown that such large reductions in vapor pressure would require negative pressures which are much too large to be consistent with a Kelvin surface tension effect. Some of these "Kelvin effect" negative pressures are greater than the probable ultimate tensile strengths of the liquids concerned.

Accordingly the more plausible interpretations of the contractions lie in one or more of the physical factors noted in category (b). That these effects cannot be ascribed wholly to either (i) or (ii) is evident, since the contractions occur with non-polar molecules as well as with molecules containing no hydrogen atoms. In case (iii) we should expect expansions at first followed by contractions as the co-operative effects develop, while in case (iv) the contractions can start from zero surface coverages. The data strongly suggest that both of these latter physical factors are operative.

We have pointed out previously that the H_2O adsorption-desorption isotherms of these carbon rods are of types usually attributed to very fine graded micropore systems.

In this respect as well as in the generality and magnitudes of the low pressure contractions our carbon rods must be regarded as differing materially from the more usual type of gas-adsorbent carbon. Average "pore sizes" of gas-adsorbent carbons are usually considered to vary from about 10 Å to 50 Å. If we may regard our rods as being finer grained than these carbons, it is evident that a considerable fraction of the micropore volume must be of molecular dimensions. Since X-ray analysis⁵ of our carbon rods indicates considerable graphitic structure, we may suppose the micropore system to consist largely of sheet-like spaces between graphite platelets (5, 7, 13), the spaces varying in thickness from a few Å upwards. Such a system will be mechanically weak toward forces perpendicular to the platelets and strong toward forces parallel to the platelets. Bearing in mind that H₂O is not held very strongly by the so-called H-type activated carbons⁶ we are led to the following speculative inferences:

1. The micropore system consists of sheet-like spaces between graphite platelets. The thickness of the spaces varies upwards from a few Å, a considerable fraction of micropore volume being composed of sheets of thickness of the order of 6 Å.
2. The surface of the carbon platelets is energetically heterogeneous, the sites consisting of areas of molecular dimensions whose potentials vary considerably.
3. The surface forces of high energy sites act on parts of polyatomic adsorbate molecules rather than on the molecules as a whole and are highly selective. Low energy sites are less specific and tend to act on the molecules as a whole.
4. The maximum adsorption potential for a given molecule occurs in spaces where two or more high energy sites are occupied simultaneously by different parts of the molecules, while the spacing of the sites is such as to permit the maximum freedom of movement of the different parts of the molecule, i.e., positions of minimum energy and/or maximum entropy.
5. When two or more sites are occupied by parts of the same molecule, the adsorption potential will be less than the sum of the potentials of the same sites for the same parts from different molecules because of the decrease in entropy involved in such "bridging" and/or because of displacement from positions of minimum energy.
6. The decrease in entropy associated with bridging is equivalent to introducing a strain in the molecule, the strain being directed along the line joining the sites bridged.
7. Because of the lack of symmetry of attractive and repulsive molecular forces, as well as because of configurational entropy considerations, tensile strains are much more probable than compressive molecular strains.
8. High energy sites for CH₃ and CH₂ groups are much more numerous than are such sites for OH groups, i.e., CH₃ and CH₂ groups are more strongly adsorbed than are OH groups.

On the basis of the above inferences we should expect ethane to exhibit high energy site "bridging" and hence contractions starting from zero surface coverages, while methanol should show little or no bridging until the adsorbate density is sufficient for bridging to develop through co-operative interactions of the —OH groups (hydrogen bonding). Thus at low surface coverage methanol molecules will be adsorbed on the

⁵The authors are indebted to Dr. W. H. Barnes, Head, Section of X-ray Diffraction, Division of Pure Physics, National Research Laboratories, for kindly doing the X-ray examination and analysis of a number of these carbon rods.

⁶High temperature activated carbons (gas-adsorbent type) have been called H carbons. These adsorbents adsorb organic solvents in preference to water or to aqueous solutions. When such carbons are immersed in aqueous NaCl, KCl etc. solutions, the solutions become markedly alkaline, while immersion in pure water has little or no effect on the pH. Prof. R. M. Barrer and W. I. Stuart have given a statistical thermodynamical treatment of the adsorption of H₂O and methanol on carbon in *J. Chem. Soc.* 3307 (1956).

high energy sites, the molecules being orientated with —OH groups away from the surface. The —OH groups being but little influenced by neighboring sites, there is little molecular strain and elementary volumes of the adsorbates are in essentially hydrostatic states of compression. Accordingly, the carbon will expand more or less isotropically so that both δv_a and δv_c are positive. At higher surface coverages interactions will develop between —OH groups from molecules held by neighboring high energy sites, leading to a tension in the molecules, the net forces tending to collapse

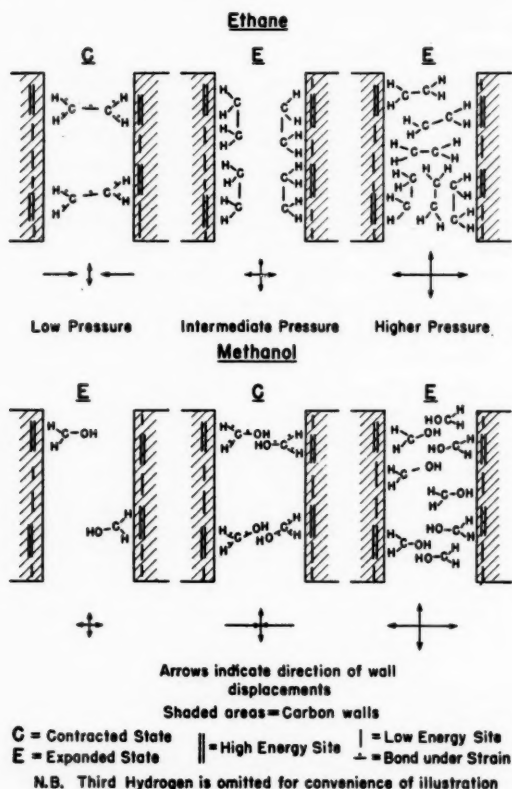


FIG. 7. A sketch illustrating molecular "bridging" (ethane) and co-operative bridging (methanol).

the narrow void spaces while increasing their areas. Thus δv_c is still positive while δv_a tends to become negative. The system being mechanically weak towards forces perpendicular to the surface, eventually δv_a becomes negative and numerically larger than δv_c . Hence the rod contracts as the co-operative effects develop. The adsorbate in this condition is of much higher density than the equilibrium vapor but the molecules are under tension and elementary volumes of adsorbate cannot be regarded as in hydrostatic states of compression. At still higher "surface coverages" as the densities approach liquid densities, interactions of the —OH groups of strongly surface held molecules will be mainly with the —OH groups from molecules other than those strongly held,

i.e., the interactions will be more generalized and elementary volumes of adsorbate once more approach essentially hydrostatic states of compression, the tension between the walls vanishing, δv_a and δv_c will become positive and the rod expand very considerably. In the case of ethane the "bridging" and contractions start from zero surface coverage since the individual molecules will seek positions where both $-\text{CH}_3$ groups are held by high energy sites on opposite walls. At higher surface coverages these sites will be occupied by parts of different molecules and the "bridging" and contractions disappear. Thus the maximum contraction with ethane should occur when the number of molecules adsorbed is somewhat less than one half the number causing the maximum contraction with methanol. Adsorption-extension behavior of higher alcohols and amines should be dominated by the hydrocarbon groups, the effect of the OH or NH_2 groups being the less the larger the hydrocarbon chain.

It is not intended to imply that the "bridging" necessarily vanishes as the density becomes high. In our opinion in the case of real systems, as the density of the adsorbate increases, in some regions or domains the "bridging" will persist while in other regions the "bridging" will vanish. The simplest cases to treat are those where either all or none of the "bridging" persists at limiting high densities.

If these speculations have any validity "bridging" molecules must be regarded as "activated" and accordingly the "catalytic activity" of the carbon in these contracted states should be high for certain types of reaction. Further, surface catalyzed reactions might yield quite different products in contracted and expanded states.

Some of the above notions are illustrated in Fig. 7.

REFERENCES

1. AMBERG, C. H. and MCINTOSH, R. *Can. J. Chem.* **30**, 1012 (1952).
2. BANGHAM, D. H. and FAKHOURY, N. *Proc. Roy. Soc. A*, **130**, 81 (1930).
3. BANGHAM, D. H. and MAGGS, F. A. P. *Proceedings of Conference on the Ultrafine Structure of Coals and Cokes*, June 24, 25, 1943, p. 101. (The British Coal Utilization Research Association, Distributing Agents, H. K. Lewis and Co. Ltd., London.)
4. BANGHAM, D. H. and RAZOUK, R. I. *Proc. Roy. Soc. A*, **166**, 572 (1938).
5. BISCOE, J. and WARREN, B. E. *J. Appl. Phys.* **13**, 364 (1942).
6. BORJE, S. *Adsorption and exchange of ions on activated charcoal*. Almqvist and Wiksells, Boktryckeri Aktiebolag, Upsala. 1944.
7. CLARK, G. L. and JOHNSTONE, H. F. O.S.R.D. Formal Report, Dec. 9, 1942.
8. FLOOD, E. A. *Can. J. Chem.* **33**, 979 (1955).
9. FLOOD, E. A. *Can. J. Chem.* **35**, 48 (1957).
10. FLOOD, E. A. and HEYDING, R. D. *Can. J. Chem.* **32**, 660 (1954).
11. FLOOD, E. A. and LAKHANPAL, M. L. *Proceedings of the Second International Congress of Surface Activity*, April 8-12, 1957, London, England. Butterworth Scientific Publications, London.
12. HAINES, R. S. and MCINTOSH, R. *J. Chem. Phys.* **15**, 28 (1947).
13. HOFMANN, VON U., RAGOSS, A., and SINKEL, F. *Kolloid Z.* **96**, 231 (1941).
14. MCBAIN, J. W., PORTER, J. L., and SESSION, R. *J. Am. Chem. Soc.* **55**, 2294 (1933).
15. MEEHAN, F. T. *Proc. Roy. Soc. A*, **115**, 199 (1927).
16. STEELE, W. A. and HALSEY, G. D. *J. Chem. Phys.* **22**, 979 (1954).
17. WIIG, E. O. and JUHOLA, A. J. *J. Am. Chem. Soc.* **71**, 561 (1949).
18. YATES, D. J. C. *Proc. Roy. Soc. A*, **224**, 526 (1954).
19. YATES, D. J. C. *J. Phys. Chem.* **60**, 543 (1956).

THE REDUCTION, ENOLATE FORMATION, AND SOLVOLYSIS OF GRIGNARD REAGENTS IN OPTICALLY ACTIVE MEDIA¹

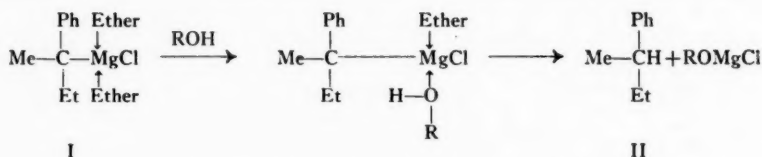
NORMAN ALLENTOFF AND GEORGE F WRIGHT

ABSTRACT

The *sec*-butylbenzene produced by solvolysis of 2-phenyl-2-chlorobutane Grignard reagent in (+) 2,3-dimethoxybutane and benzene is optically inactive. The 2- \downarrow -isopropyl-4- \uparrow -methylcyclohexanols obtained by the reducing action of isopropyl Grignard reagent on racemic 2- \downarrow -isopropyl-4- \uparrow -methylcyclohexanone in (+) dimethoxybutane are optically active to the extent of 6 and 15%. The bromomagnesium enolates obtained by the action of isopropyl Grignard reagent on racemic 2- \downarrow -isopropyl-4- \uparrow -methylcyclohexanone in (+) dimethoxybutane regenerate the parent ketone in an optically inactive state but the diastereomeric 2- \uparrow -isopropyl-4- \uparrow -methylcyclohexanone also produced is optically active to the extent of about 6%.

When Grignard reagents are prepared in optically active polyethers they react with mercuric chloride (7), oxygen, ethanol (5), or compounds containing carbonyl groups (7, 1) to give products in which one enantiomer predominates. Exceptions are the products of reaction with formaldehyde and with organic halides (7). The study has now been extended so as to resurvey the solvolysis reaction and also to examine the reactions involving so-called reduction and enolate formation which occur when Grignard reagents are treated with ketones.

Since the solvolytic reaction previously examined (5) involved an unusual Grignard reagent which might be considered to be an enolate, we have now prepared the simple tertiary Grignard reagent, I, from 2-phenyl-2-chlorobutane, in benzene containing 2 moles of (+) 2,3-dimethoxybutane, and have treated it slowly with *n*-butanol. The product is not detectably active although a rotation of 36.5° has been predicted (20) for fully resolved 2-phenylbutane (*sec*-butylbenzene) (II). Evidently the minimal steric effect,



apparent even in the simplified formulation portrayed above, is not sufficient to direct the hydrogen preferentially by one of the two reaction paths leading to enantiomeric forms of II. However, it should be noted also that solvolysis, unlike ketone addition, does not involve a reversible co-ordination such as seems to prevail during Grignard addition to the carbonyl group.

We have chosen racemic 2- \downarrow -isopropyl-4- \uparrow -methylcyclohexanone (III, menthanone) as the ketone for study of reduction and enolate formation. It has been shown by use of ethylzinc iodide (11) that III does not exist detectably in an enol form although these authors report propane equivalent to 51% of the ketone by treatment with isopropyl bromide Grignard reagent. Moreover reduction has been shown to occur (10) in the same reaction, giving alcohols which comprise 17–20 molar per cent of the reaction product. Finally no significant amount of simple carbonyl addition occurs in the reaction.

¹Manuscript received March 18, 1957.

Contribution from the Department of Chemistry, University of Toronto, Toronto, Ontario.

The isopropyl bromide Grignard reagent has been prepared (73% yield) in benzene containing 1 molar equivalent of (+) 2,3-dimethoxybutane and has been treated slowly with an equivalent amount of racemic 2- \downarrow -isopropyl-4- \uparrow -methylcyclohexanone. The four products have been separated, first by boric acid esterification of the alcohols, and secondly by chromatography on silicic acid, using the chromatoplate technique as a qualitative and semiquantitative guide. These products are described in Table I.

TABLE I

REACTION PRODUCTS FROM RACEMIC 2- \downarrow -ISOPROPYL-4- \uparrow -METHYLCYCLOHEXANONE AND ISOPROPYL BROMIDE GRIGNARD REAGENT IN BENZENE AND (+) DIMETHOXYBUTANE BASED ON THE OPTICAL ROTATORY RELATIONSHIP: III, -29.6° ; V, -49.4° ; VI, $+19.7^\circ$; IV, $+85.1^\circ$

Products	Yield		Rot., obs. theor.	% Product		% Yields, enantiomers	
	%	$[\alpha]_D$		+	-	+	-
2- \downarrow -Isopropyl-4- \uparrow -methyl- \uparrow -cyclohexanol (menthanol) V	7.5	$-3.10 \pm .17$.063	46.8	53.2	3.5	4.0
2- \downarrow -Isopropyl-4- \uparrow -methyl- \downarrow -cyclohexanol (neomenthanol) VI	6	$-2.6 \pm .2$.13	43.5	56.5	2.6	3.4
2- \downarrow -Isopropyl-4- \uparrow -methylcyclohexanone (menthanone) III	64	$+0.01 \pm .04$	0	50	50	32	32
2- \uparrow -Isopropyl-4- \uparrow -methylcyclohexanone (isomenthanone) IV	6	$-5.4 \pm .2$.06	47	53	2.8	3.2

By comparison of the observed optical rotations of these products with the rotations (top, Table I) of the pure enantiomers (29, pp. 513-515; 32) the ratio "observed/theoretical" is obtained and from these ratios the percentage of enantiomers in each product. In consideration of the several compound-yield percentages the enantiomer-yield percentages (last columns, Table I) are recorded. Totalling these yields with respect to the enantiomeric relationships (top, Table I) one obtains for the products derived from levo-III the summation 4%, 2.6%, 32%, 2.8% = 41.1% and for dextro-III the summation 3.5%, 3.4%, 32%, 3.2% = 42.1%. These percentages ought to be identical, since the intrinsic enantiomerism in the racemic reagent III is unaffected by the Grignard reactions which it has undergone.

It is obvious that the asymmetric resolutions reported previously (7, 5) differ from the present reactions with menthanone in one important respect. The former resolutions involved inactive Grignard reagents which are known to be capable (probably via equilibrium with $R_2Mg + MgX_2$ (30)) of enantiomeric equilibration. Thus the enantiomer withdrawn for asymmetric reaction is quickly replaced by this equilibration. On the other hand the equal amounts of (+) and (-) menthanone must be represented by this equality among the final products. Since the optically inactive menthanone reacts completely with an equivalent amount of Grignard reagent (final Gilman test is negative) and a stable co-ordination complex resisting the reduction, enolate, and Michler's ketone reaction is improbable, the summation of optical activity in the products should equal zero.

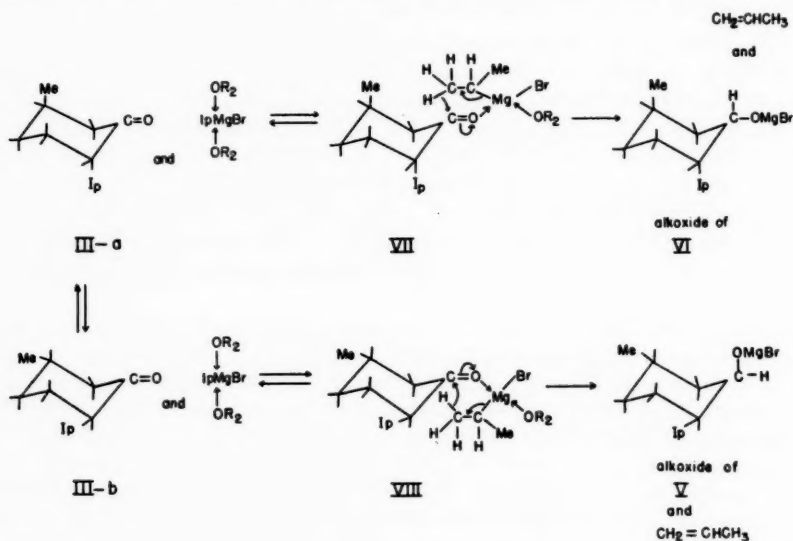
The 0.7% discrepancy between the enantiomer yields represents either a 2% or a 25% experimental error in accounting for the products, depending upon whether or not one considers the optically inactive product (menthanone) to be significant to the stereochemistry of the reaction. Since we consider the production of menthanone to be an important part of the entire reaction we accept the lower figures of error. In doing so

we assume confidently on the basis of the experimental techniques that the enantiomeric distribution of Table I applies also to the 16.5% of products which have not been isolated.

The Reduction Reaction

It may be seen in Table I that the amount of reduction (13.5%) is less than was reported for the interaction of the same reagents in diethyl ether (10). This difference is not unexpected because previously (1) it has been found that the course of reaction is strongly dependent on the type of co-ordinating ether that is involved in the system. Also the presence of optical activity in the 2- \downarrow -isopropyl-4- \uparrow -methyl- \uparrow -cyclohexanol (menthanol, V) and the 2- \downarrow -isopropyl-4- \uparrow -methyl- \downarrow -cyclohexanol (neomenthanol, VI) is expected from the reactions of optically active Grignard reagents with ketones (23, 31). It is notable that one of the diastereomeric alcohols is over twice as optically active as the other although the yields are about equal.

One may accept the proposal by Whitmore that the reduction involves a cyclic transitory intermediate in which the hydrogen on the carbon β to the magnesium atom is transferred to the carbonyl group in the six-membered cycle. Indeed this transference has been demonstrated by use of a deuterated Grignard reagent (9). Adapting this concept to the reaction of isopropyl Grignard reagent in (+) dimethoxybutane with 2- \downarrow -isopropyl-4- \uparrow -methylcyclohexanone, and arbitrarily assuming a crown ring, the a - a constellation of one enantiomer of the ketone is represented as III- a . One may expect



that the quasi-cyclic intermediate (VII) will be formed in preference to the alternative ("below the ring", not shown) in which the quasi-cycle would be in steric conflict with the isopropyl group. In consequence one might expect neomenthanol (VI) to be the principal product from the constellation III- a . But in this event the axially disposed ring-methyl substituent in VII ought to cause sufficient distortion as to favor strongly one diastereomer of VII (resulting from interaction with the enantiomeric influence of (+) dimethoxybutane, OR₂) over the other, which would be formed from isopropyl bromide Grignard reagent and the enantiomer of the constellation III- a . Therefore the

high enantiomeric preponderance found during formation of neomenthanol (VI) would not be unexpected.

The $e-e$ constellation of 2- \downarrow -isopropyl-4- \uparrow -methylcyclohexanone is shown as III-*b*, actually as the other enantiomer in order to maintain positional uniformity in the illustration. The equatorial substituents in III-*b* ought not to hinder appreciably either the formation of the quasi-cyclic intermediate VIII, which would lead to menthanol (V), or the alternative ("above the ring", not shown) which would lead to 2- \downarrow -isopropyl-4- \uparrow -methyl- \downarrow -cyclohexanol (neomenthanol, VI). But in either VIII or the alternative intermediate the distorting effect of the equatorial methyl or isopropyl group should be minimal with respect to the enantiomeric character of (+) dimethoxybutane. Consequently the relative stabilities of the two diastereomeric intermediates of VIII or of its alternative ought to be quite similar. Lack of diastereomeric preponderance would thus lead to lack of enantiomeric preponderance in the products, menthanol and neomenthanol, expected from III-*b*. Thus in summation of expected products from III-*a* and III-*b* one would anticipate a preponderance of enantiomerism in the neomenthanol.

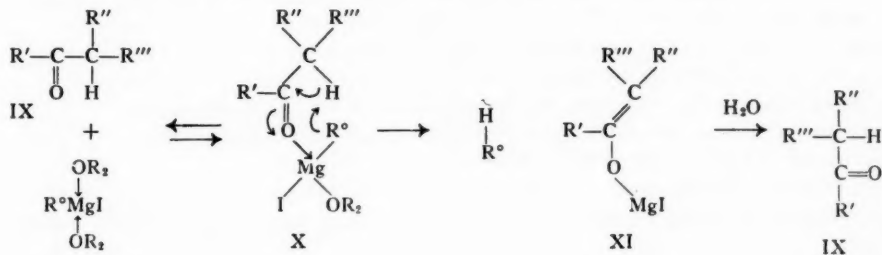
This argument is a speculation based on the observation that (+) dimethoxybutane induces over twice as much optical activity in neomenthanol as it does in menthanol. We believe that the speculation is justified because it stresses the significance of mechanical distortion in processes of asymmetric synthesis or resolution where a reversibly formed intermediate is involved (1).

Actually the most tenuous part of the argument involves the assumption of a crown constellation which until recently (19) was thought to be characteristic of cyclohexanes. This generalization now seems to be invalid. The simple Sachse-Mohr alternative (the boat constellation) cannot fit the explanation for the enantiomeric difference between menthanol and neomenthanol. However a situation not unlike that imposed by the "crown" will exist in the "flexible" constellation, which is replacing the oversimplified "boat" of Sachse-Mohr. Therefore the argument of mechanical distortion is not vitiated by these recent stereochemical revisions.

The Enolate Formation

The idea that enolate formation in Grignard reaction is not directly related to spontaneous enolization of the ketone was put forward by Lutz and Kibler (21), who described the process as a 1,4-addition to the typical linkage $A-CH_2-C=O$ in which A is hydrogen or halogen. By a slight elaboration of this concept the extent of enolate formation has been attributed (24) to the characteristic of the intermediate complex A, shown below, rather than to its essential parts.

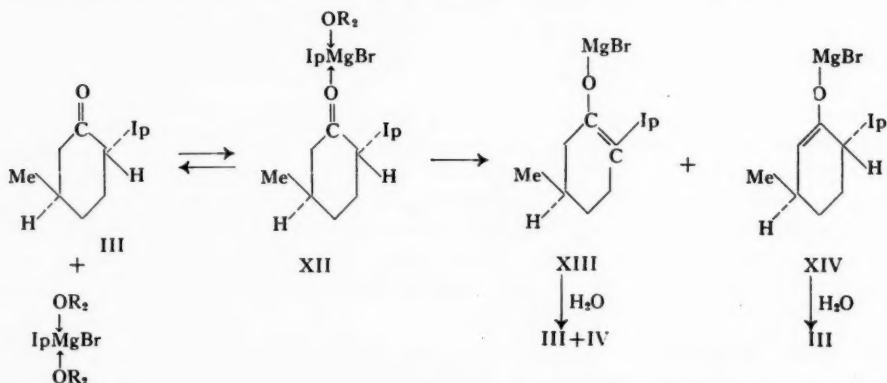
Consideration of the quasi-cyclic intermediate X shows that if one of the ketone substituents, say R'' , is non-symmetrical, then X consists of two diastereomers if it contains an optically active co-ordinating ether (OR_2). But these two diastereomers



(by reference to non-symmetric groups called *d*-ketone:*d*-ether and *l*-ketone:*d*-ether) may decompose at different rates reversibly to ketone IX and Grignard reagent, or irreversibly to enolate XI.

The 6% yield of 2- \uparrow -isopropyl-4- \uparrow -methylcyclohexanone (IV, isomenthanone), which is optically active to the extent of 6%, must have been regenerated from an enolate like XI. On the other hand there is the possibility that all or part of the 64% yield of 2- \downarrow -isopropyl-4- \uparrow -methylcyclohexanone (menthanone, III) might be optically inactive because it is in fact unchanged starting material. This possibility is unlikely. The ketone has been added slowly in order to avoid coating of reagent by product salts. Moreover the Gilman test is negative subsequent to addition of one equivalent of reagent. The presence of an unreactive complex inert toward Michler's ketone and toward enolization is unexpected in a system where it is known that the alternative, reduction, can occur. Therefore it seems reasonable to assume that the inactive ketonic product III also is regenerated from an enolate of type XI.

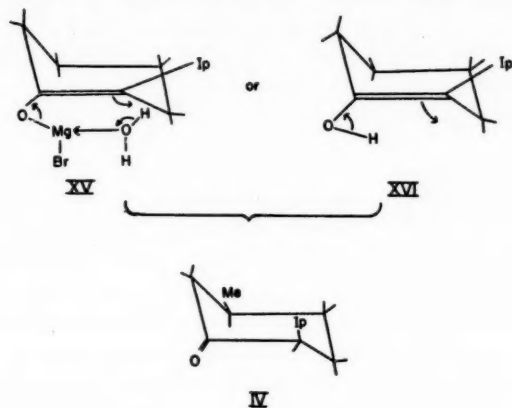
Actually two enolates may arise by action of Grignard reagent on 2- \downarrow -isopropyl-4- \uparrow -methylcyclohexanone of which XIII would seem to be a possible source of III and IV,



but XIV could regenerate only III. But if the enolate XIV were formed from racemic ketone III then XIV would be optically inactive (as would XI if R''' = H) despite the presence of optically active ether in the co-ordination complexes X or XII. On the other hand the ketone III would be optically active if it were regenerated from XIII, which produces optically active 2- \uparrow -isopropyl-4- \uparrow -methylcyclohexanone, IV. Since the ketone III regenerated in 64% yield is optically inactive, it seems worth while to consider the possibility of its formation from the enolate XIII.

It has been concluded from consideration of thermodynamic data (3) that cyclohexene exists in the symmetrical half-chair constellation of atoms. However, this symmetry cannot be expected to persist in substituted cyclohexenes. The distortion of a trisubstituted cyclohexene such as the enolate XIII probably cannot be represented by any orthodox constellation of atoms. For convenience it will be described as a "chair" in which methyl is approximately equatorial while isopropyl is displaced above the position of minimal energy for *sp*² orbital distribution, while hydroxyl (as shown in 16) or its bromomagnesium equivalent (shown as a transitory hydrate in 15) is displaced below the position of minimal energy.

Now intramolecular ketonization from either XV or XVI would be expected to produce 2- β -isopropyl 4- β -methylcyclohexanone, IV. Contrariwise, the formation of 2- β -isopropyl-4- β -methylcyclohexanone (III, menthanone) would be improbable. Of course this constellation, or any other one, is not rigid. But when the degree of improbability is included with a facile alternative for enolate formation ($\text{III} \rightarrow \text{XIV} \rightarrow \text{III}$) it is not



unexpected that the regenerated reactant III should be optically inactive ($0.01 \pm 0.04^\circ$) within the limits of our precision.

The authors are grateful to Science Service, Canadian Department of Agriculture, for expenditure of funds which made the research possible.

EXPERIMENTAL*

The Chromatoplate

This technique, invaluable for diagnosis in purification of organic compounds, separation of reaction mixtures and of a multitude of column chromatograph or countercurrent extraction samples, has been described in detail (17, 22, 27, 28). Slight modifications of the method of Rigby and Bethune are reported here as they are applicable to the present study. A glass sheet 25X25 cm., sand-blown on one side, was laid horizontally and was flanked by two longer guide sheets of glass which were raised 0.5 mm. above the surface of the middle sheet. About 60 ml. of a mixture of 80% Fisher precipitated silicic acid and 20% powdered plaster of Paris was stirred rapidly with just enough water to give a smooth slurry and then was poured rapidly onto the glass sheet and was levelled by means of a glass rod sliding on the guide sheets. The plate was then dried at 90° for at least 4 hours.

The samples and controls were applied as 0.01 ml. spots of 10% solution in hexane or chloroform along a line 4 cm. from one edge of the plate. The plate was then placed in a closed glass tank with the edge along which the spots were placed dipping into the developing medium of depth 1 cm. When the solvent front had ascended about 15 cm. (1 to 2 hours) the plate was removed, aerated at $20-25^\circ$, and sprayed with a 5% solution of absolute nitric acid in concentrated sulphuric acid. Then the plate was heated at 150° in an oven in order to make the spots visible. Other, more specific, sprays were used as needed.

*Melting points have been corrected against reliable standards.

Racemic Menthaneone

Optically inactive menthanol, $([\alpha]_D^{20} (-) 0.03 \pm 0.06^\circ, 20\% \text{ in ethanol})$ was oxidized according to Beckman (4) in 86% yield, b.p. 78–81° (8 mm.), d_4^{20} 0.899, n_D^{20} 1.4500. Development on the chromatoplate with 8% ethyl acetate in hexane showed isomenthaneone (R_f 0.53) as well as menthanone (R_f 0.72). Attempted purification by the method of Cooke and Macbeth (used by them for determination of the ultraviolet absorption spectrum of menthanone!) (8) via the semicarbazone actually increased the amount of impurity. For purification a 15-g. portion of distilled oxidation product was dissolved in 45 ml. of hexane and placed in a flat-bottomed side-arm test tube 35 mm. O.D. under a nitrogen atmosphere and was chilled to -70° and seeded or scratched to induce crystallization. After 8 hours the liquor was removed with a close-fitting filter stick and the crystals were dried *in situ* under reduced pressure in the presence of calcium chloride and paraffin. The 90% recovery was recrystallized (82% recovery) and then distilled, b.p. 93–94° (15 mm.), d_4^{20} 0.893, n_D^{20} 1.4500, homogeneous according to the chromatoplate, ultraviolet absorption: single maximum at 290 $m\mu$, E 21.6 (2.65 g. per l. in absolute ethanol), $[\alpha]_D^{20} (+) 0.02 \pm 0.04^\circ$.

Racemic 2- \downarrow -Isopropyl-4- \uparrow -methylcyclohexanone (Menthaneone) with Isopropyl Bromide Grignard Reagent in Benzene and (+) Dimethoxybutane

Isopropyl bromide was washed at 4° with 70% sulphuric acid, water, and 20% aqueous potassium carbonate, then dried with anhydrous potassium carbonate and distilled, b.p. 60–61°. To 2.50 g. (0.103 atom) of purified magnesium (1) under purified nitrogen was added a few milliliters of a solution of 12.3 g. (0.1 mole) of isopropyl bromide in 12 ml. (0.1 mole) of (+) 2,3-dimethoxybutane (7) and 60 ml. of benzene distilled from sodium benzophenone ketyl (dielectric constant at 20°, 2.284). After a few minutes of stirring with gentle warming the system gave a positive Gilman test. When addition was complete (30 minutes) the system was stirred 90 minutes longer; basic magnesium content was 73%, 0.073 mole. Then, at 4°, 11.3 g. (0.073 mole) of menthanone in 25 ml. of benzene was added during 70 minutes, and afterward stirred for 10 hours at 4–25°. A Gilman test was negative. After hydrolysis with 100 ml. of saturated ammonium chloride and ice the aqueous layer was twice extracted with 50-ml. portions of benzene. The combined benzene solution, washed twice with 25-ml. portions of saturated aqueous sodium chloride and dried with sodium sulphate, was distilled, finally at 0.5 mm., b.p. 49–65°, 9.21 g., 82% weight yield, d_4^{20} 0.895, $[\alpha]_D^{21} -1.01 \pm 0.04^\circ$. The chromatoplate showed menthanone R_f 0.67, isomenthaneone R_f 0.55, neomenthanol R_f 0.40, and menthanol R_f 0.32, and qualitatively a 1:3 ketone-alcohol ratio.

Separation of Ketones from Alcohols

An estimated twofold excess (0.26 g., 0.0042 mole) of boric acid was mixed with 4 g. of the ketone-alcohol mixture and maintained at 90° (250 mm.) for 3 hours while much of the boric acid dissolved. Then the pressure was reduced to 12 mm. to remove water. Subsequently the flask was heated to 100° under 0.25 mm. to remove 3.29 g. (82% of the original mixture), $[\alpha]_D^{21} (-) 0.61 \pm 0.02^\circ$, neat. The residual oily solid (0.91 g.) represented esters equivalent to 0.73 g. (18%) of menthanols. Since a control experiment showed that this separation of menthanones and menthanols was virtually quantitative the yield of ketones was 67% and of alcohols 15% of that possible from the Grignard reaction.

The borate residue was suspended in 5 ml. of water and was steam-distilled. The 100 ml. of distillate was saturated with sodium chloride and thrice extracted with petroleum ether. The 100 ml. of extract, dried with magnesium sulphate, was distilled, finally

at 54° (0.4 mm.), 0.53 g. (73% recovery), $[\alpha]_D^{21} (-) 2.19 \pm .06^\circ$. The chromatoplate showed that these alcohols were contaminated with ketones.

Separation of the Menthnols

(a) 2- \downarrow -Isopropyl-4- \uparrow -methyl- \uparrow -cyclohexanol (Menthanol)

A stepped glass column (12) was constructed from a 10-cm. length of tubing, 2.9-cm. I.D., sealed to a 12-cm. length of 2.2-cm. I.D. sealed to a 12-cm. length 1.4-cm. I.D., and each section was filled with a mixture of 4:1 Fisher reagent silicic acid - Celite washed with acetone, then water, and dried at 90°. Each section was capped, top and bottom, with filter paper disks resting on glass wool pads with the small intervening space packed with glass beads to ensure mixing of the eluate as it passed from one section to the next. Since the adsorbent in the column and the eluent (93:7 hexane - ethyl acetate) were similar to those used for the chromatoplate, the latter was used to evaluate the 13-ml. fractions which were eluted from the column. The eluates were evaporated *in vacuo* at room temperature in order to minimize loss of the alcohols. No product was obtained from the first eight fractions. The next 26 ml. of the eluate contained about 0.11 g. of 2- \downarrow -isopropyl-4- \uparrow -methylcyclohexanone (menthanone) and 0.13 g. of 2- \downarrow -isopropyl-4- \uparrow -methyl- \downarrow -cyclohexanol (neomenthanol). The next 39 ml. contained 0.022 g. of unseparated mixture while the remaining 91 ml. of eluate contained 0.171 g. of almost pure 2- \downarrow -isopropyl-4- \uparrow -methyl- \uparrow -cyclohexanol (menthanol), $[\alpha]_D^{21} -3.10 \pm .17^\circ$ (9% solution in ethanol), i.e. resolution to the extent of 6.2% of authentic levo-menthanol, $[\alpha]_D^{20} -48.8$. Yield is 7.5% of that possible from the ketone originally added to the Grignard reagent, based on chromatoplate evidence of the composition of the 0.022 g. nonseparated mixture and assuming that the alcohol-ketone ratio 30:11 found in the eluted product was also characteristic of the crude alcohol fraction when applied to the column.

(b) 2- \downarrow -Isopropyl-4- \uparrow -methyl- \downarrow -cyclohexanol (Neomenthanol)

The mixture of menthanone and neomenthanol (0.24 g.), separated from the Hagdahl column, $[\alpha]_D^{20} (-) 1.41 \pm .09^\circ$, neat, contained 0.13 g. of neomenthanol by chromatoplate estimation, so the activity of the neomenthanol must have been $[\alpha]_D^{20} (-) 2.6 \pm .2^\circ$ if the menthanone were inactive. Estimated yield from chromatoplates was 6% of the ketone originally treated with Grignard reagent. To 0.22 g. of the menthanone-neomenthanol fraction was added 0.31 g. (0.8×10^{-4} moles) of 88% phosphoric acid, corresponding to 0.13 g. (8.4×10^{-4} moles) of neomenthanol. The waxy mixture formed upon stirring was dissolved in 1 ml. of isohexane,* then filtered and cooled at -20°. The crystalline neomenthanol - phosphoric acid derivative (6) (44% on H_3PO_4 basis) was filtered off at 0° and vacuum-dried, 0.068 g., m.p. 81-85°. This product was recrystallized from 0.75 ml. of isohexane, recovery 61%, m.p. 85-86° (6), $[\alpha]_D^{20} (-) 2.4 \pm .4^\circ$ (15.8% in 95% ethanol). Assuming, as was found for the menthanol derivative, that the rotation of the phosphoric acid complex in 95% ethanol approximates that of its neomenthanol content alone, this rotation indicates that our neomenthanol has about 15% of enantiomeric preponderance, i.e. $[\alpha]_D^{20} (-) 3.0 \pm .6^\circ$; in close agreement with that estimated from the composition and rotation of the menthanone-neomenthanol mixture.

Phosphoric Acid - 2- \downarrow -Isopropyl-4- \uparrow -methyl- \uparrow -cyclohexanol ($H_3PO_4 \cdot 3$ Menthanol)

(a) From Levo-menthanol

When 2.0 g. (0.0128 mole) of powdered levo-menthanol was mixed with 0.50 g. (0.0045 mole) of 88% phosphoric acid and the white solid product was slowly crystallized

*Refers to commercial hexane.

from 12 ml. of dry hexane at 0°, a 32% yield of derivative, 0.81 g., m.p. 73–74°, was obtained, $[\alpha]_D^{21} (-) 40.1 \pm 2^\circ$ (6% solution in ethanol). The X-ray diffraction powder pattern with Cu K_α (Ni filtered) radiation in d spacings, Å, and relative intensities $[I/I_1]$ was [10] 5.82; [8] 4.75; [7] 4.39; [5] 4.20; [1] 7.46, 6.41, 3.56; [0.5] 5.15, 3.29.

(b) *From Racemic Menthanol*

A similar preparation gave a 40% yield, m.p. 71–72°, with diffraction pattern: [10] 11.3, 5.75, 4.70; [9] 4.10; [8] 4.41; [4] 5.14; [3] 3.67; [2] 3.87; [1] 9.93, 7.59, 6.43, 2.90; [0.5] 3.12, 2.99, 2.74.

(c) *From Partially Active Menthanol*

Although the derivatives are unstable and especially sensitive toward water, the melting point of the levo complex was consistently higher than that of the inactive complex prepared identically. This property together with the small but real differences in diffraction patterns indicates that the two derivatives are crystallographically similar but not identical. The results of cocrystallization are in agreement. Thus when mixtures of levo and racemic menthanol were converted to the phosphoric acid derivatives the properties shown in Table II were observed, rotations in ethanol. Neither prolonged time of crystallization nor stirring during crystallization affected the specific activity.

TABLE II
PROPERTIES OF PARTIALLY ACTIVE MENTHANOL - PHOSPHORIC ACID DERIVATIVES

Menthanols		M.p.	Cryst.	% Original activity	% Recovery
Levo, g.	Racemic, g.				
0.51	2.01	70.6–72	Once	74	52
0.5	0.05	68–69	Twice	72	35
0.1	0.5	69–71	Twice	74	66

(d) *From Menthanol Formed by Reduction of Menthanone by Isopropyl Grignard Reagent in (+) Dimethoxybutane*

From 0.158 g. (1×10^{-3} mole) of the menthanol isolated in the present study was obtained, by the procedure described above, 0.97 g. (49%), m.p. 69–71°, $[\alpha]_D^{21} (-) 1.6 \pm 3^\circ$ (5% in ethanol). A mixture melting point with the derivative from racemic menthanol was not depressed. On the basis of activity losses described in procedure (c) the 6.3% resolution was confirmed.

Separation of the Menthanones

(a) *2-†-Isopropyl-4-†-methylcyclohexanone (Isomenthanone)*

The mixture of ketones separated by distillation from the borate esters, $[\alpha]_D^{21} (-) 0.61 \pm 0.02^\circ$, was dissolved in 21 ml. of hexane and was chromatographed on the Hagdahl column. The first eluate, 2.16 g., optically inactive, was entirely menthanone according to the chromatoplate. Subsequently the eluates gave 0.80 g., a mixture containing about 30% of isomenthanone and 70% of menthanone according to the chromatoplate. A third column chromatogram gave an 85% recovery comprising 0.065 g., entirely menthanone, then 0.30 g. containing a trace of isomenthanone, and finally 0.32 g., $[\alpha]_D^{21} (-) 3.78 \pm 0.09^\circ$ (neat), containing, according to the chromatoplate, an estimated 0.227 g. of isomenthanone. Since the menthanone found in the product was optically inactive, the isomenthanone (5% of the ketone treated with isopropyl Grignard reagent) comprising 70% of the 0.32 g. mixture was inferred to be of $[\alpha]_D^{21}$ about $(-) 5.4 \pm 0.02^\circ$. Since (+)

isomenthanone is reported to have a rotation of 85° (32) the Grignard reaction resulted in a 6% induction of optical activity in this product.

The isomenthanone in the mixture was characterized on the basis that the racemic compound formed by its semicarbazone is less soluble in alcohols than the enantiomeric semicarbazones or the diastereomeric menthanone semicarbazones (32, 26, 25). Following a reported procedure (15) 1.20 g. (7.8×10^{-4} mole) of the mixture, $[\alpha]_D^{21} (-) 3.78 \pm 0.09^\circ$, reported above was added to a solution of 0.15 g. of sodium acetate trihydrate and 0.103 g. (9.2×10^{-4} mole) of semicarbazide hydrochloride in 1.5 ml. of water; then ethanol was added to make the system homogeneous. After 1 day at 25° ammonia was added (pH 8) and then water. The mixed semicarbazones, 0.121 g. (74%), m.p. $152-187^\circ$, $[\alpha]_D^{19} (-) 3.7 \pm 1.7^\circ$ (1.2% in chloroform), were twice crystallized from a minimum of boiling methanol and once from hot 95% ethanol to give 0.0103 g., m.p. $208-210^\circ$, of optically inactive isomenthanone semicarbazone. A mixture melting point with an authentic sample, m.p. $211-212^\circ$, was not lowered.

(b) *2-Isopropyl-4- β -methylcyclohexanone (Menthanone)*

The chromatographic separations described above allow the recovery of menthanone from the Grignard reaction to be estimated reliably at 64% of that originally used. Two-thirds of this menthanone was chromatographically homogeneous. Pure menthanone was also separated by direct chromatography of the reaction product, before the borate esterification step. For purposes of positive identification, 1 g. was distilled, b.p. 85° (11 mm.), n_D^{20} 1.4503, d_4^{20} 0.894, $[\alpha]_D^{20} (+) 0.01 \pm 0.04^\circ$ (neat). The ultraviolet spectrum showed the absorption of racemic menthanone; E_{\max} at $289 \mu = 21.8$.

2-Phenyl-2-chlorobutane Grignard Reagent in Benzene and (+) 2,3-Dimethoxybutane

To 12 g. (0.5 mole) of purified magnesium (1) was added 10 ml. of a solution of 8.44 g. (0.05 mole, washed and dried by potassium carbonate and used at once) of 2-phenyl-2-chlorobutane, n_D^{20} 1.5215, d_4^{20} 1.025, b.p. 49° (0.01 mm.) (18), in 12.0 g. (0.10 mole) of (+) 2,3-dimethoxybutane and 10 ml. of pure benzene. When the vigorously-stirred system was heated the reaction was initiated with strong evolution of heat. The Gilman test was slow in developing but was positive. The remaining halide was added during 150 minutes. The basic magnesium content was 90% of theoretical after 40 minutes of subsequent stirring.

sec-Butylbenzene

The Grignard reagent described above was cooled to 44° and solvolyzed by the addition of 3.7 g. (0.05 mole) of *n*-butanol in 10 ml. of benzene during 100 minutes with constant stirring; a Gilman test was then negative. The system was poured into 100 ml. of cold 10% hydrochloric acid, the benzene layer separated, and the aqueous layer was washed with 50 ml. of benzene. The benzene solution after threefold washing with water and drying with sodium sulphate was distilled, finally at 8 mm. Fraction 1, 0.35 g. (5%), b.p. $47-49^\circ$, n_D^{20} 1.4907, d_4^{20} 0.867, $[\alpha]_D^{20}$ $0.00 \pm 0.06^\circ$ (neat); fraction 2, 3.40 g. (51%), b.p. $50-58^\circ$, n_D^{20} 1.4951, d_4^{20} 0.873, $[\alpha]_D^{27} (-) 0.06 \pm 0.02^\circ$ (neat). The flask retained a high-boiling residue, 1.02 g. (15%). Literature constants are n_D^{21} 1.4894 (14), n_D^{20} 1.4902 (29, p. 101), n_D^{19} 1.5044 (16), d_D^{20} 0.862 (29, p. 101) to 0.864 (13). Fraction 2 was chromatographed in 8 ml. of hexane through Alcan alumina (activated at 180°) in a 1.5×22.5 cm. column. In the first 50 ml. of hexane eluate 85% of the hydrocarbon was found and distilled, n_D^{20} 1.4931, d_4^{20} 0.866. These constants were unchanged by subsequent treatment of the substance with concentrated sulphuric acid. The hydrocarbon was fractionally distilled

and the heart-cut, 0.66 g., b.p. 178°, was collected, n_D^{20} 1.4937, d_4^{20} 0.863. The ultraviolet absorption maxima (0.658 g. per l.) in isooctane were. 264 m μ , 0.764; 258 m μ , 0.986; 252 m μ , 0.835; as compared with E_{\max} of 0.739, 0.982, 0.815 reported previously (2). This *sec*-butylbenzene was inactive, $[\alpha]_D^{20}$ (+)0.02 \pm .06° (neat).

REFERENCES

1. ALLENTOFF, N. and WRIGHT, G. F. J. Org. Chem. (In press, 1957).
2. AMERICAN PETROLEUM INSTITUTE. Ultraviolet spectral data. Research Project 44, No. 5 (1900).
3. BECKETT, C. W., FREEMAN, N. K., and PITZER, K. S. J. Am. Chem. Soc. **70**, 4227 (1948).
4. BECKMAN, E. Ann. **250**, 322 (1889).
5. BHARUCHA, K. R., COHEN, H. L., and WRIGHT, G. F. J. Org. Chem. **19**, 1097 (1954).
6. BLAGDEN, J. W. and HUGGETT, W. E. J. Chem. Soc. 317 (1934).
7. COHEN, H. L. and WRIGHT, G. F. J. Org. Chem. **18**, 432 (1953).
8. COOKE, R. G. and MACBETH, A. K. J. Chem. Soc. 1408 (1938).
9. DUNN, G. E. and WARKENTIN, J. Can. J. Chem. **34**, 75 (1956).
10. GASTAMBIDE, B. Bull. soc. chim. France (5), **22**, 866 (1955).
11. GRIGNARD, V. and BLANCHON, H. Bull. soc. chim. France (4), **49**, 23 (1931).
12. HAGDAHL, L. Science tools. L.K.B. Produkten Fabriksaktie-Bolag, Stockholm, **1**, 21 (1954).
13. HARRISON, P. W. B., KENYON, J., and SHEPHERD, J. R. J. Chem. Soc. 658 (1926).
14. HEILBRON, I. and BUNBURY, H. M. (Editors). Dictionary of organic compounds. Vol. I. Eyre and Spottiswood, London. 1953. p. 390.
15. HUGHESDON, R. S., SMITH, H. G., and READ, J. J. Chem. Soc. 2916 (1923).
16. KENYON, J., PHILLIPS, H., and PITTMAN, V. P. J. Chem. Soc. 1072 (1935).
17. KIRCHNER, J. G., MILLER, J. M., and KELLER, J. G. Anal. Chem. **23**, 420 (1951).
18. KLAGES, A. Ber. **35**, 3506 (1902).
19. KUMLER, W. D. and HUITRIC, A. C. J. Am. Chem. Soc. **78**, 3369 (1956).
20. LEVENE, P. A. and ROTHEN, A. J. Org. Chem. **1**, 76 (1936).
21. LUTZ, R. E. and KIBLER, C. J. J. Am. Chem. Soc. **62**, 360 (1940).
22. MILLER, J. M. and KIRCHNER, J. G. Anal. Chem. **25**, 1107 (1953).
23. MOSHER, H. S. and LA COMBE, E. J. Am. Chem. Soc. **72**, 3994 (1950).
24. ORGANIC ANALYSIS. Interscience Publishers, Inc., New York. 1953. p. 191.
25. PICKARD, R. H. and LITTLEBURY, W. O. J. Chem. Soc. 109 (1912).
26. READ, J. and COOK, A. M. R. J. Chem. Soc. 2782 (1925).
27. REITSEMA, R. H. Anal. Chem. **26**, 960 (1954).
28. RIGBY, F. L. and BETHUNE, J. L. Proc. Am. Soc. Brewing Chemists, 174 (1955).
29. RODD, E. H. (Editor). Chemistry of carbon compounds. Vo. IIB. Elsevier Publ. Co., Amsterdam. 1953.
30. SCHLENK, F. and SCHLENK, T. Ber. **62B**, 920 (1929).
31. VAVON, G., RIVIERE, C., and ANGELO, B. Compt. rend. **222**, 959 (1946).
32. ZEITSCHEL, O. and SCHMIDT, H. Ber. **59**, 2298 (1926).

THE INFRARED AND RAMAN SPECTRA OF TOLUENE, TOLUENE- α - d_3 , *m*-XYLENE, AND *m*-XYLENE- $\alpha\alpha'$ - d_6 ¹

J. K. WILMSHURST² AND H. J. BERNSTEIN

ABSTRACT

The infrared spectra of toluene, toluene- α - d_3 , *m*-xylene, and *m*-xylene- $\alpha\alpha'$ - d_6 have been obtained from 2 to 30 μ for the vapors and liquids. The Raman spectra of the liquids have also been obtained photoelectrically together with depolarization ratios. Vibrational assignments have been made for the four molecules consistent with vapor band contours, polarization data, the Teller Redlich ratio rule, and a modified ratio rule due to Fitzer and Scott.

The infrared and Raman spectra of toluene and *m*-xylene have been investigated by numerous workers (8) and vibrational assignments have been made by Pitzer and Scott (8). Recently Randle and Whiffen (10) have studied a number of methyl benzenes in the 10 μ region in an effort to determine the rocking frequencies associated with the methyl group and their assignments for these modes differ from those of Pitzer and Scott (8). The study of the far infrared spectrum of the methyl benzenes (9) also gave data conflicting with the assignments of Pitzer and Scott.

Toluene- α - d_3 and *m*-xylene- $\alpha\alpha'$ - d_6 have recently been prepared in these laboratories (11) and it appeared that a study of these two molecules should assist in determining the frequencies associated with the methyl group and may also aid in verifying the complete assignment of the two molecules. With this in mind, the infrared spectra of toluene, toluene- α - d_3 , *m*-xylene, and *m*-xylene- $\alpha\alpha'$ - d_6 have been obtained for both the liquid and the gaseous states, and the Raman spectra recorded for the four molecules in the liquid state. Complete assignments for the a_1 , b_1 , and b_2 modes and partial assignments for the a_2 modes have been made by analogy with Ingold's (6) assignment for benzene, assuming the Mair and Hornig (7) alternative for ν_{14} and ν_{15} . The present assignments are also consistent with vapor band contours, depolarization ratios, the Teller Redlich product rule, and a modified form of this rule suggested by Pitzer and Scott (8).

A complete assignment of the a_1 , b_1 , and b_2 frequencies in toluene-*p*- d has also been made.

EXPERIMENTAL

The infrared spectra were obtained with a Perkin Elmer model 12C double pass spectrometer equipped with LiF, CaF₂, NaCl, KBr, and CsBr optics. A 1 meter cell was used for the vapor spectra, the pressure being the vapor pressure of the liquid at 25° C. To observe some of the weaker bands in the vapor a small dish of liquid was placed inside the instrument housing in addition to the 1 meter cell. The Raman spectra were recorded photoelectrically on a White Raman spectrometer (15) and depolarization ratios measured by the method of Edsall and Wilson (4).

EXPERIMENTAL RESULTS

The infrared spectra of toluene and toluene- α - d_3 for the liquid and vapor are given in Figs. 1 and 2, and the infrared spectra of *m*-xylene and *m*-xylene- $\alpha\alpha'$ - d_6 for the liquid

¹Manuscript received April 12, 1957.

Contribution from the Division of Pure Chemistry, National Research Council, Ottawa, Canada.

Issued as N.R.C. No. 4406.

²National Research Council Postdoctorate Research Fellow, 1955-57.

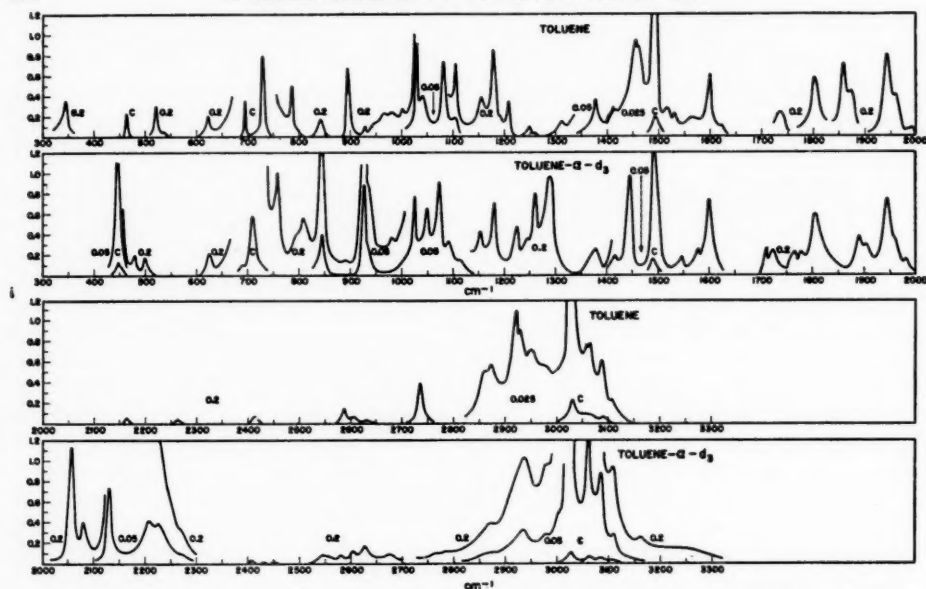


FIG. 1. The infrared spectra of toluene and toluene- α - d_3 in the liquid phase. Cell thickness in mm. as indicated. c = capillary film.

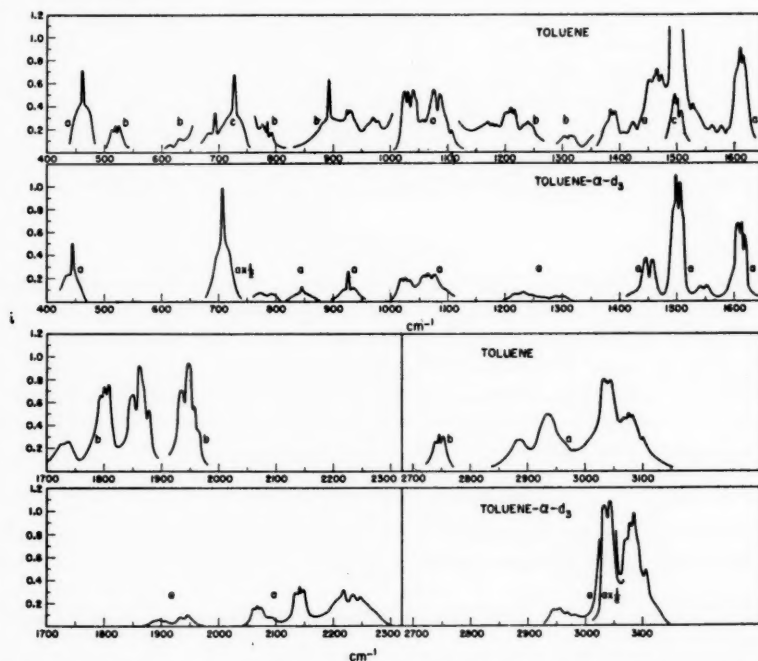


FIG. 2. The infrared spectra of toluene and toluene- α - d_3 in the vapor phase. The pressure of the vapor is the vapor pressure of the liquid at 20°C . a = 1 meter cell, b = 1 meter cell + dish, c = 10 cm. cell.

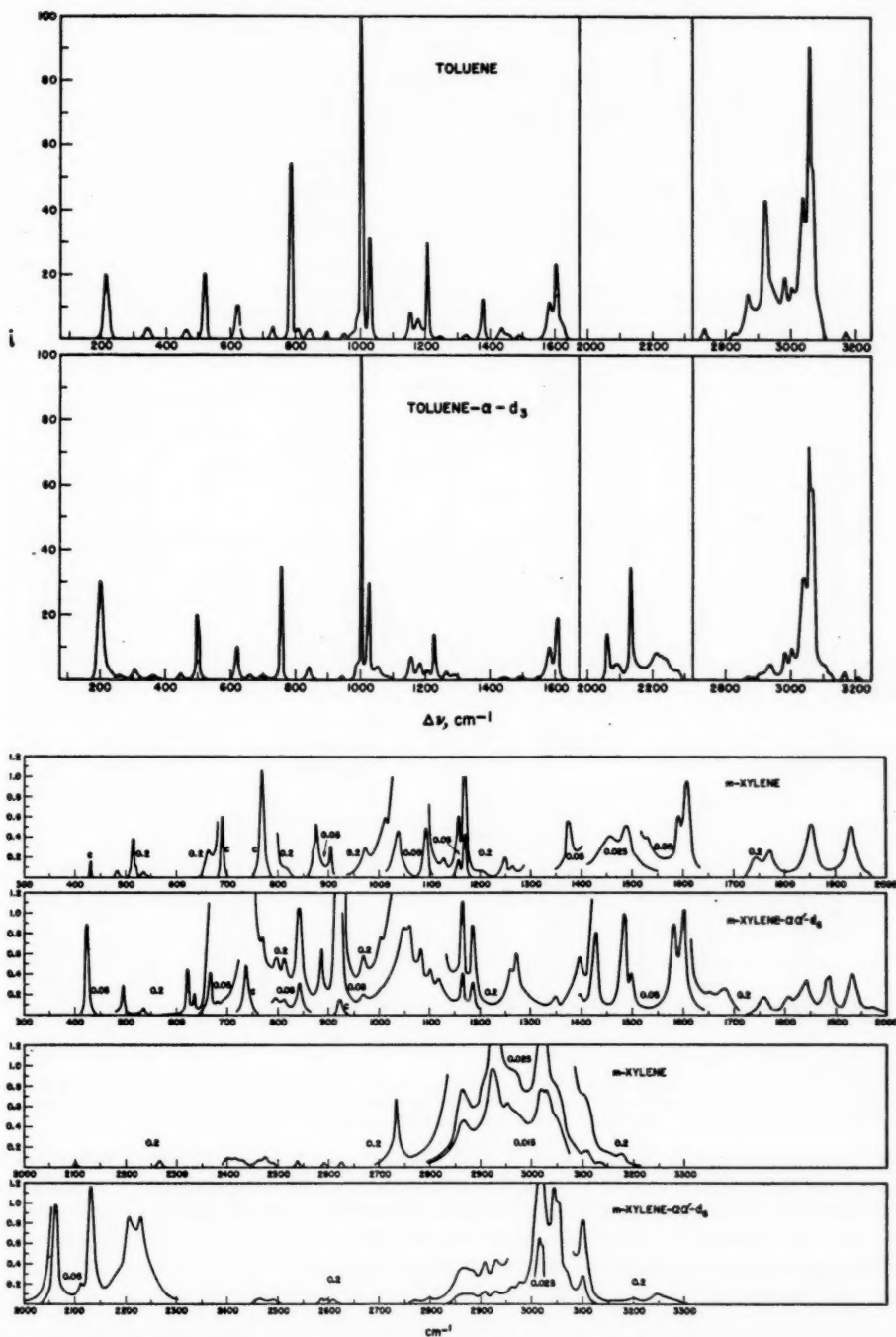


FIG. 3. (Top) The Raman spectra of toluene and toluene- α - d_3 in the liquid phase.

FIG. 4. (Bottom) The infrared spectra of *m*-xylene and *m*-xylene- $\alpha\alpha'$ - d_2 in the liquid phase. Cell thickness in mm. as indicated. c = capillary film.

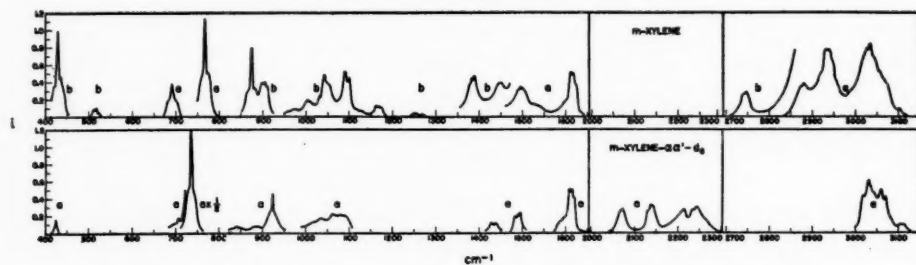


FIG. 5. The infrared spectra of *m*-xylene and *m*-xylene- $\alpha\alpha'$ - d_6 in the liquid phase. The pressure of the vapor is the vapor pressure of the liquid at 20°C. *a* = 1 meter cell, *b* = 1 meter cell + dish.

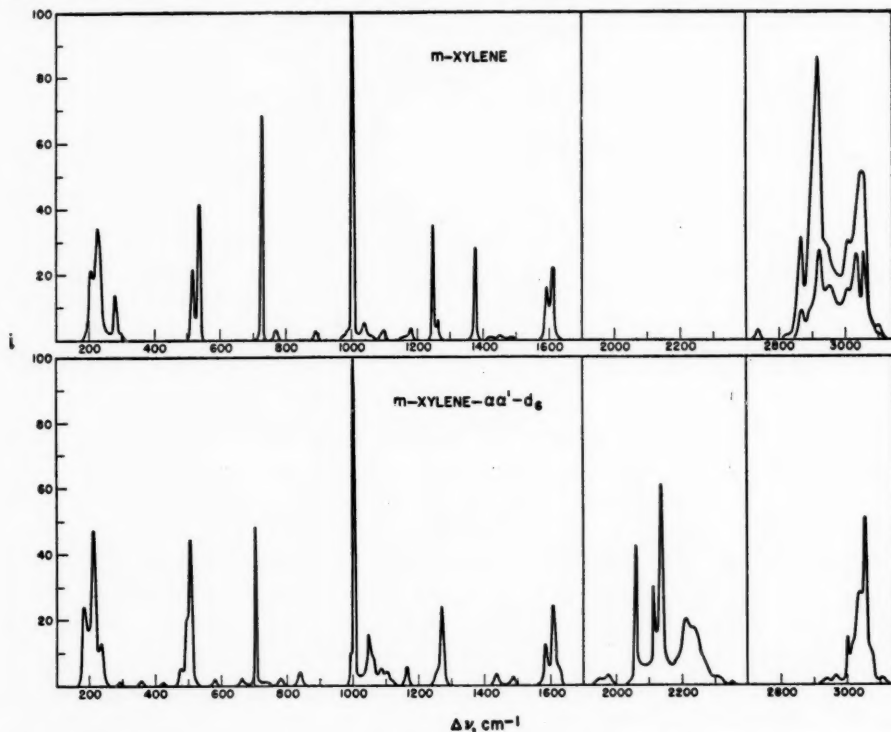


FIG. 6. The Raman spectra of *m*-xylene and *m*-xylene- $\alpha\alpha'$ - d_6 in the liquid phase. In *m*-xylene, the polarized bands around 3000 cm^{-1} overlap some of the weaker depolarized bands. The depolarized component is also shown in the figure in the 2800–3100 cm^{-1} region.

and vapor are given in Figs. 4 and 5. The Raman spectra of toluene and toluene- α - d_3 and of *m*-xylene and *m*-xylene- $\alpha\alpha'$ - d_6 are shown in Figs. 3 and 6 respectively. The observed spectra and assignments for toluene, toluene- α - d_3 , and toluene-*p*- d are given in Tables I, II, and III respectively and the fundamentals are given in Table VI. The observed spectra and assignments for *m*-xylene and *m*-xylene- $\alpha\alpha'$ - d_6 are given in Tables IV and V and the fundamentals are given in Table VII.

TABLE I
 VIBRATIONAL ASSIGNMENT FOR TOLUENE

Infrared				Infrared			
Liquid	Vapor	Raman	Assignment	Liquid	Vapor	Raman	Assignment
345 m		216 (2) dp	b_1 Fundamental	1455 vs	1452 } $B?$	1457	dp b_1 Fundamental
464 vs	450 } 462 } (C)	344 (0) p?	b_1 Fundamental	1460 vs	1465 } B	—	b_1 Fundamental
	470 }	465 (0) dp	b_2 Fundamental	1492 vs	1497 } A	1491	dp a_1 Fundamental
521 m	519 } (A)	521 (2) p	a_1 Fundamental		1501 }		
537 w	525 }	—	1004 - 465 = 539 (B_2)	1516 m	1521 } C?		729 + 785 = 1514 (B_2)
623 m	614 } (B)	623 (1) dp	b_1 Fundamental		1527 }		
	631 }			1530 m	1533 }		695 + 842 = 1537 (B_1)
695 vs	683 } C		b_2 Fundamental	1565 m	1561 }		729 + 842 = 1571 (B_1)
	694 }				1572 }		695 + 895 = 1590 (A_1)
729 vs	714 } C	730 (0) dp	b_2 Fundamental		1588 }		
	728 }			1590 s	1611 } A	1585	dp a_1 Fundamental
	736 }				1616 }	1604	dp b_1 Fundamental
785 m	776 } A	786 (6) p	a_1 Fundamental		1619 }		
7967 vw	791 }	809 (0) p	344 + 464 = 808 (B_1)	1622 m		1622	dp 729 + 895 = 1624 (A_1)
842 m		843 (0) dp	a_2 Fundamental	1735 m	1727 } B		842 + 965 = 1737 (B_1)
895 m-s	880 } C	896 (0) dp	b_2 Fundamental		1737 }		
	893 }			1802 ms	1794 }		785 + 1030 = 1815 (A_1)
	903 }			1858 ms	1800 } A		
929 w	918 } A?		2 × 464 = 928 (A_1)		1807 }		
	924 }				1851 }		785 + 1081 = 1866 (B_1)
946 w	929 }	950 (0)	729 + 216 = 945 (A_1)	1873 m	1878 } C?		695 + 1178 = 1873 (B_2)
966 m	961 } C?		b_2 Fundamental	1942 ms	1936 }		785 + 1155 = 1940 (B_1)
	969 }				1947 }		521 + 1455 = 1976 (B_1)
981 m	977 }	981 (0) p?	464 + 521 = 985 (B_2)	1950 m	1957 } B?		785 + 1209 = 1994 (A_1)
		994 (0)	a_2 Fundamental		1965 }		2 × 1004 = 2008 (A_1)
1002 m		1004 (10) p	a_1 Fundamental	1983 w			2 × 1081 = 2162 (A_1)
1029 s	1024 } A	1030 (3) p	a_1 Fundamental	1992 w			1105 + 1178 = 2283 (B_1)
	1031 }			2164 w			2 × 1209 = 2418 (A_1)
1041 ms	1041 } ?	—	b_2 Fundamental	2263 w			1004 + 1585 = 2589 (A_1)
	1056 }			2413 w			1004 + 1604 = 2608 (B_1)
1081s	1076 } B	—	b_1 Fundamental	2587 w			1178 + 1455 = 2633 (B_1)
	1086 }			2607 w			
1105 ms	1094 } B?	1155 (1) dp	b_1 Fundamental	2632 w			
	1107 }				2741 }		
1155 m	1160 }	1178 (0) dp	a_1 Fundamental	2736 m	2747 } A	2736	p 2 × 1377 = 2754 (A_1)
1178 ms	1177 } A				2753 }		
	1184 }			2862 s		2827	dp 1460 + 1377 = 2837 (B_1)
1209 m	1202 } A	1208 (3) p	a_1 Fundamental		2879 }		1377 + 1492 = 2869 (A_1)
	1210 }			2873 s	2886 } A	2870 (1) p	2 × 1436 = 2872 (A_1)
1249 w	1240 } A	1244 (0)	785 + 464 = 1249 (B_1)		2897 }	2920 (4) p	a_1 Fundamental
	1245 }			2923 vs	2928 }		b_2 Fundamental
1260 w	1305 } B	—	1804 - 345 = 1280 (A_1)	2930 vs	2936 }		
	1313 }		464 + 842 = 1306 (B_1)		2946 }		
1311 w	1320 } A		521 + 785 = 1306 (A_1)	2952 s	2957 } B?	2955	dp b_1 Fundamental
		1329	344 + 994 = 1338 (B_2)		2965 }		
1377 ms	1378 } A	1379 (1) p	a_1 Fundamental	2981 s	3006 } A	2983 (2) dp	2 × 1492 = 2984 (A_1)
	1391 }				3012 }	3003 (1) p	a_1 Fundamental
1415 w	1407 }		695 + 729 = 1424 (A_1)	3032 vs	3034 } B	3039 (4) dp	b_1 Fundamental
	1423 } C?	1436	dp b_2 Fundamental		3045 }	3056 (9) p	a_1 Fundamental
	1435 }			3061 s			1604 + 1457 = 3061 (A_1)
				3067 s	3068 } A	~3067	p a_1 Fundamental
					3078 }		
				3090 s	3083 }	~3086	sh. p b_1 Fundamental
				3110 ms	3102 ?	—	1604 + 1492 = 3096 (B_1)
						3170	p 2 × 1585 = 3170 (A_1)

Toluene and Toluene- α - d_3

Neglecting interaction terms in the potential function between the methyl group and the aromatic ring, the secular equation for toluene can be factorized as if the molecule possessed C_{2v} symmetry when the vibrations divide into symmetry species as $\{13a_1 + 13b_1\}$ (planar) and $\{4a_2 + 9b_2\}$ (nonplanar). All modes are Raman active, while only the a_1 , b_1 , and b_2 modes are infrared active.

TABLE II
 VIBRATIONAL ASSIGNMENT FOR TOLUENE- α - d_3

Infrared				Infrared			
Liquid	Vapor	Raman	Assignment	Liquid	Vapor	Raman	Assignment
		201 (3) dp	b_2 Fundamental	1578 m			500 + 1092 = 1592 (B_1)
		233 (0)	992 - 758 = 234 (A_2)	—	~1599 } A	1583 (1) dp	a_1 Fundamental
		258 (0)	709 - 446 = 263		1607 } B	1607 (2) dp	b_1 Fundamental
		307 (0) dp	b_1 Fundamental	1599 s	1614		
		362 (0) pf	a_1 Fundamental	1711 m	1619		1003 + 709 = 1712 (B_2)
446 vs	436 } C	448 (0)	b_2 Fundamental	1723 m			1025 + 709 = 1734 (B_2)
	444 }			1766 m			625 + 1154 = 1779 (A_1)
	~455 }			1778 m			758 + 1025 = 1783 (A_1)
480 m		498 (2) p	a_1 Fundamental	1805 ms			362 + 1445 = 1807 (B_2)
500 m		621 (1) dp	b_1 Fundamental		1886 }		
625 m		699 (0)	b_1 Fundamental	1890 m	1897 }		709 + 1181 = 1890 (B_2)
691 ms	~697 }				1907 }		
709 vs	707 } C		b_2 Fundamental	1904 m			758 + 1154 = 1912 (B_1)
	718 }			1944 ms	1934 } B		500 + 1445 = 1945 (B_1)
758 ms		758 (4) p	a_1 Fundamental	~1960 m	1947 }		362 + 1607 = 1969 (B_2)
797 m			307 + 498 = 805 (B_1)	1981 m			1225 + 758 = 1983 (A_1)
809 m			362 + 448 = 810 (B_1)		3062 }		
	~836 }	842 (0) dp	a_1 Fundamental	2058 ms	2066 }	2059 (1) p	2 \times 1027 = 2054 (A_1)
845 s	845 } C		b_2 Fundamental		2074 }		
	~856 }		2 \times 446 = 892 (A_1)	2081 m	2088 }	2089 (0) p	2 \times 1051 = 2102 (A_1)
891 w	919 }				2093 }		
	927 }		b_2 Fundamental	2131 s	2135 }	2131 (3) p	a_1 Fundamental
927 s	927 } C				2141 }		
	935 }				2147 }		
~934 m			b_1 Fundamental	2208 ms	~2210 }	2210 (1) p	b_2 Fundamental
981 w		946 (0) dp	448 + 498 = 946 (B_2)		2218 }		
			b_2 Fundamental	2227 ms	2235 }	2235 (1) dp	b_1 Fundamental
		992 pf	a_1 Fundamental	~2275 m	~2299 }	2274 (0) p	1092 + 1181 = 2273 (B_1)
1003 w	1020 }	1003 (10) p	a_1 Fundamental				1181 + 1225 = 2406 (A_1)
1025 s	1020 } A	1027 (3) p	a_1 Fundamental	2407 w			845 + 1583 = 2428 (B_2)
	1034 }				2431 w		992 + 1445 = 2437 (B_2)
1080 s	~1048 }	1081 (0) pf	$a_1 + b_2$ Fundamental	2452 w			2 \times 1225 = 2450 (A_1)
	1054 } A			2547 w			1050 + 1491 = 2541 (A_1)
	1059 }			2582 w			1003 + 1583 = 2586 (A_1)
1073 s	1086 }	1076 (0) dp?	b_1 Fundamental	2605 w			1003 + 1607 = 2610 (B_1)
1092 ms	~1094 }		b_1 Fundamental	2628 w			1181 + 1445 = 2626 (B_1)
1113 m			500 + 625 = 1125 (B_1)	2677 w			1073 + 1607 = 2680 (A_1)
1154 m		1153 (0) pf?	b_1 Fundamental	~2765 w			1181 + 1583 = 2764 (A_1)
1181 ms		1181 (0) pf?	a_1 Fundamental	2785 w			1181 + 1607 = 2788 (B_1)
~1203 w		1205 (0) pf?	362 + 842 = 1204 (A_1)	2870 m		2869	2 \times 1445 = 2890 (A_1)
1225 m	1219 }	1225 (1) p	a_1 Fundamental	2938 ms	2945 }	2937 (0) dp?	1445 + 1491 = 2936 (B_1)
1245 w	1233 }		2 \times 625 = 1250 (A_1)		2955 }	2983 (1) pf?	2 \times 1491 = 2982 (A_1)
1260 ms	~1245 }	1281 (0) p	500 + 788 = 1283 (A_1)	~2979 ms	2970 }	3003 (1) p	a_1 Fundamental
	1259 }			~3005 ms	2982 }		
1289 ms	~1270 }		446 + 842 = 1288 (B_1)	3028 vs	3034 }	3039 (3) dp	b_1 Fundamental
	1291 }				3044 }	3056 (7) p	a_1 Fundamental
~1293 ? m	1301 }				3072 }		
1379 m			2 \times 691 = 1382 (A_1)	3064 vs	3079 }	3064 (6) p	a_1 Fundamental
1416 m	~1425 }		2 \times 709 = 1418 (A_1)		3085 }		
1445 s	1447 } B	1442	b_1 Fundamental	3086 s	3093 }	3098	b_1 Fundamental
	1458 }				3106 }		
1491 s	~1495 }	1495	a_1 Fundamental?	3110 ms	~3130 }	3117	1607 + 1495 = 3102 (B_1)
	1499 }			3163 m		3166 (0) p	2 \times 1583 = 3166 (A_1)
	1506 }					3211 (0) p	2 \times 1607 = 3214 (A_1)
	~1511 }						
1547 m	1541 }		709 + 845 = 1554 (A_1)				
	1552 }						

The a_1 Species

The strong polarized bands in the Raman spectrum of liquid toluene at ~3067, 3056, 3003, 2920, 1379, 1208, 1030, 1004, 786, and 521 cm^{-1} and in toluene- α - d_3 at 3064, 3056, 3003, 2131, 1225, 1027, 1003, 758, and 498 cm^{-1} can be assigned as a_1 fundamentals with reasonable certainty. The infrared bands of gaseous toluene at 3076, 3008, 1501, 1385, 1210, 1177, 1031, 785, and 519 cm^{-1} and of gaseous toluene- α - d_3 at 3079, 2141, 1054, and 1026 cm^{-1} having three maxima corresponding to P , Q , and R branches with PR separation* of about 14 cm^{-1} are also a_1 fundamentals.

*The PR separation was calculated from the formula of Badger and Zumwalt (2). The moments of inertia of toluene were calculated assuming $r_{\text{CH}} = 1.09$, $r_{\text{CCH}_3} = 1.51$, $r_{\text{CC}} = 1.40$ and gave

$$I_A = 154 \times 10^{-40} \text{ g.cm}^2, \quad I_B = 306 \times 10^{-40} \text{ g.cm}^2, \quad I_C = 460 \times 10^{-40} \text{ g.cm}^2$$

TABLE III
 VIBRATIONAL ASSIGNMENT FOR TOLUENE-*p-d*

Infrared, liquid	Raman	Assignment	Infrared, liquid	Raman	Assignment
	208 (1)	b_1 Fundamental	1310 w		$453 + 863 = 1316 (A_1)$
	338 (4)	b_1 Fundamental	1351 wm		$517 + 836 = 1353 (B_1)$
	453 (4)	b_2 Fundamental	1380 s	1379 (1)	a_1 Fundamental
	517 (3)	a_1 Fundamental	1420 w		b_2 Fundamental
	616 (2)	b_1 Fundamental	1454 (s)		b_1 Fundamental
693 (s)		b_2 Fundamental	1470 (4)		b_1 Fundamental
710 (s)		b_2 Fundamental	1497 (s)		a_1 Fundamental
726 (s)		$208 + 517 = 725 (B_2)$	1510 w		$710 + 803 = 1513 (A_1)$
785 (m)	784 (5)	a_1 Fundamental	1601 (2)		a_1 Fundamental
803 (m)		b_1 Fundamental	1608 (s)		b_1 Fundamental
836 (s)		b_1 Fundamental	1675 wm		$693 + 987 = 1680 (B_2)$
863 m		b_2 Fundamental	1735 w		$710 + 1029 = 1739 (B_2)$
893 w		$208 + 693 = 901 (A_1)$	1789 wm		$803 + 987 = 1790 (B_2)$
917 w		$208 + 710 = 918 (A_1)$	1845 w		$863 + 987 = 1850 (B_2)$
944 w		$338 + 616 = 954 (A_1)$	1894 mw		$693 + 1206 = 1899 (B_2)$
983 w	987 (10)	a_1 Fundamental	2230 m		$785 + 1454 = 2239 (B_1)$
1013		$208 + 803 = 1011 (A_1)$	2252 wm		$1080 + 1179 = 2259 (B_1)$
1029 (s)	1028 (1)	a_1 Fundamental		2266 (1)	a_1 Fundamental
1040 (s)		b_2 Fundamental		2288 (4)	$836 + 1454 = 2290 (A_1)$
1076 sh		b_1 Fundamental	2580 vw		$1080 + 1497 = 2577 (B_1)$
1090 (s)		b_1 Fundamental	2717 w		$1111 + 1608 = 2719 (A_1)$
1111 (s)		b_1 Fundamental	2833 s		$2 \times 1420 = 2840 (A_1)$
1121 m		$338 + 785 = 1123 (B_1)$	2898 s		$2 \times 1454 = 2908 (A_1)$
1126 m		$517 + 616 = 1133 (B_1)$		2922 (2)	a_1 Fundamental
1151 m		b_1 Fundamental	2959 s		$b_1 + b_2$ Fundamental
1179 m	1178 (1)	a_1 Fundamental	2994 s		$2 \times 1497 = 2994 (A_1)$
1206 w	1209 (2)	a_1 Fundamental		3054 (6)	$a_1 + b_1$ Fundamental

In all the aromatics, two bands occur in the Raman spectrum at 1600 cm^{-1} . In benzene (6) these two bands arise because of Fermi resonance of $\nu_1 + \nu_8$ with the fundamental ν_8 , but in the aromatics with less than a threefold symmetry axis they are taken as the two components of the doubly degenerate mode ν_8 in benzene (1, 3, 6). Thus in toluene and toluene- $\alpha-d_3$ the two bands are taken as the a_1 and b_1 components of ν_8 in benzene, but since the a_1 component should be strongly depolarized (14) they cannot be distinguished on the basis of the depolarization data. In the infrared spectrum of the liquids only one strong band is observed, while in the vapor, the band contours show an overlapping of two bands. The 1585 cm^{-1} Raman band is taken as the a_1 component. This completes the a_1 assignment in toluene, and the remaining assignment in toluene- $\alpha-d_3$ is chosen by analogy with toluene. Thus ν_{9a} and ν_{19a} in toluene- $\alpha-d_3$ are taken at 1181 and 1491 cm^{-1} respectively, in agreement with ν_{9a} and ν_{19a} at 1178 and 1492 cm^{-1} in toluene. The 1491 cm^{-1} band in toluene- $\alpha-d_3$, although we assign it to an a_1 mode, appears to be a B type band but this may be due to overlapping with an overtone or interference due to water vapor.

The b_1 Species

The infrared bands at 2960, 1613, 1469, 1155, 1105, 1081, and 621 cm^{-1} in toluene vapor and at 3098, 3038, 2241, 1453, and 1072 cm^{-1} in toluene- $\alpha-d_3$ vapor are type B bands with no central maxima and are assigned as b_1 fundamentals. ν_3 , ν_{6b} , and ν_{8b} should not be affected by deuterium substitution and are chosen at 1092, 621, and 1607 cm^{-1} in toluene- $\alpha-d_3$ consistent with the corresponding bands in toluene. ν_{7b} and ν_{20b} again should not be affected by deuterium substitution and are chosen in toluene at 3039 and 3090 cm^{-1} to be consistent with the assignments in toluene- $\alpha-d_3$. ν_{14} , which has dropped from 1310 cm^{-1} in benzene to 1155 cm^{-1} in toluene, drops further on deuterium substitution to 1092 cm^{-1} in toluene- $\alpha-d_3$ coincident with ν_3 .

The methyl bending frequency ν_{9b} is assigned to the infrared band and weak Raman band at 344 cm^{-1} in toluene and the Raman band at 307 cm^{-1} in toluene- $\alpha-d_3$, while ν_{18} is assigned as 1155 and 1154 cm^{-1} in toluene and toluene- $\alpha-d_3$ respectively.

TABLE IV
 VIBRATIONAL ASSIGNMENT FOR *m*-XYLENE

Infrared			Raman	Assignment	Infrared			Raman	Assignment
Liquid	Vapor				Liquid	Vapor			
			206 (2) dp	a_1 Fundamental	1458 s	~1450 broad		1424 (0)	$a_1 + b_1$ Fundamental
278 w			227 (3) dp	b_2 Fundamental		1490		1452 (0)	$a_1 + a_2 + b_2$ Fundamental
			280 (1) dp	a_2 Fundamental	1489 s	1496 } A		1496 (0)	b_1 Fundamental
404 w			299 (0) p†	b_1 Fundamental		1498			
	~420				~1510 m	1508			431 + 1094 = 1525 (B_2)
	428			b_2 Fundamental		1525 m			2 × 769 = 1538 (A_1)
431 vs	(435)			206 + 227 = 433 (B_2)		1532			
	~440				1593 s	~1595		1593 (1) dp	a_1 Fundamental
484 w				691 - 206 = 485 (B_2)		1613			
	511				1610 s	1618		1613 (2) dp	b_1 Fundamental
515 m	517 } A		518 (2) dp	b_1 Fundamental		1624			
	524				1745 m				870 + 876 = 1746 (A_1)
520 w				727 - 206 = 521 (A_1)	1772 m				538 + 1248 = 1786 (A_1)
536 w			538 (4) p	a_1 Fundamental	1854 m				769 + 1094 = 1863 (B_2)
663 m				280 + 404 = 684 (B_2)	1932 m				691 + 1248 = 1939 (B_2)
					~1966 w				727 + 1248 = 1975 (A_1)
691 vs	~683			b_2 Fundamental	2101 w				518 + 1593 = 2111 (B_1)
	692				2267 w				1094 + 1158 = 2252 (B_1)
	~702		727 (7) p	a_1 Fundamental	2400 w				1161 + 1248 = 2409 (B_1)
					2416 w				1170 + 1248 = 2418 (B_1)
769 vs	~755		771 (0) dp	b_2 Fundamental	2431 w				2 × 769 + 905 = 2443 (B_1)
	767 } C				2463 w				1003 + 1458 = 2461 (A_1)
	774				2475 w				1003 + 1489 = 2492 (B_1)
~816 w				2 × 404 = 808 (A_1)	2492 w				905 + 1593 = 2498 (B_1)
~870 m				b_2 Fundamental	2538 w				1094 + 1458 = 2552 (A_1)
	~863				2592 w				1003 + 1593 = 2596 (A_1)
876 m	874 } C			b_2 Fundamental	2626 w				1158 + 1489 = 2647 (A_1)
	883		892 (0) dp	a_2 Fundamental		2740			
					2733 m	2748 } A + B†	2734 (0) p	2 × 1375 = 2750 (A_1, B_1)	
905 m	898 } A			b_1 Fundamental		2752			
	910						~2829 (0) p†	1375 + 1458 = 2833 (B_2)	
	960				2864 s	2875 } A†	2867 (3) p	2 × 1452 = 2904 (A_1)	
973 w	967 } A†	~978 (0) dp	280 + 691 = 971 (B_1)		~2904 m	2882	~2895	dp† 1424 + 1486 = 2910 (A_1, B_1)	
	973		~999 (0) p	227 + 771 = 998 (A_1)					
			1003 (10) p	a_1 Fundamental	2923 s	2921 } B	2923 (0) p	$a_1 + a_2 + b_1 + b_2$ Fundamental	
1013 w	1005 } A			2 × 515 = 1030 (A_1)		2933			
	1011					2939			
	1016				2953 m	2948 } B	~2955 (3) dp	$a_1 + b_1$ Fundamental	
1039	1031		1039 (0) p	$a_2 + b_2$ Fundamental		2955			
	1042				~2970 m	2960 } B		2 × 1489 = 2978 (A_1)	
	~1052		~1061 (0)	2 × 538 = 1076 (A_1)		~2994	3007 (3) p†	a_1 Fundamental	
1094 s	1090 } B	1097 (0) p†	$a_1 + b_1$ Fundamental			3118 } B†		1458 + 1593 = 3051 (A_1)	
	1099				3020 s	3028			
1128 w	1116 } B			431 + 691 = 1122 (A_1)	3030 s	3035	3034	dp	b_1 Fundamental
1158 m	1128					3044			
	1163	~1161 (0) dp†	b_1 Fundamental		~3052 m	3057 } A	3056 (5) p	a_1 Fundamental	
1170 s	1169 } A	1173 (0) dp	b_1 Fundamental			~3073			
~1200 w	1175						3067	p†	a_1 Fundamental
1250 w		1248 (4) p	a_1 Fundamental		~3082 m		3079	1489 + 1610 = 3099 (A_1)	
1265 w	1255 } B†	1263 (1) p	538 + 727 = 1265 (A_1)		3108	3102 } B†	~3101	206 + 2923 = 3129 (A_1)	
	1267				3133 m	3115		227 + 2923 = 3150 (B_2)	
1375 s	1378 } A + B	1377 (3) p†	$a_1 + b_1$ Fundamental		3176 w			2 × 1593 = 3186 (A_1)	
	1388								

The internal methyl bending frequency at 1455 cm^{-1} in toluene is considered to drop to 1073 in toluene- α - d_3 coincident with ν_{18b} , while the b_1 rocking mode in toluene is placed coincident with ν_{18b} at 1081 cm^{-1} and drops to 934 cm^{-1} in toluene- α - d_3 .

The b_2 Species

The type b_2 vibrations should give rise to C type bands with a very strong Q branch and these were observed at 2936, 895, 729, 695, and 464 cm^{-1} in toluene and at 2218, 927, 845, 707, and 446 cm^{-1} in toluene- α - d_3 . The band at 691 cm^{-1} in toluene- α - d_3 is assigned as ν_4 consistent with the corresponding band at 695 cm^{-1} in toluene while ν_6 and ν_{17b} are chosen at 966 and 216 cm^{-1} in toluene and at 981 and 201 cm^{-1} in toluene- α - d_3 respectively.

The internal methyl bending frequency in toluene is placed at 1436 cm^{-1} and in

TABLE V
 VIBRATIONAL ASSIGNMENT FOR *m*-XYLENE- $\alpha\alpha'$ - d_2

Infrared				Infrared			
Liquid	Vapor	Raman	Assignment	Liquid	Vapor	Raman	Assignment
		186 (2) dp	a_1 Fundamental	1583 s	1587 } B	1587 (1) dp	a_1 Fundamental
		213 (5) dp	b_2 Fundamental		1596 }		
		236 (1) dp	a_1 Fundamental	1603 s	1610 }	1611 (3) dp	b_1 Fundamental
		294 (0)	b_1 Fundamental		1616 }		
		350 (0)	a_2 Fundamental		1620 }	1625	$213 + 1429 = 1642 (B_2)$
424 s	~ 418 } C	426	b_2 Fundamental	1651 w			$812 + 842 = 1654 (A_1)$
	~ 424 }	479 p	$667 - 186 = 481 (B_2)$	1682 m			$2 \times 842 = 1684 (A_1)$
495 m	~ 430 }	495 (2) dp	b_1 Fundamental	1759 w			$507 + 1271 = 1778 (A_1)$
526 w		507 (5) p	a_1 Fundamental	1809 w			$737 + 1032 = 1819 (B_2)$
		582	$236 + 294 = 530 (B_2)$	1843 m			$236 + 1611 = 1847 (B_2)$
622 m			$2 \times 294 = 588 (A_1)$	~ 1891 m			$704 + 1185 = 1890 (B_1)$
635 w			$213 + 424 = 637 (A_1)$	1887 m			$812 + 1082 = 1894 (B_2)$
667 s		662	b_2 Fundamental	1933 m		1951	$667 + 1271 = 1938 (B_2)$
682 m			$186 + 507 = 693 (A_1)$	1971 w		1977	$704 + 1271 = 1975 (A_2)$
~ 696 w	706 ?	704 (5) p	a_1 Fundamental		~ 2067 }		
	~ 728 }			2062 s	2073 } A	2063 (4) p	$2 \times 1049 = 2098 (A_1)$
737 vs	~ 738 } C	738	b_2 Fundamental		~ 2077 }	2114 (3) p	$2 \times 1064 = 2128 (A_1)$
	~ 744 }			2113 m			
770 m			$350 + 424 = 783 (B_1)$	2132 s	2133 }	2138 (6) p	$a_1 + b_1$ Fundamental
797 m		781	$294 + 495 = 789 (A_1)$		2138 }		
812 m			$294 + 507 = 801 (B_1)$	~ 2186 m	2143 }	2181	dpf $2 \times 1102 = 2204 (A_1)$
			b_2 Fundamental	2207 s	~ 2200 }	2210 (2) dp	$a_2 + b_2$ Fundamental
		840	a_1 Fundamental		2215 }		
			b_2 Fundamental	2230 s	2234 }	2236 (2) dp	$a_1 + b_1$ Fundamental
842 s	~ 833 } C		b_2 Fundamental		2244 }	2236	pf $1082 + 1165 = 2248 (B_1)$
	~ 841 }					2236	$2 \times 1165 = 2330 (A_1)$
	~ 850 }			2464 w		2310	$1155 + 1183 = 2331 (A_1)$
886 m	~ 881 } A		b_1 Fundamental	2491 w		2351	$1185 + 1271 = 2457 (B_1)$
	~ 891 }			2587 w			$1082 + 1429 = 2511 (A_1)$
922 vs	~ 917 } C		$a_2 + b_2$ Fundamental	2596 w			$1033 + 1583 = 2586 (A_1)$
	~ 923 }			2609 w			$1118 + 1485 = 2603 (A_1)$
969 m	~ 930 }			2771 w			$1185 + 1429 = 2615 (B_1)$
		994 (1) p	$a_1 + b_1$ Fundamental	2800 w			$1186 + 1603 = 2789 (A_1)$
1003 w	~ 1017 }	1003 (10) p	$2 \times 495 = 990 (A_1)$	2887 m			$1272 + 1603 = 2875 (B_1)$
1048 s	1036	1049 (2) p	$a_1 + b_1$ Fundamental	2880 m			$667 + 2230 = 2897 (A_1, A_2)$
1060 s	1062 } B	1064	dp $a_1 + b_1$ Fundamental	2909 m			$1429 + 1485 = 2914 (B_1)$
	1069 }			2931 m		2937	
1082 s	1078 } B	1098	dp a_1 Fundamental	2963 m		2965	$2 \times 1485 = 2970 (A_1)$
	1087 }			2978 m			$842 + 2132 = 2974 (B_2)$
1102 m		1104	pf $a_2 + b_2$ Fundamental			3002 (2) p	a_1 Fundamental
1118 m		1119	b_1 Fundamental	3016	3020	3018 (1) pf	$1436 + 1587 = 3023 (A_1)$
1166 s		1165	dp b_1 Fundamental	3025 s	3031 }		$1429 + 1603 = 3032 (B_1)$
1186 s			b_1 Fundamental	3045 s	3037 }	3040 (3) dp	b_1 Fundamental
1261 m		1254	$424 + 842 = 1266 (A_1)$	~ 3054 s	3043 }		
1272 m		1271 (3) p	a_1 Fundamental			3057 (5) p	a_1 Fundamental
~ 12907 w			$213 + 1082 = 1295 (B_2)$	~ 3068 m	3061 } B	3075 (1)	a_1 Fundamental
1340 w			$186 + 1105 = 1352 (B_1)$		3071 }		
1397 m			$667 + 737 = 1404 (A_1)$	3101 s	3106 }	3106	$1003 + 2138 = 3141 (A_1)$
1429 s	1430 } B	1436	pf a_1 Fundamental		3114 }		$969 + 2230 = 3199 (A_1)$
	1439 }			3109 w			$1048 + 2207 = 3255 (B_2, A_2)$
	1485 }			3247 w			
1435 s	1490 } A	1487	b_1 Fundamental				
	1495 }						
1498 m			$424 + 1082 = 1506 (B_2)$				

toluene- α - d_3 at 1051 cm^{-1} , while the methyl rocking frequency in toluene- α - d_3 is assigned to the type C band at 927 cm^{-1} , the corresponding mode in toluene being taken as 1041 cm^{-1} .

The a_2 Species

The a_2 vibrations are active only in the Raman effect and, by analogy with benzene, bands are chosen at 994 and 843 cm^{-1} in toluene, and 992, 842, and 362 cm^{-1} in toluene- α - d_3 . The remaining band in toluene was calculated by application of Pitzer's product rule (8) to benzene to be at 407 cm^{-1} .

Toluene- p - d

The assignment for toluene- p - d was made using the published Raman (12) and infrared (13) data. Strong Raman lines were assumed to belong to the a_1 species and the assignments were made by analogy with toluene.

TABLE VI
FUNDAMENTAL FREQUENCIES IN TOLUENE, TOLUENE- α - d_3 , AND TOLUENE- p - d

Frequency	Benzene	Toluene	Toluene- α - d_3	Toluene- p - d	Frequency	Benzene	Toluene	Toluene- α - d_3	Toluene- p - d
a_1					b_1 (continued)				
ν_1	992	786	758	784	ν_{1b}	1150	(1155)	1154	1111
ν_2	3062	3056	3056	3054	ν_{1bb}	1033	1081	1073	1080
ν_{6a}	606	521	498	517	ν_{1bl}	1480	1455	1445	1454
ν_{7a}	3047	1208	1225	1209	ν_{20b}	~3080	3090	3086	(3054)
ν_{8a}	~1595	1585	1583	1601	ν_{CH_2}	—	2952	2227	2959
ν_{9a}	1178	1178	1181	1179	$\delta'CH_3$	—	1460	(1073)	1470
ν_{12}	~1010	1004	1003	987	ν_{CH_3}	—	(1081)	934	~1076
ν_{13}	~3062	3003	3003	2266					
ν_{13a}	1033	1030	1027	1028	b_2				
ν_{19a}	1480	1492	1491	1497	ν_4	~705	695	691	693
ν_{20a}	~3080	3067	3064	(3054)	ν_5	985	966	981	803
ν_{CH_2}	—	2920	2131	2922	ν_{10b}	849	895	845	863
δCH_3	—	1377	1050	1380	ν_{11}	671	729	709	710
b_1					ν_{16b}	405	464	446	453
ν_8	~1326	1105	1092	836	ν_{17b}	~970	216	201	208
ν_{8b}	606	623	621	616	ν_{CH_2}	—	2930	2208	2959
ν_{7b}	3047	3039	3039	(3054)	$\delta'CH_3$	—	1436	(1051)	1420
ν_{8b}	~1595	1604	1607	1608	ν_{CH_3}	—	1041	927	1040
ν_{9b}	1178	344	307	338	a_2				
ν_{14}	1310	1155	(1092)	1151	ν_{10a}	849	843	842	—
					ν_{16a}	405	407*	362	—
					ν_{17a}	~970	994	992	—

() Frequency used twice. * Calculated from Pitzer's rule (8).

TABLE VII
FUNDAMENTAL FREQUENCIES FOR *m*-XYLENE AND *m*-XYLENE- $\alpha\alpha'$ - d_4

Frequency	Benzene	<i>m</i> -Xylene	<i>m</i> -Xylene- $\alpha\alpha'$ - d_4	Frequency	Benzene	<i>m</i> -Xylene	<i>m</i> -Xylene- $\alpha\alpha'$ - d_4
a_1				b_1 (continued)			
ν_1	992	727	704	ν_{20b}	3080	3030	3040
ν_2	3062	3056	3057	ν_{CH_3}	—	(2923)	(2138)
ν_{6a}	606	538	507	ν_{CH_3}	—	(2953)	(2230)
ν_{7a}	3047	3007	3002	δCH_3	—	(1375)	(1048)
ν_{8a}	~1595	1593	1583	$\delta'CH_3$	—	(1424)	(1060)
ν_{9a}	1178	206	186	ν_{CH_3}	—	(1094)	(969)
ν_{12}	~1010	1003	1003				
ν_{13}	~3062	1248	1271	b_2			
ν_{13a}	1033	1094	1082	ν_4	~705	691	667
ν_{19a}	1480	1458	1429	ν_5	985	876	842
ν_{20a}	~3080	3067	3068	ν_{10b}	849	227	213
$\nu_{CH_3}(s)$	—	2923	2138	ν_{11}	671	769	737
$\nu_{CH_3}(a)$	—	2953	2230	ν_{16b}	405	428	424
$\delta CH_3(s)$	—	1375	1048	ν_{17b}	~970	870	812
$\delta'CH_3(a)$	—	1424	1060	ν_{CH_2}	—	2923	2207
ν_{CH_3}	—	(1094)	969	$\delta'CH_3$	—	(1458)	1102
b_1				ν_{CH_3}	—	1039	922
ν_2	~1326	1158	1118	ν_{CH_3}	—	—	—
ν_{6b}	606	518	495	a_2			
ν_{7b}	3047	1170	1186	ν_{10a}	849	280	236
ν_{8b}	~1595	1610	1603	ν_{16a}	405	404	359
ν_{9b}	1178	404	294	ν_{17a}	~970	892	840
ν_{14}	1310	1200	1186	ν_{CH_2}	—	(2923)	(2207)
ν_{15}	1150	1158	1166	δCH_3	—	(1458)	(1102)
ν_{18b}	1033	905	886	ν_{CH_3}	—	(1039)	(922)
ν_{19b}	1480	1489	1485	ν_{CH_3}	—	—	—

() Frequency used twice.

m-Xylene and *m*-Xylene- $\alpha\alpha'$ - d_6

Both these molecules belong to point group C_{2v} , and the vibrations can be divided into symmetry species as $\{16a_1+15b_1\}$ (planar) and $\{7a_2+10b_2\}$ (nonplanar). The separation between the two methyl groups is sufficiently large that it would be unlikely that any interaction should occur between the internal modes of the two groups. Thus of the internal methyl modes the $5a_1$ frequencies should be identical with the corresponding $5b_1$ frequencies and the $3a_2$ frequencies should be identical with the corresponding $3b_2$ frequencies.

The a_1 Species

The strong polarized Raman bands at 3067, 3056, 3007, 2923, 1377, 1248, 1003, 727, and 538 cm^{-1} in *m*-xylene and at 3057, 3002, 2138, 1271, 1049, 1003, 704, and 507 cm^{-1} in *m*-xylene- $\alpha\alpha'$ - d_6 can be assigned with reasonable certainty to a_1 type vibrations. The infrared bands at 1593 and 1094 cm^{-1} in *m*-xylene and at 3067, 1583, 1429, 1082, and 1060 cm^{-1} in *m*-xylene- $\alpha\alpha'$ - d_6 have B type contours and are also taken as a_1 fundamentals.

Since the a_1 and b_1 methyl internal vibrations would be coincident, the band contours may be of a 'hybrid' type between A and B and such bands are observed at 1375 cm^{-1} in *m*-xylene and at 2138 cm^{-1} in *m*-xylene- $\alpha\alpha'$ - d_6 .

The unresolved band at 1458 cm^{-1} in *m*-xylene is taken as ν_{19a} , the counterpart of the type B band at 1429 cm^{-1} in the deuterated molecule, while the band at 206 cm^{-1} in *m*-xylene is assigned to ν_{9a} , the corresponding band in *m*-xylene- $\alpha\alpha'$ - d_6 being taken as 186 cm^{-1} .

The internal methyl frequencies can be assigned by analogy with toluene. Thus besides the bands at 2923 and 1375 cm^{-1} , which are certainly polarized and are analogous to the bands in toluene at 2920 and 1377 cm^{-1} , the bands at 2953 and 1094 cm^{-1} (coincident with ν_{18a}) analogous to bands at 2952 and 1081 cm^{-1} in toluene are chosen. The remaining unsymmetrical CH_3 bending mode should occur around 1400 cm^{-1} but is probably overlapped in the infrared spectrum by the strong 1450 cm^{-1} band. It is associated with the Raman line at 1424 cm^{-1} .

The b_1 Species

The bands at 3030, 1610, 1489, 1170, 905, and 515 cm^{-1} in *m*-xylene and at 1603, 1485, and 886 cm^{-1} in *m*-xylene- $\alpha\alpha'$ - d_6 have A type contours and can be assigned as type b_1 vibrations. The bands at 3040, 1186, and 495 cm^{-1} in *m*-xylene- $\alpha\alpha'$ - d_6 corresponding to the b_1 modes in *m*-xylene at 3030, 1170, and 515 cm^{-1} are also taken as b_1 modes. The bands at 1200 and 1158 cm^{-1} in *m*-xylene (1186 and 1166 cm^{-1} in *m*-xylene- $\alpha\alpha'$ - d_6) are taken as ν_{14} and ν_{15} respectively, while ν_{9b} , the methyl bending mode, is assigned to the band at 404 cm^{-1} in *m*-xylene, falling to 294 cm^{-1} in *m*-xylene- $\alpha\alpha'$ - d_6 . ν_3 is taken as 1158 in *m*-xylene, coincident with ν_{15} , falling to 1118 in *m*-xylene- $\alpha\alpha'$ - d_6 .

This completes the assignment of the aromatic ring, and the internal methyl vibrations are taken as coincident with the corresponding a_1 frequencies.

The b_2 Species

The bands at 876, 769, 691, and 428 cm^{-1} in *m*-xylene and at 2207, 922, 842, 737, and 424 cm^{-1} in *m*-xylene- $\alpha\alpha'$ - d_6 having a C type contour with a very strong Q branch are taken as b_2 fundamentals. The band at 1039 cm^{-1} in *m*-xylene tends to have some b_2 type structure and is also taken as a b_2 fundamental. The remaining b_2 fundamentals in *m*-xylene are taken as 870 and 227 cm^{-1} (812 and 213 cm^{-1} in *m*-xylene- $\alpha\alpha'$ - d_6) for

the aromatic ring and at 2923 and $\sim 1458 \text{ cm}^{-1}$ for the methyl group. The internal methyl bending vibration in *m*-xylene- $\alpha\alpha'$ - d_6 is placed at 1102 cm^{-1} .

The a_2 Species

The internal methyl vibrations should have the same frequencies as the b_2 modes and are assigned accordingly.

The aromatic vibrations in *m*-xylene are assigned, by analogy with benzene, to the Raman bands at 892 and 280 cm^{-1} and to the infrared band at 404 cm^{-1} coincident with ν_{9b} . In *m*-xylene- $\alpha\alpha'$ - d_6 the Raman bands at 840, 359, and 236 cm^{-1} are taken as their counterparts.

DISCUSSION

The assignments of the aromatic vibrations in toluene and *m*-xylene can be partly checked by the application of a modified product rule (8) as first suggested by Pitzer and Scott (PS).

This rule defines the product ratio τ as

$$\tau = \frac{\prod_i \nu_{si} \prod_j I_{uj}^{\frac{1}{2}} \prod_r M_{ur}^{\frac{1}{2}}}{\prod_i \nu_{ui} \prod_j I_{sj}^{\frac{1}{2}} \prod_r M_{sr}^{\frac{1}{2}}}$$

where s indicates the substituted compound and u the unsubstituted compound. I is a moment of inertia and M a mass.

The methyl group is considered as an 'isotope' of hydrogen of mass 15 and for each methyl-ring stretching motion the square root of the mass ratio is $(1/15)^{\frac{1}{2}} = 0.258$, while for a bending motion one considers the moments of inertia of the attached group with respect to the point of attachment on the ring, obtaining $(1.2/41)^{\frac{1}{2}} = 0.171$.

Applying this rule, the assignments of the ring vibrations in toluene and *m*-xylene were compared with those in benzene. The calculated and observed ratios are given in Table VIII.

TABLE VIII
THE PRODUCT RATIOS FOR THE RING VIBRATIONS

Species	Benzene-toluene		Benzene- <i>m</i> -xylene	
	Calc.	Obs.	Calc.	Obs.
a_1	0.258	0.243	0.044	0.044
a_2	1.00	(1.00)*	0.171	0.170
b_1	0.171	0.169	0.044	0.045
b_2	0.171	0.169	0.171	0.176

* Used to calculate ν_{18a} .

A check on the assignments of the methyl vibrations and the internal consistency of the aromatic frequencies between the isotopic molecules is obtained by an application of the Teller Redlich product rule, which applies rigorously in this case. Calculated and observed product ratios for toluene and toluene- α - d_3 , toluene and toluene- p - d , and *m*-xylene and *m*-xylene- $\alpha\alpha'$ - d_6 are given in Table IX.

The present investigation indicates that the internal methyl vibrational frequencies in the methyl benzenes can be taken as shown in Table X, the asymmetrical C—H stretching and CH_3 bending modes being a little doubtful owing to overlapping by other vibrations especially in the undeuterated methyl compounds, but the symmetrical CH_3

TABLE IX
 TELLER REDLICH PRODUCT RATIOS FOR THE DEUTERATED MOLECULES

Species	Toluene-toluene- α - d_3		Toluene-toluene- p - d		m -Xylene- m -xylene- $\alpha\alpha'$ - d_6	
	Calc.	Obs.	Calc.	Obs.	Calc.	Obs.
a_1	0.508	0.519	0.711	0.742	0.182	0.232
a_2	0.895*	0.887	1.00	—	0.352*	0.357
b_1	0.375	0.414	0.721	0.735	0.185	0.227
b_2	0.380	0.407	0.727	0.730	0.369*	0.391

*Torsional mode factorized out.

 TABLE X
 INTERNAL METHYL VIBRATIONAL FREQUENCIES

	Present investigation		Pitzer and Scott		Randle and Whiffen
	Toluene	m -Xylene	Toluene	m -Xylene	Toluene
$\nu_{CH_3}(s)$	2920	2923	2950	2950	—
$\nu_{CH_3}(a)$	2952	2953	2950	2950	—
$\nu_{CH_3}(a)$	2930	~2923	2950	2950	—
$\delta_{CH_3}(a)$	1460	~1458	1495	1470	—
$\delta_{CH_3}(a)$	1436	1424	1455	1448	—
$\delta_{CH_3}(s)$	1377	1375	1380	1375	—
τ_{CH_3}	~1081	~1094	1190	1090	1041
τ_{CH_3}	1041	1039	1060	1031	1041

stretching and deformation vibrations being definitely established. It is fairly certain that one component of the CH_3 rocking mode is at $\sim 1040\text{ cm}^{-1}$ in the undeuterated methyl derivatives, a conclusion also reached by PS and Randle and Whiffen (10), but whereas the latter authors assumed that the degeneracy of this mode was not removed by the aromatic ring, we prefer to assume that the other component is at around 1080 cm^{-1} to be consistent with the assignment in the deuterated molecules. This is the same conclusion arrived at by PS for m -xylene but in the case of toluene PS considered the other component to be at 1190 cm^{-1} , not consistent with the present data on the deuterated molecule.

The present assignment for toluene agrees with that of PS for the a_1 and a_2 vibrations, but whereas we only observed two of the a_2 modes and calculated the remaining mode ν_{16a} to be at 407 cm^{-1} , PS report a Raman line at 405 cm^{-1} . Apart from the difference due to using the Mair and Hornig alternative for ν_{14} in the present assignment, two other differences from the PS assignment occur. ν_{19b} assigned by PS to 1310 cm^{-1} is assigned here to the very strong infrared band at 1485 cm^{-1} which they had assigned as a methyl bending mode. However, the presence of this strong band in toluene- α - d_3 at the same position identifies it with a ring mode and the assignment here is consistent with corresponding assignments in other aromatics. ν_3 is lowered from 1282 cm^{-1} in the PS assignment to 1105 cm^{-1} here. The assignment of the b_2 modes agrees with that of PS with the exceptions of the internal methyl rocking mode, which is assigned here at 1041 cm^{-1} consistent with Randle and Whiffen (10) as compared to the PS assignment at 1190 cm^{-1} .

In m -xylene ν_{19a} assigned by PS at 1320 cm^{-1} is assigned here to the strong infrared band at 1458 cm^{-1} consistent with corresponding assignments in other aromatics. Other a_1 modes assigned by PS at 1167 and 224 cm^{-1} are assigned here at 1094 and 206 cm^{-1} .

consistent with band contours and the product rule. In the b_1 species, apart from the Mair and Hornig alternative for ν_{14} used here, the present assignment differs from that of PS mainly with respect to the low frequency mode ν_{9b} assigned by PS to a Raman band at 310 cm^{-1} . In the infrared, two bands are observed in this region at 280 and 404 cm^{-1} and since ν_{9b} is infrared active it should be assigned to one of these frequencies. If the former band at 280 cm^{-1} is chosen, then to obtain agreement with the PS product rule, it is necessary to raise all the higher frequencies around $\sim 900\text{--}1200\text{ cm}^{-1}$ up to around 1200 cm^{-1} , which is inconsistent with band contour data and corresponding assignments in toluene and other aromatics. However, a choice of the band at 404 cm^{-1} for ν_{9b} gives a much more "realistic" assignment for the frequencies in the $900\text{--}1200\text{ cm}^{-1}$ region consistent with the PS product rule. This high frequency for ν_{9b} as compared to its a_1 counterpart at 206 cm^{-1} indicates appreciable coupling of the methyl bending modes with the ring vibrations. In the b_2 modes PS assigns ν_{16b} as 485 cm^{-1} , but the band contours observed here definitely establish this at 428 cm^{-1} . The agreement with the product rule is then improved by increasing ν_{10b} from 200 cm^{-1} in the PS assignment to 227 cm^{-1} here. The a_2 assignment of PS for the ring modes of 830 , 439 , and 276 cm^{-1} is modified here to 892 , 404 , and 280 cm^{-1} . The assignments of PS for the internal methyl vibrations in *m*-xylene are essentially the same as those obtained in the present investigations.

The C—CH₃ stretching frequency in toluene might be expected to occur around 1050 cm^{-1} , somewhat higher than that in ethane, while the aromatic ring breathing mode may be expected at around 980 cm^{-1} . However, the two bands are actually observed at 1208 and 786 cm^{-1} indicating that the two modes of vibration are interacting to a considerable extent. This same phenomena of an 'anomalously' high C—CH₃ frequency and 'anomalously' low ring frequency is observed in all the methyl benzenes and is greatest in hexamethyl benzene (5) where $\nu_{\text{CCH}_3} = 1385\text{ cm}^{-1}$ and $\nu_{\text{ring}} = 553\text{ cm}^{-1}$. It is of interest to see if a simple normal coordinate calculation on hexamethyl benzene will explain these frequencies and give reasonable values for the force constants.

Assuming a potential energy function for the a_{1g} modes of hexamethyl benzene as

$$\text{I} \quad 2V = 6k_1 Q_{\text{CCH}_3}^2 + 6k_2 Q_{\text{CC}}^2 + 12d Q_{\text{CCH}_3} Q_{\text{CC}},$$

we obtain on expanding the secular equation

$$\begin{aligned} \text{II} \quad \lambda_1 + \lambda_2 &= k_1 \left(\frac{1}{M_{\text{C}}} + \frac{1}{M_{\text{CH}_3}} \right) + \frac{k_2 - 2d}{M_{\text{C}}}, \\ \lambda_1 \lambda_2 &= (k_1 k_2 - d^2) \frac{1}{M_{\text{C}} M_{\text{CH}_3}}. \end{aligned}$$

Assuming firstly that $d = 0$, solution of II for k_1 and k_2 gave only imaginary roots, but assuming that $k_1 = 5 \times 10^5$ dynes cm^{-1} , then solution of II gave $d = 0.31 \times 10^5$ dynes cm^{-1} and $k_2 = 7.35 \times 10^5$ dynes cm^{-1} . The nice agreement between k_2 observed here and that of 7.62 calculated from benzene (14) shows that relatively small coupling between the C—CH₃ and ring breathing modes which have nearly the same 'group' frequencies (i.e. around 1050 and 980 cm^{-1} respectively) accounts for the observed large 'splitting' at 1385 and 553 cm^{-1} respectively.

The present assignments for toluene and *m*-xylene do not affect the statistical thermodynamic functions as calculated by PS appreciably, the calculated entropy at 298.16° K . assuming free rotation of the methyl groups being in toluene: $76.80\text{ cal. deg}^{-1}\text{ mole}^{-1}$ (PS = $76.73\text{ cal. deg}^{-1}\text{ mole}^{-1}$) and in *m*-xylene: $85.77\text{ cal. deg}^{-1}\text{ mole}^{-1}$ (PS = 85.88

cal. deg.⁻¹ mole⁻¹), agreeing within the experimental error with the experimental values (8) for toluene: 76.44 ± 0.3 cal. deg.⁻¹ mole.⁻¹ and *m*-xylene: 85.60 ± 0.3 cal. deg.⁻¹ mole.⁻¹.

REFERENCES

1. ANDERSON, F. A., BÄK, B., BRODERSEN, S., and RASTRUP-ANDERSEN, J. *J. Chem. Phys.* **23**, 1047 (1955).
2. BADGER, R. M. and ZUMWALT, L. R. *J. Chem. Phys.* **6**, 711 (1938).
3. CORRISIN, L., FAX, B. J., and LORD, R. C. *J. Chem. Phys.* **21**, 1170 (1953).
4. EDSALL, J. T. and WILSON, E. B., Jr. *J. Chem. Phys.* **6**, 124 (1938).
5. HASTINGS, S. H. and NICHOLSON, D. E. To be published.
6. HERZFELD, N., INGOLD, C. K., and POOLE, H. G. *J. Chem. Soc.* 316 (1946).
7. MAIR, R. D. and HORNIG, D. F. *J. Chem. Phys.* **17**, 1236 (1949).
8. PITZER, K. S. and SCOTT, D. W. *J. Am. Chem. Soc.* **65**, 803 (1943). (This gives a summary of work up to 1943.)
9. PLYLER, E. K. *Discussions Faraday Soc.* **9**, 100 (1950).
10. RANDLE, R. R. and WHIFFEN, D. H. *J. Chem. Soc.* 3497 (1955).
11. RENAUD, R. and LEITCH, L. C. *Can. J. Chem.* **34**, 98 (1956).
12. SMITH, C. H., CHOPPIN, A. R., and NANCE, O. A. *J. Am. Chem. Soc.* **72**, 3260 (1950).
13. TURKEVICH, J., MCKENZIE, H. A., FRIEDMAN, L., and SPURR, R. *J. Am. Chem. Soc.* **71**, 4045 (1949).
14. WHIFFEN, D. H. *Proc. Roy. Soc. (London), A*, **248**, 131 (1955).
15. WHITE, J. U., ALPERT, N., and DEBELL, A. G. *J. Opt. Soc. Amer.* **45**, 154 (1955).

THE INFRARED SPECTRA OF HUMIC ACIDS AND RELATED MATERIALS¹

R. M. ELOFSON

ABSTRACT

The infrared spectra of a number of humic acids and related materials obtained by the potassium bromide pressed pellet technique are summarized. Acidic properties of humic acids are largely due to clearly defined carboxylic acid frequencies at $3.9\ \mu$ and 5.8 to $5.85\ \mu$. These bands are shifted in the expected manner by preparation of the sodium salts. Autoclaving of humic acids from lignite and from hydroquinone removes the carboxylic acid bands and produces material having bands in the long wave-length region that are at the same position as bands shown by bituminous coal and autoclaved cellulose. The potassium bromide technique has also revealed in the infrared spectra of low rank material a band at $6.65\ \mu$ which decreases markedly with increase in rank and may be related to the degree of condensation of aromatic nuclei.

INTRODUCTION

The term "humic acids" is applied to the brown or black amorphous solids obtained when alkali extracts of low rank coal, soil, or peat are acidified. The alkali-soluble, acid-insoluble materials obtained when coal is oxidized by a variety of oxidizing agents are also called humic acids or regenerated humic acids. Similar products—which may be termed synthetic humic acids—are obtained by the oxidative polymerization of hydroquinone and other phenols.

Breger (5) noted some similarity between Brauns native spruce lignin and humic acids extracted from peat. Cannon and Sutherland (9) reported that the infrared spectra of humic acids derived from coal differ from those of the parent coal and resemble those of graphitic and mellitic acids. Friedel and Pelipetz (12) and Friedel and Queiser (13) have compared the chars obtained from cellulose and sucrose with bituminous coal. In the most complete study of the spectra of the humic acids, Hadži (15) and Čeh and Hadži (11) have examined a number of humic acids obtained from coal, hydroquinone, and glucose in nujol mulls. Gordon *et al.* (14), van Krevelen *et al.* (18), and Bergmann and co-workers (4) have studied the spectra of a large number of coals by the KBr pressed pellet technique.

The present paper is an attempt to show the relationships existing between various humic acid preparations as revealed by infrared spectroscopy. In order to show the relationship of these substances to lignin and coal, spectra have also been prepared of coal, lignin, and charred cellulose. To gain as much knowledge as possible of the spectral range from 2 to $15\ \mu$, the KBr pressed pellet technique of Schiedt (17) was utilized. This technique has made it possible to observe a number of new features in the spectra of humic acids and coal.

EXPERIMENTAL

All spectra were obtained with a Perkin Elmer Model 21 recording infrared spectrophotometer.

Potassium bromide pellets were prepared by grinding the sample either in a hand mullite mortar or in a mechanical mullite mortar, and finally mixing thoroughly with powdered spectral grade potassium bromide obtained from the Harshaw Chemical

¹Manuscript received November 9, 1956.

Contribution from the Research Council of Alberta, Edmonton, Alberta.

Company. The mixture was then pressed into a pellet in an evacuable die supplied by the Perkin Elmer Corporation, at a pressure of 40,000 lb./sq. in.

By this technique, with varying concentrations of a humic acid preparation, it was found possible to obtain satisfactory semiquantitative results with short grinding times. In order to avoid oxidation, samples of coals and the harder chars were not submitted to prolonged periods of grinding. This results in a considerable amount of absorption due to scattering in addition to the development of inherent background absorption in these harder materials.

Fig. 1 shows a spectrum obtained from humic acids which had been prepared by oxidizing hydroquinone.

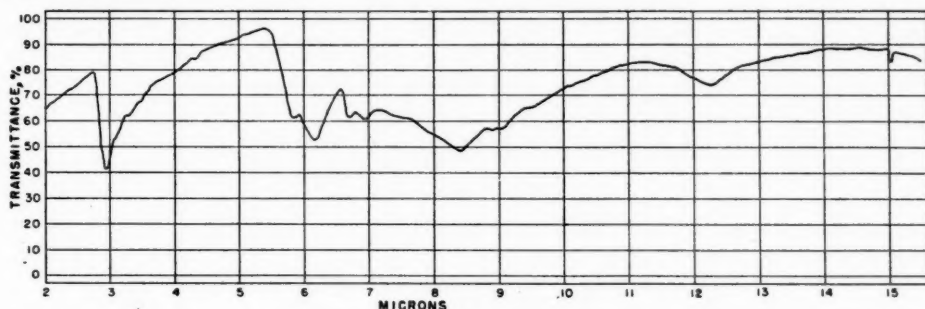


FIG. 1. Infrared spectrum of humic acids from hydroquinone; conc. 0.2% in KBr pellet 0.8 mm. thick.

Fig. 2 summarizes the spectra obtained from 12 materials. This was done by calculating the density by the base line technique. Inevitably some arbitrary decisions had to be made where bands appeared close enough to each other to interfere seriously, but in such cases consistent methods were employed throughout the series.

Table I contains a summary of the source and elemental analysis of the materials used in the investigation.

TABLE I
HUMIC ACID PREPARATIONS

Material	Source	Analysis, dry ash-free basis	
		Carbon, %	Hydrogen, %
Hydroquinone humic acids	Oxidation with $\text{Na}_2\text{S}_2\text{O}_8$	63.41	3.33
Peat humic acids	Extraction according to Arnold, Lowry, and Thiessen (2)	54.20	4.33
Nitro humic acids	Oxidation of Taylorton lignite with 30% HNO_3	56.97	3.48
Lignite humic acids	Extraction of weathered lignite with alkali	64.49	4.03
Klason lignin		59.70	4.48
Humic acid char	Hydroquinone humic acids heated to 320° C. for 48 hours	81.9	3.54
Humic acid char	Lignite humic acids heated to 320° C. for 48 hours in presence of water vapor	82.8	4.74
Cellulose char 195° C.	Cellulose heated to 195° C. for 2 hours	64.77	4.94
Cellulose char 420° C.	Cellulose heated to 420° C. for 2 hours	84.11	3.95
Lignite	Vitrain Taylorton, Sask.	71.8	5.14
Bituminous coal	Vitrain Bruceton, Pa.	83.0	5.1
Subbituminous coal	Vitrain Edmonton, Alta.	76.9	5.00

DISCUSSION

An examination of the spectra of humic acids, chars, and coals illustrates that these substances bear a resemblance to one another. However, important differences do exist. These features are best brought out by comparing some individual bands appearing in Fig. 2.

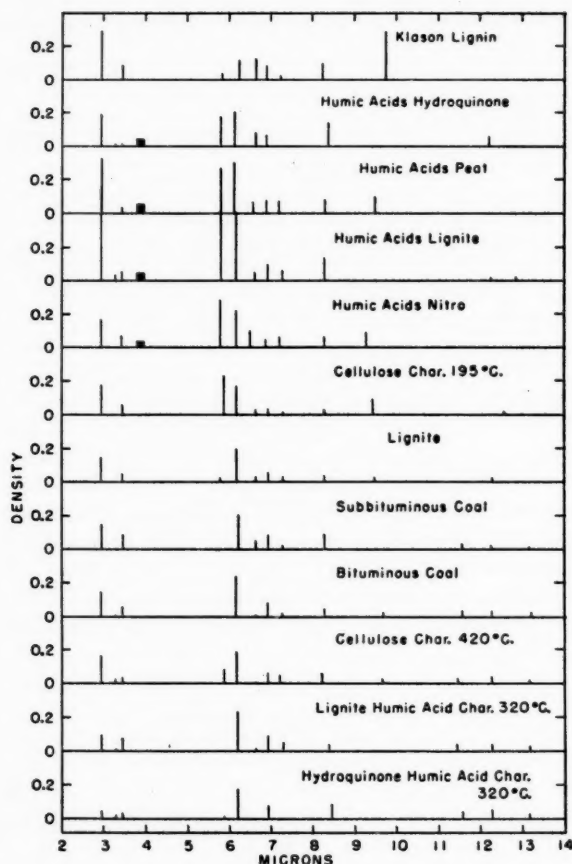


FIG. 2. Summary of spectra of humic acids and related materials; conc. 0.2% in KBr pellets 0.8 mm. thick.

The 6.2 μ Band

All the materials studied in this investigation have an intense band at approximately 6.2 μ which does not vary greatly in intensity, with the exception of Klason lignin in which it is apparently about half as intense as in the other materials. The peak appears to occur at rather low wave-lengths in humic acid spectra: peat humic acids, 6.13 μ ; hydroquinone humic acids, 6.15 μ ; nitro humic acids, 6.18 μ ; and lignite humic acids, 6.17 μ . For the coals the band occurs close to 6.20 μ as noted by many workers (4, 5, 6, 8, 12, 16, 18). Significantly, in high temperature cellulose char it is higher—6.21 μ —

than in low temperature cellulose char in which it occurs at $6.19\ \mu$. In lignin the peak appears at $6.25\ \mu$.

It is not the purpose of this paper to comment on the possible structures producing this band. The band does appear in carbonized material from all sources and, therefore, seems to be due primarily to carbon-carbon unsaturation, although as suggested by Brown (6) and by Friedel and Queiser (13) oxygen-containing structures may be important, particularly in humic acids which have the band at lower wave-lengths.

The Carboxylic Acid Bands

The humic acid preparations all have marked absorption at 5.80 to $5.85\ \mu$ which must undoubtedly be a carbonyl absorption. The cellulose chars show absorption in this region although at slightly longer wave-lengths, and do not dissolve in alkali. The humic acid preparations have a distinct but very broad absorption band in the region of $3.9\ \mu$ which can be safely associated with the strongly associated OH bands of the CO_2H group. In the cellulose chars this band could not be detected, which agrees with the lack of alkali solubility of these materials. The occurrence of the carbonyl stretching band at wave-lengths as low as $5.8\ \mu$ seems surprising since ordinary aromatic acids in the solid state absorb at about $5.9\ \mu$. α - β -Unsaturated acids absorb at somewhat shorter wave-lengths, and perhaps this indicates that the humic acids are attached to nuclei which have a greater degree of bond fixation than is found in ordinary benzene carboxylic acids (3).

In agreement with the findings of Čeh and Hadži (11), confirmation of the presence of CO_2H groups has been obtained by examining the spectra of the sodium salts. Spectra of the sodium salts of both lignite humic acids and hydroquinone humic acids showed the replacement of the bands at $5.8\ \mu$ with strong bands at 6.30 to $6.35\ \mu$ together with evidence of increased absorption in the region of $7.30\ \mu$, and Bellamy (3) regards these observations as evidence for the ionized carboxyl group. In his first paper Hadži (15) suggested that the lack of any band in the vicinity of $11\ \mu$ was evidence against the presence of carboxylic acid groups. However, these bands are usually weak or absent in the solid state.

The Carbon-Hydrogen Vibrations

Bands at $7.3\ \mu$ are observed in coal, in coal humic acids, and in carbonized cellulose. This band is commonly attributed to the symmetrical deformation of the CH_3 group attached to another carbon. There is no reason to doubt this assignment in these materials. This band is not observed in humic acids derived from hydroquinone. On the other hand, strong bands are observed at $6.9\ \mu$ in all these spectra, which must be only partly due to CH_2 and CH_3 deformations since these bands should be of medium intensity, judging by the intensity of $3.45\ \mu$ bands. Particularly in the materials derived from hydroquinone, the $6.9\ \mu$ band should be weak if it is derived entirely from CH_2 and CH_3 groups. However, this band has been commonly assigned to the CH_2 group by previous workers (12, 14, 16, 18).

The $6.65\ \mu$ Band

The $6.65\ \mu$ band is intense and sharp in lignin and to some extent in the hydroquinone humic acids, although in the latter case more severe oxidizing conditions appear to cause a decreased intensity of the band. This band is still very distinct in peat humic acids although it occurs at a slightly lower wave-length. It appears quite distinctly in lignite humic acids, lignite, subbituminous coal, and low temperature cellulose char. The band

is very weak in bituminous coal and occurs at a slightly longer wave-length. In the other three char preparations the band is weak or non-existent.

At this time it is only possible to speculate on the reason for the decrease in intensity of this band in the above series. The 6.6–6.7 μ band is widely used for diagnosis of aromatic systems (3). It has been shown by the results of deuteration that while it is mainly a skeletal mode of the benzene ring, the hydrogen atoms of the benzene ring are involved (1). The band is completely absent in the spectrum prepared in this laboratory on hexamethylbenzene. Therefore it could be inferred that increased substitution should on the average lower the intensity of this band. The band appears to be present in some condensed aromatic systems and absent in others (10). On the whole, however, increase in condensation of the aromatic rings would be expected to lower the intensity, particularly if the resulting systems were heavily substituted with peripheral aliphatic and alicyclic groups as envisaged by Brown and Hirsch (7).^{*} This peak is not observed in the nitro humic acids; instead, in agreement with Hadži (11), a very distinct band at 6.40 to 6.45 μ is observed which is undoubtedly due to the nitro-group.

Absorption in the Long Wave-length Region

It is well known that bituminous coal shows three distinct bands at 11.6, 12.25, and 13.25 μ ; these bands are also shown by high temperature cellulose char (9). Heating of lignite humic acids to 320° C. for 48 hours produces material showing these bands; this fact, together with the disappearance of carbonyl absorption at 5.8 μ and decrease of OH absorption at 2.95 μ , is evidence for the *in vitro* conversion of humic acids to material the spectrum of which at least approximates very closely that of bituminous coal. More significantly, heating the hydroquinone humic acids produced a char having a spectrum in which the bands at 5.8 μ and 6.6 to 6.7 μ have disappeared but in which new bands show at 11.6, 12.3, and 13.25 μ which are almost identical to those shown by bituminous coal.[†]

The assignment of the bands in the long wave-length region has always been to aromatic substitution. Friedel (12) believes that these bands can be explained by substitution patterns on the benzene nucleus, whereas Bergmann (4) has suggested that these waves correspond to substitutions on the phenanthrene nucleus.[‡] In any event, the identical position of these bands in high rank coals and chars from cellulose and humic acids strongly suggests that the skeletal structures of all these materials must be similar.

ACKNOWLEDGMENT

Thanks are extended to the following members of the Research Council for their assistance: Mr. William Dammeyer for determining the spectra, Mr. John Fryer for the elemental analyses, and Dr. J. C. Wood for the Klason lignin. Thanks are also ex-

^{*}Some substitution patterns can cause very pronounced lowering of the intensity of the 1500 cm^{-1} band; cf. 9,10-disubstituted anthracenes, anthraquinone, dibenzanthrone, etc. The studies of Cannon and Sutherland (10) indicate that in the benzene series the 1500 cm^{-1} band weakens drastically in penta- and hexa-substituted compounds. Both van Krevelen and Brown, as well as this study, have noted low absorption due to aromatic CH in the low rank coals, indicating a high degree of substitution in the low rank coals. Polymers containing isolated benzene rings, e.g. polystyrene, have very strong 1500 cm^{-1} bands. Tetraphenylmethane (four benzene rings) has a much stronger 1500 cm^{-1} band than benzantracene; Ref. 10 contains many other examples. Compare the apparent molecular extinction coefficients per benzene ring in the series benzene, ϵ 80; naphthalene, ϵ 2, 27; anthracene, ϵ 3 at 1550 cm^{-1} , 8; phenanthrene ϵ 3, 20; benzantracene, ϵ 4, 18. (Jones, R. N. and Sandorfy, C. Chemical applications of spectroscopy. Interscience Publishers Inc., New York, N. Y.)

[†]Hydroquinone itself was not affected by autoclaving under these conditions.

[‡]Brown discussed the position of the long wave-length bands in terms of the number of neighboring hydrogen atoms on each benzene ring whether isolated or condensed. He did not arrive at any conclusion regarding isolated or condensed systems below about 90° C.

tended to Dr. I. Wender of the Bruceton Laboratories of the U.S. Bureau of Mines, for the sample of Bruceton vitrain.

REFERENCES

1. ANGUS, W. R., BAILEY, C. R., HALE, J. B., INGOLD, C. K., LECKIE, A. H., RAISIN, C. G., THOMPSON, J. W., and WILSON, C. L. *J. Chem. Soc.* 971 (1936).
2. ARNOLD, C. L., LOWRY, A., and THIESSEN, R. *Fuel*, **14**, 107 (1935).
3. BELLAMY, L. J. *The infrared spectra of complex molecules*. Methuen and Co. Ltd., London, 1954. Chap. 10.
4. BERGMANN, G., HUCK, G., KARWEIL, J., and LUTHER, H. *Brennstoff-Chem.* **35**, 175 (1954).
5. BREGER, I. A. *Fuel*, **30**, 204 (1951).
6. BROWN, J. K. *J. Chem. Soc.* 744 (1955).
7. BROWN, J. K. and HIRSCH, P. B. *Nature*, **175**, 229 (1955).
8. CANNON, C. G. *Nature*, **171**, 308 (1953).
9. CANNON, C. G. and SUTHERLAND, G. B. B. M. *Trans. Faraday Soc.* **41**, 279 (1945).
10. CANNON, C. G. and SUTHERLAND, G. B. B. M. *Spectrochim. Acta*, **4**, 373 (1951).
11. ČEH, M. and HADŽI, D. *Fuel*, **35**, 77 (1956).
12. FRIEDEL, R. A. and PELIPETZ, M. G. *J. Opt. Soc. Amer.* **43**, 1051 (1953).
13. FRIEDEL, R. A. and QUEISER, J. A. *Anal. Chem.* **28**, 22 (1956).
14. GORDON, R. R., ADAMS, W. N., PITT, C. J., and WATSON, C. H. *Nature*, **174**, 1098 (1945).
15. HADŽI, D. *Acad. Sci. et Art. Sloven. Class. III, Ser. A*, 108 (1951).
16. KIRKBY, W. A., LAKEY, F. R. A., and SARJANT, R. J. *Fuel*, **33**, 480 (1954).
17. SCHIEDT, U. *Z. Naturforsch.* **8b**, 66 (1953).
18. van VUCHT, H. A., RIETVELD, B. J., and van KREVELEN, D. W. *Fuel*, **34**, 50 (1955).

NOTES

THE USE OF A TWYMAN-GREEN TYPE INTERFEROMETER TO MEASURE DIFFUSIVITIES IN AN ELECTRODEPOSITION CELL

ROBERT N. O'BRIEN*

A modified Twyman-Green type of split beam interferometer was built for use with a copper sulphate electrodeposition cell as shown in Fig. 1. The diagram shows the two copper electrodes end-on between the two glass flats. The remainder of the cell consisted of a perspex cup to hold the flats and electrolyte. The electrodes were two pieces of copper, 3 mm. apart, and the depth of electrodes and solution was 2 mm. The light used was an ordinary sodium vapor lamp.

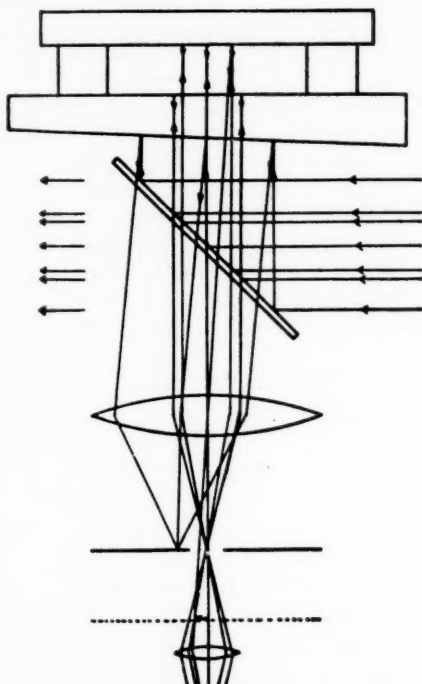


FIG. 1

An electrical circuit using a lead-acid storage cell as a source of power with a potential divider and an ammeter and voltmeter was used. Various solutions were tested and from interferograms obtained it was concluded that the perturbations of the interference fringe pattern, although changing in amplitude, always had the same general configuration. All possible ranges of current density were tried, various ions were added, and chelating agents giving charges of $+2$, 0 , and -2 on the chelated copper ion were used.

*Now at Division of Pure Chemistry, National Research Council, Ottawa, Canada.

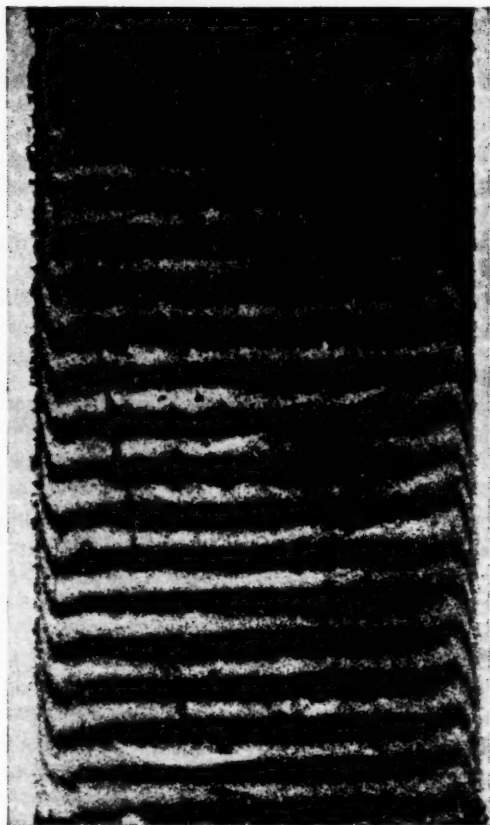


FIG. 2.

Fig. 2 shows a typical interferogram obtained at 0.125 amp. per sq. dm. and 0.117 v. with a 0.2 *M* solution of $\text{CuSO}_4 \cdot 5\text{H}_2\text{O}$. The relatively long straight section of fringe in the middle has been called the "general pattern" and each other part that is sufficiently well defined has been called a "wave" and numbered. Starting at either electrode, the nearest straight part is the first wave and the second and third are called the second and third wave respectively.

When the current is switched on, the fringes first pivot about a central point and then develop the waves shown in Fig. 2. The waves intensify with increasing current density. In the first crude apparatus built it was impossible to obtain sufficient resolving power to produce enough data on the first wave to establish the factors on which it depends, but there were indications that the fringe shift was proportional to current density but not the same for all solutions. The general pattern shift was different in magnitude for each solution and depended on current density. The dependence was linear with the limits of the accuracy of the measurements. The second and third wave gave good linear plots of current density versus fringe shift and the slope was exactly the same for all solutions including chelated ones. This suggests that the physical phenomena associated with these waves are general processes occurring in all conducting

solutions, such as polarization at electrodes. The relative thicknesses of the various parts of the solution where the various waves developed can be seen in Fig. 2. They were about 0.125 mm., 0.296 mm., and 0.421 mm. for the first, second, and third waves respectively.

The third wave represents a decrease (relatively) in concentration in the cathode pattern if it is accepted that optical contours represent concentration contours. The second wave then represents an increase in concentration, or really a decrease in concentration gradient.

Assuming again that the optical density is directly proportional to the chemical concentration, apparent diffusivities corresponding to the implied concentration gradient were calculated. They were, at 21.5° C. for CuSO_4 , using only the cathode side of the pattern (except for the "over-all diffusivity") and Fick's first law $J = -D \, dc/dx$:

General pattern	$1.5 \times 10^{-6} \text{ cm.}^2 \text{ sec.}^{-1}$
First wave	1.5×10^{-3}
Second wave	-9.3×10^{-4}
Third wave	7.6×10^{-2}
Over-all	3.1×10^{-6}

All of the values except the "over-all" are relative to the "general pattern". The over-all diffusion coefficient was found by taking the total fringe shift from the anode to the cathode, and the over-all distance between the electrodes as the concentration gradient, and it is this value that is to be compared with that of 3.8×10^{-6} given in International Critical Tables.

A more sophisticated apparatus has been designed and further work is intended. Meanwhile it is thought that the values found are probably correct to $\pm 20\%$, and that the modulation of the fringe system deserves early reporting.

Greater details of the experimental data obtained, which run to about 200 interferograms, are to be published shortly in "Electroplating and metal finishing". A complete treatment appears in the author's Ph.D. Thesis submitted to the Metallurgy Department, Manchester University.

ACKNOWLEDGMENT

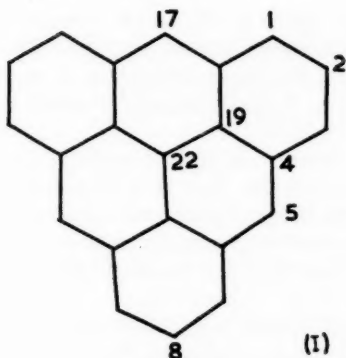
All the data for the above were obtained at the University of Manchester under the direction of Prof. F. C. Thompson and H. J. Axon to whom thanks are due for encouragement and advice.

RECEIVED FEBRUARY 20, 1957.

A NOTE ON THE HYDROCARBON DIBENZO(*cd,mn*)PYRENE

M. W. LISTER

The fused aromatic ring compound dibenzo(*cd,mn*)pyrene, $\text{C}_{22}\text{H}_{12}$ (I) has the peculiarity that no Kekulé type formula can be written for it. It is easily found by trial and error that at least two carbon atoms are left unattached to double bonds. These atoms can be in various combinations of the 1, 5, and 19 type of positions, and in these positions there need only be two such unattached atoms. If any of the unattached atoms are in a 2, 4, or 22 type of position, there must be at least four of them. If we allow Dewar



(1)

type formulae, with bonds between para positions, two atoms still remain unattached; but a bond between meta positions (e.g. 5 to 19) can remove such unattached atoms. These considerations suggest that the molecule might be paramagnetic with two unpaired electron spins. The molecule is too complicated to treat by the valency bond method in detail. However, the molecular orbital treatment is possible, and the object of this note is to report the results of this treatment. These results also suggest that the molecule should be paramagnetic, that is, that it should have a triplet ground state.

Since the compound does not seem to have been prepared, the results are perhaps of somewhat academic interest, but they show a rather unusual relation between the molecular orbital and valency bond pictures. Also, this seems to be the simplest aromatic molecule in which this type of paramagnetism might be expected to occur.

It did not seem worth while to calculate the energy levels by anything more than the simplest approximation, as this is sufficient to establish the probability of paramagnetism; and there are no experimental data available for a more detailed comparison. Accordingly, if the molecular orbitals are of the form $\Psi = \sum c_n \psi_n$, where ψ_n are the $2p$ orbitals on carbon, then minimizing the energy in the usual way (1, 4) gives a secular determinant $|H_{rs} - E S_{rs}|$ in which the terms were taken to be as follows (E is the energy of the molecular orbital): If $r = s$, all H_{rs} are taken as having the same value, E_0 . Where r and s are neighbors, all H_{rs} are taken as having some other identical value, β . Otherwise H_{rs} is assumed equal to zero. S_{rs} is unity for $r = s$, but otherwise S_{rs} is taken to be zero. These are the usual first approximations.

Dibenzo(*cd,mn*)pyrene has D_{2h} symmetry, but the molecular orbital wave functions, which are antisymmetric in the plane of the molecule, will in effect only have C_{2v} symmetry (like ammonia). For the C_{2v} symmetry group, the character table is as follows (e.g. (3)): A_1 : 1,1,1; A_2 : 1,1,-1; E : 2,-1,0. The first number refers to the identity operation, the second to rotations, and the third to reflections. If we take the molecular orbitals belonging to the A_1 representation, there must be six of these because there are six essentially different positions in the molecule. The A_1 part of the character table requires that the c_n coefficients are the same for all atoms in any one type of position, so we get a sixth order determinant whose roots are $E_0 \pm 2.633\beta$, $E_0 \pm 1.524\beta$, and $E_0 \pm 0.863\beta$.

For the A_2 representation, only atoms in the 1 and 4 types of position do not have zero coefficients; this gives two more levels: $E_0 \pm \beta$.

The remaining 14 levels of the E representation must occur in pairs of equal energy. The simplest way of finding these levels is to take the molecular orbitals as having a

planar node running through atoms 17, 22, and 8. This gives a ninth order determinant whose roots are: $E_0 \pm 2.149\beta$, $E_0 \pm 1.543\beta$, $E_0 \pm \beta$, and E_0 . The $E_0 \pm \beta$ levels coincide with the A_2 levels, but these are triply degenerate levels as can be seen by actually working out the coefficients, c_n . Each of the other E levels is doubly degenerate, so that we now have the complete 22 levels.

There are 22 aromatic electrons, and as β is negative, in the ground state these will go in as follows: two in $E_0 + 2.633\beta$, four in $E_0 + 2.149\beta$, four in $E_0 + 1.543\beta$, two in $E_0 + 1.524\beta$, six in $E_0 + \beta$, two in $E_0 + 0.863\beta$, and the remaining two can go one each in the two E_0 levels. Thus the situation is similar to that in the oxygen molecule, so presumably the last two electrons will have unpaired spins. Hence the molecular orbital method also predicts a paramagnetic molecule.

The total energy is $22E_0 + 30.810\beta$. Localized molecular orbitals give an energy of $22E_0 + 20\beta$, so the resonance energy is 10.810β . This is 1.80β per ring; compare naphthalene on the same approximation at 1.84β per ring, or anthracene at 1.77β per ring ((5), or Ref. 3, p. 256). Alternatively the total energy can be written as $22(E_0 + 1.40\beta)$; this also is comparable to naphthalene at $10(E_0 + 1.37\beta)$, or anthracene at $14(E_0 + 1.38\beta)$. These quantities are fairly constant for a number of fused ring hydrocarbons, and in this respect dibenzo(*cd,mn*)pyrene falls into line.

If the c_n values are worked out for each level, we get the patterns of nodes in the molecular orbitals. The A_1 levels have triangular nodes, rather like two-dimensional radial nodes (like the $2s$ orbit in hydrogen), while the E levels have planar nodes (like the $3d$ or $2p$ orbits in hydrogen). On the basis of this analogy, it is interesting to note that the order of the levels is: the lowest level, $E_0 + 2.633\beta$, has of course no nodes like a $1s$ orbit; next, the $E_0 + 2.149\beta$ level has one planar node like a $2p$ orbit; the $E_0 + 1.543\beta$ level has two planar nodes like a $3d$ orbit; and the fourth level, $E_0 + 1.524\beta$, has a triangular node like a $2s$ orbit. Thus the order of the levels is different from what might be expected from this analogy.

If the coefficients, c_n , are chosen so that pairs of degenerate orbits are orthogonal, it is possible to calculate the distribution of electron charge. If the energy levels are taken to the nearest 0.0001β , all atoms appear to have a net charge less than 0.001 electron charge. This is to be expected as this is an alternant hydrocarbon, and Coulson and Rushbrooke (2) have shown that the net charge on atoms of alternant hydrocarbons is zero.

Finally it may be mentioned that a somewhat better approximation will not change the relative positions of the levels. If S_{rr} is not zero for neighbors (6), the relative energies will change somewhat, but not their number or their order. The same applies if H_{rr} for next nearest neighbors is not zero, at least for any reasonable value as compared with β .

1. COULSON, C. A. Valence. Clarendon Press, Oxford. 1952. p. 239.
2. COULSON, C. A. and RUSHBROOKE, G. S. Proc. Cambridge Phil. Soc. **36**, 193 (1940).
3. EYRING, H., WALTER, J., and KIMBALL, G. E. Quantum chemistry. John Wiley & Sons, Inc., New York. 1944. p. 384.
4. HUECKEL, E. Z. Physik, **70**, 204 (1931).
5. HUECKEL, E. Z. Physik, **76**, 628 (1932).
6. WHELAND, G. W. J. Am. Chem. Soc. **63**, 2025 (1941).

RECEIVED APRIL 23, 1957.
DEPARTMENT OF CHEMISTRY,
UNIVERSITY OF TORONTO,
TORONTO, ONTARIO.

National Research Council Postdoctorate Research Fellow 1955-. Present address: 28 Wairere Ave., Mt. Albert, Auckland, New Zealand.

TABLE I
THE "SENSITIVE" METHYLENE FREQUENCIES IN THE METHYLENE HALIDES

	δ_{CH_2}	w_{CH_2}	t_{CH_2}	r_{CH_2}
CH_2F_2^1	1508	1435	1262	1176
CH_2FCI^1	1470	1351	1236	1004
$\text{CH}_2\text{FBr}^{2-a}$	1461	1313	1227	939
CH_2Cl_2^1	1424	1262	1159	898
CH_2ClBr^1	1402	1225	1130	852
$\text{CH}_2\text{ClI}^{2-a}$	1392	1183	—	801
CH_2Br_2^1	1385	1190	1096	813
$\text{CH}_2\text{BrI}^{2-a}$	1374	1150	1065	754
CH_2I_2^1	1351	1107	1035	717

^aRaman data only.

¹Plyler, E. K. and Benedict, W. S. *J. Research Natl. Bur. Standards*, **47**, 202 (1951).

²Delwaulle, M. L. and Francois, M. F. *J. phys. radium*, **7**, 15 (1946).

all four points lie on the best line parallel to the ordinate, giving a minimum total deviation of the points from the 'theoretical' curves. The intersection of this line with the abscissa would then give the sum of the "group electronegativities" of the substituents. Alternatively, the "group electronegativities", as determined in Part I (3) from the sensitive methyl frequencies (Table II), can be used and the methylene frequencies plotted on Fig. 1 in the same manner as for the halides. This latter procedure has been followed in the present work and the plots are given superimposed on Fig. 1. Table III compares

TABLE II
SOME "GROUP ELECTRONEGATIVITY" VALUES

Group	Electronegativity ^a
HO—	3.86
H ₂ N—	3.63
O ₂ N—	3.47
Cl ₃ C—	3.25
Cl ₂ HC—	3.22
ClH ₂ C—	3.22
N≡C—	3.11
—O ₂ C—	2.98
HOOC—	2.97

^aDetermined from the methyl rocking and symmetrical deformation frequencies (3).

TABLE III
CALCULATED AND OBSERVED VALUES OF THE "SENSITIVE" METHYLENE FREQUENCIES

	δ_{CH_2}		w_{CH_2}		t_{CH_2}		r_{CH_2}	
	Obs.	Calc.	Obs.	Calc.	Obs.	Calc.	Obs.	Calc.
$\text{CH}_2\text{Cl}(\text{CCl}_3)^1$	1426	1438	1283	1286	1206	1182	958	932
$\text{CH}_2(\text{CN})_2^2$	1422	1435	1265	1280	1214 ^a	1178	936	925
$\text{CH}_2(\text{Cl})_3^3-a$	1416	1430	1269	1270	1180	1168	932	912
$\text{CH}_2(\text{CO}_2)_2^4-a$	1420	1423	1259	1256	1175	1156	922	893

^aRaman data.

¹Nielsen, J. R., Liang, C. Y., and Daash, L. W. *J. Opt. Soc. Amer.* **43**, 1071 (1953). The assignment of the δ , w , and t methylene frequencies has been interchanged to agree with the data here and is now consistent with the depolarization data for the deuterated material (Allen, G. and Bernstein, H. J. *Can. J. Chem.* **32**, 1124 (1954)).

²Halverson, F. and Francel, R. J. *J. Chem. Phys.* **17**, 694 (1949).

³Cheng, H.-C. *Z. physik. Chem. B*, **26**, 288 (1934).

⁴Wilmschurst, J. K. Unpublished data.

the observed frequencies (δ , w , t , and r) for some methylene compounds with the calculated frequencies obtained using the "group electronegativities" from Part 1 (3) and the 'theoretical' curves of Fig. 1. The agreement is very satisfactory.

In all the monomethylene compounds considered here, the sensitive methylene frequencies behave as group frequencies and always occur in the order $\delta > w > t > r$. In dimethylene compounds the situation is complicated by the possibility of interaction between the two methylene groups and by the presence of rotational isomers. However, if one assumes that the dimethylene unit is made of two single methylene units having identical frequencies, and that only like frequencies interact, e.g. the two δ modes together, the two w modes together, then the pairs of resulting frequencies of the dimethylene system should lie equally separated about the corresponding methylene frequency of the lone CH_2 unit as mean. This is illustrated in Table IV for 1,2-dichloroethane (1) where

TABLE IV
SENSITIVE FREQUENCIES FOR $\text{ClCH}_2\text{CH}_2\text{Cl}$ ^a

Frequency	Trans	Mean	Gauche	Mean	Calc.
δ	1448 1453	1450	1433 1429	1431	1436
w	1301 1231	1266	1312 1286	1299	1282
t	1265 1128	1197	1207 1143	1175	1178
r	992 773	883	944 880	912	927

^aBrown, J. K. and Sheppard, N. *Trans. Faraday Soc.* **48**, 128 (1952).

the calculated frequencies were obtained from Fig. 1 using the "group electronegativities" of Part 1. The good agreement obtained in 1,2-dichloroethane suggests that, even in dimethylene compounds, the sensitive methylene frequencies can be regarded as group frequencies, interactions occurring only between like modes.

When the CH bending frequency (taking the mean of the a' and a'' components where necessary) in the trihalomethane series (Table V) is plotted against the sum of the electronegativities (2) of the halide atoms, a smooth curve is obtained (Fig. 2). With

TABLE V
THE METHINE BENDING FREQUENCY IN THE TRIHALOMETHANES

HCF ₃ ¹		1372	
HCF ₂ Cl ¹	1347		1311
HCF ₂ Br ²	1344		1276
HCFCl ₂ ¹	1304		1242
HCFClBr ^{3-a}	1302		1205
HCFBr ₂ ^{3-a}	1293		1170
HCCL ₃ ¹		1214	
HCCl ₂ Br ¹	1211		1168
HCClBr ₂ ¹	1189		1144
HCBBr ₃ ¹		1142	
HCL ₃ ¹		1064	

^aRaman data.

¹Plyler, E. K. and Benedict, W. S. *J. Research Natl. Bur. Standards*, **47**, 202 (1951).

²Palm, A., Voelz, F. L., and Meister, A. G. *J. Chem. Phys.* **23**, 726 (1955).

³Glockler, G. and Leader, G. R. *J. Chem. Phys.* **8**, 699 (1940).

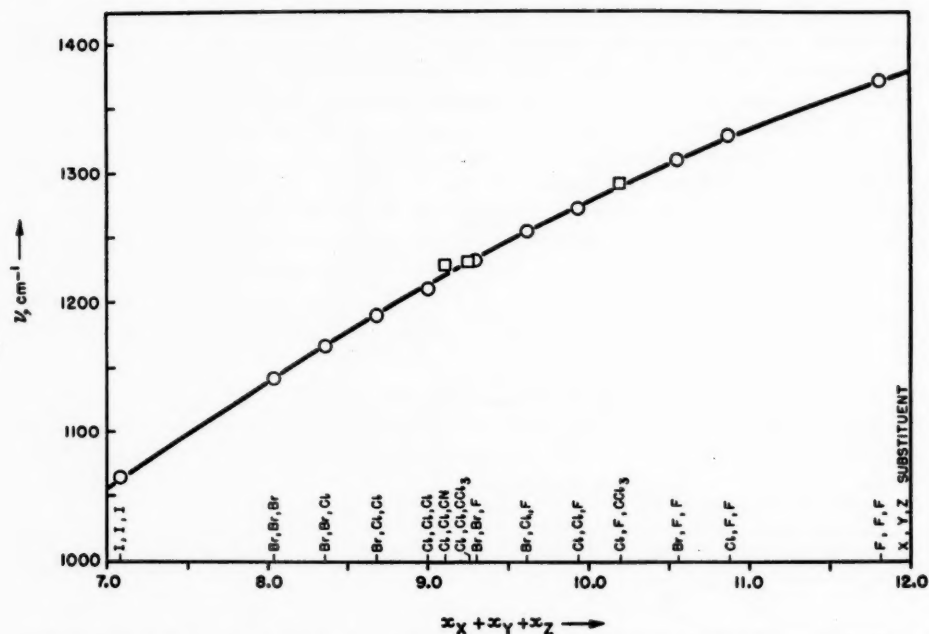


FIG. 2. The plot of the "sensitive" methine frequency against the sum of the electronegativities of the substituents: O trihalomethanes, □ other methine derivatives.

other molecules of the general type HCXYZ, where at least one of the substituents X, Y, or Z is not a halide atom, the CH bending frequency can be fitted to Fig. 2 to obtain values of the "group electronegativities," or alternatively, the "group electronegativities" as determined in Part 1 (3) can be used to plot the bending frequency on Fig. 2. Using the latter approach, the plots of some methine compounds are superimposed on Fig. 2 and the observed and calculated frequencies compared in Table VI. The agreement is excellent.

It is very gratifying to find that the "group electronegativities" as determined from the sensitive methyl frequencies (3) can be used to predict the sensitive methylene

TABLE VI
CALCULATED AND OBSERVED VALUES OF THE "SENSITIVE"
METHINE FREQUENCY

	δ_{CH} obs.	δ_{CH} calc.
CHFCI(CCl ₃) ^{1,a}	1322 } 1262 }	1292
CHCl ₂ (CCl ₃) ²	1252 } 1210 }	1231
CHCl ₂ (CN) ^{3,a}	1258 } 1200 }	1229
		1227

^aRaman data only.

¹Glockler, G. and Sage, C. *J. Chem. Phys.* **9**, 387 (1941).

²Nielsen, J. R., Liang, C. Y., and Daasch, L. W. *J. Opt. Soc. Amer.* **43**, 1071 (1953).

³Cheng, H.-C. *Z. physik. Chem. B*, **26**, 288 (1934).

and methine frequencies with such accuracy. This lends support to the consideration of a "group electronegativity" and is in agreement with the fact that in these three series the same effect is operative.

1. BROWN, J. K. and SHEPPARD, N. *Trans. Faraday Soc.* **48**, 128 (1952).
2. GORDY, W. *Phys. Rev.* **69**, 604 (1946).
3. WILMSHURST, J. K. *J. Chem. Phys.* **26**, 426 (1957).

RECEIVED MARCH 14, 1957.
PURE CHEMISTRY DIVISION,
NATIONAL RESEARCH COUNCIL,
OTTAWA, CANADA.

NOTES ON THE PREPARATION AND USE OF ^{14}C -LABELLED VITAMIN K_1 AND VITAMIN K_3

R. J. WOODS AND J. D. TAYLOR¹

The synthesis of labelled vitamin K_1 (2[^{14}C]-methyl-3-phytyl-1,4-naphthoquinone) by the condensation of isophytol and 2[^{14}C]-methyl-1,4-dihydroxynaphthalene (vitamin K_3 hydroquinone) previously reported from these laboratories (4) has been modified and an alternative method of separating the reaction products developed (cf. 1). The condensation mixture was found to have reached its final state after it had been stirred for 1 hour at 50° C.; the longer reaction time reported previously is unnecessary. Slightly better yields were obtained by substituting phytol for isophytol; phytol acetate gave the same yield as the free alcohol.

Both vitamin K_1 and vitamin K_3 labelled with ^{14}C appear to undergo appreciable self-decomposition when stored in the dark at 5° C. The labelled vitamin K_1 was best purified by chromatography just before use and the vitamin K_3 purified, if necessary, by vacuum sublimation. Self-decomposition of other compounds labelled with ^{14}C has been observed (5, 6).

Phytol and isophytol give isomeric products when used in the vitamin K_1 synthesis (3) though both forms are reported to have the same biological effectiveness when administered to vitamin K deficient chicks and rabbits rendered hypoprothrombinemic with dicumarol. Results obtained using [^{14}C]-labelled vitamin K_1 prepared from both phytol and isophytol suggested that the two forms may be deposited to a different extent in the skeletal muscle of the rat following intravenous injection.

EXPERIMENTAL

Vitamin K_3

A sample of 2[^{14}C]-methyl-1,4-naphthoquinone (28.5 mg., specific activity 9.2×10^6 disintegrations per minute per mg.) was found to have darkened appreciably after being stored 23 months in a sealed vial in the dark, at 5° C. The sample was resublimed to give the pure quinone (24.1 mg.) and a small quantity of oily residue (3.45 mg.). Inactive 2-methyl-1,4-naphthoquinone was added to a solution of the residue in chloroform, the solvent evaporated, and the quinone recovered by sublimation. The recovered quinone contained 0.15% of the total activity originally present. Assuming that the residue was material changed as a consequence of radioactive decay it was calculated that approximately 29 molecules were changed per 100 electron volts of energy liberated.

Preparation of Vitamin K_1

2[^{14}C]-methyl-1,4-naphthoquinone (241 mg.) in 10 ml. ether was shaken with a solution of sodium hydrosulphite (0.5 g.) in 4 ml. water until the color of the mixture faded to

¹National Research Council student.

pale yellow. The ethereal solution was separated, dried over magnesium sulphate, and evaporated to give 2^[14C]-methyl-1,4-dihydroxynaphthalene.

To the dry hydroquinone were added a solution of phytol (280 mg.) in 3 ml. pure dry dioxane and a solution of boron trifluoride in ether (0.1 ml., 45% BF₃) and the mixture was stirred for 1 hour at 50° C. under dry nitrogen. The resulting solution was diluted with 20 ml. light petroleum (Skelly F) and extracted with four 5-ml. portions of Claisen alkali (35 g. potassium hydroxide in 25 ml. water, diluted to 100 ml. with methanol) containing 10% of a saturated aqueous solution of sodium hydrosulphite. The combined alkaline extract was shaken with three 15-ml. portions of Skelly F, diluted with 40 ml. of a 1% aqueous solution of sodium hydrosulphite, and extracted with ether. The ether extract was washed with a little water, dried over magnesium sulphate, and concentrated to 10 ml. in a stream of nitrogen. Silver oxide (600 mg.) was added and the mixture stirred for 1 hour, filtered, and evaporated in a stream of nitrogen. Solvent was removed from the residue *in vacuo* to give ^[14C] vitamin K₁ as a clear golden oil (132 mg., 21% yield based on the 2^[14C]-methyl-1,4-naphthoquinone taken). The oil was identified by its ultraviolet absorption spectrum, by paper chromatography, and by isotope dilution. Isotope dilution, using authentic 2-methyl-1,4-naphthoquinone, and paper chromatography showed the oil to be completely free from ^[14C] vitamin K₃. Isotope dilution using authentic vitamin K₁ showed that the oil contained 96% ^[14C] vitamin K₁, based on the specific activity of the starting material.

Unreacted 2^[14C]-methyl-1,4-dihydroxynaphthalene was recovered from the alkaline sodium hydrosulphite solution by acidifying with dilute sulphuric acid and extracting with ether. The ether solution was dried over magnesium sulphate and evaporated, the residue extracted with a little dry ether, filtered, and the filtrate evaporated to give the hydroquinone (56 mg.). Thus the yield of ^[14C] vitamin K₁ was 28%, based on the ^[14C] vitamin K₃ used up.

Rather better yields were obtained by working on a slightly larger scale. ^[14C] vitamin K₃ (690 mg.) gave ^[14C] vitamin K₁ in 38% yield, based on the vitamin K₃ used up, or 24% conversion if based on the amount of vitamin K₃ originally taken. Inactive 2-methyl-1,4-dihydroxynaphthalene (1 g.) gave vitamin K₁ hydroquinone in 40–60% yield (25–32% conversion).

Purification of Vitamin K₁

Labelled vitamin K₁ was stored under nitrogen in sealed ampoules, kept in the dark at 5° C. During storage the clear yellow oil gradually darkened though authentic, non-radioactive, vitamin K₁ stored in a similar manner showed no change.

Labelled vitamin K₁ (26 mg., specific activity 1.7×10^6 disintegrations per minute per mg.) which had been stored 8 months was dissolved in 0.5 ml. benzene and adsorbed onto a column of Folin's Permutit (0.8 cm.³ \times 15 cm.) moistened with Skelly F. The mobile yellow band was eluted with Skelly F containing 20% (v/v) benzene and the solvent evaporated under reduced pressure to give ^[14C] vitamin K₁ (16.3 mg., 95% pure—determined by the Irreverre-Sullivan reaction (2)). The eluate collected both before and after the main fraction was evaporated and gave about 2.6 mg. of less pure ^[14C] vitamin K₁. The colored decomposition product was strongly adsorbed on the column but could be eluted with diethyl ether; it was recovered after evaporating the ether *in vacuo* as a red-brown oil (7.1 mg.).

Approximately 390 molecules of ^[14C] vitamin K₁ were lost for each 100 electron volts liberated by radioactive decay.

Chromatography on Folin's Permutit separated vitamin K₃ from vitamin K₁ but did not separate the other materials obtained during the condensation of vitamin K₃ hydroquinone and phytol.

Vitamin K₁ Isomers

Intravenous administration of [¹⁴C] vitamin K₁ prepared from phytol resulted in the deposition of $8.0 \pm 1.5\%$ (standard deviation) of the injected ¹⁴C in the skeletal muscle of albino rats (12 rats) whereas with [¹⁴C] vitamin K₁ prepared from isophytol (11 rats) the deposition was $12.6 \pm 4.3\%$ (standard deviation). The results are calculated on the basis that dry skeletal muscle comprises 27% of the live weight of a rat. No significant differences were found in the deposition of ¹⁴C in the livers, spleens, or blood.

ACKNOWLEDGMENT

The authors gratefully acknowledge their indebtedness to the Atomic Energy Control Board (R. J. W.) and the National Research Council (J. D. T.) for financial support through Dr. J. W. T. Spinks and Dr. L. B. Jaques.

1. HIRSCHMANN, R., MILLER, R., and WENDLER, N. L. *J. Am. Chem. Soc.* **76**, 4592 (1954).
2. IRREVERRE, F. and SULLIVAN, M. X. *Science*, **94**, 497 (1941).
3. ISLER, O. and DOEBEL, K. *Helv. Chim. Acta*, **37**, 225 (1954).
4. LEE, C. C., HOSKIN, F. C. G., TREVOY, L. W., JAKES, L. B., and SPINKS, J. W. T. *Can. J. Chem.* **31**, 769 (1953).
5. LEMMON, R. M. *Nucleonics*, **11** (10), 44 (1953).
6. TOLBERT, B. M. *et al.* *J. Am. Chem. Soc.* **75**, 1867 (1953).

RECEIVED APRIL 8, 1957.
DEPARTMENTS OF CHEMISTRY AND PHYSIOLOGY,
UNIVERSITY OF SASKATCHEWAN,
SASKATOON, SASKATCHEWAN.

HELVETICA
CHIMICA
ACTA

SCHWEIZERISCHE
CHEMISCHE GESELLSCHAFT
Verlag Helvetica Chimica Acta
Basel 7 (Schweiz)

Seit 1918 **40**
Jahre

Es sind noch
lieferbar:

Neudruck zum Teil ab Lager
Vol. I–XIV (1918–1931)
Vol. XVII–XX (1934–1937) Auslieferung erfolgt demnächst!
Vol. XV, XVI, XXI–XXV (1932, 1933, 1938–1942) in Vorbereitung.

Originalausgaben, zum Teil druckfrisch
Vol. XXVI–XXXIX (1943–1956)

Diverse Einzelhefte ab Vol. XV
Preise auf Anfrage. Nur solange Vorrat

Abonnemente: laufender Jahrgang Vol. XL (1957) Fr. 80.–plus Porto

Das wissenschaftliche Organ der

SCHWEIZERISCHEN
CHEMISCHEN
GESELLSCHAFT

CANADIAN JOURNAL OF CHEMISTRY

Notes to Contributors

Manuscripts

(I) **General.** Manuscripts, in English or French, should be typewritten, double spaced, on paper $8\frac{1}{2} \times 11$ in. The original and one copy are to be submitted. Tables and captions for the figures should be placed at the end of the manuscript. Every sheet of the manuscript should be numbered.

Style, arrangement, spelling, and abbreviations should conform to the usage of this journal. Names of all simple compounds, rather than their formulas, should be used in the text. Greek letters or unusual signs should be written plainly or explained by marginal notes. Superscripts and subscripts must be legible and carefully placed.

Manuscripts and illustrations should be carefully checked before they are submitted. Authors will be charged for unnecessary deviations from the usual format and for changes made in the proof that are considered excessive or unnecessary.

(II) **Abstract.** An abstract of not more than about 200 words, indicating the scope of the work and the principal findings, is required, except in Notes.

(III) **References.** References should be listed alphabetically by authors' names, numbered, and typed after the text. The form of the citations should be that used in this journal; in references to papers in periodicals, titles should not be given and only initial page numbers are required. The names of periodicals should be abbreviated in the form given in the most recent *List of Periodicals Abstracted by Chemical Abstracts*. All citations should be checked with the original articles and each one referred to in the text by the key number.

(IV) **Tables.** Tables should be numbered in roman numerals and each table referred to in the text. Titles should always be given but should be brief; column headings should be brief and descriptive matter in the tables confined to a minimum. Vertical rules should be used only when they are essential. Numerous small tables should be avoided.

Illustrations

(I) **General.** All figures (including each figure of the plates) should be numbered consecutively from 1 up, in arabic numerals, and each figure referred to in the text. The author's name, title of the paper, and figure number should be written in the lower left corner of the sheets on which the illustrations appear. Captions should not be written on the illustrations (see Manuscripts (i)).

(II) **Line Drawings.** Drawings should be carefully made with India ink on white drawing paper, blue tracing linen, or co-ordinate paper ruled in blue only; any co-ordinate lines that are to appear in the reproduction should be ruled in black ink. Paper ruled in green, yellow, or red should not be used unless it is desired to have all the co-ordinate lines show. All lines should be of sufficient thickness to reproduce well. Decimal points, periods, and stippled dots should be solid black circles large enough to be reduced if necessary. Letters and numerals should be neatly made, preferably with a stencil (do NOT use type-writing), and be of such size that the smallest lettering will be not less than 1 mm. high when reproduced in a cut of suitable size.

Many drawings are made too large; originals should not be more than 2 or 3 times the size of the desired reproduction. In large drawings or groups of drawings the ratio of height to width should conform to that of a journal page but the height should be adjusted to make allowance for the caption.

The original drawings and one set of clear copies (e.g. small photographs) are to be submitted.

(III) **Photographs.** Prints should be made on glossy paper, with strong contrasts. They should be trimmed so that essential features only are shown and mounted carefully, with rubber cement, on white cardboard with no space or only a very small space (less than 1 mm.) between them. In mounting, full use of the space available should be made (to reduce the number of cuts required) and the ratio of height to width should approximate that of a journal page ($5\frac{1}{2} \times 7\frac{1}{2}$ in.); however, allowance must be made for the captions. Photographs or groups of photographs should not be more than 2 or 3 times the size of the desired reproduction.

Photographs are to be submitted in duplicate; if they are to be reproduced in groups one set should be mounted, the duplicate set unmounted.

Reprints

A total of 50 reprints of each paper, without covers, are supplied free. Additional reprints, with or without covers, may be purchased.

Charges for reprints are based on the number of printed pages, which may be calculated approximately by multiplying by 0.5 the number of manuscript pages (double-spaced typewritten sheets, $8\frac{1}{2} \times 11$ in.) and including the space occupied by illustrations. An additional charge is made for illustrations that appear as coated inserts. The cost per page is given on the reprint requisition which accompanies the galley.

Any reprints required in addition to those requested on the author's reprint requisition form must be ordered officially as soon as the paper has been accepted for publication.

Contents

	Page
The Hysteresis Loop in Adsorption Isotherms on Porous Vycor Glass and Associated Dimensional Changes of the Adsorbent. II— <i>H. W. Quinn and R. McIntosh</i>	745
Preparation of Erucic and Nervonic Acids Labelled with Carbon-14— <i>K. K. Carroll</i>	757
Effect of Changes in Hydration on Recoil Fragments in Neutron-Irradiated Permanganates— <i>J. R. Bolton and K. J. McCallum</i>	761
Hydride Transfer to Carbonium Ions. I. The Mechanism of the Reduction of Triphenylmethyl Carbonium Ion in Formic Acid— <i>Ross Stewart</i>	766
Free Radicals by Mass Spectrometry. XIII. The Mercury Photosensitized Decomposition of Allene and Butadiene: The C_3H_3 Radical— <i>J. Collin and F. P. Lossing</i>	778
The Reaction of Unsaturated Carbohydrates with Carbon Monoxide and Hydrogen. I. Branched-chain Carbohydrate from 3,4,6-Tri-O-acetyl-D-galactal— <i>A. Rosenthal and D. Read</i>	788
The Fractionation of Polysaccharides by the Method of Ultrafiltration— <i>K. C. B. Wilkie, J. K. N. Jones, Barbara J. Escell, and R. E. Semple</i>	795
The Structure of Aluminum Di- and Tri-soaps— <i>A. E. Leger, R. L. Haines, C. E. Hubley, J. C. Hyde, and H. Shaffer</i>	799
Equilibrium Constants for the Sulphur Isotope Exchange between SO_2 and H_2SO_4 — <i>H. B. Dunford, A. G. Harrison, and H. G. Thode</i>	817
Sensitized Photolysis— <i>Ikuzo Tanaka and E. W. R. Steacie</i>	821
The Reaction of Nitrous Acid with 4-Substituted Thiosemicarbazides— <i>Eugene Lieber, C. N. Pillai, and Ralph D. Hites</i>	832
Chemistry of 2,3,5,6-Tetrahydro-1-imidas(1,2-a)imidazole— <i>A. F. McKay, M.-E. Kreling, G. Y. Paris, R. O. Braun, and D. J. Whittingham</i>	843
The Production of Titanium Trichloride by Arc-Induced Hydrogen Reduction of Titanium Tetrachloride— <i>T. R. Ingraham, K. W. Downes, and P. Marier</i>	850
Atisine: Further Degradation— <i>D. Dvornik and O. E. Edwards</i>	860
Bis-organomagnesium Reactions. I. Effect of Solvation on Enolization— <i>C. A. Guthrie, E. Y. Spencer, and George F Wright</i>	873
Détermination du degré de solvatation du mono-n-butoxytrichlorotitane dans le butanol— <i>Jacques Archambault and Roland Rivest</i>	879
Stresses and Strains in Adsorbate-Adsorbent Systems. IV. Contractions of Activated Carbon on Adsorption of Gases and Vapors at Low Initial Pressures— <i>M. L. Lekhanpal and E. A. Flood</i>	887
The Reduction, Enolate Formation, and Solvolysis of Grignard Reagents in Optically Active Media— <i>Norman Allentoff and George F Wright</i>	900
The Infrared and Raman Spectra of Toluene, Toluene- α - d_3 , <i>m</i> -Xylene, and <i>m</i> -Xylene- $\alpha\alpha'$ - d_4 — <i>J. K. Wilmshurst and H. J. Bernstein</i>	911
The Infrared Spectra of Humic Acids and Related Materials— <i>R. M. Eloffson</i>	926
 Notes:	
The Use of a Twyman-Green Type Interferometer to Measure Diffusivities in an Electrodeposition Cell— <i>Robert N. O'Brien</i>	932
A Note on the Hydrocarbon Dibenzo(cd,mn)pyrene— <i>M. W. Lister</i>	934
"Sensitive" Vibrational Frequencies. Part 2. The Methylene and Methine Frequencies and Their Relation to Electronegativity— <i>J. K. Wilmshurst</i>	937
Notes on the Preparation and Use of ^{14}C -Labelled Vitamin K_1 and Vitamin K_2 — <i>R. J. Woods and J. D. Taylor</i>	941

